A Lake Sediment Study of Particulate Flux in the Humber Catchment Using Magnetic Techniques

Daniel Barlow

A thesis submitted in fulfilment of the requirements
for the degree of Doctor of Philosophy
to the University of Edinburgh
1998

Abstract

At present there is a poor understanding of changes in rates of erosion over long time periods and in the link between erosion and sediment delivery in Britain. Using a catchment study approach sediment accumulation rates in cores from the three lakes Semer Water, Gormire and Hornsea Mere have been used to reconstruct changes in sediment yield over time periods of up to 10 000 years, and estimate the mean annual flux of sediment to the Humber estuary. Each of the sites lies in a catchment of differing land use, relief and geology but taken together they are representative of the Humber catchment.

Sediment cores obtained from Gormire and Hornsea Mere have been correlated successfully using variations in mineral magnetic signature. The magnetic minerals are dominated by bacterial magnetosomes at Hornsea Mere and by a combination of bacterial magnetosomes and topsoil at Gormire. Sediment accumulation rates have been converted into sediment yields using a ^{137}Cs and ^{210}Pb chronology, sediment accumulation area, sediment density, organic carbon and carbonate data. At Gormire yields increased from just 7 t km^{-2} a^{-1} in the early Holocene to 78 t km^{-2} a^{-1} for the period 1949-1994. Sediment yields at Hornsea Mere increased dramatically from 12 t km^{-2} a^{-1} in the period 1730-1963 to 52 t km^{-2} a^{-1} between 1963 and 1979, but declined slightly to 41 t km^{-2} a^{-1} in the most recent period 1979-1994.

Sediment accumulation in three cores from Semer Water has been used to determine a mean sediment yield of 6.3 t km^{-2} a^{-1} since 1950. Unusually thick sediment sequences were identified upstream of the existing lake Semer Water in the Raydale valley. Resistivity profiles and gouge cores were used to map the extent of these deposits and ^{14}C and pollen analysis used to establish their chronology. The combined sediment mass of Semer Water and Raydale deposits has been calculated at 11 million tonnes. This translates into a mean Holocene sediment yield of 28 t km^{-2} a^{-1}. The topography of five representative gullies was used to calculate the potential volume of sediment produced from gully erosion in the catchment. This technique indicates that the entire mass of sediment deposited in Raydale during the Holocene may have been produced from gully and channel erosion.

Sixteen catchment and land use characteristics have been determined for 30 British lakes and reservoirs previously studied for sediment flux. Using stepwise regression a model has been constructed relating sediment flux catchment area, catchment soil erosion susceptibility and a slope length factor. The regression equation has an R^2 value of 79%.

Combining a sediment delivery ratio with sediment flux estimates from (i) Semer Water and Gormire, and (ii) published lake and reservoir sediment studies from sites in the Humber catchment, sediment flux to the Humber estuary is estimated at between 40 000 and 110 000 t a^{-1}.

Acknowledgements

I would like to thank Dr. Roy Thompson for his supervision over the past four years and for painstakingly reading earlier drafts of this thesis. Professor Frank Oldfield has also offered advice and encouragement on many occasions. I wish to thank my colleagues in this NERC LOIS Special Topic; Dr. George Wolffe, Mrs Liz Fisher and Miss. Becci Wake at the University of Liverpool. My thanks are extended to Dr. P. O'Sullivan for suggesting I write the initial speculative letter to Professor F.Oldfield inquiring about the possibility of doing a Ph.D.

Mr Alan Pike maintained the coring equipment and accompanied me on fieldwork on many occasions. I also owe thanks to Mr. Alex Jackson and Mr. Jim Smith for fieldwork assistance. I am very grateful to Dr. Bob McCulloch for preparing the pollen samples, Mr. Geoff Angell for help with X-ray diffraction and Mrs. Ann Menim for laboratory assistance. Dr. Peter Appleby provided the ^{210}Pb and ^{137}Cs chronologies and the ^{14}C AMS sample preparation was undertaken at the NERC radiocarbon laboratory in East Kilbride. Dr. Per Sandgren kindly converted the radiocarbon ages into calendar years. NERC and the department Mobil fund provided financial assistance which enabled me to attend short courses on diatom and pollen analysis at the Environmental Change Research Centre, University College London. My thanks are extended to Mr. Justin MacNeil for computing assistance over the past couple of months. This research was funded by NERC.

I wish to thank all the landowners in the Semer Water catchment who gave us permission to obtain cores and undertake resistivity surveys over their land. I would especially like to thank the Sowerby family at Carr End Farm, Raydale for granting us unlimited access with the Giddings corer. Mr. Alan Ball provided advice about the Yorkshire Wildlife Trust nature reserve in the Semer Water catchment and the staff at English Nature offices in Leyburn and Hull supplied information about the Sites of Special Scientific Interest within each of the three catchments. I would like to thank the Henderson family for granting permission to take cores from Gormire.

I owe a great deal to many friends in Edinburgh, in particular Helen and Teresa for all their support and Nick, Yvonne and Peter for sharing many good times. Thanks to Mr Nick Cogzell for correcting my English in earlier drafts of this thesis and thanks to Craig and Dan for continuing to be two exceptional friends for the duration of the Ph.D. I would particularly like to thank Anna Vickery for her love and support over the past two years. Finally I could not have wished for a more supportive family, thanks a lot Mum, Dad, Marts and Lucy.

Contents

List of Figures

List of Tables

Chapter 1

Introduction

1.1 Land Ocean Interaction Study

The Ph.D. project involves the application of lake sediment cores to characterise and quantify sediment flux in three catchments within the Humber region. The project aims to reconstruct variations in particulate flux through the Holocene period.

The research was funded via the University of Liverpool through the NERC Land Ocean Interaction Study (LOIS). The six year LOIS study is the largest and most ambitious Community Research Project ever undertaken by NERC. It follows the government's recognition of the poor current level of understanding of the land ocean interface and the need to develop policy to manage and protect the coastal zone. The following quotation from the LOIS implementation plan summarises the need for such a project.

> "It is important that such policies should be underpinned by a coherent scientific understanding of the region, the materials that traverse it and the transformations that occur within it. Most importantly there is a concern about change, particularly that originating from the activities of man."
> (Gray *in* NERC LOIS Implementation Plan 1994, page ii)

By quantifying the flux, storage and transformation of materials at the coast, and by evaluating how these processes change with time and space, computer models can be devised to predict future processes and to model the effects of differing scenarios.

The NERC LOIS project is concerned primarily with the marine environment, and is subdivided into 7 components as follows:

- Rivers
- Atmosphere } Rivers, Atmosphere, Estuaries and Coasts Study (RACS)
- Estuaries
- Land-Ocean Evolution Perspective Study (LOEPS)
- Shelf Edge Study (SES)
- North Sea Modelling Study (NORMS)
- Data

This Ph.D. project falls within the realms of LOEPS which aims to quantify changes in sediment flux to the marine environment via the Humber estuary during the Holocene.

Three lake catchments within the Humber region were selected for study in the Ph.D project:

- Semer Water
- Gormire
- Hornsea Mere

Sediment cores taken from each of these lakes have been used in assessing erosion rates within each catchment. Figure 1.1 illustrates the extent of the Humber catchment and the location of Semer Water, Gormire and Hornsea Mere within the Humber drainage basin. Semer Water is one of only two natural freshwater lakes within the Yorkshire Dales National Park. The large upland agricultural catchment lies on Carboniferous limestone and is predominantly rough grazing land. Hornsea Mere is a low lying coastal lake, sited on the plain of Holderness. Arable cropland is the principal land use within the catchment, which is underlain by Cretaceous chalk. Gormire is situated on the eastern fringe of the North York Moors. The comparatively small wooded catchment is steep and sited on lower Jurassic bedrock. The geological and land-use characteristics of each catchment differ significantly but are representative of much of the Humber catchment. More detailed information pertaining to the characteristics of each catchment is provided in Chapter 3.

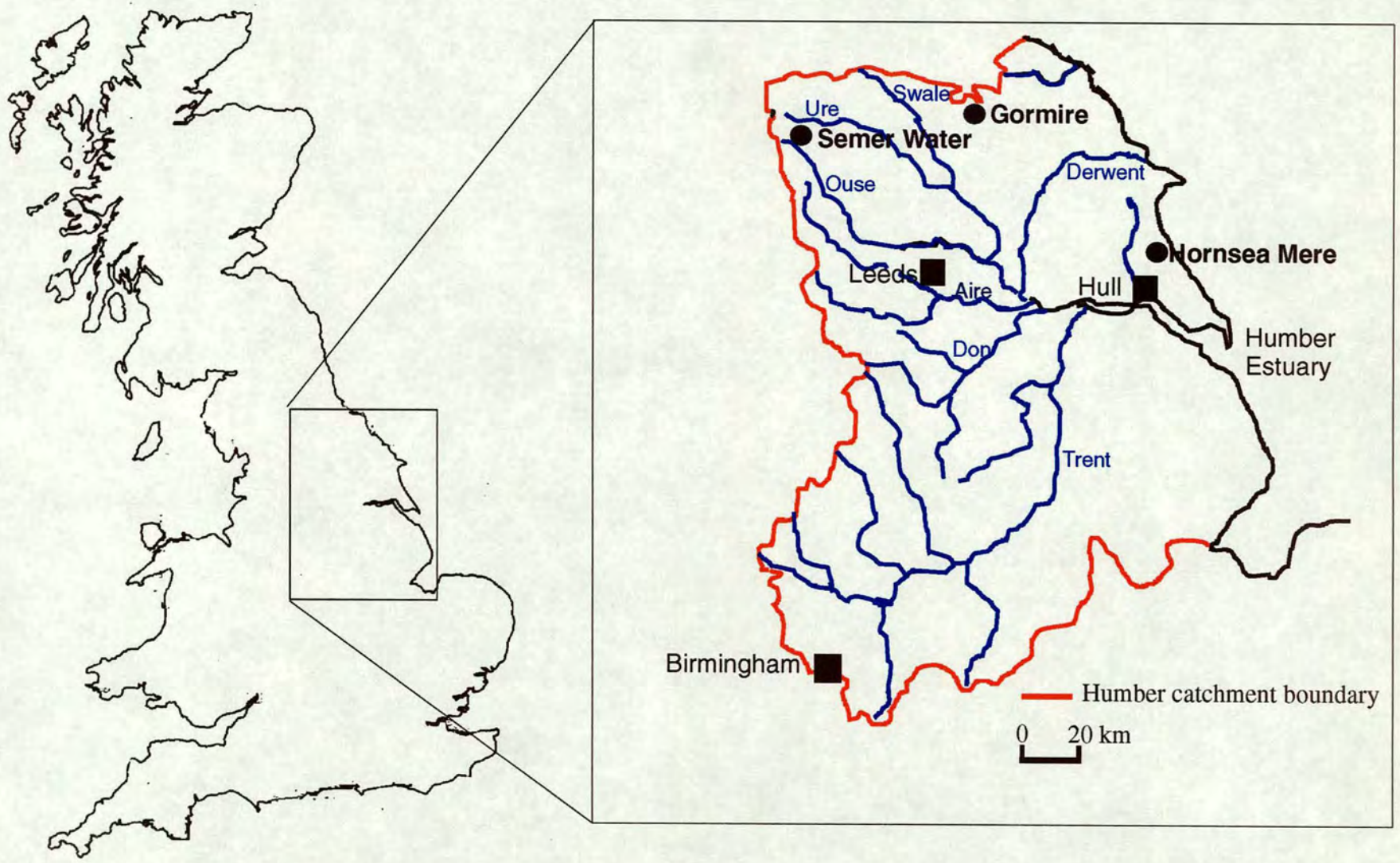

Figure 1.1 The location of Semer Water, Gormire and Hornsea Mere within the Humber catchment The major rivers within the Humber catchment are also shown.

1.2 Project Rationale

1.2.1 Sediment Yields

Despite previous studies on erosion, understanding of quantitative estimates of erosion rates remains poor, particularly on an historical perspective and for such large geographical areas. As reported by Moore and Newson (1986), long records of erosion are unusual in Britain. Indeed Foster *et al.* (1990) reported that by 1990 fewer than ten multiple core lake sediment records had been published in the World. Consequently very little information on erosion rates within British catchments is available over long time periods. The rate of erosion is defined as the mass of sediment physically removed from a given area over a given time. In this study erosion rates are expressed in tonnes per kilometre square per year (t km^{-2} a^{-1}). In Britain work has tended to consider the relatively recent time period, primarily relating to just the past two centuries. The British work covers many important changes including variations in erosion associated with shifts in agricultural and forestry practises, and urbanisation. However, other fundamental changes concerning more historical land use patterns and other human activities are largely undocumented.

Many previous studies reporting erosion rates assume that a uniform rate of soil loss has occurred over the whole of the catchment. A variety of studies have illustrated that sediment is often removed from specific areas within a catchment, and that the extent and location of these areas depend on a number of factors including topography, geomorphology, climate and landuse. Reporting of erosion assuming such a uniform rate of loss is thus often inaccurate, and does little to contribute to our understanding of soil erosion processes. Recent research has begun to address this issue and efforts have been made to link sedimenting material in lakes to specific sources. In this way current work attempts to reconstruct, for example, the varying proportions of material derived from slopes and channel banks. Recent work also aims to establish sediment budgets and models of sediment loss. Such work is

particularly important as it enables us to increase our understanding of geomorphological processes, and when coupled to a variety of dating techniques, the timescales over which these processes occur.

1.2.2 Characterisation

The characterisation of lake sediments is an important aspect of any study which attempts to assess changes in sediment flux. Changes in catchment processes relating to changes in primary source material are likely to be reflected in sediment cores by way of different mineralogies as evident, for example, in X-ray diffraction and mineral magnetic studies. Pollen analysis can be a useful palaeoecological indicator. Palynology can be employed both to illustrate changes in vegetation within the catchment, and also to date sediments. Complementary work is being undertaken at the University of Liverpool to characterise the organic fraction of the sediments from each of the three sites.

1.2.3 Economics

As reported by Walling (1988), the erosion of soil particles can result in on-site problems including reductions in soil depth, fertility and, ultimately, crop productivity. Off-site problems include the sedimentation of channels and reservoirs downstream. Myers (1993) estimates that, globally, approximately 75 billion tons of soil are eroded annually, the majority of which comes from the World's croplands. Thus each decade the global soil budget is being depleted by c. 7% (Walling 1988). According to Pimental *et al.* (1976), in the past two centuries the US has lost one third of its top soil. The UNEP (1980) report suggests that soil continues to be lost from over 6 million hectares per year. As a consequence roughly 80% of the worlds agricultural land is deemed to be suffering from 'moderate to severe erosion' and a further 10% 'slight to moderate erosion' (Speth 1994). The variability in rates of erosion across the world is huge. Fournier (1960) reports that with average erosion rates of 1000 to 2000 t km^{-2} a^{-1}, losses in Asia, Africa and South America are

greatest, and losses lowest in the US and Europe where the average yield is c. 0 to 600 t km^{-2} a^{-1}. These losses from predominantly agricultural areas contrast with those associated with undisturbed forests which range from only 0.4 to 5 t km^{-2} a^{-1} (Bennett 1939).

A number of authors have attempted to calculate the financial implications of erosion in terms of both on and off-site costs. Brown (1948) estimated that the impacts of sediment erosion downstream in U.S. cost in the region of $175 million dollars annually, Walling (1988) translates this into a 1988 value of c. 1000 million dollars. Pimentel (1995) suggests that, whilst the resulting decline in soil fertility in the US costs approximately $27 billion dollars, the off-site environmental impact equates to an additional 17 billion US dollars (1992 dollars) a year. Thus, he suggests that in the U.S., the annual cost of sediment erosion resulting from agriculture is in the region of $44 billion per year, equivalent to about $100 per hectare of pastureland and cropland.

1.3 Project Aims

The main aims of this study can be summarised as follows:

1) To obtain estimates of sediment yield from three catchments in the Humber region.

2) To employ these sediment yield estimates to obtain an estimate of the flux of material to the Humber estuary from the Humber catchment.

3) To establish a database of long term sediment yields obtained from lake or reservoir sediment studies in Britain of a comparable nature to the Humber lake studies.

4) To use the database to investigate links between sediment yield and catchment characteristics.

Chapter 2

Background

2.1 Magnetics

Magnetic techniques can be employed to characterise lake sediment in a rapid and non-destructive manner. Variations in magnetic signature with depth in sediment cores can be employed to correlate cores taken from a single lake. Comparison of the magnetic characteristics of catchment sediment samples with those of lake sediment cores can also be used to assist in identifying the source of sedimenting material.

2.1.1 Magnetic Minerals

Iron is an abundant element, constituting 5% by weight of the Earth's crust (O'Neill 1985). Within the crust it occurs predominantly as oxides, hydroxides, sulphides and silicates. These minerals can be either magnetic or non-magnetic and transfer between the two magnetic states can occur as a result of a variety of surface processes such as, for example, weathering. This study involves three magnetic minerals of detrital origin, the iron oxides magnetite and haematite and the iron hydroxide goethite. These three magnetic minerals are derived from the catchment either as eroded topsoil or as primary unweathered material. The iron oxide magnetite (Fe_3O_4) is probably the most abundant magnetic mineral in sediments, soils and rocks. It is ferrimagnetic and is the strongest common natural magnetic mineral. In comparison the iron oxide haematite (Fe_2O_3) is magnetically weak. Goethite (FeOOH) is the most magnetically stable iron hydroxide. The study also involves three further magnetic minerals, the authigenic iron sulphide, greigite, bacterial magnetosomes and anthropogenically produced magnetite spherules.

2.1.2 Magnetic Parameters

A number of magnetic parameters can be employed to assist in the identification of magnetic minerals. Table 2.1 summarises the magnetic parameters employed in this study, their interpretation, the symbols used to represent them in this thesis the units used in this thesis and their interpretation. Typical magnetic properties of magnetite, haematite and goethite are given in Table 2.2.

Table 2.1. Selected magnetic parameters employed in this study and their interpretation. (After Oldfield and Maher (1984) Thompson (1986), Thompson and Oldfield (1986), Maher (1988), Oldfield (1990), Oldfield and Richardson (1990) and Higgitt *et al.* 1991).

Abbreviation	Magnetic parameter/units	Interpretation
χ	Magnetic susceptibility. ($\mu m^3 kg^{-1}$)	Approximately proportional to the ferrimagnetic mineral concentration of a sample. Can exhibit grain size dependency.
χfd	Frequency dependant susceptibility. % of low field susceptibility ($\chi fd\%$)	Indicates the presence of fine, viscous grains at the boundary between superparamagnetic (SP) and stable single domain (SSD) grains. Often characteristic of topsoil.
ARM	Anhysteretic remanent magnetisation ($mA\ m^2\ kg^{-1}$)	The magnetisation acquired in a decreasing alternating field in the presence of a weak steady field. Indicative of the concentration of fine (SSD) ferrimagnetic minerals.
χARM	Susceptibility of ARM ($\mu m^3 kg^{-1}$)	ARM divided by the steady field and hence expressed as a susceptibility.
IRM	Isothermal remanence magnetisation ($mA\ m^2\ kg^{-1}$)	The magnetization acquired in a given field. Provides a rough indication of magnetic concentration. Usually expressed as a proportion of the SIRM. This ratio can be employed to

		indicate the significance of 'soft' or 'hard' magnetic components.
SIRM	Saturation isothermal remanence magnetisation ($mA\ m^2\ kg^{-1}$)	The magnetisation acquired in a high field (usually 1T). Grain size and concentration dependent. SSD grains acquire greater remanence than multidomain (MD) grains.
ARM/χ	($kA\ m^{-1}$)	Related to variations in grain size of ferrimagnetic minerals. Small (SSD) grains tend to result in higher values.
ARM/SIRM (A/S)	(dimensionless)	Indicative of grain size variations in ferrimagnetic minerals. Higher values indicative of greater proportion of SSD grains, or interacting chains of magnetosomes.
S_{100}	IRM_{100}/SIRM (dimensionless)	The proportion of the SIRM acquired in a forward dc field of 100 mT. Can be indicative of the proportion of haematite/goethite and magnetite in a sample with higher values indicating greater magnetite dominance.
S_{20}	IRM_{20}/SIRM (dimensionless)	The proportion of the SIRM acquired in a forward dc field of 20 mT. Can be indicative of the significance of magnetically very soft material, e.g. atmospheric magnetic spherules.
Back IRM	($mA\ m^2\ kg^{-1}$)	dc demagnetisation of SIRM.

Table 2.2 Magnetic properties of magnetite, haematite and goethite.

Mineral	χ ($\mu m^3 kg^{-1}$)	ARM ($mA\ m^2\ kg^{-1}$)	SIRM ($Am^2\ kg^{-1}$)	ARM/χ ($kA\ m^{-1}$)	S_{100}	A/S
Magnetite (soft)	560	18	9	0.03	0.97	0.02
Magnetite (hard)	400	110	22	0.3	0.85	0.005
Haematite	0.6	~0.0	0.24	-	0.003	0.001
Goethite	0.7	~0.0	0.05	-	0.02	0.001

2.1.3 Early Magnetic Research

The application of magnetic techniques to the study of such processes as erosion, in the 1970s to 1990s, was facilitated by important theoretical research into the physical basis of magnetisation conducted earlier this century. For example Nagata (1942) studied a variety of magnetic characteristics of igneous rocks. These included remanent magnetisation, susceptibility, hysteresis loops and temperature dependant susceptibility. A further important development was comprehensive rock magnetic work on synthetic material. In particular Parry (1965) studied the effect of grain size on the magnetic signature of rocks and determined the coercivity of remanence, volume susceptibility and saturation remanence of dispersed magnetite powders of the range of grain sizes commonly found in natural materials.

On the basis of the high coercivity of haematite, Collinson (1968) used measurements of susceptibility in high fields, of between 300 and 1000 mT, to indicate the haematite content of sediments. As shown by Collinson (1968) magnetite and maghemite do not contribute significantly to the susceptibility and isothermal remanent signature of red beds, as small amounts of such minerals will be saturated in fields beyond 250 mT. The straight line portion of the magnetisation curve (between c. 300 and 800 mT) can thus be employed as a high field susceptibility and be used to calculate haematite concentrations.

Further research has focused on the application of measurements of isothermal remanent magnetisation to study the magnetic mineralogy of red bed sediments (Dunlop 1972). On the basis of the different coercivities of magnetite and haematite reported by Roguet (1954) (magnetite tends to have low coercivities, usually less than 100 mT whilst values for haematite can often be between 2000 - 3000 mT), the coercivity spectra can be used to identify magnetite and haematite in red sandstones and clays. Isothermal remanence curves for red bed samples illustrate the significance of the hard (haematite) component in sandstones. In contrast limestones had no increase in remanence above 1000 mT indicating the absence of a hard

haematite or goethite component. Dunlop (1972) found the argillite samples to be characterised by both a considerable soft and hard component and hence a mixed magnetic mineralogy.

Following on from Le Borgne's work (1955), Mullins and Tite (1973) carried out the first comprehensive mineral magnetic studies of soils in the 1970s. In particular they employed soil samples known to contain single domain (SD) grains of magnetite or maghemite and samples of artificially prepared SD size magnetite to investigate frequency dependant susceptibility. Mullins and Tite (1973) found that susceptibility varied linearly with the logarithm of frequency and that frequency dependence was strongest for ultrafine magnetic grains common in many topsoils. Samples of multi-domain (MD) magnetite, when subjected to comparative measurements in contrast, did not exhibit any significant frequency dependent behavior.

2.1.4 The Origin of the Magnetic Signature in Lake Sediments

The mineral magnetic study of lake sediments from Lough Neagh, Northern Ireland (Thompson *et al.* 1975) indicated that the magnetic signature resulted from the input of detrital geological material. However, research undertaken since 1975 has illustrated that the magnetic characteristics of lake sediments may not result exclusively from the input of primary ferrimagnetic minerals of geological origin. Secondary magnetic minerals produced in the soil (Le Borgne 1955) can dominate the magnetic characteristics of lake sediments (Higgitt 1985). The magnetic signature can also be influenced by diagenesis, authigenesis, bacterial magnetite, dissolution and the input of anthropogenic magnetic spherules. The following text briefly reviews the evidence for each of these potential sources and Table 2.3 summarises selected magnetic characteristics which can be employed to assist in the identification of each source.

2.1.4.1 Geological

Using a combination of magnetic, thermomagnetic, chemical, x-ray and electron microprobe analyses Thompson *et al.* (1975) found the susceptibility of Holocene sediments in Lough Neagh, Northern Ireland to be a function of detrital titanomagnetite. All samples produced similar IRM acquisition curves, reaching saturation by 1 T, and were indicative of the presence of titanomagnetite. The alternating field demagnetisation of IRM similarly suggested the remanence carrier to be magnetite. A positive linear correlation between initial susceptibility and IRM was observed in samples taken from a range of depths in the sediment and different areas of the lake. Thompson *et al.* suggested that either the IRM was produced by just one magnetic mineral or the proportions of magnetic minerals remained constant downcore. Thompson *et al.* propose that the slope of the linear relationship between susceptibility and IRM indicated that titanomagnetite was the dominant magnetic mineral. With a Curie point of 580 °C the magnetic extract from the gyttja is dominated by magnetite-rich titanomagnetite. Thompson *et al.* also note that the composition of the gyttja magnetic extract is similar to those observed in basaltic titanomagnetite grains. X-ray and electron probe analyses undertaken on magnetic extract from Lough Neagh samples showed grains to be characterised by a high iron content, a titanium content in excess of 5% by weight, aluminium and manganese contents of c. 1% and traces of magnesium and chromium. The authors conclude that the detrital titanomagnetite producing the magnetic susceptibility in Lough Neagh sediment originates from Tertiary basalts in the Lough Neagh catchment.

2.1.4.2 Topsoil

The production of maghemite and magnetite, observed at or near the soil surface (Mullins 1977), have been found to contribute significantly to the magnetic signature

of lake sediments, particularly in sites characterised by magnetically weak bedrock. Studies undertaken at Jackmoor Brook (Oldfield *et al.* 1979) and at the Petit Lac d'Annecy (Higgitt 1985) have reported significantly higher magnetic concentrations in lake and river sediments than those found in the parent geological material. At sites where the primary ferrimagnetic minerals cannot account for the high concentrations observed in the sediment samples, and where there is a dependence of susceptibility on frequency, the magnetic signature has been attributed to high concentrations of secondary magnetic oxides observed in the surface soils.

2.1.4.3 Bacteria

Blakemore (1975) isolated iron containing bacteria from marine sediment which displayed a preferred orientation in weak magnetic fields. Working on magnetotactic spirillum cultured from freshwater sediment Frankel *et al.* (1979) used Mossbauer spectroscopic analysis to demonstrate the presence of iron, in the form of magnetite, in the magnetotactic cells. More recently studies by Moskowitz *et al.* (1993) have indicated that the acquisition of remanent magnetisation in fine-grained sediment can be attributed to magnetite biomineralisation (by micro-organisms). Long chains of magnetosomes synthesised by magnetotactic bacteria have been identified in a wide variety of environments including marine (Hesse 1994) and freshwater (Vali *et al.* 1987, Snowball 1994) sediments. Figure 2.1 illustrates a chain of magnetosomes identified in sediment from Hornsea Mere. The formation of bacterial chains is believed to result in an energetically favourable arrangement of magnetosomes within the cell. Moskowitz *et al.* (1993) propose that the chains acquire a post depositional remanent magnetisation following the deaths of the cells and incorporation into the sediment.

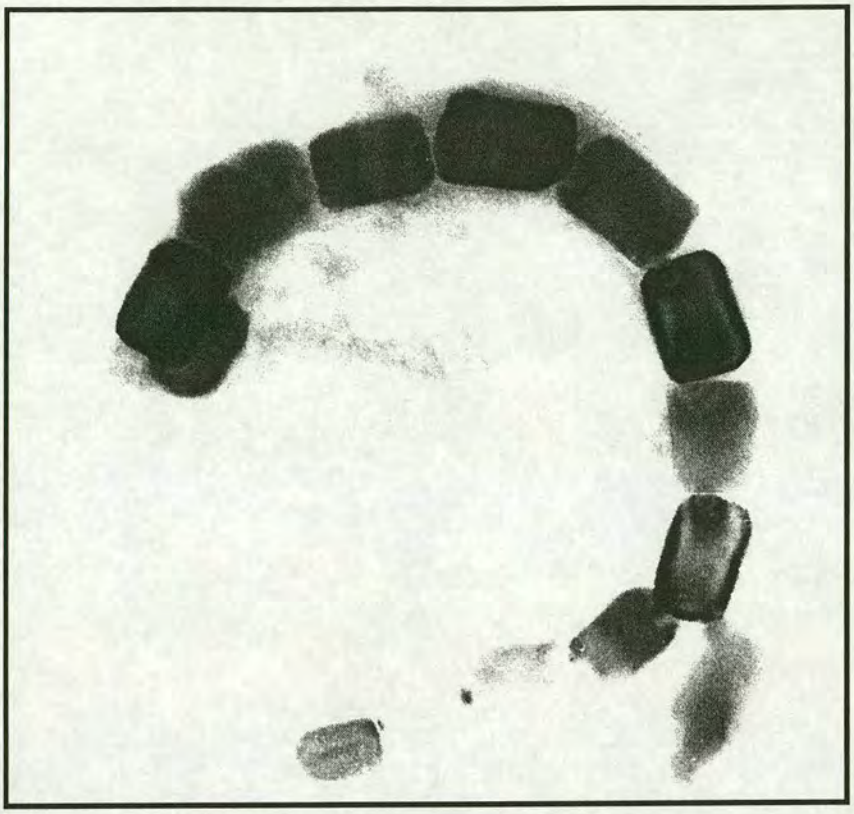

Scale 180 000:1

Figure 2.1 A transmitting electron microscopy image of a chain of bacterial magnetosome cells extracted from sediment at Hornsea Mere by M. Hanzlik (Institut für Allgemeine und Angewandte Geophysik und Geophysikalisches Observatorium der Ludwig-Maximilians-Universität München).

The occurrence of bacterial magnetite can override any detrital magnetic signature, consequently the identification of bacterial magnetosomes is important before the magnetic signature attributable to fine grained magnetite can be employed in source provenance studies (Van der Post *el al.* 1997). Amongst others, Moskowitz *et al.* (1993) and Oldfield (1994), have proposed magnetic methods which can be employed to infer the presence of bacterial magnetosomes. Oldfield (1994) suggests that where the magnetic properties of the sediment are controlled by the presence of magnetite/maghaemite, and the measurements of frequency dependant susceptibility and χARM/SIRM ratio implies a grain size indicative of stable single domain grains or smaller, then the ratios χARM/χ and χARM/χfd can be employed to distinguish fine-grained magnetite of detrital origin from that of bacterial origin. Values of χARM/χ in excess of 40 and χARM/χfd greater than 1000 correspond to samples

expected to contain bacterial magnetite. Oldfield (pers. comm.) reports that the χARM/SIRM ratio can be employed as a proxy indicator of the strength of the bacterial magnetosome component. Values in excess of 2 x 10^{-3} metres per amp (m/A) have often been reported for samples with a high concentration of bacterial magnetite. However a number of authors (Dunlop 1986, Cisowski 1981) have observed high ARM/SIRM ratios (up to c. 0.20) in rocks and synthetic analogs composed of non-interacting SD particles and thus high ARM/SIRM quotients alone are not exclusive to bacterial magnetosomes. Alongside remanence ratios, bi-plots employing a stability parameter (e.g. ARM_{40}/SARM, or S_{100}) can assist in the identification of bacterial magnetite. Confident identification of the presence, and to some degree the significance of, magnetotactic bacteria requires magnetic extraction techniques coupled with transmitting electron microscopy (TEM) studies. TEM images also provide information on the preservation state of chains of magnetotactic bacteria.

2.1.4.4 Atmospheric

A number of studies have illustrated the significance of atmospheric loadings of magnetic minerals into the upper levels of lake sediments (Anderson *et al.* 1988). Oldfield *et al.* (1981) and Richardson (1986) has documented increases in atmospheric pollution of this kind in peat. Figure 2.2 shows increased magnetic deposition over the past two centuries at a site in Finland (Oldfield *et al.* 1981). The pollutants take the form of spherules produced from power station fly-ash, and are most clearly detected where the background magnetic signature resulting from the input of detrital material is low. The atmospheric spherules are predominantly soft multidomain magnetite and can thus be identified using a ratio such as S_{20}.

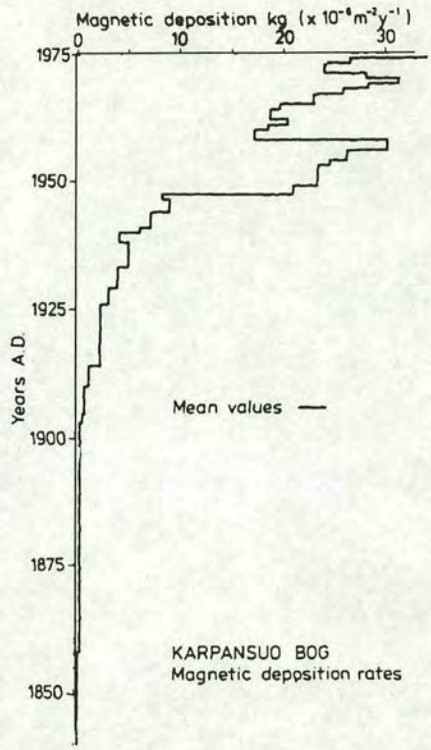

Figure 2.2 A record of atmospheric magnetic deposition in Karpansuo Bog, Finland. Dates determined using moss increment counting, annual magnetite deposition estimated using SIRM values (from Oldfield *et al.* 1981). The figure illustrates a gradual increase in magnetic deposition in the period c.1900-1945 followed by a sudden rapid increase in deposition at a date of c. 1945. Since c. 1945 magnetic deposition rates have varied between 18 and 35 kg x 10^{-6} m^{-2} y^{-1}.

2.1.4.5 Diagenetic and Authigenic Magnetic Minerals.

Hilton and Lishman (1985) and Hilton *et al.* (1986) suggest that the magnetic mineral signature recorded in organic rich sediments of productive lakes may result primarily from magnetic minerals of diagenetic or authigenic origin. Diagenetic magnetic minerals are those magnetic minerals produced from existing magnetic or non-magnetic minerals in the sediment. Hilton and Lishman (1985) noted that the intensity of magnetic susceptibility in sediment samples from Esthwaite Water was lowered when the samples were allowed to oxidise. A number of further studies including that undertaken by Anderson and Rippey (1988) at Lough Auber, Northern

Ireland have concluded that diagenetic changes are controlled by the eH (oxidising potential) and pH of the sediment pore water.

Authigenic magnetic minerals are produced as a result of chemical or biogenic processes occuring within the sediment. Snowball and Thompson (1988) and Hilton (1990) have demonstrated the presence of the ferrimagnetic sulphide, greigite (Fe_3S_4), in high concentrations in sediments from Loch Lomond and Esthwaite Water respectively. High concentrations of greigite in sediments can be inferred from a high SIRM/χ ratio, greater than 60 kA m^{-1}, where a significant hard remanence component indicative of a haematite or goethite is absent. The presence of greigite in sediments also tends to result in steep remanence acquisition and loss curves in fields typically between 50 and 80 mT (Snowball and Thompson 1988).

2.1.4.6 Dissolution

Canfield and Berner (1987) studied variations in concentrations of magnetite and hydrogen sulphide (H_2S) with depth in sediments from Long Island Sound. The dissolution of magnetite during burial was observed and the rate of dissolution was found to be proportional to the concentration of dissolved sulphide in the pore waters. Using a scanning electron microscope Canfield and Berner (1987) observed that where magnetite is in contact with concentrations of H_2S in excess of 1 millimolar for long time periods (several hundred years) magnetite dissolution can be accompanied by pyrite replacement. Anderson and Rippey (1988) has similarly reported the diagenetic dissolution of magnetite in organic rich, strongly reduced sediments typically found in hyper-eutrophic lakes. Snowball (1993) reports that the magnetic signature in lake sediments affected by magnetite dissolution can be employed to record palaeoredox conditions and indicate episodes of climate change. Working on sediment cores taken from lakes in the the Kårsa valley, Sweden, Snowball (1993) proposed that periods of low sediment accumulation in the Holocene climate optimum combined with higher organic carbon resulted in strongly

reducing conditions and ultimately the dissolution of magnetite. In contrast magnetite is preserved during periods of higher sedimentation rates and lower organic carbon contents when the glaciers reformed.

The process of dissolution diagenesis can often be detected within the magnetic signature by noting, for example, steep declines in those parameters indicative of concentration alongside corresponding declines in the ratios ARM/SIRM and ARM/χ. Reductions in these ratios indicate the preferential removal of fine grains. Magnetite appears to be more susceptible to dissolution than haematite and goethite, therefore the ratio between hard and soft magnetic remanence can similarly be employed similarly to indicate the action of diagenesis (Oldfield, pers. comm).

2.1.4.7 A Summary of the Characteristic Magnetic Properties of Different Source Materials

Table 2.3. A summary of selected magnetic characteristics employed to identify the source of magnetic signature.

Geological material, heavy mineral concentrations		
Magnetite	ARM/χ	0.1 kA m^{-1}
	ARM/SIRM	0.005 (SD) - 0.02 (MD)
	Soft S_{100}	0.85 (SD) - 0.97 (MD)
Haematite/Goethite	ARM/χ	0 kA m^{-1}
	ARM/SIRM	0
	Hard S_{100}	0.06-0.3
Goethite	Hard IRM_{2T}/IRM_{4T}	<0.75
	IRM_{4T}/χ	<200 kA m^{-1}
Top soil:	High χarm/SIRM	0.5-1.8 x 10^{-3} m/A
	High χfd	>5%

Magnetotactic bacteria:	High ARMs	1 mA m^2kg^{-1}
	High ARM/SIRM	0.2-0.3.
Anthropogenic input:	Very soft, high S_{20}	c. 0.15.
Authigenic iron sulphides:	SIRM/χ	>60 kA m^{-1}.

Dissolution diagenesis: Steep declines in concentration indicators (χ, ARM, IRM) and parallel declines in the ARM/χ and ARM/SIRM quotients.

2.2 Catchment Studies of Sediment Erosion - Previous Research.

By World standards sediment yield in Britain is generally low (Moore and Newson 1986). The low yields can be attributed to low peak rainfall intensities (Rodda 1970) and relatively dense vegetation and crop cover (Fleming 1969). In Britain bedload sediment tends to be greatest in bare upland gullies and suspended loads highest in areas of bare lowland farming i.e. during cultivation periods prior to crop growth (Moore and Newson 1986). Sediment transport occurs largely as a result of channelized, as opposed to sheet, flow in these upland gully and bare lowland agricultural sites (Moore and Newson 1986). The development of artificial drainage channels associated with farming and forestry practises in upland catchments has, in recent times, given rise to significant increases in rates of erosion. McManus (1986) notes that in comparison to many other countries, little research has been undertaken in Britain in terms of the development and application of successful erosion measurement and prediction techniques.

2.2.1 River Sediment Discharge Data

A variety of authors have employed river sediment discharge data to calculate average erosion rates within the contributing catchment area. The first recorded

attempts were made by Geikie (1868) who employed average sediment discharge data from the Mississippi to relate water discharge in a variety of British rivers to sediment discharge and thus calculate the solutional lowering of a variety of catchments including the following:

River	Drainage basin lowering (mm a^{-1})
Thames	0.03
Tay	0.17
Forth	0.10
Boyne	0.05

An interval of nearly 100 years elapsed before further work was undertaken. Hall (1967) determined the suspended, bed and solution loads of the River Tyne and Derwent in Northumberland. Employing an in-situ sediment density of 1.59 g cm^{-3} Hall calculated surface lowering rates of 0.068 mm a^{-1} and 0.117 mm a^{-1} in two sub-catchments draining into the Tyne. Sediment fluxes in the Plynlimon catchment in Wales have been studied in detail for the past 20 years and a six fold increase in bedload yield has been reported as a result of digging open forest ditches (Moore and Newson 1986). In an attempt to determine the loss of sediment to the North Sea by way of the Forth and Tay estuaries McManus (1986) studied erosion within catchments in the South Grampian Highlands between 1973 and 1984. Using figures for years with similar average river discharge conditions McManus (1986) calculated total sediment yield from catchments above gauging stations in the Forth and Tay River systems (Table 2.4).

Table 2.4 Sediment yield determined from sediment discharge data within catchments in the Forth and Tay River systems (McManus 1986).

River	Site	Years	Area (km^2)	Sediment yield ($t\ km^{-2}\ a^{-1}$)
Earn	Kinkell	1973-74	591	41.8-131.5
Earn	Forteviot	1973-74	782	67.3-128.8
Almond	Almondbank	1972-75	175	17.3-64.9
Lvon	Comrie Bridge	1972-75	391	24.4-59.7
Tay	Pitnacree	1972-75	1150	26.5-80.7
Tay	Caputh	1972-75	3212	43.1-201.7
Tummel	Ballinluig	1972-75	1720	26.0-104.4
Isla	Forter	1975-80	73	12.2-17.3
Isla	Wester Cardean	1975-80	367	39.3-106.9
Forth	Gargunnock	1975-80	397	163.8-296.1
Teith	Bridge of Teith	1975-80	518	8.9-12.3
Ardoch B	Doune Castle	1976-80	48	11.0-18.3
Allan W	Kinbuck	1975-80	161	10.6-19.7

Table 2.4 illustrates (i) the extent of variations in sediment flux within each catchment area during the monitoring period and (ii) the wide range of sediment yield values found between sites. The large variations in sediment yields observed over a time period of just a few years illustrate the need for sediment flux records which span longer timescales in order to determine long term trends, as opposed to short term variability. Appendix A summarises a range of suspended sediment loads determined for a variety of British catchments. Suspended sediment loads are shown to vary from less than 1 $t\ km^{-2}\ a^{-1}$ to nearly 500 $t\ km^{-2}\ a^{-1}$.

Studies of reservoir sedimentation have been employed to estimate sediment yield for a variety of catchments in the UK. Following the draining of the Strines reservoir in Yorkshire in 1956 Young (1958) determined the volume of material deposited in the 87 years between construction and drainage and found this an annual lowering of the catchment surface by 0.005 inches (which is equivalent to a sediment flux of 52.5 $t\ km^{-2}\ a^{-1}$). Kirkby (1967) studied erosion in the Water of Deugh drainage basin in Galloway. By measuring the volume of material accumulated behind a dam an

erosion rate equivalent to 42.4 t km^{-2} a^{-1} was found for the period 1937-1960. Butcher *et al.* (1993) employed echo sounding surveys to establish changes in volume of 28 reservoirs in the southern Pennines since their construction. In addition the density and organic content of sediment samples obtained from each reservoir was determined and the data used to calculate sediment yields ranging between 2.9 t km^{-2} a^{-1} and 289.46 t km^{-2} a^{-1}. Appendix B summarises records of sediment yield obtained from a range of reservoir sediment studies in Britain. The range of sediment yields reported is vast, though an average yield of between 30 t km^{-2} a^{-1} and 60 t km^{-2} a^{-1} can be taken as representative for Britain.

2.2.2 Lake Sediment Cores

During the past two decades research on longer term sediment records, both in terms of quantifying sediment yield and investigating the source areas of sedimenting material, has been undertaken using lake sediments to provide an account of changes in sediment yields and sediment processes in a historical context within catchments. Such studies have developed from the drainage basin approach (Smith 1969, Omernik and Griffith 1991) in which the area of study is defined by a physical boundary (the watershed) separating precipitation draining into one catchment from another. The drainage basin therefore provides a defined unit in which to study hydrological, geomorphological, chemical or biological processes. The lake-watershed ecosystem framework (Borman and Likens 1969, Oldfield 1977 and O'Sullivan 1979) has developed this approach further. Coupling observations and experiments of the contemporary system to lake sediment based reconstructions of long term changes, the lake-watershed ecosystems can provide an ideal framework to study ecological and physiographic changes over varying timescales (Oldfield 1977). As Dearing *et al.* (1990) note, catchment based studies of sediment movement can be employed to overcome several difficulties associated with small plot studies of sediment erosion. The first of these difficulties relates to the time periods studied. Whilst significant variations in yield and source may be observed on a short time

scale it is difficult to be sure how they compare with longer term trends and whether they actually record specific thresholds and indeed responses. Secondly, catchment studies avoid the problems associated with identifying the precise source area of sedimenting material in small scale studies. Catchment areas generally have well defined boundaries and thus the source of eroding material is limited to within this boundary.

Davis (1976) provided one of the first examples of the application of lake sediment cores in the reconstruction of sediment yields with time. Her study was undertaken at Frains Lake, Michigan, North America. She compared rates of sediment accumulation under forest in primeval times with those under farmland in the 146 years after woodland clearance (Figure 2.3). The chronology of sedimentation was determined using radiocarbon dates and pollen analyses. The sediment deposited since the forest clearance phase was identified by the characteristic increase in the proportion of pollen from agricultural weeds and accompanying decrease in tree pollen. A radiocarbon dated core obtained from the centre of the lake indicated that rates of sediment accumulation were found to be relatively uniform during the Holocene period with an average sedimentation rate of 0.67 mm per year (Kerfoot 1974). Similarly sedimentation rates of 0.7 mm per year were calculated for a core from the north shore for the pre-settlement period. Thus the accumulation rate at the marginal site is very similar to that at the centre of the lake. On the basis of these two cores a sediment yield of 9 t km^{-2} a^{-1}, prior to human settlement, was calculated. After settlement yields increased dramatically by a factor of approximately ten. Post-settlement sediment yield estimates were calculated at the adjacent Murray lake. Yields of between 10 - 15 t km^{-2} a^{-1} at Murray Lake compare closely with those obtained from Frains Lake.

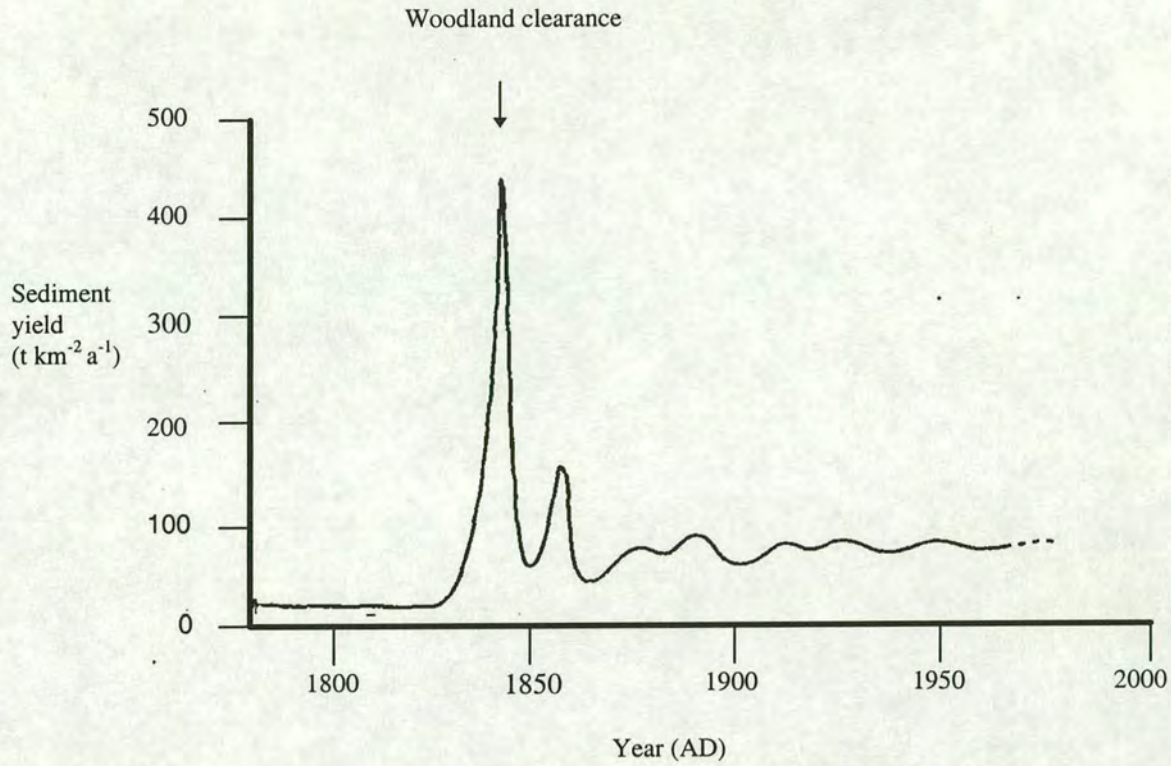

Figure 2.3 A lake sediment based study of changes in sediment yield with time at Frains Lake, Michigan, North America (from Davis 1979). A very marked peak in sediment yield occurs immediately following a phase of forest clearance.

Pennington (1978) employed pollen analysis techniques together with ^{14}C dating to determine land use and erosion rate changes associated with the impact of human activity on catchments in the English Lakes. She observed a decrease in the organic content of sediments since c. 5000 BP and associated it with the destruction of the primary forest. Pennington (1978) also found that at Barfield Tarn in Cumbria the rate of sedimentation since 5000 BP has increased by a factor of six. Increased rates of sediment accumulation were also recorded after 2500 BP. She believes this latter increase to also result from further periods of tree clearance. A similar pattern in sediment accumulation rates to that of Barfield has been observed in sediments taken from Ennerdale water. Here a rapid increase in sediment accumulation rate is found for material rich in *Calluna* (heather) pollen. Once again a link between lake sediment accumulation and deforestation is found as the *Callunetum* is believed to

have developed on the upland catchment following the period of prehistoric deforestation. Pennington (1981) also noted that in lake sediments from Blelham Tarn an increase in deposition rates is recorded post c. 2500 B.P. Again the change in accumulation rate correlates with pollen evidence for deforestation. Thus there are numerous examples of linkages between land-use, erosion and lake sediment accumulation. However rather few such linkages have been studied in a quantitative way.

2.2.3 The Application of Magnetic Methods to Catchment Studies: A History of Developments

2.2.3.1 Pre 1970

The development of mineral magnetic techniques have contributed significantly to studies of erosion during the post-glacial period. Le Borgne (1955, 1960) undertook studies linking surface processes to a characteristic magnetic signature. His study of the magnetism of top soil preceded research by Radhakrishnamurty *et al.* (1968), which illustrated how episodes of tephra deposition could be recorded from magnetic susceptibility records of deep sea stratigraphy.

2.2.3.2 The 1970s

In the 1970s the development of magnetic methods in catchment studies evolved from the palaeomagnetic research of Mackereth (1971) and Thompson (1973) which concentrated on establishing proxy sedimentation timescales in Windermere and Lough Neagh. Thompson (1973) and Thompson *et al.* (1975) reported that cores could be correlated using variations in magnetic susceptibility with depth, and that these were in agreement with those correlations obtained when measurements of

magnetic declination on the same samples were employed. Figure 2.4 illustrates the susceptibility based correlation of four cores taken from Antrim Bay, Lough Neagh. Thompson *et al.* (1975) thus proposed that the use of whole core susceptibility scanning provided a rapid and non-destructive method of multiple core correlation. The magnetic signature obtained by measuring both natural and laboratory induced remanence parameters in this initial study was attributed to the inwash of detrital catchment derived minerals into the sediment (cf Section 2.1.4.1). The research showed magnetic susceptibility to be related to the amount of allochthonous mineral material derived from the catchment as a result of erosion of substrates and soils. Comparison of profiles of *Gramineae* (grass) and the agricultural weed *Plantago lanceolata* (ribwort plantain) with the susceptibility profile provided evidence of the relationship between erosion and susceptibility (Thompson *et al.* 1975). The authors proposed that pollen diagrams are a good indicator of forest clearance and the extension of farming. Increases in soil erosion between c. 3000 - 200 BP (mid-to-late Littletonian period) have been attributed to the effects of forest clearance within the Lough Neagh catchment.

Thompson *et al.* (1975) also noted that peaks in total iron content in cores from Lough Neagh and Lough Fea showed a degree of correlation with peaks in magnetic susceptibility. This correlation is attributed to the significance that detrital magnetite makes to the iron content of the sediments at these horizons. However the imperfect correlation between total iron content and magnetic susceptibility was interpreted as indicating that magnetite does not usually dominate the iron content of lake sediments.

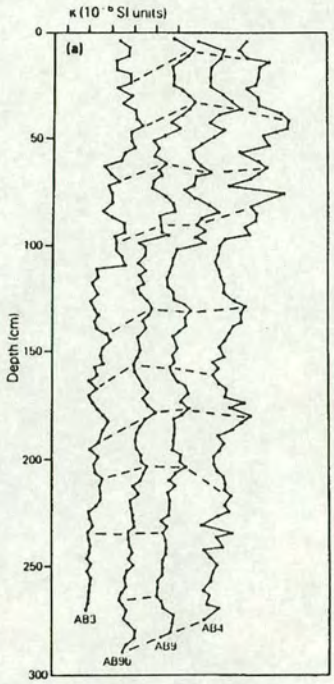

Figure 2.4 Correlation of four cores from Antrim Bay, Lough Neagh, Northern Ireland using magnetic susceptibility (from Thompson and Oldfield 1986).

The initial study of post glacial sediments in Lough Neagh provided the first example of the application of magnetic studies to erosion research. The study implied that mineral magnetic measurements could be employed to both assist in the improvement of quantitative accounts of sedimentation and also to link variations in sedimentation rates to catchment processes.

2.2.3.3 Post 1979

The first study which employed magnetic techniques to correlate cores and determine sediment input for specific periods (on a whole lake basin scale) was undertaken by Bloemendal (1979) at Llyn Goddionduon, North Wales. A grid of over 100 one-metre Mackereth cores was obtained, and the cores correlated using volume susceptibility scans. Specific horizons were dated using a combination of ^{14}C and ^{137}Cs. Sediment yields were calculated for three specific time periods (Appendix C). The most significant changes in mineral magnetic properties with depth in the cores were interpreted as reflecting changes in water level and a forest fire within the catchment. As illustrated in Figure 2.5 sediment deposition is not uniform across the lake basin. The effect of sediment focusing (Davis and Ford 1982) is clearly evident with some areas of the lake basin receiving particularly high volumes of sediment and other areas particularly low. Figure 2.5 also indicates the variability in sediment distribution with time. This multi-core approach to lake basin research thus allowed a detailed reconstruction of accounts of temporal and spatial changes in sediment deposition to be determined. Magnetic techniques have been employed in a variety of studies which have attempted to reconstruct records of sediment yield and sediment source with time. Appendix C summarises sediment yield results obtained from a number of lake sediment studies in British catchments. Sediment yields are shown to vary from just 2 t km^{-2} a^{-1} in the early Holocene at Llyn Geirionydd, North Wales (Snowball and Thompson 1992) to 421 t km^{-2} a^{-1} at Loe Pool, Cornwall (O'Sullivan 1982). The particularly high sediment yield at Loe Pool coincides with a period of intensive mining activity in the Loe Pool catchment. At the majority of sites an increase in sediment yields with time is observed.

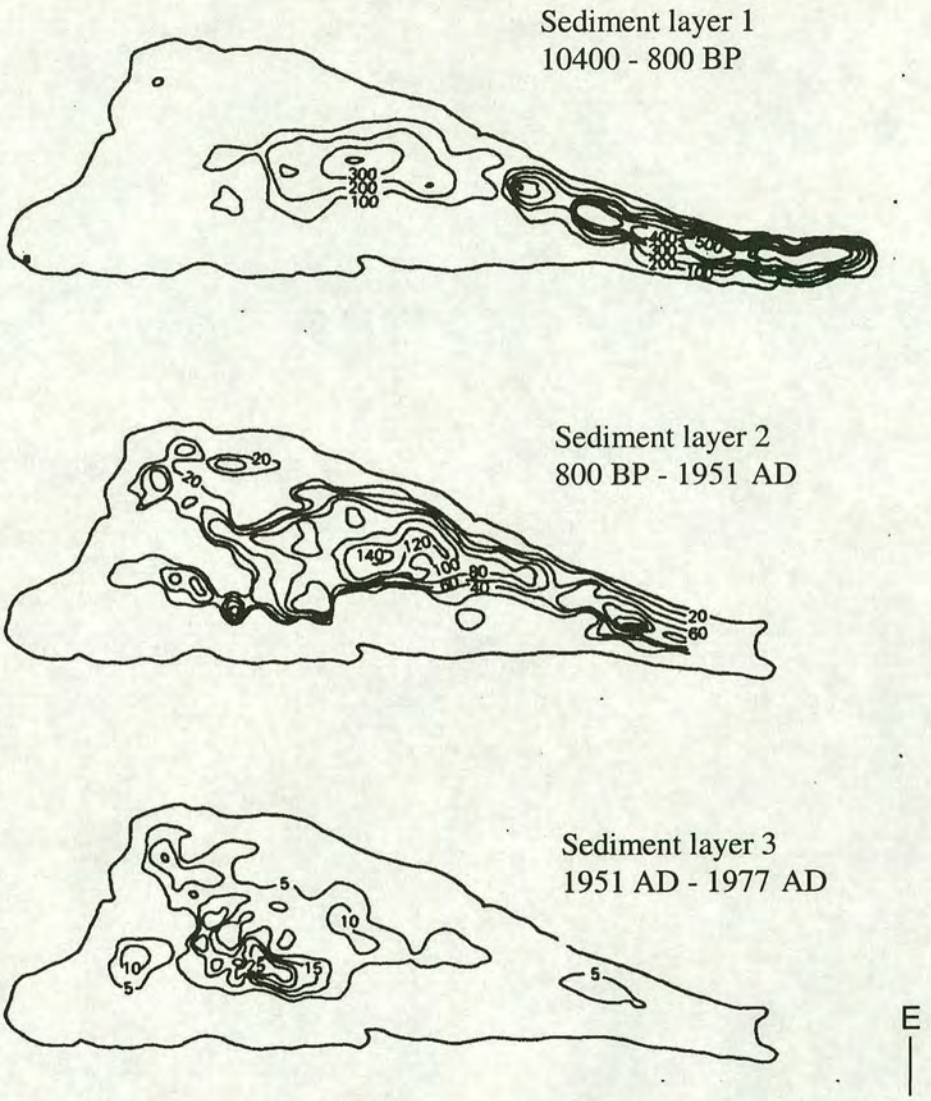

Figure 2.5 Changes in the pattern of sediment acccumulation (cm) with time in Llyn Goddionduon, North Wales (from Thompson and Oldfield 1986, after Bloemendal 1982). In sediment layer 1 sediment accumulation is greatest in the narrow southern part of the lake, in sediment layers 2 and 3 accumulation is greatest in the centre of the lake.

Thompson and Morton (1979), working on sediments obtained from Loch Lomond, noted that susceptibility measurements correlated with particle size distribution. Peaks and troughs in susceptibility were shown to correlate with horizons of finer and coarser particles respectively (Figure 2.6). The authors concluded that susceptibilty measurements of lake sediment cores could be employed to determine a

lake sediment lithostratigraphy. Thompson and Morton (1979) reported that particle size also controls other magnetic parameters, for example SIRM. As in the Lough Neagh sediments (Thompson *et al.* 1975) a link between high percentages of non-arboreal pollen (for example *Gramineae, Plantago lanceolata* and *Calluna*) and high susceptibility values was observed. In Loch Lomond magnetic concentration is linked with an increase in fine particle size material, presumably resulting from an increase in erosion of fine particles from surface materials.

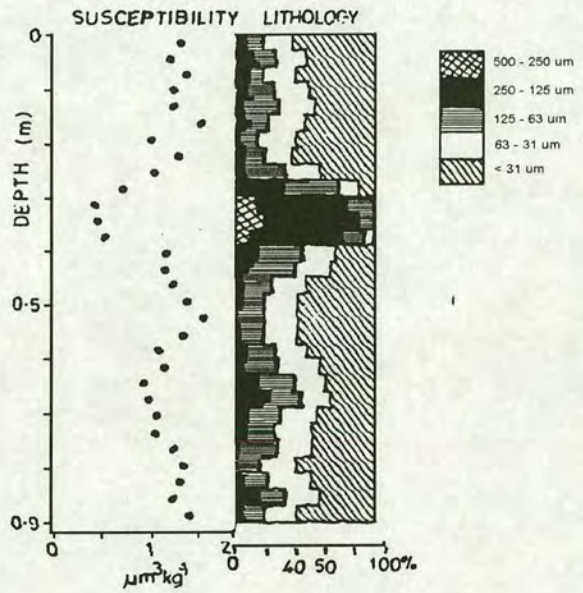

Figure 2.6 A comparison of susceptibility with particle size in a core from Loch Lomond (from Thompson and Morton 1979). The susceptibility minima at a depth of c. 0.3-0.4 m correlates with a very high proportion of coarse grained sediment of 125-500 μm. Two other less prominent troughs in susceptibility at depths of c. 0.05 and 0.6-0.7 m also correlate with high proportions of coarse sediment of between 125 and 250 μm.

Since 1979 a number of studies have employed magnetic measurements in an attempt to identify the source of sedimenting material. In their study of the Jackmoor Brook catchment, Devon, Oldfield *et al.* (1979) compared measurements of the magnetic properties of suspended river sediments with those of potential sources including bank-side material, parent bedrock material and top soil. As illustrated in Table 2.5

magnetic enhancement of the topsoil over and above that of bedrock was observed. Using back IRM curves measured on catchment and bulk suspended sediment samples, the authors concluded that the most significant source of the suspended sediments is the catchment surface material.

.

Table 2.5 Magnetic characteristics of suspended sediments and potential sediment sources in the Jackmoor Brook catchment (after Oldfield et al., 1979).

	χ ($\mu m^3 kg^{-1}$)	SIRM ($mA\ m^2\ kg^{-1}$)	SIRM/χ ($kA\ m^{-1}$)	$-IRM_{100}$/SIRM
Woodland topsoil	>2.5	>10	~4	1
Well-drained cultivated topsoil	0.2-2	1-10	5-7	0.28-0.8
Poorly drained and gleyed soils	0.06-0.4	0.5-3.5	~10	~0.4
Parent material	<0.1	1-2	>10	-0.8 to -0.6
Suspended sediments	0.25-0.75	2.5-9	~10	0.06-0.4

Oldfield *et al.'s* (1979) study also developed the concept of magnetic fingerprinting further by illustrating how the composition of suspended sediment changes during the course of a storm. Initially the sediment was dominated by top soil but as the storm progressed the importance of channel derived material increased. Whilst noting that the Jackmoor brook site was ideal for such a study because of (i) the absence of glacial drift material, (ii) the homogeneous nature of the parent material and, (iii) the easily distinguishable top soil and substrate material, the authors suggested that the magnetic fingerprinting approach could be adopted elsewhere in catchments with other geological, hydrological and land-use characteristics.

More recently Oldfield *et al.* (1985) and Thompson and Oldfield (1986) reported on a study undertaken in the Rhode River Watershed. In Rhode River they found that soil horizons could be characterised by their mineral magnetic properties. The unweathered parent materials were characterised by low SIRM and low χfd% values. In contrast weathered subsoils had intermediate magnetic values, while high values were recorded in the surface soils. Four magnetic components were identified within

the soils and subsoils. These were a primary ferrimagnetic component, a secondary antiferromagnetic component, a secondary ferrimagnetic component and a paramagnetic component. By employing SIRM and χfd measurements the origin of both suspended sediments (within streams and estuarine waters) and the sediments deposited within the estuary were determined. Oldfield *et al.* (1979) distinguished material derived from soil and sub-soil and also, using magnetic measurements undertaken on specific particle size splits, attributed the source of the sediment to specific soil horizons .

Oldfield (pers.comm.) suggests that three conditions need to be met in order to use magnetic fingerprinting to identify sediment sources. Firstly, a degree of weathering and soil formation needs to have occurred. Secondly, the iron oxides in the potentially eroding material must be stable over a considerably longer time period than that over which erosion and sedimentation rates and processes are being studied. Thirdly, the magnetic properties of eroded sediment must be unaltered by diagenesis. Thus for magnetic measurements to be applicable in sediment source tracing, the magnetic properties employed must be indicative of specific sources and also the source materials must account for a significant portion of the magnetism of the sediment under study.

Another approach using magnetism in the study of the flux of material through catchments is through the use of sediment traps. Dearing and Flower (1982) reported on the collection of contemporary sediment samples using sediment traps in Lough Neagh. They made susceptibility measurements on 98 soil samples and 8 stream bedload samples collected within the Lough Neagh catchment and they noted a strong positive correlation between rainfall and the susceptibility of sedimenting material collected in a trap in Antrim Bay. They attributed the positive correlation to the transport of greater concentrations of silt during high river levels following heavy rainfall. The correlation between susceptibility and rainfall was not observed at a second sediment trapping site which, unlike the Antrim Bay trap was a long way from any large inflowing rivers. Dearing and Flower (1982) suggested that most of

the silt entering the second trap does so as redeposited sediment and thus the correlation was not observed. The authors propose that the high susceptibility of material from the Antrim Bay traps indicates erosion of channel banks. The banks provide a source of silt material which is transported by elevated stream flows after heavy rain. Upon this understanding Dearing and Flower (1982) have reassessed the susceptibility signature recorded in a 3 m core from Antrim Bay (Thompson *et al.* 1975) and suggest that the 3 m susceptibility record indicates a gradual increase in channel erosion intensity within the Lough Neagh catchment since 5000 BP. High levels of channel bank erosion occurring in the period c. AD 1500-1700 have been linked to the large scale woodland clearance within Ulster during this time (McCraken, 1944, 1947, 1959 *in* Battarbee 1978).

Magnetic techniques have frequently been applied to assist in identifying the source of eroded material in lake sediment studies. In a study of Lake Bussjösjön, Sweden, Dearing *et al.* (1990) employed magnetic techniques to construct a record of sediment yield and determine changes in the relative amounts of topsoil and subsoil/channel bank sediment through the Holocene period. Dearing *et al.* (1990) employ the characteristically high HIRM values to identify detrital haematite and goethite present in the unweathered parent material. The presence of secondary ferrimagnetic minerals (c.f. Dearing *et al.* 1986) within the catchment soils (ultrafine magnetite and maghemite) can be observed using χfd. Therefore the ratio of HIRM/χfd can be employed to distinguish material derived from top soils with that derived from unweathered parent material. Cores representing sediment deposited in the period 1700 - 1950 have been interpreted in terms of differing proportions of eroded top soil and parent material using the HIRM/χfd ratio. Values of the HIRM/χfd ratio before c. 1900 show minimal variation (Figure 2.7) and with a mean of c. 10 kA m^{-1} the values are typical of fine grained topsoil. Since 1900 values have fluctuated more significantly between c. 7 kA m^{-1} (1985) and 295 kA m^{-1} with higher values indicating the erosion of unweathered subsoil. Significant subsoil peaks have been dated to c. 1920, 1945, 1955-1960, 1970 and 1975. In the twentieth century the

sediment record indicates that top soil has dominated the composition of the sediments in the periods 1925-40, 1950-1955 and 1980-1985.

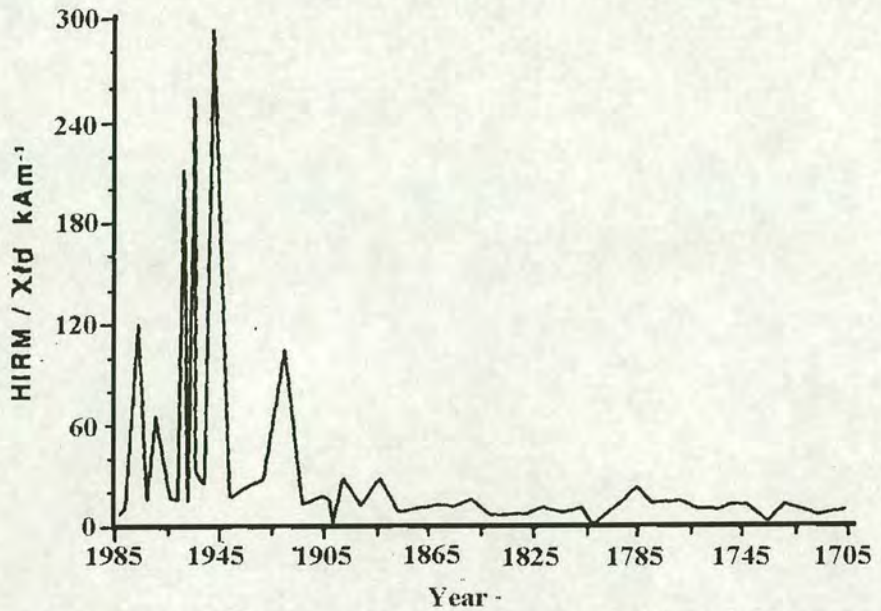

Figure 2.7 Changes in the proportion of topsoil and parent material at Lake Bussjösjön, Sweden since 1700. Higher HIRM/χfd values are characteristic of subsoil and lower values of topsoil (from Dearing *et al.* 1990). In the period 1705 - 1900 the magnetic record indicates that topsoil is the dominant source of eroding material. The figure illustrates several significant peaks in subsoil erosion in the period post c. 1900.

The Holocene record at Bussjösjön has also been interpreted using changes in the HIRM/χfd ratio to indicate changes in the relative amounts of eroding top soil and subsoil (Figure 2.8). However the low concentrations of ferrimagnetic minerals makes interpretation difficult. The authors identified sub-soil as making a significant contribution in the period pre 9000 BP, however they noted that this signal could in fact reflect an immature soil signal, i.e. soil with low secondary ferrimagnetic concentrations and hence a high HIRM/χfd ratio. After 2500 BP three specific periods have been identified where the subsoil contribution has been particularly significant (c. 2500-2200 BP, c. 1800-1500 BP, c. 1250-500 BP) and three periods when the contribution from top soil has been high (c. 2000-1800 BP, c. 1500-1250 BP and after 500 BP).

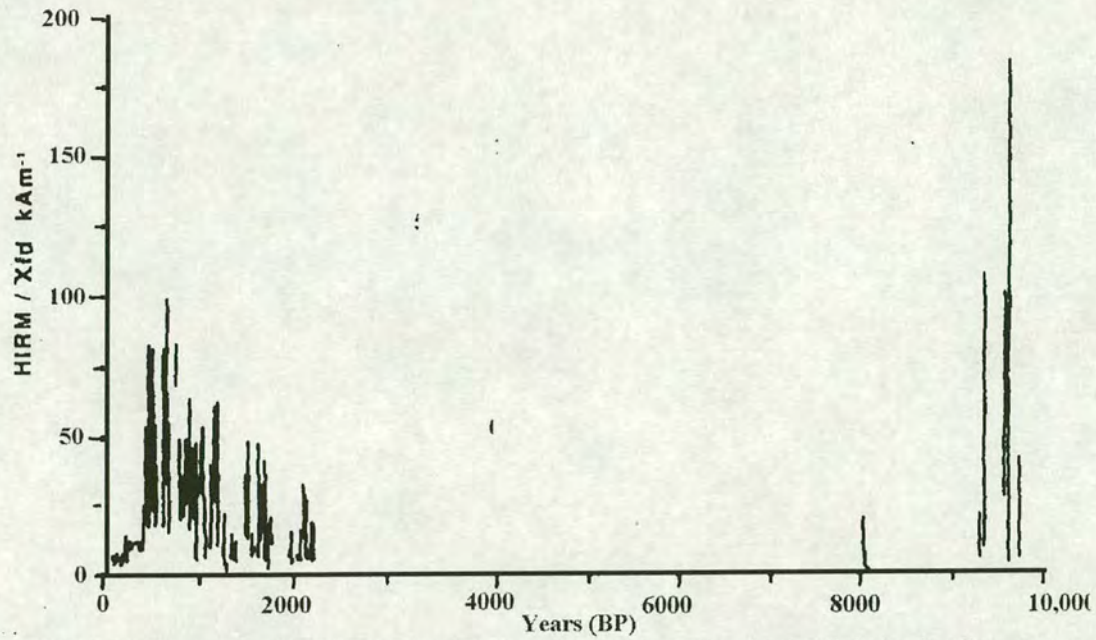

Figure 2.8 A Holocene record of changes in the proportions of topsoil and subsoil derived sediment at Lake Bussjösjön, Sweden (from Dearing *et al.* 1990). Subsoil is shown to make a particularly significant contribution to the lake sediment in the early Holocene (pre c. 9000 years BP) and during several periods after 2500 BP.

Sandgren and Fredskild (1991) have, in a similar manner to Dearing *et al.* 1990, related changes in downcore magnetic signature in cores from four lakes in Greenland to catchment disturbance. Using magnetic susceptibility six distinct magnetic units have been identified at each site (Table 2.6).

Table 2.6 Environmental changes related to susceptibility units (after Sandgren and Fredskild 1991).

Susceptibility Unit	Relative trend	Environmental interpretation
A	Rapidly increasing, prominent χ peak.	Unstable, severe soil erosion due to reappearance of sheep-breeding man in beginning of 20th Century
B	Rebound to lower χ values	Stable/stabilizing; due to disappearance of Norsemen in the 15th Century
C	χ peak	Disturbance due to arrival of Norsemen around AD 1000
D	Low χ	Stable environment
E	Decreasing χ	Stabilizing environment
F	High χ	Unstable environment

Since the mid 1980s a variety of research has been published concerned with modelling the magnetic signature within sediments. Thompson (1986) reports on the use of a SIMPLEX model which employs magnetic remanence hysteresis parameters to calculate the proportion of different minerals in simple two mineral mixtures. Yu and Oldfield (1989) have employed the magnetic characteristics of sediment and source material in the Rhode River catchment, U.S.A to construct quantitative source mixing models. Using mass specific and magnetic ratio parameters Yu and Oldfield (1989) were able to calculate the relative contribution from different source material to the clay and silt fraction of lake sediment cores.

A maximum likelihood unmixing algorithm has been applied to magnetic and radioactive measurements of stream bedload samples in a catchment containing an iron ore mine in the Western Ghats of South India (Shankar *et al.* 1994). 11 magnetic measurements and two natural radioactivity measurements were obtained on the 39 source samples and 22 bedload samples. These two techniques enable not only material derived from an iron ore mine to be distinguished from catchment source material (Figure 2.9) but also the relative proportions of the two in stream bedload samples to be calculated. Magnetite has been identified as the primary magnetic mineral in both the catchment and stream bedload samples, varying in concentrations from c. 0.02% in one sample to in excess of 50% in the primary iron ore. Results illustrate that upstream of the mine workings, stream samples comprise over 97% catchment material whilst downstream of the mine outfall the contribution of suspended sediment mine waste component increases dramatically and is modelled as averaging 47% of the bedload (Figure 2.10).

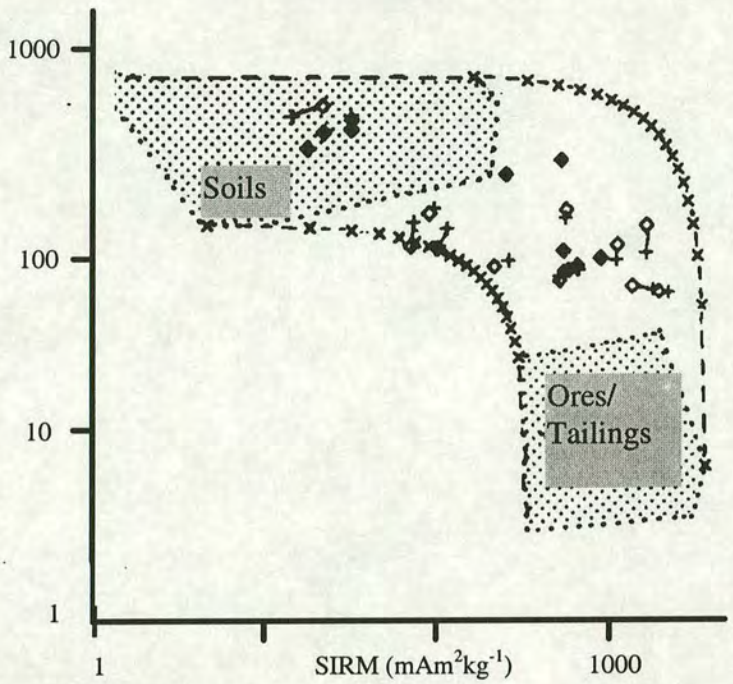

Figure 2.9 Unmixing bedload samples from the Bhadra River, India using SIRM and alpha activity (from Shankar *et al.* 1994). The ores and tailings are shown to be characterised by lower alpha activitiy and higher SIRM values than the catchment soils.

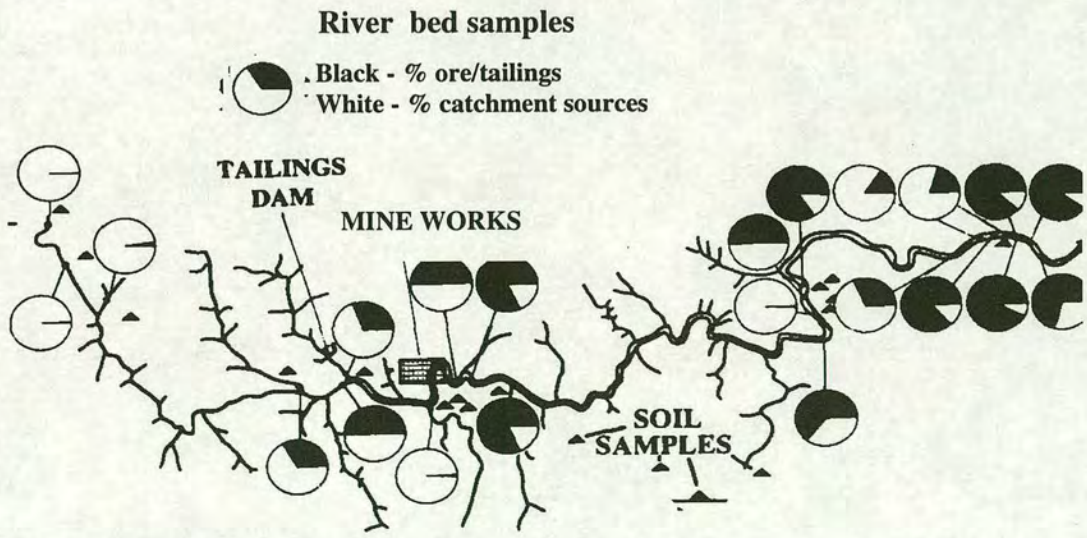

Figure 2.10 Variations in the proportions of ore/tailing material and catchment material in the Bhadra River catchment, India. Pie diagrams calculated using unmixing calculations based on two natural radioactivity measurements and 11 artificial magnetic measurements (from Shankar *et al.* 1994).

2.3 Modelling Sediment Erosion

2.3.1 Linking Sediment Accumulation to Sediment Yield

As a starting point the following equation can be employed to determine sediment yield in lake catchments

$$Y = M/A \qquad (2.1)$$

where Y is sediment yield (t km^{-2} a^{-1}), M is the mass of material deposited in the basin annually (t a^{-1}) and A is the catchment area (km^2).

However, as Walling (1983,1988) notes, sediment yield determined from lake sediment based studies does not take account of the deposition of material during transport on route from source to sink, whether it be in river channel or overland within the catchment. Research by Owens (1990) illustrates the significance of sediment storage in an upstream valley in the Slapton Ley catchment. Based on data from historical maps, aerial photography, interviews with farmers and ^{137}Cs, Owens reports that some 34 070 tonnes of material is stored in just one sediment sink at Deer Bridge. When coupled to the sediment yield data obtained from lake cores collected at Slapton Ley (Crick 1985) the volume of material stored in the Deer Bridge sediment sink results in sediment yields from the Start catchment of between 82 and 148 t km^{-2} a^{-1} depending on the age of the sink. This compares to a mean yield, calculated from lake sediment core data alone, of 53.5 t km^{-2} a^{-1} for the two sub-basins draining into the lower ley. The research in the Slapton Ley catchment by Owens (1990) illustrates an example of the errors associated in expressing sediment yields based on lake core data alone within catchments where the storage of material is high. Such research clearly implies that significant quantities of sediment eroded from catchments may not be transported downstream to lakes but will be deposited en-route within the drainage basins, for example on floodplains.

Sediment yield is therefore a function not only of the rate of soil loss but also of the efficiency with which it is delivered via the processes of surface runoff and channel flow (Jackson *et al.* 1986). Thus in order to relate sediment yield to erosion the sediment delivery ratio (D) must be considered. Haan *et al.* (1994) define the sediment delivery ratio as

$$D = G/(Y.A) \qquad (2.2)$$

where G is the gross erosion occurring in the catchment per year (t a^{-1}).

Sediment yield in lake catchments therefore becomes

$$Y = (M.D)/A \qquad (2.3)$$

There are a variety of difficulties in selecting a sediment delivery ratio, D, for a given catchment as there are a range of factors which can influence it. Indeed Haan *et al.* (1994, page 293) state that

> "It should be pointed out that the degree of understanding of sediment delivery ratios is probably less than any other area of sedimentation."

Nevertheless a number of researchers have attempted to quantify the significance of the various processes. Vanoni (1975) suggests that in basins larger than 1 km^2 often less than 25% of the material eroded reaches a given point downstream, whilst theoretical work undertaken by Trimble (1981) suggests that in fact sediment delivery may fall to a mere 6%.

The American Society of Civil Engineering (A.S.C.E, 1975) have adopted the following empirical relationship

$$D=0.36A^{-0.2}$$

where A is the catchment area in km^2. Figure 2.11 illustrates the relationship between sediment delivery ratio and drainage basin area developed by the A.S.C.E. It should be noted however that this relationship has not been verified in Europe and has been criticized in many North American studies (Trimble, 1981).

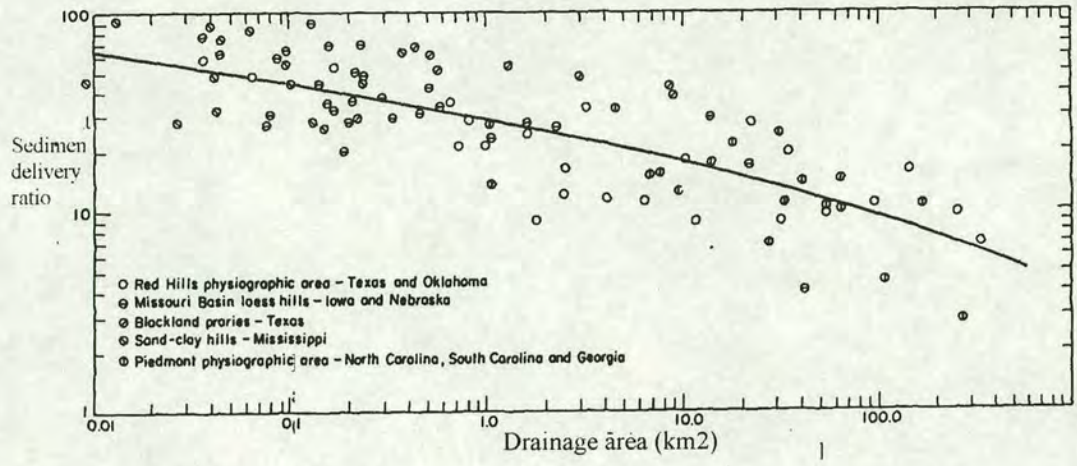

Figure 2.11 The relationship between sediment delivery ratio and drainage basin area developed by Boyce (1975).

Sediment delivery is seen to vary from more than 90% in some small catchments to less than 10% in the largest catchments in Figure 2.11.

2.3.2 Linear Relationships Between Sediment Yield and Catchment Characteristics

Turning to the global scale links between sediment yield and a number of physical parameters such as catchment area and relief have been investigated previously in various regions of the world. On the basis of discharge and sediment data for 60 large catchments Strakhov (1967) produced a map illustrating the global pattern of erosion (Figure 2.12). Strakhov illustrated that in large basins variations in suspended sediment yield of between 1 m^3 km^{-2} a^{-1} and 4000 m^3 km^{-2} a^{-1} and dissolved sediment yield of between 1 m^3 km^{-2} a^{-1} and 450 m^3 km^{-2} a^{-1} can be accounted for by physiography, soil type, vegetation cover and climate. Strakhov identifies two particular zones of erosion illustrated by Figure 2.12. First a temperate moist belt in the northern hemisphere is broadly bounded to the south by the annual +10°C isotherm. This zone is characterised by an annual precipitation of between 150 and 600 mm. It has low erosion rates typically less than 10 t km^{-2} a^{-1} (diagonal stripes and horizontal dashes in Figure 2.12). The second zone includes parts of

North America, South America, Africa and south eastern Asia. His second region corresponds to the area between the +10°C isotherm in the northern hemisphere and the +10°C in the southern hemisphere. This second zone is characterised by an average annual precipitation of between 1200 and 1300 mm. Here erosion is high, typically between 50 to 100 t km^{-2} a^{-1}, though rising to values in excess of 1000 t km^{-2} a^{-1} in the Indus, Ganges and Brahmaputra basins. Britain, along with most of Europe falls into his low erosion zone.

Links between spatial scale and yield have been studied by many authors previously. Brune (1950) studied sediment loads for a range of drainage basins in the Sangamon River Watershed, Illinois, America. He noted that average rates of sediment production decreased with increasing drainage area (Figure 2.13). Following on from the work of Brune *et al.* Flaxman and Hobba (1955) surveyed sedimentation in 38 stockponds in the Columbia River Basin. They observed that drainage basin area was one of five factors accounting for 80% of the variation in sediment accumulation in the stockponds studied. Langbein and Schumm (1958) employed American gauging station data for 94 catchments and reservoir sedimentation data for 163 catchments to study the relationship between effective precipitation and erosion. They found that sediment yields reached a peak at the precipitation boundary between desert shrub and grassland conditions. Particularly dry regions and more humid ones are characterised by much lower yields. Langbein and Schumm (1958) suggested that the low sediment yields in very dry regions could be explained by the low runoff resulting from precipitation levels of less than 300 mm a^{-1}. Schumm (1963) also noted the effect of relief ratio (maximum basin relief/length) on sediment yield. He found an exponential increase between annual sediment yield and relief ratio in drainage basins of area 2.6 km^2 and greater.

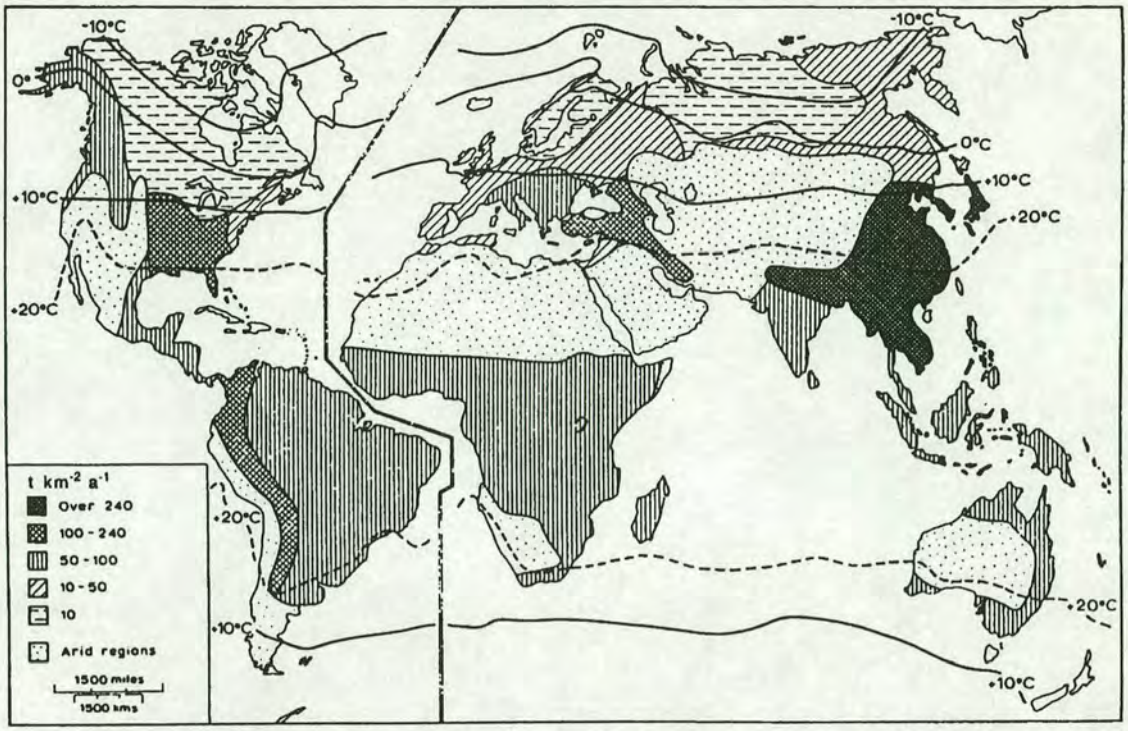

Figure 2.12 Global rates of erosion (Strakhov 1967, modified by Goudie 1995). Two zones of differing erosion are identified. In the northern hemisphere a temperate moist belt characterised by an annual precipitation of between 150 and 600 mm has low erosion rates, typically less than 10 t km^{-2} a^{-1} (diagonal stripes and horizontal dashes). The second zone covers the area between the +10 °C isotherm in the northern hemisphere and the +10 °C isotherm in the southern hemisphere. This second zone is characterised by average annual precipitation of between 1200 and 1300 mm and erosion is typically between 50 and 100 t km^{-2} a^{-1}.

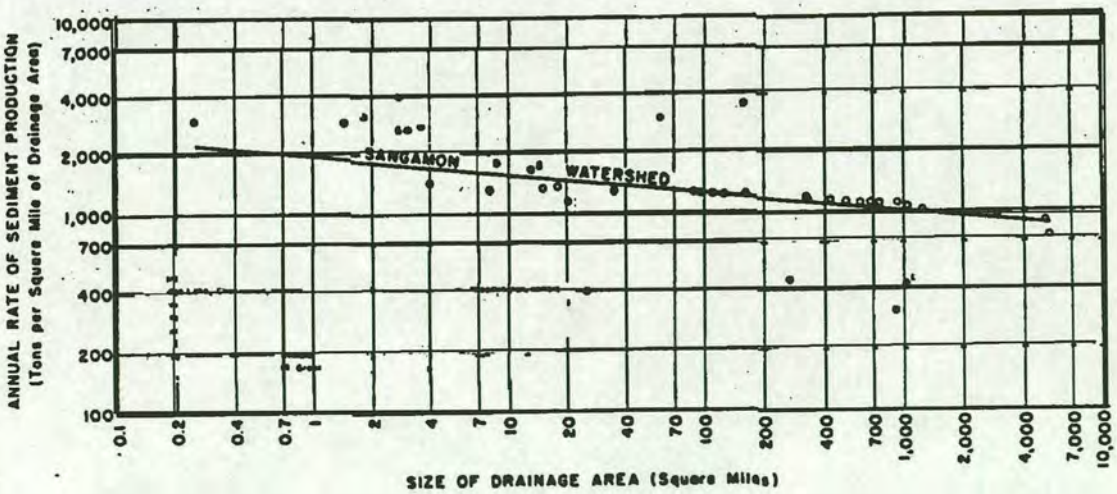

Figure 2.13 The relationship between rate of sediment production and spatial scale for a variety of catchments in the Sangamon River Watershed, Illinois, America (from Brune 1950). The figure shows a general decline in the rate of sediment production with increasing drainage area.

Amongst others, Dearing and Foster (1993) have postulated links between the catchment to lake ratio (CLR) and sediment yields. The authors plot the relationship between CLR and sediment yield for 20 studies of erosion for a variety of studies in different environments in the World (Figure 2.14). As illustrated in Figure 2.14 they propose that the data can be divided into two groups. One group (upperline) represents sites where recent maximum sediment yield under cultivation/moorland has been plotted and the second group (lower line) illustrates maximum sediment yields under forest (Dearing and Foster, 1993). Both groups display a decrease in sediment yield as CLR increases. The authors propose that the negative correlation can be explained by two factors first, the increase in storage as catchment area increases and second, the erosion pathways between slopes, channels and the lake which increase at a slower rate than catchment area. Dearing and Foster (1993) therefore suggest that, assuming other factors to be constant, for sites where the CLR is less than 10 sediment is more likely to originate from slope or surface processes than channel banks. In larger catchments, where the CLR is greater than 10, a channel network is supported and thus the significance of channels as a sediment source increases.

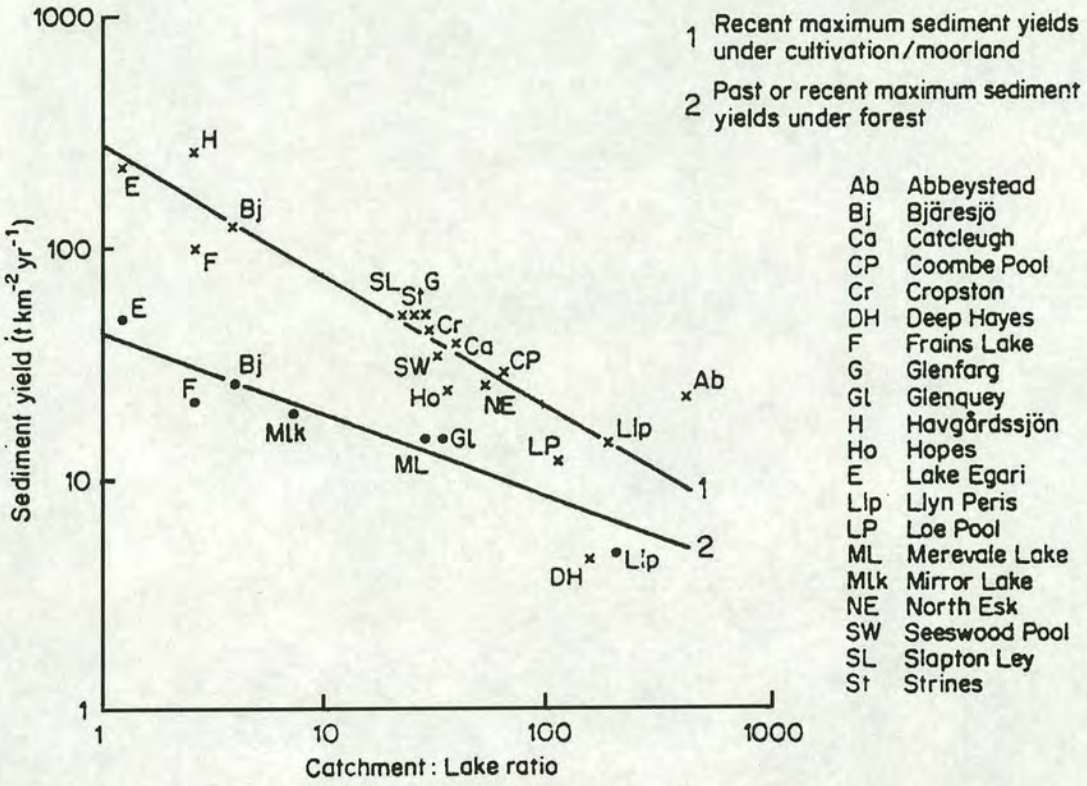

Figure 2.14 The relationship between catchment to lake ratio and sediment yield for 20 studies (from Dearing and Foster 1993). Dearing and Foster (1993) have grouped the sediment yield and catchment:lake ratio data into two groups, an upper set comprising yield estimates obtained from catchments which are cultivated or moorland and a lower set which comprises sediment yield estimates from forested catchments.

2.3.3 Modeling Sediment Yields and Processes

Following on from the work of Flaxman and Hobba (1955), Langbein and Schumm (1958) and Schumm (1963) more complex models of sediment yields and processes have been developed. Dickinson (1990) notes that models have been constructed to predict sediment yields and describe processes on a variety of scales, ranging from small one metre square plots to large catchments. Dickinson proposed that the models enable us to (i) extend databases, (ii) determine spatial and temporal variations/patterns (iii) establish important processes and (iv) investigate the effects of potential strategies to control erosion.

Studies of soil erosion have employed a variety of models. Traditionally the models have tended to be based on empirical equations, though more recently much attention has been focused on what Foster (1990) terms 'process based technology'. Gregory and Walling (1973), identify three kinds of empirical models:

Black box	-	Only the main inputs and outputs are studied
Grey-box	-	Some detail of how the system works is known
White-box	-	All details of how the system operates are known

Black box models are the simplest relating, for example, sediment yield to rainfall. As reported by Morgan most models of soil erosion fall into the grey-box category. Having identified the most significant factors such models are based on deriving a regression equation from the relationship between certain physical parameters and sediment loss (Morgan 1995). One such empirical model is that of Fournier (1960). Using data from 78 drainage basins Fournier derived the following equation between sediment yield, precipitation, altitude and basin slope:

$$\log Qs = 2.65 \log p^2/P + 0.46 (\log H) (\tan S) - 1.56$$

Qs	Mean annual sediment yield (g/m^2)
p	Highest mean monthly precipitation (mm)
P	Mean annual precipitation (mm)
H	Mean catchment altitude (m)
S	Mean basin slope (degrees).

Such empirical equations cannot be reliably employed outwith their data range. Fournier (1960), aware of the models limitations, produced a further four regression equations applicable to distinct relief and climate conditions. These four equations relate sediment yield to a precipitation index, namely p^2/P (Figure 2.15).

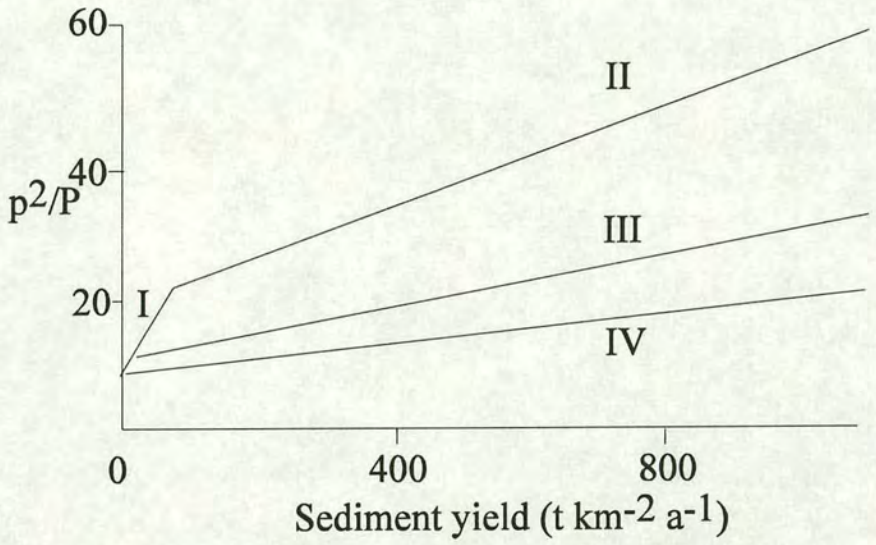

Figure 2.15 The relationship between sediment yield and p^2/P index (after Fournier 1960).

I Low relief (mean valley floor gradient <1:100, $p^2/P > 20$

Sediment yield = 6.14 (p^2/P) - 49.78

II Low relief (mean valley floor gradient <1:100, P>600 mm

Sediment yield = 27.12 (p^2/P) -475.40

III High relief (mean valley floor gradient ≥ 1:100), P>600 mm

Sediment yield = 52.49 (p^2/P) - 513.20

IV High relief (mean valley floor gradient ≥ 1:100), 200 ≤ P ≤ 600 mm

Sediment yield = 91.78 (p^2/P) -737.62

These regression curves produced by Fournier (1960) provide a measure of seasonal variations in precipitation and reflect the important effects of intense rainfall and vegetation on controlling erosion rates (Douglas 1967).

The most widely employed empirically based model is the Universal Soil Loss Equation (USLE). This well known model was developed by Wischmeier and Smith (1978) from a database consisting of more than 10 000 plot-years of data. Plots studied ranged in length from 11 to 189 metres and spanned a variety of soils, slope steepness, vegetation and climate in eastern America.

The model has the form:

$$E = R \cdot K \cdot LS \cdot C \cdot P$$

Where

E = Mean annual soil loss

R = Rainfall erosivity factor

K = Soil erodibility factor

L = Slope length

S = Slope steepness

C = Crop management factor

P = Erosion control practise factor

K represents mean annual soil loss per unit of R, therefore E has the same units as K. Multiplication of K in t ha^{-1} by R (in metric units) provides the value of E in t/ha (Morgan, 1980).

The USLE was designed for estimating interrill and rill erosion over time on small field plots. The equation was not designed to estimate soil loss for specific storm events. A number of authors have expressed concerns regarding the application of the USLE to larger areas (Meade 1982). As noted by Foster (1982), the USLE is not designed to predict gully or channel bank erosion or account for the deposition of material on hillslopes or channels and hence assumes a sediment delivery ratio of one. Thus catchment studies which incorporate the USLE to estimate erosion need to add a sediment delivery term (D) to the equation. Other limitations which have been identified in the USLE include the narrow database upon which it was built, i.e.

agricultural American sites, and theoretical problems, for example, the lack of interaction terms.

As a result of the limitations posed by empirical models additional efforts have been made towards the development of models which are better suited to predicting the distribution of sediment loss and runoff spatially on an individual storm basis as well as estimating total soil loss. Further improvements in erosion modeling are more likely to arise from models which incorporate key hydrological and erosion processes rather than from small developments based on the USLE. However, as noted by Rose *et al.* (1988 *in* Dickinson *et al.* 1990), contemporary understanding of the processes surrounding the transport and detachment of soil remains inadequate and hence hampers efforts to obtain reliable input data and to validate models. The development of physically based models is therefore at an early stage, and thus Morgan (1995) reports that in practical terms estimates of erosion obtained from empirical models (grey-box) are often more reliable than those based on physical processes (white-box). Modelling of erosion in lake catchments is considered further in Chapter 3.

2.4 Summary

- Magnetic techniques can be applied to assist in the correlation of lake cores and in the identification of source material in catchment studies of sediment flux. However, interpretation of the lake sediment magnetic signature is made complex by the fact that the signal is influenced by a number of factors, and is thus not always a result of the input of catchment detrital material alone.

- In the United Kingdom records of sediment yield over time periods of more than a few years are rare. Variability in sediment flux and sediment delivery over such short periods of time prevents reliable catchment process-response relationships to be determined.

- Links between a range of catchment characteristics and sediment yields have been investigated for a wide variety of catchments. The USLE was developed to model sediment losses from small plot areas using data for sites in eastern America and is not necessarily applicable in other climatic/geographical regions or in large/regional catchments.

Chapter 3

Methodology

3.1 Background to the Study Sites

3.1.1 Semer Water

Semer Water (Nat. Grid. Ref. SD918874) is situated in the Ure drainage basin, four miles south-east of Hawes in Wensleydale, North Yorkshire. The watershed falls largely within the parish of Bainbridge. The lake is of glacial origin, resulting from the slumping, burial and subsequent melting of an ice block at the front of the Wensleydale glacier (Squance 1980). Semer Water is impounded to the north east by a glacial moraine. The valley bottom consists of fluvial glacial deposits underlain by rocks formed in the Upper Palaeozoic. These are of the Millstone Grit Series in which the Upper part of the Carboniferous Yoredale series, comprising limestone, shale and sandstone, can be found (HMSO 1954). Extensive areas of heavily eroded Pennine blanket peat occur to the southern extent of the drainage basin. Figure 3.1 illustrates the surface geology of the area. The lake covers approximately 0.27 km^2 (Squance 1980) and drains a catchment of 43.6 km^2. Thus the catchment to lake ratio (CLR) is 164:1.

Semer Water is fed predominantly by the Crooks Beck, to the south-west. Several smaller streams including Little Ings Beck at the eastern edge also flow into the lake. The lake is drained by just one outflow, the River Bain, at the north-eastern margin.

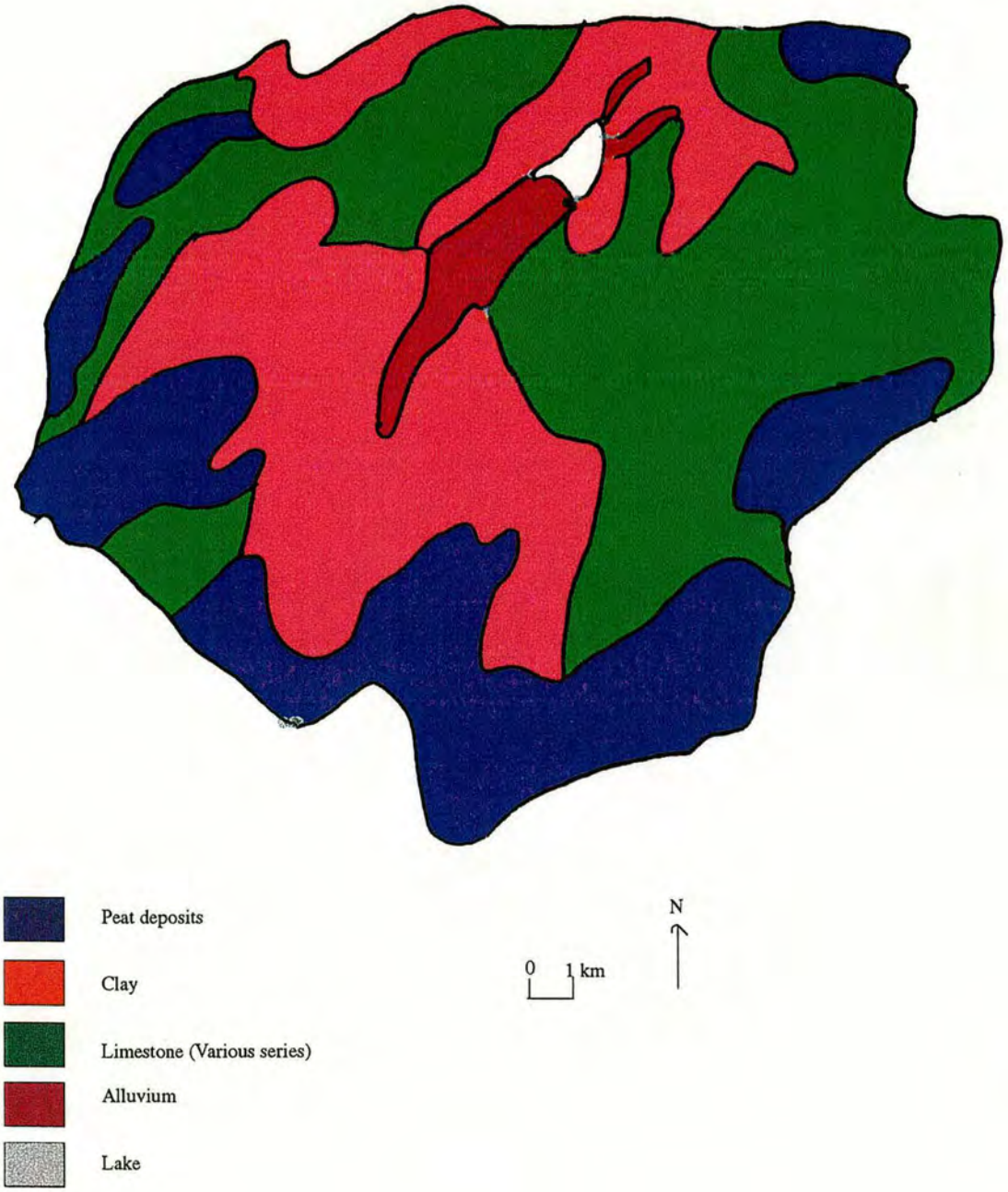

Figure 3.1 Surface geology of the Semer Water catchment, based on Geological Drift Map 50, scale 1:63,360 (from Barlow 1994). The drift geology of the catchment is dominated by a combination of peat, particularly at the towards the southern edge, clay and limestone. The lake lies at the north eastern head of substantial alluvium deposits.

Land use within this upland, agricultural catchment comprises 69.7% rough grazing, 25.6% grassland for grazing/hay and silage and 4.7% woodland/forest (Barlow 1994). The majority of the woodland/forest occurs in the form of a large coniferous plantation in the Raydale valley covering 1.7 km^2. With the exception of 0.08 km^2 of mixed conifers planted in 1900, all the trees are Sitka Spruce (*Picea Sitchensis. Bong. Carr.*) planted between 1966 and 1970 (Letters; Mr G.Hay of Tilhill Economic Forestry Ltd, 16th November 1993; Ms E. Berridge of the Yorkshire Dales National Park, 20th October 1993). An area of 0.22 km^2, bordering the south-western margin of the lake, is managed as a nature reserve by the Yorkshire Wildlife Trust. The Nature Conservancy Council (NCC, 1986) reported that approximately 1 km^2 of the catchment, including the lake itself, has been designated a Site of Special Scientific Interest (SSSI). A significant component of the catchment is a part of the designated Ministry of Agriculture, Farming and Foods (MAFF) Environmentally Sensitive Area (ESA) scheme (MAFF 1982).

The topography is typical of that found in the Yorkshire Dales. Stepped valley sides are formed as a result of the geological sequence of harder and softer limestones. At higher altitudes a layer of peat overlies the gritstone capped limestone (Jarvis *et al.* 1984). The fertile valley floor gives rise to steep sided rugged open fell to the south, west and east. The lake lies at an altitude of 215 metres whilst the catchment boundary on the east, south and west is between 400 to 600 metres above sea level.

Local residents report that the lake level was reduced in 1939-1940 as a result of a the deepening of the outflow (River Bain). A sketch in Turner's 'Yorkshire 4' sketchbook of 1816 indicates that the lake was indeed considerably larger in the early 1800s, extending up the Raydale valley towards Marsett. The lake lowering has fortunately provided an extensive area of the Raydale valley, previously occupied by Semer Water. This allowed us to get heavy coring equipment onto the former lake bed and collect extremely thick lake sediment sequences (cf Chapter 5).

The vegetational history of the site can be inferred from pollen diagrams produced for Malham (Pigott and Pigott 1963) which lies 20 km south of Semer Water. At Malham the Late-Glacial period is characterised initially by high concentrations of *Pinus* and smaller concentrations of *Betula* and *Juniperus* in Zone II. In Zone III *Betula* becomes the dominant tree and the presence of open herbaceous vegetation is indicated by pollen grasses, sedges, *Artemisia*, *Rumex* and *Helianthemum.* Zones IV and V are characterised by an abrupt decline in *Juniperus* which coincides with a sharp rise in *Corylus*. A rise in herb pollen, absent in Zones Vi and VIIa, in subzone VIIb is attributed to late-Neolithic clearance. Further rises in herb pollen and the presence of cereal pollen grains in Zone VIII coincide with the Iron Age. A continuing increase in the herb to tree pollen ratio indicative of steady destruction of woodland is associated with the Norse settlement of the Craven uplands followed by the use of Malham Moor as a sheep walk in the Middle Ages. We may infer that erosion episodes at Semer Water are likely to coincide with late-Neolithic clearances and Norse settlements recorded in the pollen record from Malham.

3.1.2 Gormire

Gormire (Nat. Grid. Ref. SE505833) is situated on the north-eastern edge of the Vale of York. The lake lies at the base of the Hambleton Hills at Whitestone Cliff, a Jurassic Gritstone escarpment. Figure 3.2 shows a simplified map of the drift geology of the Gormire catchment. The lake is located on the Late Devensian glacial limit (Penny 1974). Kendall and Wroot (1924) propose that the Whitestone Cliff escarpment provided a barrier at which ice accumulated and that the lake itself occupies a marginal drainage channel which became blocked by a landslip from the escarpment. Kendall and Wroot (1924) suggest that the drainage channel originally drained from north to south inline with other less significant adjacent channels, including Butterdale, which lies east-south-east of Gormire.

Gormire has an area of approximately 0.07 km^2 and drains a steep, relatively small catchment of about 35 ha giving rise to a CLR of 7:1. The lake lies at an altitude of 150 m, and the catchment boundary varies in altitude from 165 m to 320 m. The dominant land cover in the catchment is mixed deciduous woodland, comprising birch (*Betula pendula*), oak (*Quercus sp.*), sycamore (*Acer pseudoplataus*), elm (*Ulmus glabra*) and ash (*Fraxinus excelsior*). The majority of the catchment, including Garbutt Wood, is designated an SSSI. Garbutt Wood, situated in the north eastern part of the catchment, is managed as a nature reserve by the Yorkshire Wildlife Trust, (NCC 1985). Blackham *et al.* (1981) have undertaken pollen analysis on two lake cores from Gormire. The early Post-Glacial period is characterised by herbaceous vegetation with high concentrations of *Gramineae* and *Cyperaceae*, alongside *Betula* and *Juniperus*. At a depth of 6 metres, corresponding to c. 10,000 BP, the pollen record is dominated by *Betula*, *Pinus*, *Ulmus*, and *Corylus,* indicating a predominantly forested catchment. Increases in *Gramineae* and *Plantago lanceolata* at a depth of about 2 metres coincide with decreases in tree pollen to values below 10% of the total dry land pollen, indicating a deforested landscape. The date of forest clearance has not been determined, although it occurs sometime after the *Alnus* rise and is believed to be late Flandrian. The decline in disturbance indicators in the uppermost sediments is attributed to the regeneration of woodland in the Gormire catchment. The pollen record identifies several phases of woodland clearance in the landscape which are likely to have resulted in high rates of sediment loss. However, without a more detailed chronology it is difficult to determine during which Holocene periods episodes of erosion may have occurred in the Gormire catchment. Collaborative researchers at Liverpool University are currently involved in a joint study of the Holocene erosion history at Gormire using pollen and magnetic techniques.

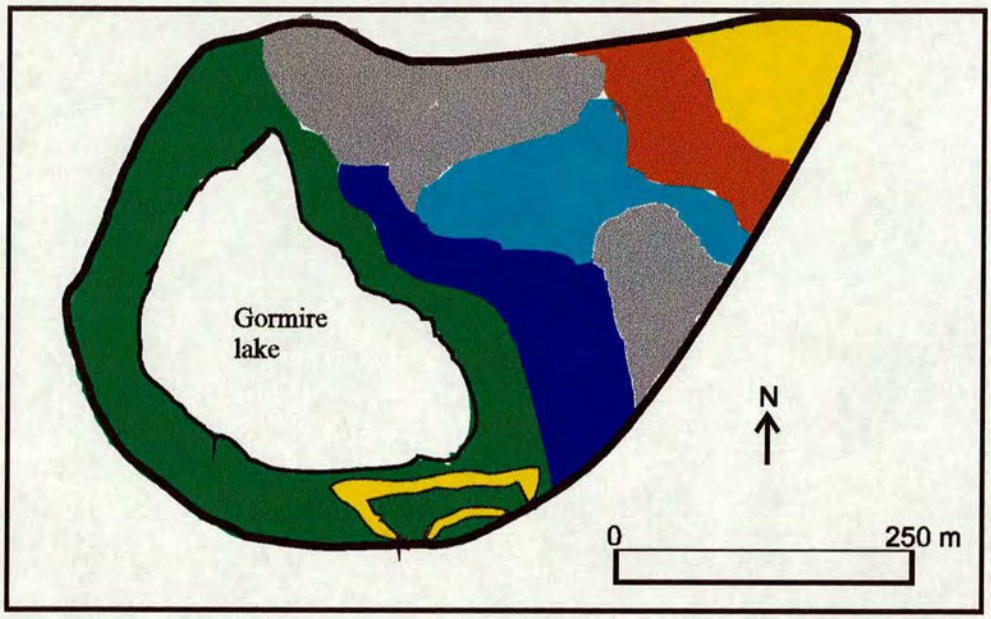

Hambleton Oolite

Birdsall Calcareous Grit

Landslip

Till

Ravenscar Group (Cloughton Formation)

Ravenscar Group (Long Nab Member)

Figure 3.2 Simplified surface geology of the Gormire catchment, based on Geological Drift Map 52(England and Wales), scale 1: 50 000. The catchment is composed of rocks formied in the middle and upper Jurassic period. The landslip cuts across the catchment from south east to north west.

3.1.3 Hornsea Mere

Hornsea Mere (Nat. Grid. Ref. TA190447) is situated close to the North Sea, 14 km north-east of Hull. It is a shallow lake (maximum depth 2m) in a lowland agricultural area. The lake lies approximately 5 metres above sea level, and the maximum altitude of the catchment boundary is c. 22 metres above this. The lake covers an area of approximately 1.2 km^2 and lies in a catchment of 16.7 km^2 resulting in a CLR of 14:1.

Cultivated arable land accounts for c. 80% of land use within the watershed, with woodland and urban land occupying the remaining c. 20% of the catchment. Cretaceous chalk underlies the glacial till deposits upon which the lake is situated. Figure 3.3 shows a simplified drift geology map of the Hornsea Mere catchment.

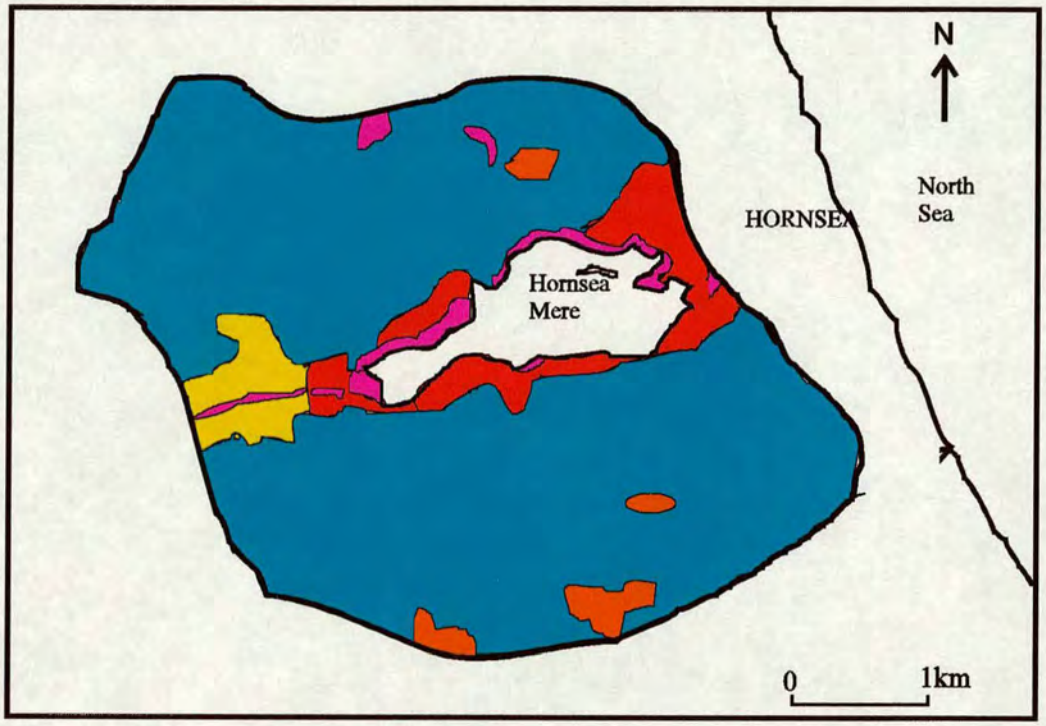

Till/Stony Clay (Glacial)

Sand and Gravel undifferentiated (Glacial)

Sand and Gravel (Glacial)

Non-Marine Sand with Peat Beds (Glacial/Post Glacial)

Alluvium (Post Glacial)

Figure 3.3 Simplified surface geology of the Hornsea Mere catchment, based on Geological Drift Map 73 (England and Wales), scale 1: 50 000. The catchment is dominated by glacial till, sand and gravel deposits with smaller deposits of post-glacial alluvium.

Palynological studies from the adjacent Hornsea Old Mere provide evidence of at least one major pre-medieval phase of forest clearance in this region (Beckett 1981). The Old Mere occupies the eastern end of the pre-glacial valley which extends

westward to Brandesburton, and includes the surviving Hornsea Mere, immediately inland from the Old Mere site. This surviving mere is drained by the Steam Dike, which runs through the centre of the Old Mere basin. A low gravel ridge separates the Old Mere from the surviving one, and a gravel rim forms distinct north and south shorelines to the basin. The presence of a terrace around the existing Hornsea Mere, at about 3m above present water level, suggests a previously higher water surface level, probably high enough to join the two meres into one lake of considerable size (Reid 1885, *in* Beckett 1981). Beckett (1981) reports that the Late Devensian vegetation is characterised initially, in Zone RB.1, by an open landscape. The increase in arboreal pollen in Zone RB.2 indicates the development of local woodland. This is followed by a decrease in tree pollen and a corresponding increase in the shrubs *Juniperus* and *Betula nana.* The development of birch woodland at c. 10,000 BP is followed by a sharp increase in *Corylus* and then *Alnus* and *Ulmus.* The *Alnus/Quercus* assemblage zone at c. 5100 BP indicates the opening up of woodland cover which is attributed to the onset of Neolithic people. However, the low concentrations and inconsistent presence of *Plantago lanceolata* is interpreted as indicating minimal arable activity. The subsequent expansion of *Tilia Cordata* and *Ulmus* is perceived to indicate forest regeneration, however the concentrations of these two taxa decline in the Bronze Age forest clearance period as indicated by the *Alnus/Gramineae* pollen assemblage zone. The drying up of the Old Mere at c. 2000 BP prevents any detailed interpretation of post-Bronze Age vegetational change. On the basis of the early Holocene pollen record (pre-2000 BP) we may infer high sediment erosion episodes associated with the onset of the Neolithic activity at c. 5100 BP and the more recent Bronze Age clearances. The current Hornsea Mere catchment is dominated by arable land and thus we might expect contemporary sediment yields to be particularly high.

3.1.4 Summary of Catchment Site Details

Figure 3.4 illustrates the simplified geology of the Humber region. The Semer Water, Hornsea Mere and Gormire catchments represent a broad cross section of the geology and land use environments found within the Humber catchment. These sites form a representative sample upon which to establish estimates of sediment yield for the whole of the Humber catchment.

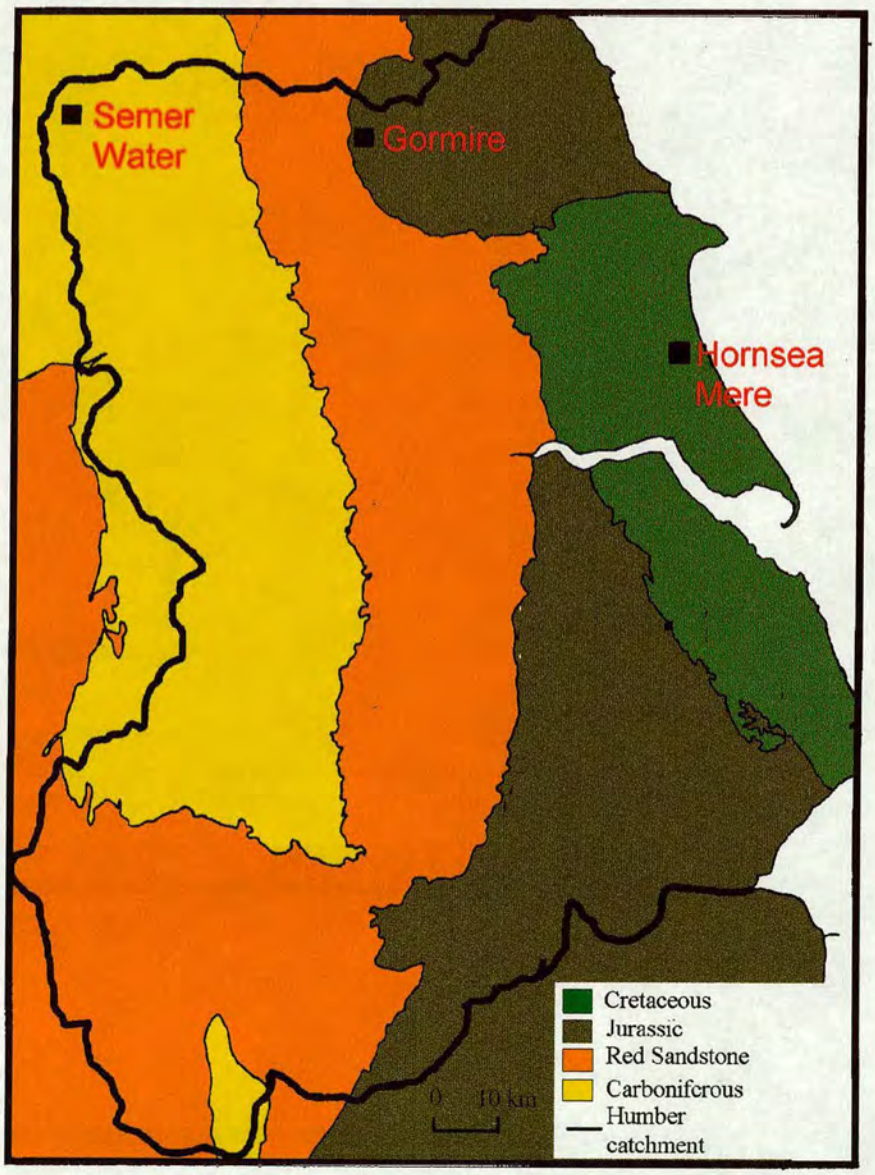

Figure 3.4 Simplified geology of the Humber catchment.

3.2 Fieldwork

3.2.1 Coring

3.2.1.1 Mackereth Coring

Lake cores were obtained using a combination of one, three and six metre long Mackereth piston corers (Mackereth 1958, 1959). These corers are operated from a boat using compressed air. The corer is lowered to the lake sediment surface so that the bell chamber rests on the surface providing a stable base for coring to take place. Compressed air is applied via an air line from the boat; this air forces the piston downwards in the coring chamber which drives the perspex coring tube (80 mm in diameter) into the sediment. Once the coring tube has penetrated the sediment to the maximum extent excess air bubbles up through relief valves on the top of the bell chamber thus illustrating the completion of the coring. The one metre corer is then pulled vertically to the surface by hand, brought aboard the boat and the core tube unscrewed. The three and six metre corers employ plastic tubing, of 53 mm internal diameter, in place of perspex core tubes. The three and six metre Mackereth corers need a significantly larger bell chamber such that, after completion of coring, sufficient compressed air may be introduced into the chambers to give the positive buoyancy necessary to raise the corer from the sediment. Figure 3.5 illustrates the operation of the one-metre corer.

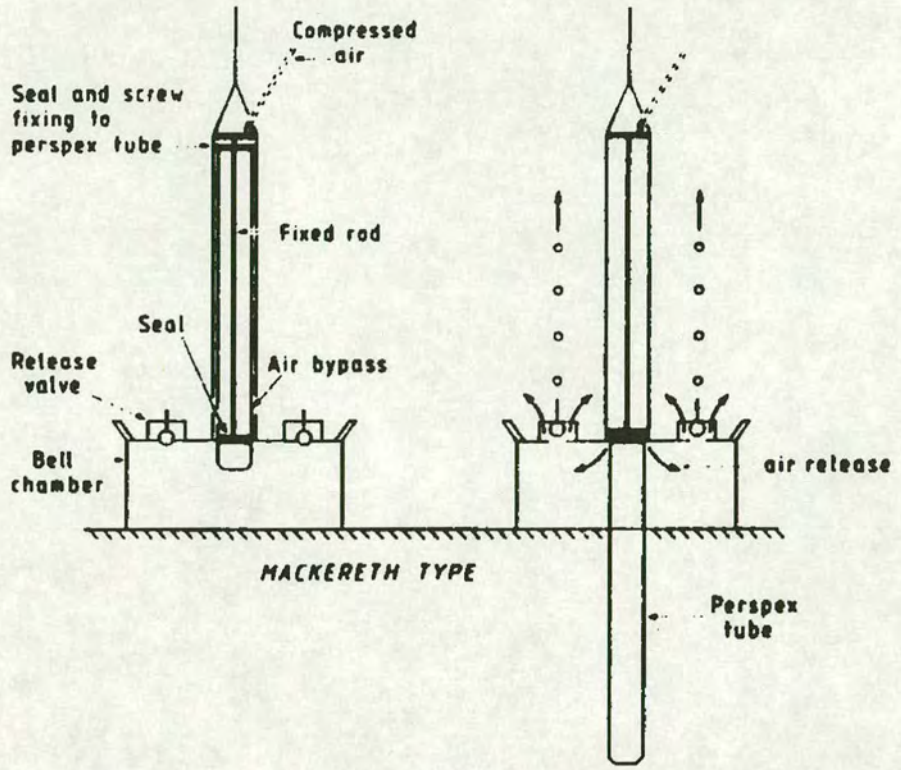

Figure 3.5 The operation of the Mackereth corer (from Foster *et al.* 1990).

3.2.1.2 Gouge Coring

A gouge corer is a hand operated corer. It comprises an open sided steel tube of 35 mm diameter which retains sediment once the gouge has been forced into the sediment and then rotated 360 ^{o}. Attached to this gouge are a series of extension rods in one metre sections. It is difficult to establish accurate sediment stratigraphies with this corer as material is subject to moving up and down the gouge. Therefore gouge corers are best suited for preliminary investigations of a site, before using either a Giddings corer, or in shallower, softer material a Russian corer to obtain a more reliable account of sediment stratigraphy.

3.2.1.3 Giddings Coring

In order to obtain terrestrial cores in Raydale, from the drained part of Semer Water, a Giddings corer was used. This hydraulic piston corer facilitates the recovery of cores in one metre sections of diameter 60 mm. The corer comprises a one metre stainless steel barrel into which a plastic core tube lining is inserted. A series of tubular steel extension rods in 225 cm sections enable cores to be obtained down to a depth of 15 metres. An auger is employed to remove the top soil and material that cannot be retrieved successfully using the core barrel, such as gravel. In this study the auger enabled coring to continue below very wet and non-cohesive sediments which simply dropped out of the core barrel as it was withdrawn from the core hole towards the surface. On later site visits the addition of a fixed, wire held, piston into the core barrel considerably improved the ability to recover the wet, non-cohesive sediments.

3.2.2 Catchment Sampling

Catchment samples were obtained from a variety of localities within each catchment, in order to gain a representative account of the potential sources of sedimenting material. Samples were also obtained from the alluvial fan at Semer Water to enable a comparison between contemporary sedimenting material with older sediments from cores from Raydale and Semer Water.

3.2.3 Resistivity Surveys

The resistivity method involves imparting artificially-generated electric currents into the ground and measuring the potential difference at the surface. Most rock-forming minerals are insulators and thus electric current is passed through the rock via the

passage of ions in pore waters. Consequently the resistivity of rocks is controlled largely by porosity. Information on subsurface structure can be gained by studying the pattern of potential differences measured at the surface. Resistivity soundings were undertaken in Raydale in order to enable the extent and volume of old lake sediment to be mapped. The contrasting porosity of the lake sediment and underlying bedrock results in deviations in the potential differences measured at the surface from those expected if the material was homogenous. The measurements were made with an Abem Terrameter using BGS-128 multi-core cable and involved a spread of five equally spaced electrodes. At each electrode spacing two Wenner offsets and three tripotential configurations were employed. In order to generate the Wenner apparent resistivities the resistance of the five measurements were combined, following Barker (1981). All soundings were obtained using an electrode spacing sequence of 0.5, 1, 2, 4, 8, 16, 32, 64 and 128 m. At each site the maximum span possible was employed. Kearey and Brooks (1984) and Milson (1989) provide a more detailed description of resistivity theory, and include information on electrode configurations, electrical profiling and depth surveying using resistivity methods.

3.2.4 Surveying

Surveying techniques have been used to determine the volume of material potentially produced by eroding gullies in the Semer Water catchment. Gullies were identified within the catchment using a combination of site visits and a 1:25 000 map, and classed into one of three size classes. Five gullies of differing proportions were surveyed in the Semer Water catchment using a TOPCON level and the average cross-sectional area of each gully calculated. On the basis of the five surveyed gullies estimates of average cross sectional area for three gully size categories have been determined.

The length of each gully identified has been determined and, using the average cross sectional area of each gully size class, the volume of material eroded from the gullies

has been calculated. In order to also take account of material derived from river beds the length of main river channels flowing into Semer Water (excluding those rivers flowing down gullies) has also been determined.

3.3 Laboratory Analysis

3.3.1 Core Sub-Sampling

All one metre Mackereth cores were extruded in the laboratory at intervals of c. 2.5 cm into perspex pots (10 cm^3). Duplicate samples were taken from each horizon and stored in a cold room for later laboratory analyses. The three and six-metre Mackereth cores and Giddings cores were all sampled into 6 cm^3 perspex cubes by splitting the core tube along its length (axis) into two 'D' shaped sections. One half of each core was wrapped in polythene tubing and archived. Samples were later removed from the archived sections for ^{14}C dating, and for additional laboratory analysis when required. The other half of the Mackereth cores were sub-sampled continuously (samples at 2.2 cm intervals) whilst the Giddings cores were sub-sampled at 5 cm intervals.

3.3.2 Magnetic Instrumentation

The magnetic measurements used in this study depend on measuring artificial magnetisations grown in the laboratory. The methods employed are outlined below. Details pertaining to the theory of magnetism are described in detail by many authors including Chikazumi (1964), Tarling (1983), O'Reilly (1984), Thompson & Oldfield (1986) and Jiles (1991). Thompson and Oldfield (1986) also provide a more detailed account of magnetic instrumentation used in this project.

The following magnetic measurements, described in section 2.1, were employed to characterise the sediment samples:

Parameter	Abbreviation	Units
Magnetic susceptibility	(χ)	($\mu m^3 kg^{-1}$)
Anhysteretic remanent magnetisation	(ARM)	(mA $m^2 kg^{-1}$)
Saturated anhysteretic remanent magnetisation	(SARM)	(mA $m^2 kg^{-1}$)
Isothermal remanent magnetisation	(IRM)	(mA $m^2 kg^{-1}$)
Saturated isothermal remanent magnetisation	(SIRM)	(mA $m^2 kg^{-1}$)

All magnetic measurements were undertaken on the wet sediment samples and then converted into mass specific units after drying for 48 hours at 30 °C. The results are expressed, where mass specific, as either mA $m^2 kg^{-1}$ or $\mu m^3 kg^{-1}$. kA m^{-1} is used for ratios between remanence magnetisation and susceptibility.

3.3.2.1 Magnetic Susceptibility (χ)

A Digico susceptibility bridge was employed for measuring magnetic susceptibility. Low frequency and high frequency susceptibility measurements were also undertaken using a Bartington Instruments magnetic susceptibility meter bridge on selected samples. The calibration of both susceptibility bridges were checked using a sample of ammonium ferrous sulphate ($(NH_4)_2Fe(SO_4)_2.6H_2O$) of known mass.

3.3.2.2 Remanent Magnetisations (ARMs and IRMs)

A peak alternating field of 99.5 mT, with a biasing direct field of 0.1 mT was employed to produce the SARM. After measurement the SARM was demagnetised

in alternating fields of 5, 10, 20, 40, and 80 milli tesla. Values of ARM in this thesis can be converted to χARM by dividing the ARM by the direct field used of 0.1mT. IRMs were induced in fields of 20, 40, 60, 80, 100, 200, 300, 1000, 2000, and 4000 milli tesla (mT). A combination of a Molspin pulse magnetiser, electromagnets and a 'TRILEC' pulse magnetiser were used to grow the IRMs. The remanent magnetisations at all stages of magnetisation or demagnetisation were measured using a Molspin spinner magnetometer (calibrated using a standard sample of magnetic tape of known magnetic moment) coupled to a BBC microcomputer. The remanence measurements were all converted into mass specific measurements by dividing by their dry mass. A variety of magnetic ratios were calculated from the susceptibility and remanence measurements including ARM/χ, SARM/SIRM, S_{100} and S_{20}.

3.3.2.3 Interpretation of Magnetic Data using Biplots

A combination of down core profiles and biplots were used to interpret the magnetic data. Biplots are a useful qualitative technique for assisting in the identification of the magnetic composition of a sample. Three bi-plots which were found particularly useful in this work are shown in Figure 3.6. Two of the three biplots employ magnetic ratios, rather than individual magnetic measurements, in order to eliminate the effects of magnetic concentration.

a) The biplot of ARM/SIRM vs S_{100} can be employed to discriminate between detrital magnetite, haematite/goethite, topsoil and bacterial magnetite. The ratio ARM/SIRM provides information on magnetic grain size and the extent of magnetic interaction between grains. Higher ARM/SIRM ratios (c. 0.2-0.3) tend to be indicative of single domain grains and a high degree of interaction. Samples with such high ARM/SIRM ratios are likely to be dominated by bacteria. Slightly lower ARM/SIRM quotients (c. 0.05 to 0.15) are typical of those found in topsoil. Low ARM/SIRM ratios (< 0.05) are characteristic of geological multi-

domain magnetite, single-domain magnetite or haematite/goethite of detrital origin. The S_{100} ratio illustrates the proportion of magnetite vs goethite/haematite present in a sample. Higher S_{100} ratios (>0.8) are indicative of magnetic properties dominated by magnetite whilst lower ratios(<0.4) indicate a more significant haematite or goethite component (Figure 3.6a)

(b) Biplots of ARM/χ vs ARM/SIRM assist in discriminating between top-soil and bacteria (Figure 3.4b). Whilst topsoil and bacteria both give rise to relatively high ARMs, topsoil is characterised by high susceptibility These two characteristics combine so that top soil dominated samples are characterised by ARM/χ ratios of c. 0-1.0 k Am^{-1}. Samples containing bacterial magnetosomes typically have ARM/χ ratios greater than 1 k Am^{-1} on account of the high ARM values found in bacteria (Figure 3.6b).

(c) A biplot of ARM vs ARM/SIRM can assist in the identification of bacterial magnetosomes, which are likely to be characterised by both high ARM values and by high ARM/SIRM ratios (Figure 3.6c).

It is important to note that in mixed assemblages these biplots reflect tendencies only. No single biplot is diagnostic.

3.3.3 Particle Size Analysis

Particle size analyses were undertaken using a Laser Coulter Counter, LS 200. The samples were pre-treated as outlined in 3.3.3.1 and 3.3.3.2 below in order to remove their organic and carbonate components before being chemically dispersed with calgon (4% sodium metahexaphosphate) and placed in an ultrasonic bath for physical dispersion before analysis. The samples were also sieved at 500 μm to remove the larger mineral and organic matter, which cannot be measured using the laser granulometer.

3.3.3.1 Carbonate Removal

1) One gram of sediment sample was added to 100ml of 20% acetic acid in a 250 ml beaker.

2) The sample was placed in an ultrasonic bath for 30 minutes and then left for 12 hours to settle.

3) The supernatant liquid was poured off and remaining sediment rinsed into 50 ml centrifuge tubes with distilled water.

4) The samples were centrifuged at 2000 rpm for 12 minutes, the supernatant poured off and the samples rinsed again with distilled water. This process was repeated until the acetic acid was very dilute.

5) The supernatant liquid was siphoned off.

3.3.3.2 Organic Carbon Removal

1) Following carbonate removal the remaining sediment was rinsed into a 50 ml beaker with a minimum amount of deionised water.

2) 30 ml of 100 vols hydrogen peroxide solution were added to each sample.

3) The beakers were placed in an ultrasonic bath for three hours at 50 ^{o}C and then left for 12 hours to settle.

4) The supernatant liquid was poured off.

5) The samples were rinsed and centrifuged several times at 2000 rpm for minutes until the sediment remained suspended.

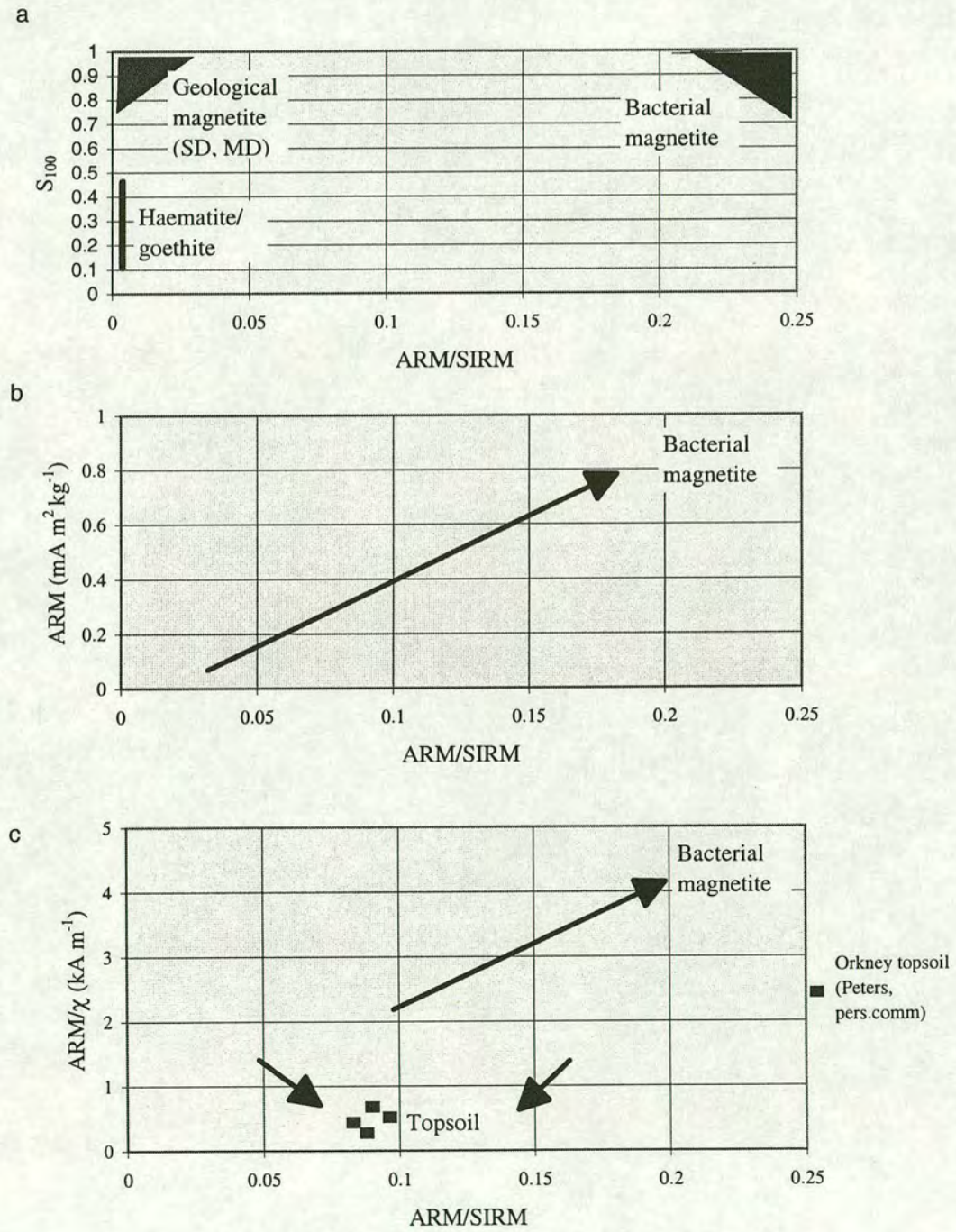

Figure 3.6 Interpretation of magnetic data using biplots. In mixed magnetic assemblages the biplots reflect tendencies only. Plot a) shows the distinction between geological magnetite, bacterial magnetite and haematite/goethite using ARM/SIRM and S_{100}. Plot b) indicates where bacterial magnetite plots on the basis of ARM and ARM/SIRM and plot c) shows the distinction between bacterial magnetite and topsoil on the basis of ARM/χ and ARM/SIRM. Data from Thompson and Oldfield (1986), Peters (1995) and Thompson (pers.comm).

3.3.3.3 Bulk Particle Size Splits

In order to obtain bulk particle size splits for magnetic measurements material was sieved at 500 μm and 63 μm. The sample was further separated at 10 μm and 2 μm using a centrifuge technique. Peters (1995) employed the following centrifuge settings for separating into three size fractions:

Size (μm)	Speed (revs/min)	Time (minutes)
10	300	3
0-2	1800	2.4

In this research better separations (validated using the laser coulter counter) were obtained using the following centrifuge settings:

Size (μm)	Speed (revs/min)	Time (minutes)
10	400	4
0-2	2500	4

Histograms of particle size vs concentration, obtained when the above centrifuge parameters were employed to split samples, are given in Appendix D.

As illustrated in Table 3.1 the particle size information produced by the Coulter Counter software has been used to group the sediment sizes into five different categories (Folk 1974) and to determine the relative contribution of each size fraction to the total sediment mass.

Table 3.1. Particle size classes employed in this study.

Fraction	Size range (μm) Folk (1974)	Size range (μm) Nearest Coulter Counter equivalent
Clay	0-3.9	0-3.8
Fine/medium silt	3.9-31	4.23-29.13
Coarse silt	31-62.5	32.43 - 61.70
Fine sand`	62.5-250	68-248.6
Medium/coarse sand	250+	276.76 +

3.3.4 X-Ray Diffraction

X-ray diffraction is a versatile, non-destructive analytical technique which can be employed to identify the mineralogy of samples. X-rays directed at a sample are diffracted at specific angles depending on the crystal lattice and thus the mineralogy of a sample. Each mineral therefore possesses a specific diffraction pattern. X-ray diffraction tends to be used as a qualitative technique, however semi-quantitative results can be obtained by comparing the peak heights produced by different minerals and inferring from these the relative proportions of each mineral (Gavish and Friedman 1973).

X-ray diffraction slides were prepared for a selection of samples from Semer Water and Raydale. A rigorous approach to sample preparation was employed. Despite initial encouraging results in the semi-quantitative determination of calcite, X-ray diffraction was not found, as originally hoped, to be of value in core correlation.

3.3.5 Chronology

A combination of ^{14}C, ^{210}Pb, ^{137}Cs dating and pollen analysis were used to establish sedimentation chronologies at each site. Eighteen ^{14}C accelerator mass spectrometry (AMS) dates have been obtained on macrofossils and wood fragments from Raydale

and Semer Water cores. The accelerator mass spectromotery (AMS) facility enables very small quantities of sample (c. 0.3 mg of carbon) to be dated. The radiocarbon ages were converted to calendar years by Per Sandgren (pers.comm) using a radiocarbon calibration program written by Stuiver and Reimer (1993). Additional datasets used in the calibration came from Pearson and Stuiver (1993) and Stuiver and Pearson (1993). Peter Appleby established sediment chronologies for cores from each site using ^{210}Pb and ^{137}Cs.

Birks (1989) has compiled isochrone maps illustrating the first post-glacial rise in pollen percentages of the major tree taxa in the British Isles. 135 radiocarbon dated pollen diagrams have enabled the construction of maps for each major taxa, illustrating the patterns and timescales of colonisation. As an example Figure 3.7 illustrates the colonisation of *Alnus glutinosa* (alder) in the British Isles. Information from such isochrone maps is employed in this study to assist in establishing chronologies for the sediment cores obtained from Raydale.

3.3.6 Pollen Analysis

In December 1995 the author attended a one week course entitled 'An introduction to pollen analysis' at the Environmental Change Research Centre, University College, London given by H.J.B. Birks. Subsequently pollen counts were undertaken on samples from Giddings cores A, B and C from Raydale. The pollen analysis simply aimed to assist in establishing a chronology by placing each sample into the local pollen assemblage zone, therefore counting was restricted to ten taxa and to the identification of two hundred pollen grains per horizon. The counting concentrated on identifying indicators of vegetation change and woodland clearance episodes, in particular the identification of well dated changes, such as the *Alnus* rise at c. 7000 - 7500 years BP in Northern England (Birks 1989). Moore *et al.* (1991) provide an illustrated account of pollen analysis techniques including its application, errors and detailed key for pollen grain identification. Pollen samples were prepared in the

Geography Department, University of Edinburgh by Dr B. McCulloch following the method described in Moore *et al.* (1991).

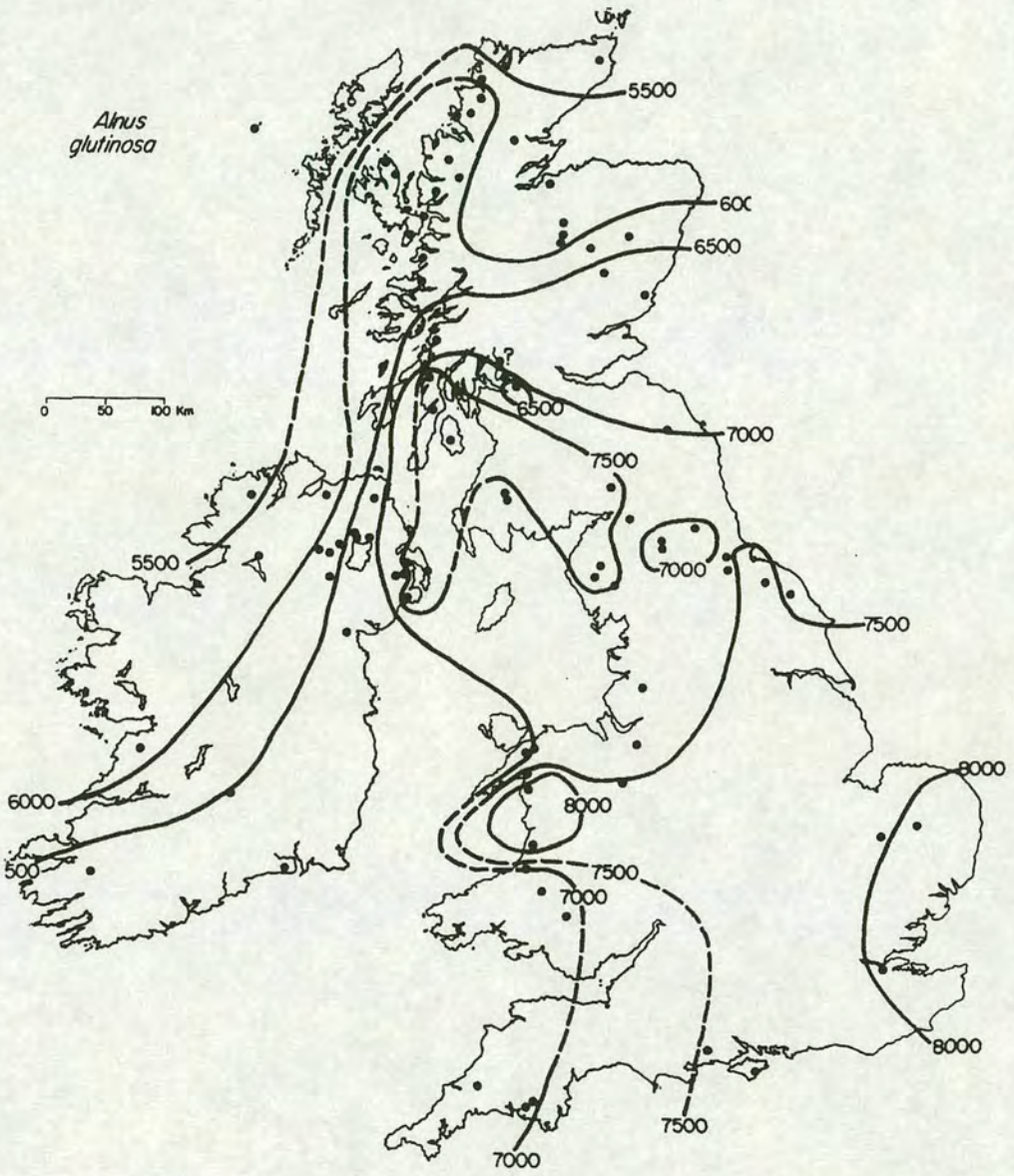

Figure 3.7 An isochrone map illustrating the colonisation of *Alnus* across the British Isles during the Holocene (from Birks 1989). Dates given are in radiocarbon years BP. The figure shows that *Alnus* colonised the British Isles from the south east, arriving in the Humber catchment between 7000 and 8000 radiocarbon years BP.

3.3.7 Sediment Composition

Bulk density was determined by dividing the dry weight of the sample by the volume of the sediment sample cube (6 cm^3) or pot (10 cm^3). The organic carbon content was estimated from loss on ignition measurements obtained by determining the loss in weight after heating the sediment samples in a muffle furnace at 550 °C for 12 hours. Bengtsson and Enell (1986) suggest that the organic carbon content is usually 50-60% of the loss on ignition. A figure of 55% is employed in this study. In order to determine the carbonate content the samples were returned to the furnace for a further 4 hours heating at 925 °C, and a further loss in weight determined, for conversion into carbonate content. Bengtsson and Enell (1986) suggest that the weight loss between 550 and 925 °C should be multiplied by 1.36 to obtain the carbonate content. Bengtsson and Enell (1986) provide a more thorough description of the determination of bulk density, water, organic and carbonate content.

3.3.8 Alpha and Beta Counting

Alpha and beta counts of natural radioactivity have, in previous studies (Shankar *et al.* 1994), assisted in the identification of source material in catchments. The technique can be carried out on the same bulk material used for the magnetic studies without the need for any pre-treatment, and thus is a rapid additional characterisation technique. In this study alpha and beta counts were measured on sediment samples from Semer Water. It was thought that the shale component of the Carboniferous series of rocks within the Semer Water catchment may contain alpha emitting members of ^{238}U and the ^{232}Th series and beta decay of ^{40}K. In this study the technique was, however, unsuccessful. The counts were exceptionally low and despite grouping samples together to get a sufficiently high count, no significant difference between samples were found.

3.3.9 Diatoms

The application of diatom analysis techniques to assist in core correlation, particularly of littoral cores at Semer Water was considered. The author attended a two week course at the Environmental Change Research Centre, University College, London on diatom analysis. However the poor preservation of the diatoms within the Semer Water sediment and the time consuming nature of diatom analysis made this technique in appropriate for the scope of this project.

3.3.10 Sediment Yield Calculation

The calculation of sediment yield is a major part of this project. The procedures used are summarised below.

1) Obtain multiple cores from the lake basin.
2) Correlate cores using whole core susceptibility scanning.
3) Sub-sample cores.
4) Correlate cores (visual, magnetics, diatoms, pollen, chemistry)
5) Determine the dry weights and dry densities.
6) Establish a chronology (^{210}Pb, ^{137}Cs, ^{14}C, pollen).
7) Determine the dry mass accumulation rate within each sediment core and obtain a mean.
8) Multiply 7) by the area of active sedimentation within the lake.
9) Divide the total mass of material deposited by the number of years in each time period to give a combined influx of allochthonous and authochthonous material.
10) Determine the average organic content (%) of sediment deposited within each time period.
11) Determine the carbonate content (%).
12) Determine the biogenic silica (diatom) component (%).
13) Subtract 10), 11), and 12) from the bulk influx 9), the result being the influx of minerogenic material into the lake per year.

14) The influx can be converted to yield by dividing by the catchment area.

A more detailed account of calculating sediment yield, including some of the limitations of the approach is provided in Dearing (1986).

3.4 Modelling

During the course of the project it became apparent that relating sediment deposition in a lake to catchment erosion was not straight forwards. Furthermore empirical relationships found by earlier workers between catchment area and lake deposition or catchment to lake area and sediment yield were found not to be entirely satisfactory. Hence a more quantitative approach was investigated. The basic idea was to try to employ a statistical approach to use catchment characteristics to improve, or modify in some way, the empirical relationships of earlier workers such as Brune (1950), Fournier (1960) or Dearing and Foster (1993) (see section 2.3.2). This involved determining the physical and land-use characteristics of some 30 catchments from Britain with sediment yield data and testing simple erosion models and relationships on the new data set. The sediment delivery factor was found to be of paramount importance in this very difficult problem. Potential data sets obtained for use in these statistical, erosion studies are described below.

3.4.1 Universal Soil Loss Equation (USLE)

As described in section 2.3.3 in order to calculate yield using the USLE the following equation is employed:

$$E = R \cdot K \cdot LS \cdot C \cdot P$$

Where E is the mean annual soil loss in tonnes per hectare (t ha^{-1}), R is the rainfall erosion factor, K is the soil erodibility factor, LS is the slope factor, C is the crop management factor and P is the erosion control practice factor. These five factors are now considered in turn.

3.4.1.1 Estimating R (rainfall erosion factor)

Morgan (1995) suggests that rainfall erosivity is a function of intensity, duration and of the mass, diameter and velocity of the raindrops. Wischmeier and Smith (1958) relate soil loss to kinetic energy (E) and the maximum 30-minute rainfall intensity (I_{30}). They proposed that an EI_{30} factor could be employed to determine the extent of erosion occurring as a function of rainfall. The rainfall erosivity factor is based on the mean annual EI_{30}. Here E is in J/m^2 and I_{30} is in mm/hr and

$$R = EI_{30}/1000$$

Morgan (1980) has mapped the UK into regions of differing erosivity (Figure 3.8). In this study of the British Isles an I_{30} value of 75 mm/h is employed throughout. This Figure represents the maximum value recommended by Wischmeier and Smith (1978).

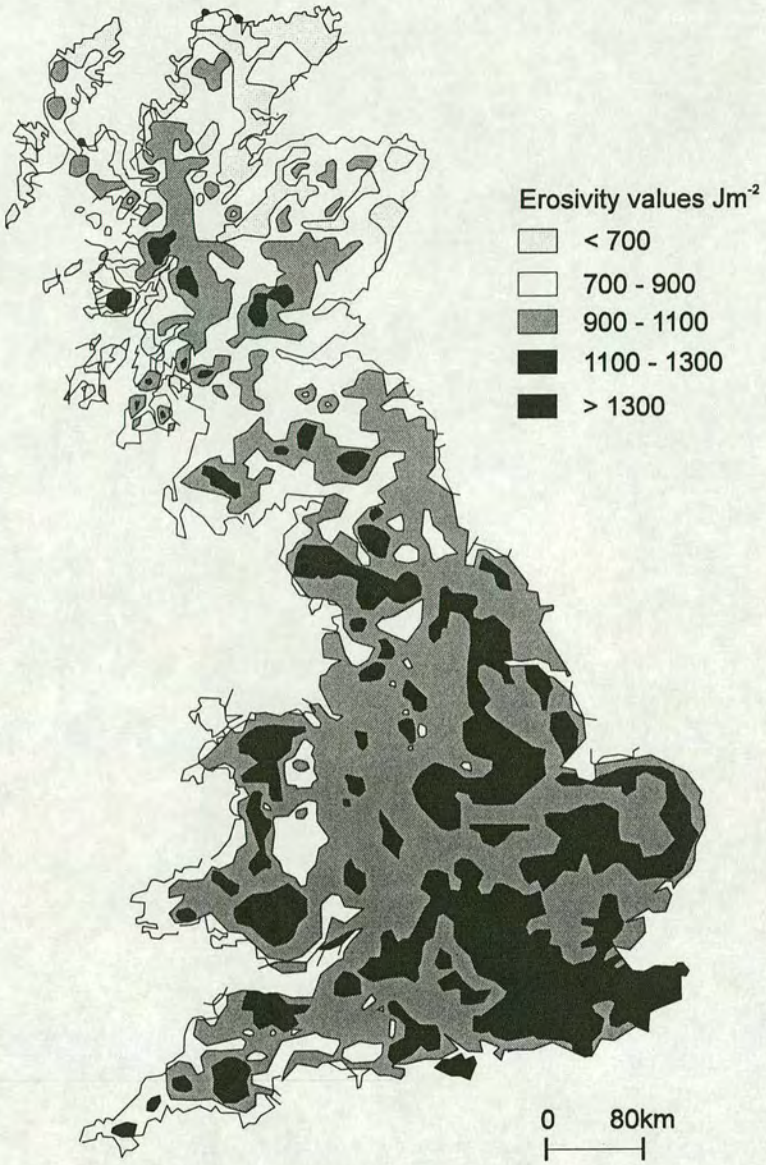

Figure 3.8 Mean annual erosivity in Great Britain (after Morgan 1980).

3.4.1.2 Estimating K (soil erodibility factor)

K is defined as mean annual soil loss per unit of R for a standard condition of bare soil, recently tilled up-and-down slope, with no conservation practice and on a slope of 5 ^{o} and 22 m in length. In this study values of K are obtained from the standard nomograph (Figure 3.9) (after Wischmeier *et al.* 1971). The parameters needed to obtain K are (i) the percentage of silt, fine sand and sand in the soil (ii) the soil structure on a scale of 1-4 and (iii) the permeability on a scale of 1 (rapid) to 6 (very slow). In this study soil maps and published soil profile analyses were used to estimate all these parameters (section 3.4.2.4).

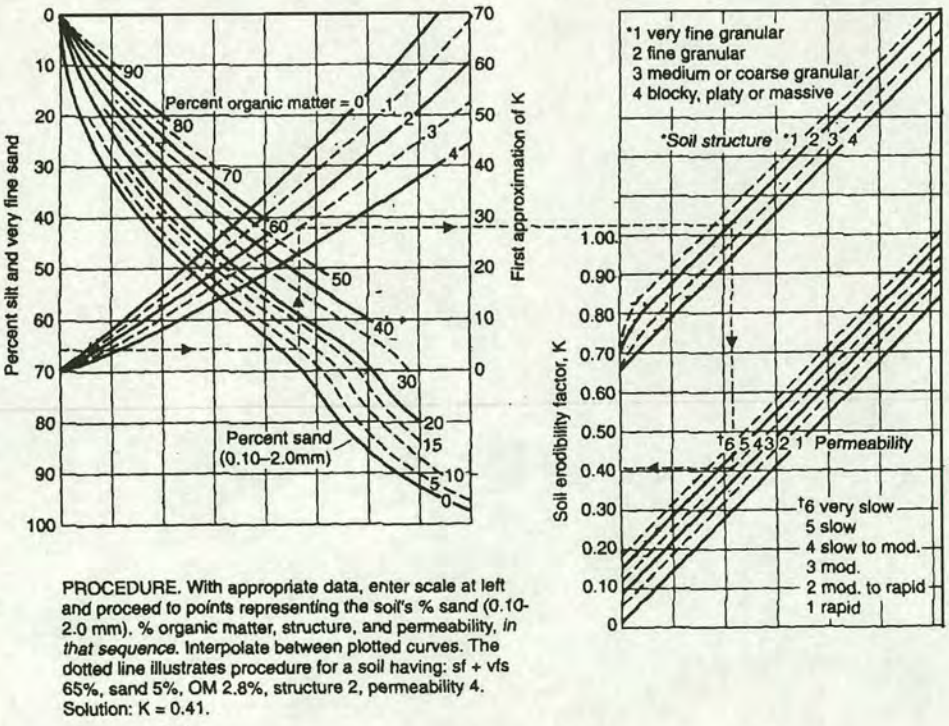

Figure 3.9 Nomograph for calculating the K value for incorporation in the Universal Soil Loss Equation (after Wischmeier *et al.* 1971). An estimate of the soil erodibility factor (K) can be gained based on the following soil characteristics: The proportion of silt and fine sand, sand, organic matter, soil structure and soil permeability.

3.4.1.3 Estimating LS (slope factor)

The factors of slope length (L) and slope steepness (S) are combined in an index which expresses the ratio of soil loss under a given slope steepness and slope length to the soil loss from the standard condition of a 5 ° slope, 22 m long, for which LS = 1.0. The following equation can be employed to determine LS:

$$LS = (x/22.13)^n (0.065 + 0.045s + 0.0065s^2)$$

Where x is the slope length (m) and s is the slope gradient in percent. The value of n should be varied according to slope steepness and is 0.5 for low slopes. Morgan (1995) discusses the selection of n values in detail. Proposed values range between 0 and 2.0. In this study a mid-point value of 1.0 has been employed.

3.4.1.4 Estimating C (crop management factor)

The crop management factor represents the ratio of soil loss under a given crop to that from bare soil. The following C values have been employed in this study (After Wischmeier and Smith 1978).

Crop	C ratio
Bare soil	1.00
Forest	0.001
Meadow grass	0.01-0.025
Wheat	0.10-0.40

The C value in catchments where arable crops are grown needs to be varied throughout the year to take account of fallow periods and variations in the density of crop cover. The year is divided into periods corresponding to different stages of crop growth. The C value is also weighted using rainfall data. Thus the proportion of the

annual rainfall falling each month is employed to calculate weighted C values for each month which are totalled to create an annual C value. Appendix E demonstrates the calculation of C values for catchments which include arable land.

In this study the dominant arable crop found in catchments studied is wheat. Winter barley may also be significant in some catchments however a C value for the latter is unobtainable, and in this study, parity with wheat has been assumed.

3.4.1.5 Estimating P (erosion control measures)

P relates to practises such as terracing. It is not applicable in this study and so can be set to 1.

3.4.2 Lake and Catchment Characteristics for use in Sediment Flux Models.

During the course of this work catchment characteristics were determined for 30 published studies reporting sediment yield on the basis of lake and reservoir sediment accumulation rates. Of the 30 sediment yield estimates 14 had been determined from reservoir re-surveys and 16 have employed lake sediment cores.

3.4.2.1 River Length

River length data were obtained for each catchment. Having defined the watershed boundary and identified all the streams draining into the lake/reservoir the length of each stream marked on a 1:25 000 OS pathfinder series map was measured using a map distance measurer and the total calculated.

3.4.2.2 Slopes

An average slope was determined for each catchment. Ten equidistant points were identified along the perimeter of each catchment. The altitude of each of these ten points was noted. A map distance measurer was then employed to measure the distance in a straight line from each of these ten points to the edge of the lake/reservoir and the gradient calculated (in terms of percentage) by dividing the altitude difference by the distance from the catchment boundary to the lake/reservoir. Finally an average slope was obtained from the ten gradients.

3.4.2.3 Catchment Altitude

The average altitude of the ten points on the catchment perimeter (employed in 3.4.2.2) was noted and an average catchment altitude estimated by adding the average boundary altitude to the altitude of the lake and dividing this sum by two. The altitude of each lake has been obtained from the 1:25 000 OS Pathfinder maps.

3.4.2.4 Soils

Information on the soil types within each catchment was obtained from Soil Survey maps of England and Wales and of Scotland. Some published papers listed the soil series and the proportion of each series within the catchment studied. In most cases information on soil type was obtained from soil survey maps (Sheets 1-6, Soil Survey of England and Wales 1983), and the proportion of each soil series within each catchment estimated directly from the maps. The physical characteristics of each soil series were obtained from of soil profiles analysed by Avery (1990), Ragg *et al.* (1984), Findlay *et al.* (1984) and Rudeforth *et al.* (1984). Information pertaining to the permeability of each soil series was obtained from the soil unit descriptions provided in the Handbook of the Soil Survey of England or Wales (1983), or the Soil

Survey of Scotland (Sheets 1-6, Macaulay Institute for Soil Research 1984). Information on organic content, silt and sand components and permeability was used to calculate the K factor for use in the USLE. Appendix E summarises the mean K value for each of the soil series present in the catchments studied

3.4.2.5 Land Use

Land use information has been obtained for each of the 30 catchments using a combination of published papers (see Appendix F) and land use maps (Macaulay Land Use Research Unit, Sheets 1-7, 1994 and Ministry of Agriculture, Fisheries and Food - Agiricultural Land Classification in England and Wales, Sheets 1-6, 1977). The land use information was employed to calculate a C factor (cf Section 3.4.1.4).

3.4.2.6 Precipitation

Annual average and maximum mean monthly precipitation data was obtained for each site from information supplied by the Climate Research Unit (CRU) at the University of East Anglia. Where precipitation data was not available for sites within the catchment precipitation data from a nearby station at a similar altitude was employed. The p^2/P index has been calculated for each site (refer to Section 2.3.3).

3.4.2.7 Lake Perimeter

The perimeter of each lake and reservoir was measured using a map distance measure. Lake perimeter relates to the length of potentially erodible lake bank.

3.4.2.8 Regression Analysis

Stepwise regression and standard regression techniques were employed in order to select the most significant catchment variables in accounting for variations in sediment flux within each catchment. These statistical analyses have been undertaken using the Minitab statistical package.

3.5 Summary

- The three catchments studied - Semer Water, Gormire and Hornsea Mere - have very different physical characteristics.

- In order to determine sediment yield within each catchment a combination of field work and laboratory analysis was undertaken. The field techniques involved sediment coring, resistivity, surveying and catchment sampling. Laboratory studies involved mineral magnetic measurements, X-ray diffraction, pollen counting and particle size analysis.

- The USLE was used to estimate soil erosion in 30 British catchments for which lake sediment estimates of yield had previously been published or were obtained in this study.

- Regression analysis was undertaken to investigate relationships between physical catchment characteristics, land use and sediment influx in Britain.

Chapter 4

Lake Semer Water

4.1 Introduction

At Semer Water catchment samples and lake sediment cores have been collected and characterised magnetically. Variations in sediment density and lithostratigraphy have also been noted. In Chapter 8 the flux of sediment into Semer Water is estimated using accumulation rates reported by Appleby (1998) for three cores from Semer Water. The sediment flux into Semer Water is then compared with that for Raydale (Chapter 5) and used to calculate sediment influx and yields for the Semer Water catchment.

4.2 Catchment Samples

Forty-two catchment samples were collected from a variety of locations within the catchment, as illustrated in Figure 4.1. Catchment material included samples from sheep erosion scars, stream beds, tractor wheelings, behind walls and within gullies (Table 4.1).

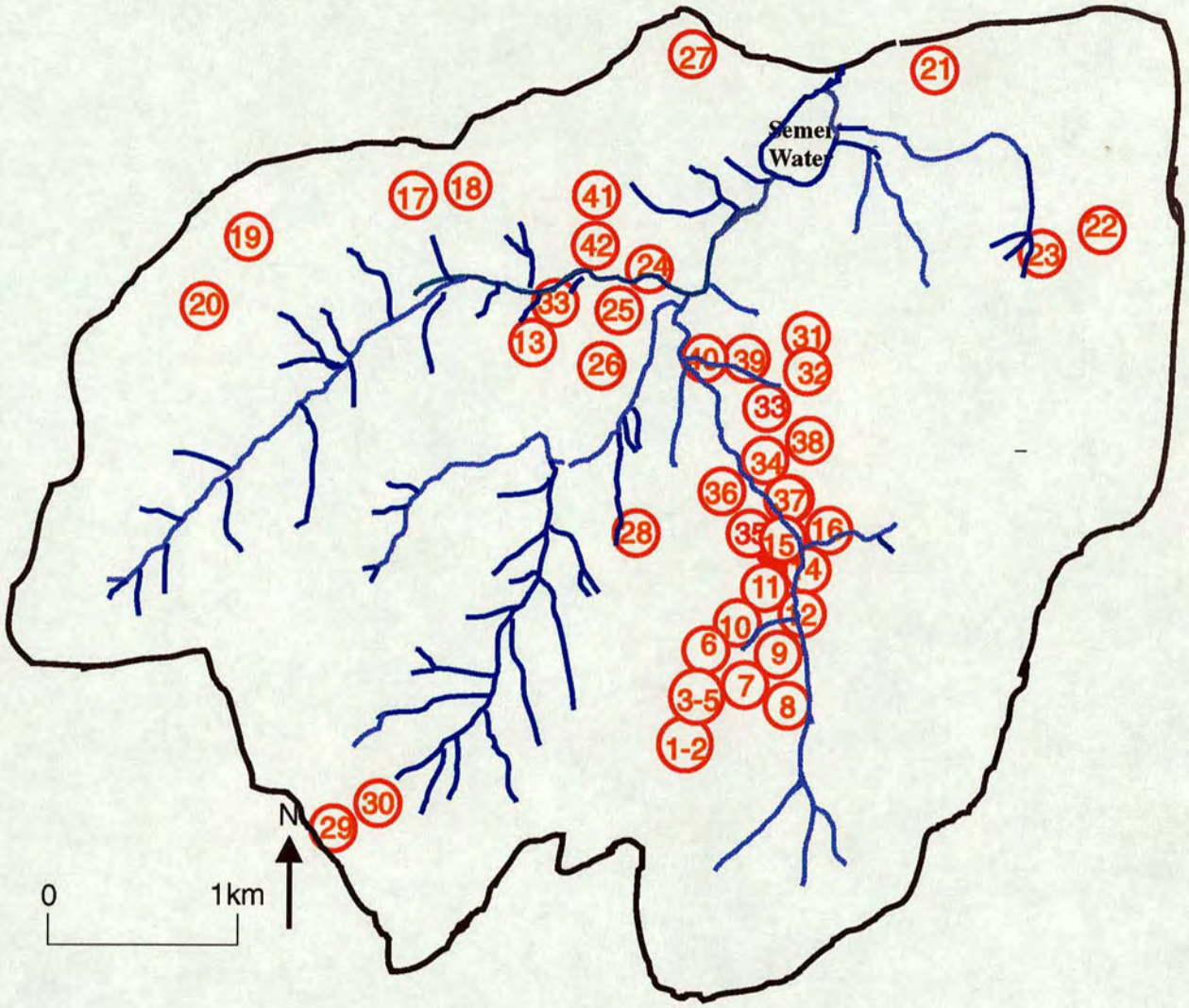

Figure 4.1 The location of catchment sample sites within the Semer Water catchment. Forty-two catchment samples were collected in total and characterised magnetically. The samples include bedload, streambank, topsoil, subsoil and gully sediment. The major river channels are also shown.

Table 4.1 The origin of catchment samples within the Semer Water catchment

Samples	Origin
1, 2 9, 10, 11, 12	Bedload
3, 4, 5, 7, 8, 13, 14, 16	Stream bank
6	Exposed glacial diamict
17, 18,	Subsoil
19, 20	Peat
21, 29, 30	Topsoil
22, 23,25, 26, 28, 40, 41, 42	Gully
24, 27	Eroding hillslope scar
36, 38, 39	Behind walls
37	Tractor wheelings
31, 33, 34, 35	Puddles

4.2.1 Magnetic Characterisation of Catchment Samples

The magnetic characteristics of Semer Water catchment samples (summarised in Table 4.2) are particularly diverse. Individual magnetic values or ratios were not found to relate to any one source.

Table 4.2 A summary of the magnetic properties of catchment samples.

	χ ($\mu m^3 kg^{-1}$)	ARM ($mA\ m^2 kg^{-1}$)	IRM_{100} ($mA\ m^2 kg^{-1}$)	SIRM ($mA\ m^2 kg^{-1}$)	A/S	S_{100}	ARM/χ ($kA\ m^{-1}$)
Mean	0.059	0.058	1.09	1.51	0.043	0.595	0.247
St dev	0.133	0.127	1.74	2.32	0.029	0.179	0.173
Min	0.000	0.000	0.01	0.02	0.015	0.171	0.034
Max	0.880	0.743	6.64	10.1	0.157	0.885	0.844

With a mean susceptibility value of just 0.059 $\mu m^3\ kg^{-1}$ the catchment samples are characterised by very low concentrations of magnetic minerals arising from the underlying, weakly magnetic, limestone bedrock. Two samples (19 and 22), were found to be characterised by particularly low S_{100} quotients of 0.171 and 0.180 respectively and by low ARM/SIRM ratios of 0.024 and 0.033 respectively, indicative of either goethite or haematite. Their IRM acquisition curves demonstrate

continued increases in magnetisation in fields up to 4T, indicating that most of the magnetic signature derives from goethite rather than haematite (Figure 4.2). These two samples have IRM_{2T}/IRM_{4T} ratios of 0.54 and 0.61 (Table 4.3). Their low IRM_{4T}/χ ratios of 6.69 and 7.77 kA m^{-1} in provide even further evidence for the presence of goethite. Appendix G includes the results of four magnetic measurements made on each catchment sample.

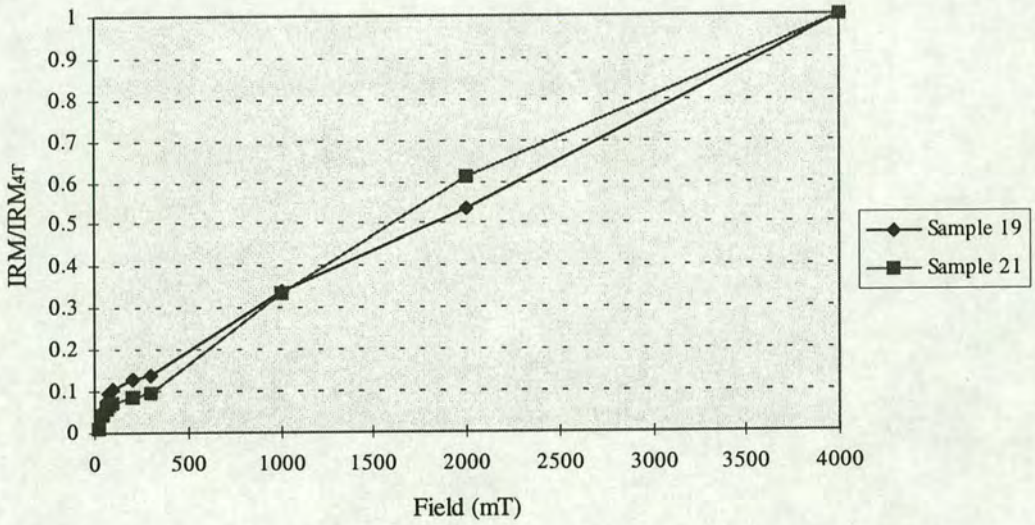

Figure 4.2 IRM acquisition curves for catchment samples 19 and 22 from Semer Water. The significant increase in magnetisation above a field of 1T infers that the magnetic signature is controlled by goethite, rather than haematite.

Table 4.3 Selected magnetic properties of catchment samples 19 and 22

Catchment sample	19	22
IRM 2T (mA m^2 kg^{-1})	3.13	2.77
IRM 4T (mA m^2 kg^{-1})	5.82	4.51
χ (μm^3 kg^{-1})	0.87	0.58
IRM_{4T}/χ (kA m^{-1})	6.69	7.77
IRM_{2T}/IRM_{4T}	0.54	0.61

Further interpretation of the magnetic signature recorded in the Semer Water catchment samples can be gained from biplots of (i) ARM/SIRM vs S_{100} and (ii) ARM/SIRM vs ARM/χ (Section 3.3.2.3). As illustrated in Figure 4.3 the forty-two catchment samples span a wide range of magnetic mineralogical compositions.

Some samples are dominated by magnetite, others by goethite/haematite while five samples are characterised by ARM/SIRM ratios in excess of 0.1 indicating the presence of either topsoil or magnetotactic bacteria. With reference to Figure 3.4a (Chapter 3) Figure 4.4 indicates that the catchment samples are characterised by low ARM/χ ratios typical of detrital or topsoil derived magnetic minerals rather than magnetotactic bacteria. No correspondence between ARM/SIRM, S_{100} or ARM/χ ratios and catchment sample origin was observed at Semer Water. Those catchment samples found to be dominated by magnetite (e.g. samples 2, 5 and 7) do not all arise from topsoil, but originate from a range of bedload and stream-bank deposits at High Lane, above Stalling Busk, Marsett Bridge and Bardale Beck. The most goethite dominated samples (19 and 22), originate from exposed glacial deposits at High Lane, above Stalling Busk, in the catchment.

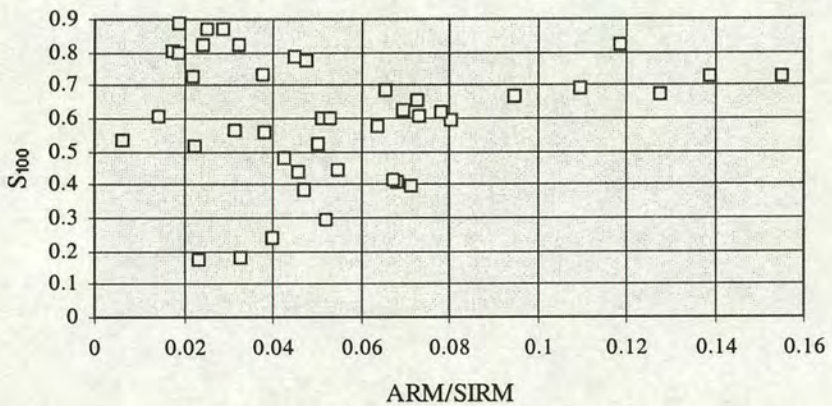

Figure 4.3 Biplot of ARM/SIRM and S_{100} ratios of Semer Water catchment samples. The biplot can be interpreted to indicate the magnetic mineralogy and hence the origin of the magnetic signature within the samples. Magnetite plots in the top left of the diagram, goethite/haematite in the bottom left and bacteria in the extreme top right (refer to Figure 3.4a, Chapter 3).

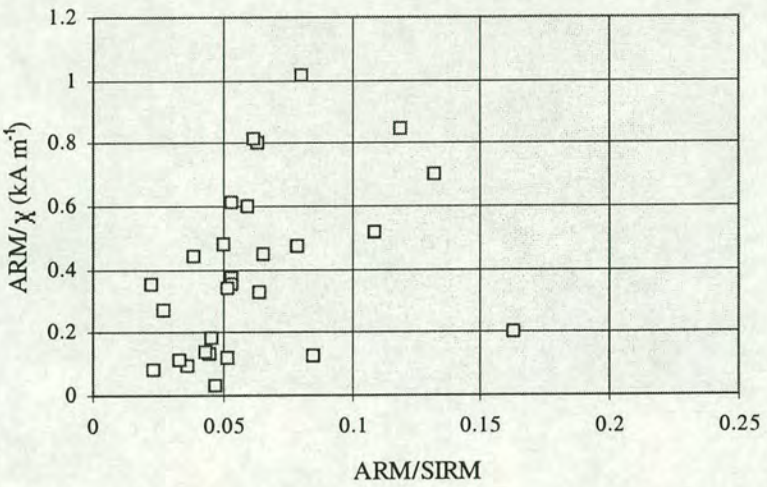

Figure 4.4 ARM/χ and ARM/SIRM ratios of Semer Water catchment samples. The biplot can be employed to distinguish between topsoil magnetic minerals (which plot towards the lower left of the figure) and magnetotactic bacteria (which plot towards the top right hand corner). The catchment samples tend to be characterised by low ARM/χ and ARM/SIRM ratios indicative of a magnetic mineralogy dominated by topsoil rather than bacterial magnetosomes (refer to Figure 3.6b, Chapter 3 for further information).

4.3 Sediment Cores

4.3.1 Collection

A suite of fifteen one-metre Mackereth cores were obtained along two transects within Semer Water in September 1994. Figure 4.5 illustrates the location of the cores and their water depths. The longer of the two transects followed a deep kettle hole trench running north east to south west. Attempts were made to obtain six-metre cores from the deepest point, 10.5 m, in the lake, however major difficulties were encountered. The longest cores obtained (SL1 and SL2) recovered only 2.25 and 2.4 m of sediment respectively and the operation had to be aborted. Figure 4.6 shows a bathymetric map compiled from water depth measurements made whilst obtaining the sediment cores and bathymetric data provided in Barlow (1994).

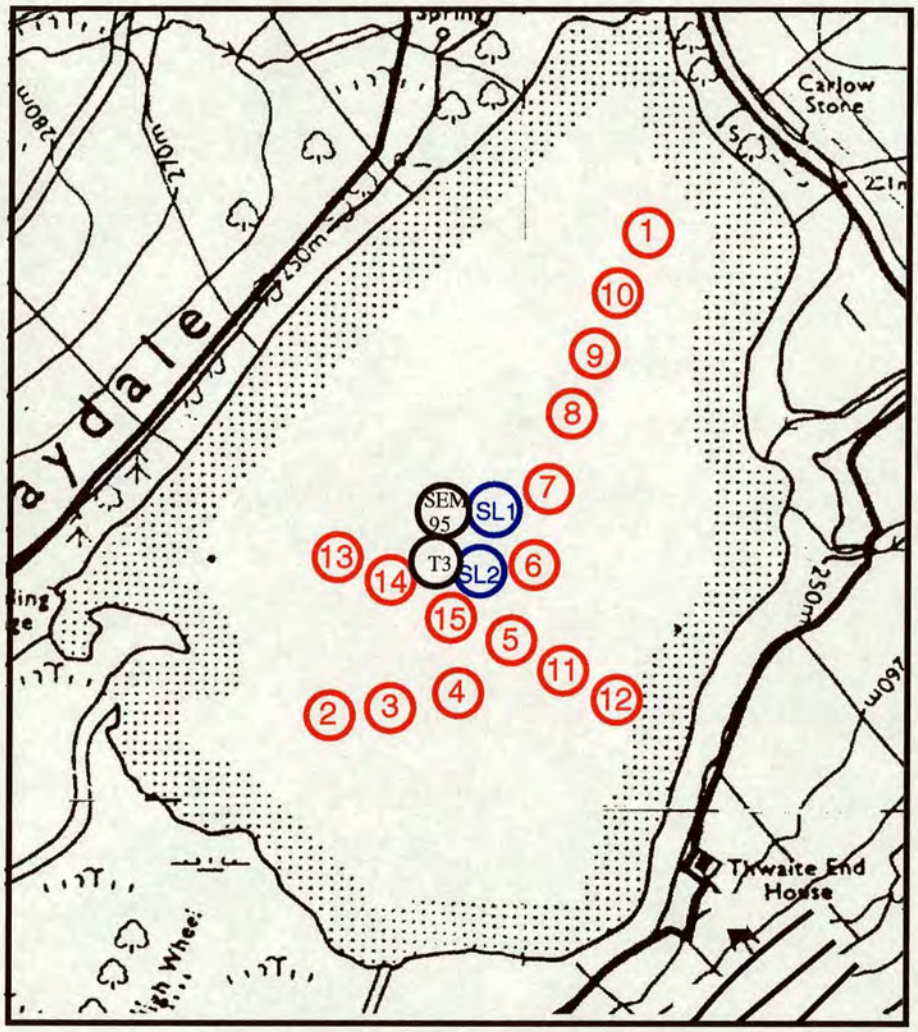

1 metre cores

3 metre cores

SEM 95 — 1 metre core obtained by the ECRC, University College, London.

T3 — 1 metre core obtained previously by Liverpool University

Core	Water depth (m)	Core	Water depth (m)
1	2.5	10	1.5
2	3.0	11	2.5
3	5.5	12	1.5
4	8.5	13	1.2
5	9.5	14	2.5
6	10.5	15	4.5
7	8.0	SL1	10.5
8	6.0	SL2	10.0
9	7.0		

Figure 4.5 The location of Mackereth cores at Semer Water. 17 Mackereth cores were collected during fieldwork in October 1994. Two cores (T3 and SEM95) had previously been collected by researchers at Liverpool and London Universities respectively.

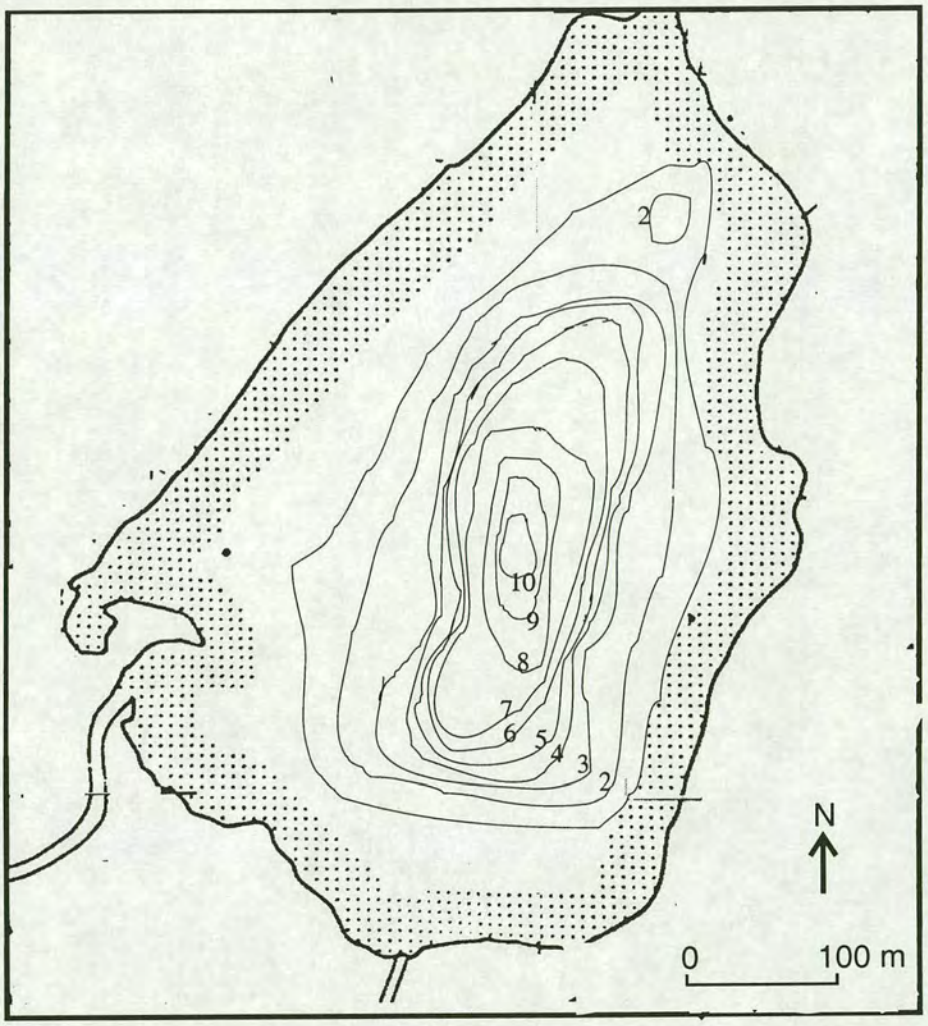

Figure 4.6 Bathymetric map of Semer Water. The water depth is contoured in metres. Based on depth water determinations made when obtaining the lake cores and bathymetric data provided in Barlow (1994).

4.3.2 Lithostratigraphy

The sediment cores collected from Semer Water display little variation in stratigraphy with depth. The cores are composed of fine grained sediment of clay/silt size. Semer Water cores SL1 and SL2 display mean sediment densities of 0.590 and 0.592 g cm^{-3} respectively (Figure 4.7). The complete sediment density data for each core is provided in Appendix H. Changes in density with depth (Figure 4.7) in core SL1 from Semer Water include specific horizons where abrupt density changes occur, these may be indicative of hiatuses in the sediment. The sudden decrease in density at a depth of 94 cm in core SL1 corresponds to an increase in the proportion of very fine sediment in the core.

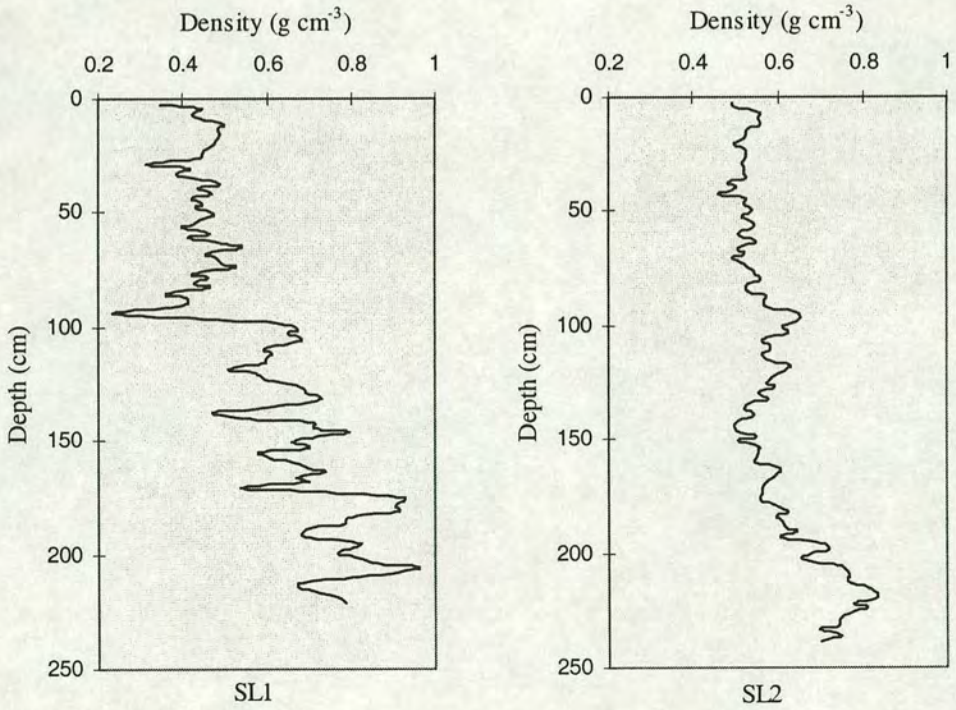

Figure 4.7 Changes in sediment density with depth in cores SL1 and SL2

4.3.3 Total Organic Carbon and Carbonate Content

The organic carbon and carbonate content of samples obtained from lake core SL1 is given in Table 4.4.

Table 4.4 Organic carbon and carbonate content of samples from core SL1.

Depth (cm)	Organic (%)	Carbonates (%)
13.1	10.6	1.6
43.8	13.5	1.4
113.8	10.7	2.6
137.9	11.4	2.3
153.2	10.6	21.4
168.5	10.6	1.6
192.6	11	2.0
210.6	9.5	3.5

The average organic content of sediment in Semer Water is 11%. The variation within the core is relatively small (std.dev. 1.1) . With the exception of one value the carbonate content varies around a mean of 2.1% (std. dev.0.7). The outlying value at a depth of 153.2 cm can probably be attributed to a shell fragment.

4.3.4 Chronology

4.3.4.1 ^{210}Pb and ^{137}Cs Activity in Cores 6, T3 and ECRC Core SEM95

^{210}Pb and ^{137}Cs analysis has been undertaken on samples from core 6 by P. Appleby at the University of Liverpool. Appleby (1998) reports a mean accumulation rate of 0.9 cm a^{-1} in core 6 for the period since 1950. Appleby (1998) has determined additional chronologies from two cores T3 and SEM95 collected by Liverpool and London Universities respectively. For core SEM95 Appleby (1998) reports an average accumulation rate of about 0.37 cm per year over the time period 1959-1993.

For core T3 Appleby estimates a sediment accumulation rate of 0.6 cm per year for the period 1979-1994.

4.3.4.2 ^{14}C Analysis

Five samples from the long cores SL1 and SL2 were dated using AMS radiocarbon analysis. Tables 4.5 summarises the results. The three samples taken from the uppermost sediment in cores SL1 (0.40 m, 0.65 m) and SL2 (0.1-0.2 m) were too young for ^{14}C dates to be determined.

Table 4.5 A summary of the Semer Water radiocarbon results

Sample	Core	Depth (m)	Composition	Publication Code	Radiocarbon age (BP± 1σ)	Calibrated age (BP) (1σ range)	
Semer Water 14	SL1	0.40	twig	AA-26406	post-1950		
Semer Water 15	SL1	0.65	root	AA-26407	post-1950		
Semer Water 16	SL2	0.10 - 0.20	twig	AA-25554	post-1950		
Semer Water 17	SL2	1.00 - 1.10	twig	AA-25555	260 ± 60	296	0-421
Semer Water 18	SL2	1.80 - 2.00	twig	AA-25556	460 ± 45	509	492-523

Notes:

i) Where a depth range is indicated more than one sample was obtained and grouped in order to provide a sufficient mass (> 0.3 mg carbon) of material for dating.

ii) Samples prepared at the NERC Radiocarbon Lab., East Kilbride and ^{14}C AMS analysis carried out by the University of Arizona NSF AMS Facility.

The AMS date of 296 BP obtained on a twig fragment from 1.00-1.10 m in core SL2 is characterised by a high potential error (age range at the 1σ level of between 0 and 421 years BP) and thus cannot be used to calculate an accurate accumulation rate for the uppermost section of the core. Using the calibrated age of 509 BP (range 492-523 at 1σ level) for a sample from a depth of between 1.80 and 2.00 m an average accumulation rate of 0.34 cm a^{-1} (range:0.32 - 0.37 cm a^{-1}) can be estimated for the period since 1441 (1950-509) (Table 4.6).

Table 4.6 Sediment accumulation rates in core and SL2

Core	Sediment range (cm)	Sediment accumulation (cm)	Time period (calendar years) (years BP± 1σ)	Sediment accumulation rate (cm a^{-1})
SL2	0-200	180-200	509 (492-523)	0.34 (0.32 - 0.37)

The sediment accumulation rates determined from the ^{14}C date is slightly lower than those reported by Appleby (1998) for cores 6, T3 and SEM95 using ^{137}Cs and ^{210}Pb dating techniques.

4.3.5 Lake Sediment Magnetic Measurements

Sediment cores obtained from Semer Water have been characterised magnetically. Four measurements (χ, ARM, IRM_{100} and SIRM) were made on samples taken at c. 2 cm intervals down each of the 17 cores. The results are tabulated in Appendix J. In order to summarise this large body of data the results are first plotted with depth for two representative cores. Figures 4.8 and 4.9 show changes in sediment density χ, ARM, IRM_{100}, SIRM, ARM/SIRM, S_{100} and ARM/χ for the deep water (6) and the shallow water cores (10). Secondly the parameters χ and ARM/SIRM are plotted with depth for the 15 surface cores (Figures 4.10 and 4.11).

Some similarities between the magnetic trends displayed in these cores are found. As illustrated in Figure 4.10 a general decline in χ can be observed in all 15 cores with more rapid decreases occurring in cores 5, 6,11 and 15. However cores 7 and 8 display a rather different trend in χ with depth. The magnetic results have been normalised by dry mass, so the changes are not simply due to water content. Figure 4.11 also shows a general increase in ARM/SIRM towards the mud/water interface. Cores 7, 8, 9 and 14 display particularly marked minimum ARM/SIRM values towards the centre of the cores.

On closer inspection it is found that these various correlations do not agree closely with one another. Variation is not uniform across the lake basin. Magnetic features occurring in some profiles are not observed in other profiles, and it is reluctantly concluded that magnetic techniques cannot be used for core correlation at Semer Water. Appleby (1998) reports that ^{210}Pb and ^{137}Cs analysis of cores T3 and SEM95 have identified the presence of hiatuses in the sediment cores collected, providing further evidence of discontinuous sedimentation in Semer Water.

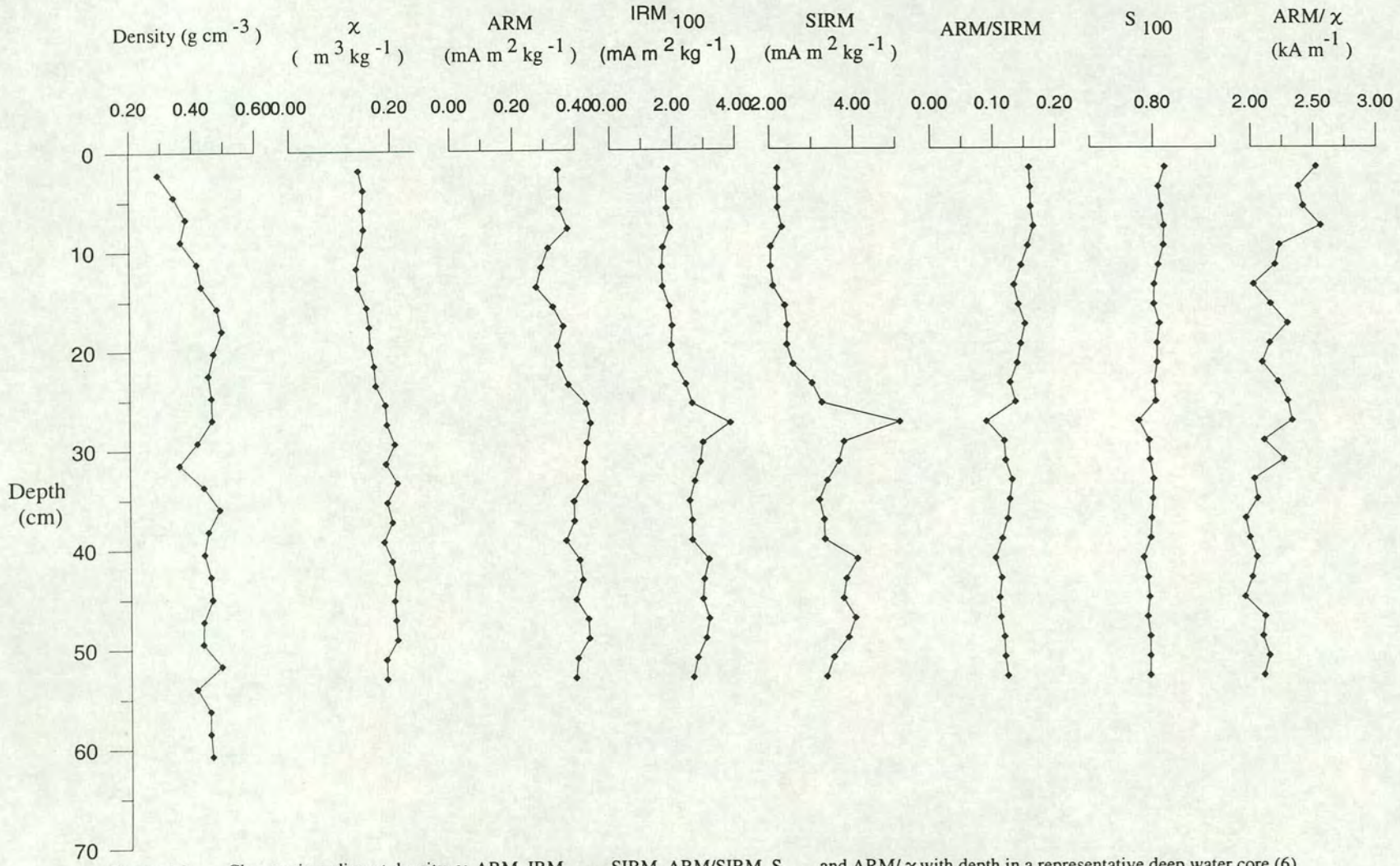

Figure 4.8 Changes in sediment density, χ ARM, IRM $_{100}$, SIRM, ARM/SIRM, S $_{100}$ and ARM/ χ with depth in a representative deep water core (6) from Semer Water. Variations in the magnetic signature with depth in core 6 are minimal. A slight decrease in susceptibility can be observed and a peak in IRM $_{100}$ and SIRM at a depth of between 25 and 30 cm is evident.

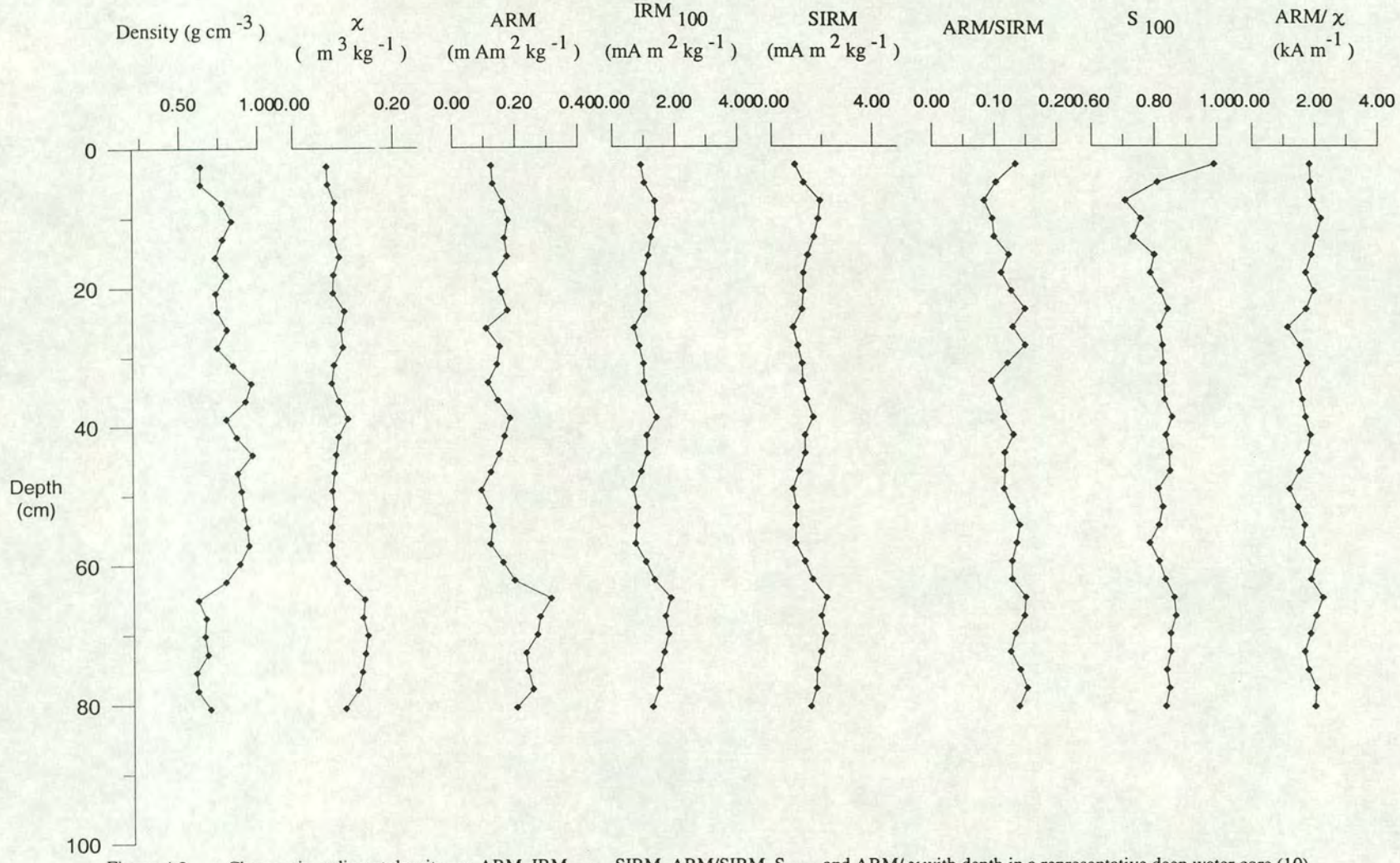

Figure 4.9 ı Changes in sediment density, χ ARM, IRM $_{100}$, SIRM, ARM/SIRM, S $_{100}$ and ARM/ χ with depth in a representative deep water core (10) from Semer Water. The uppermost 60 cm of core 10 displays minimal variation in χ ARM, IRM $_{100}$, SIRM however a marked increase in density at a depth of c. 65 cm corresponds a decline in all four magnetic concentration indicators (χ ARM, IRM $_{100}$ and SIRM.

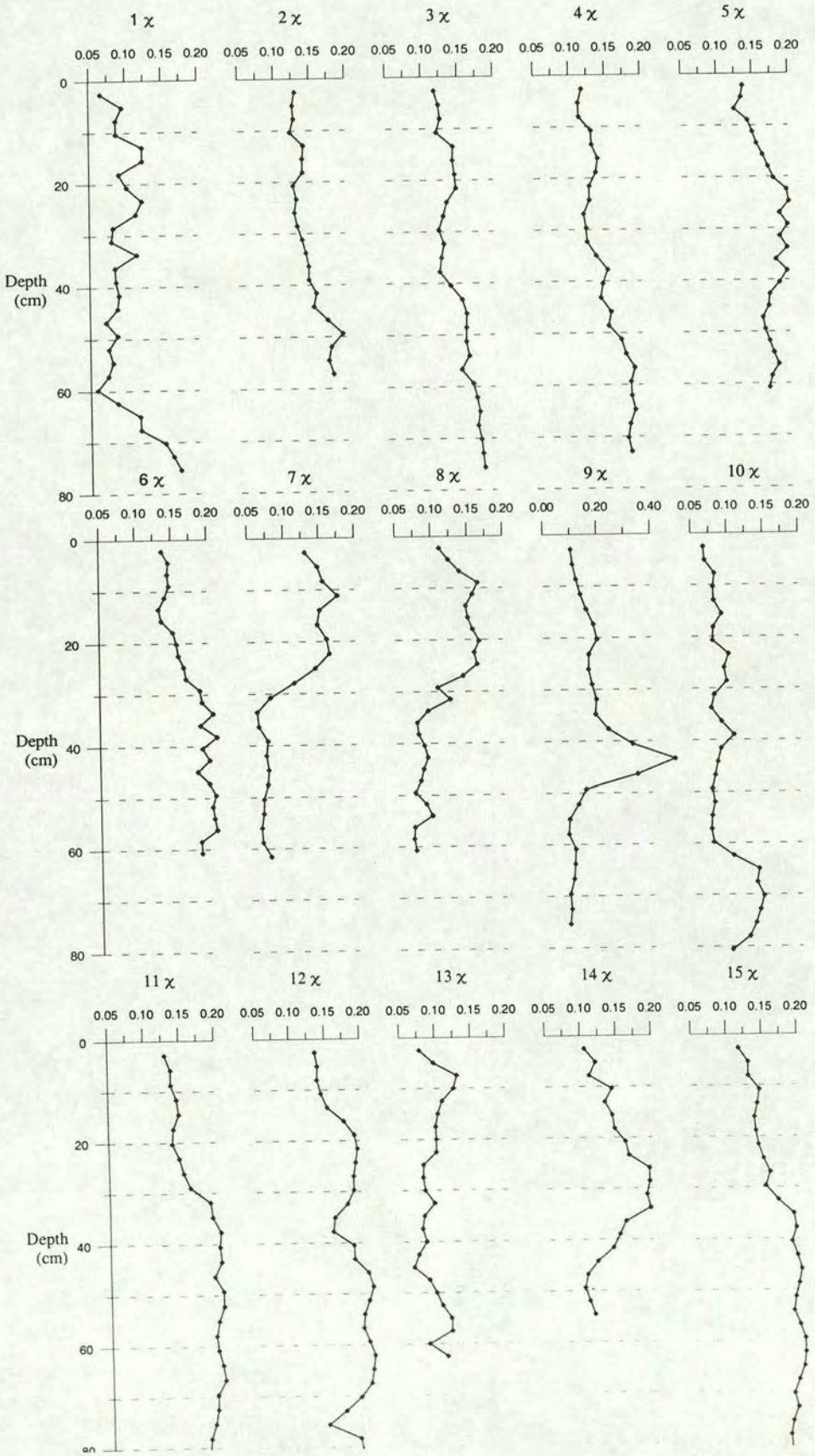

Figure 4.10 Variation in susceptibility ($\mu m^3\ kg^{-1}$) with depth in cores 1-15 from Semer Water. A general decline in susceptibility can be observed in all cores. Cores 5, 6, 11 and 15, which all originate from the deepest part of Semer Water, display a more rapid decrease in susceptibility.

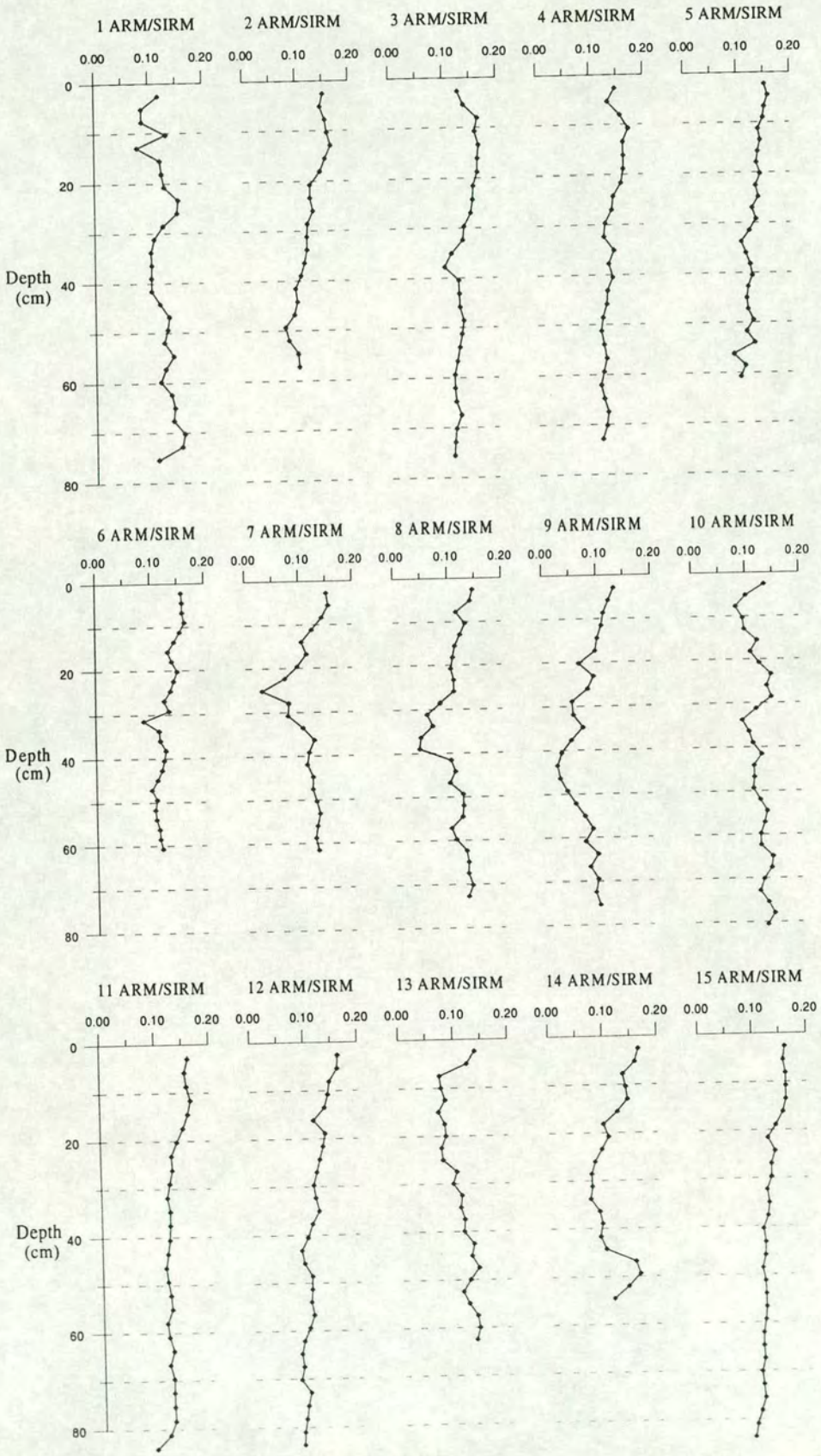

Figure 4.11 Variation in ARM/SIRM ratio with depth in cores 1-15 from Semer Water. Most cores show an overall increase in ARM/SIRM towards the surface. Cores 7, 8, 9 and 14 show marked minimum ARM/SIRM values towards the centre of the core.

On account of the heterogeneous magnetic signal within and between Semer Water lake sediment cores the magnetic characteristics of the two longest cores (SL1, SL2), spanning the longest time period, can be taken to be most representative of the lake sediments as a whole. Table 4.7 summarises the magnetic characteristics of these two cores.

Table 4.7 A summary of the magnetic properties of samples from lake cores SL1 and SL2.

	χ ($\mu m^3 kg^{-1}$)	ARM ($mA\ m^2 kg^{-1}$)	IRM_{100} ($mA\ m^2 kg^{-1}$)	SIRM ($mA\ m^2 kg^{-1}$)	A/S	S_{100}	ARM/χ ($kA\ m^{-1}$)
Mean	0.159	0.32	2.43	3.06	0.105	0.80	2.00
Std dev	0.045	0.10	1.02	1.38	0.027	0.06	0.34
Min	0.072	0.08	0.51	0.64	0.065	0.68	0.82
Max	0.249	1.53	5.45	6.82	0.183	0.95	2.88

Interpretation of the magnetic signature recorded in the Semer Water lake samples can be gained from biplots of (i) ARM/SIRM vs S_{100} and (ii) ARM/SIRM vs ARM/χ (Section 3.3.2.3). Figure 4.12 demonstrates where the lake samples plot on the ARM/SIRM vs S_{100} biplot, having ARM/SIRM and S_{100} ratios from 0.065 to 0.183 and 0.68 to 0.95 respectively. The ARM/SIRM ratios are much higher than those of 'geological' minerals and appears to be indicative of the presence of magnetotactic bacteria or topsoil. The mean S_{100} ratios are typical of sediment samples dominated by magnetite as opposed to haematite or goethite. The lake samples are characterised by high ARM/χ ratios of up to 2.88 kA m^{-1} indicating that the magnetic signature results from magnetotactic bacteria, rather than topsoil (Figure 4.13).

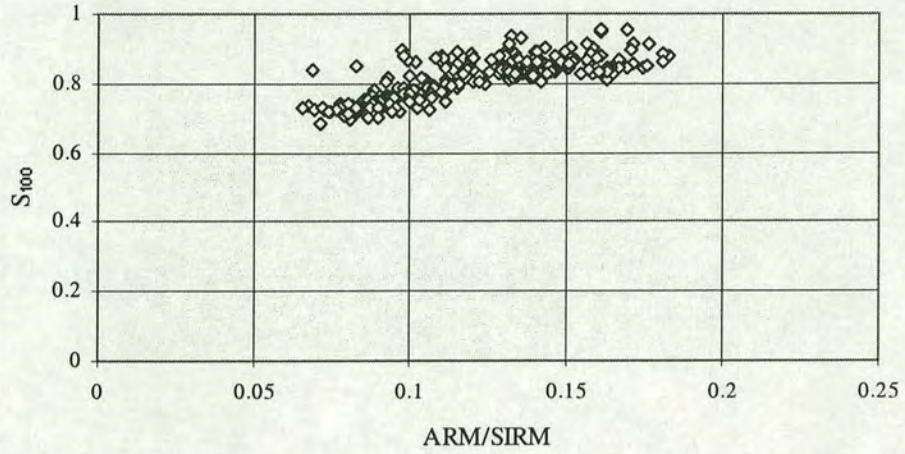

Figure 4.12 Biplot of ARM/SIRM and S_{100} ratios for Semer Water lake sediment samples. The biplot can be used to indicate the origin of the magnetic signature within the lake sediment samples (refer to Figure 3.6a, Chapter 3 and Figure 4.3). With ARM/SIRM and S_{100} ratios of between 0.065 to 0.183 and 0.68 to 0.095 respectively the magnetic signature within the lake sediment samples is characteristic of a mineralogy dominated by magnetotactic bacteria or topsoil.

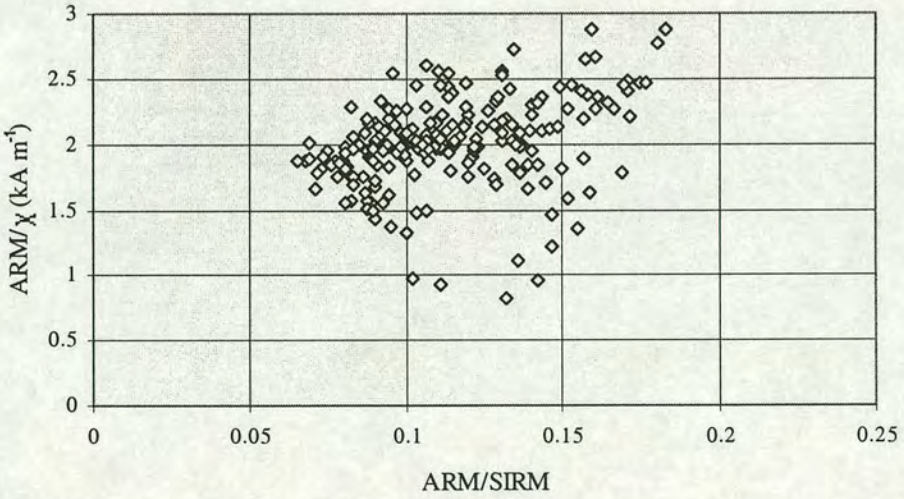

Figure 4.13 Biplot of ARM/SIRM and ARM/χ ratios for Semer Water lake sediment samples. The biplot can be used to distinguish between detrital/topsoil magnetic minerals and magnetotactic bacteria (refer to Figure 3.6b, Chapter 3 and Figure 4.4). The samples are characterised by high ARM/χ ratios of up to 2.88 kA m^{-1} indicating that the magnetic signature results from magnetotactic bacteria rather than topsoil.

4.4 Comparison of Catchment Sample and Lake Sample Magnetic Data

Figures 4.14 and 4.14 compare the ARM/SIRM, S_{100} and ARM/χ ratios for the catchment and lake sediment samples. A clear distinction is evident between the catchment samples and lake samples. The magnetic properties of the catchment samples are influenced by detrital magnetite, goethite and topsoil (Section 4.2.1) whilst the lake samples are suspected to contain bacterial magnetosomes superimposed on low concentrations of detrital magnetite and goethite and perhaps topsoil.

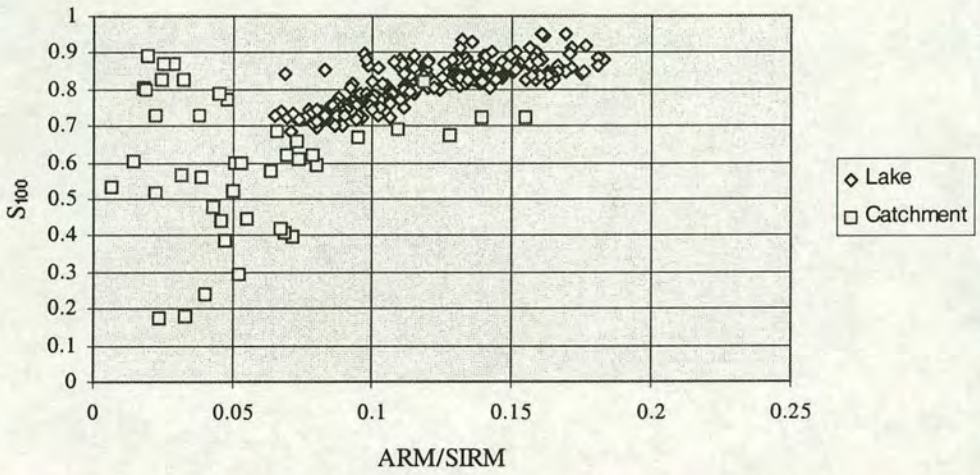

Figure 4.14 A comparison of ARM/SIRM and S_{100} ratios for Semer Water lake and catchment samples. The catchment samples tend to have lower ARM/SIRM ratios than lake sediment samples and include samples with much lower S_{100} values indicating that the catchment samples contain geological magnetite and goethite whilst the magnetic mineralogy of the lake sediment samples is dominated by bacterial magnetosomes (refer to Figure 3.6b, Chapter 3 and Figure 4.4 for additional details pertaining to the interpretation of magnetic mineralogy using a biplot of S_{100} and ARM/SIRM).

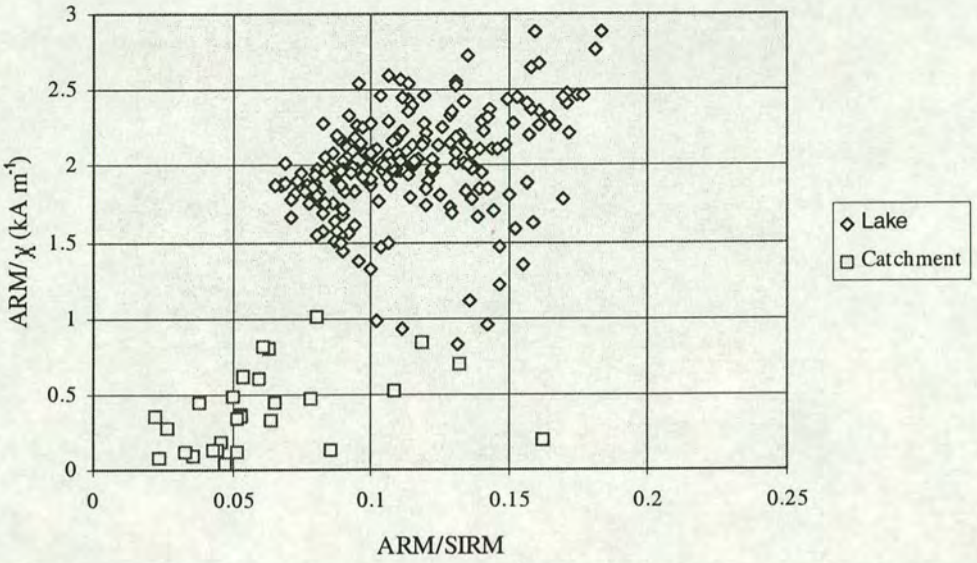

Figure 4.15 A comparison of ARM/SIRM and ARM/χ ratios for Semer Water lake and catchment samples. The catchment samples tend to be characterised by lower ARM/χ, indicative of topsoil, than the lake sediment samples (refer to Figure 3.6b, Chapter 3 and Figure 4.4).

4.5 Summary

- Catchment samples obtained from Semer Water have been characterised magnetically. The magnetic signature is shown to arise from a combination of detrital magnetite, goethite and topsoil.

- The 17 Mackereth lake cores obtained from Semer Water are composed of clay/silt size material and display little variation in lithology with depth.

- Magnetic characterisation of lake cores from Semer Water shows the magnetic signature to arise from a mixture of detrital magnetite as well as bacterial magnetite.

- Based on chronologies determined from ^{210}Pb and ^{137}Cs Appleby reports average sediment accumulation rates of 0.9, 0.6 and 0.37 cm a^{-1} since c. 1950.

Chapter 5

Raydale

5.1 Introduction

Following the failure to collect long sediment cores at Semer Water, I decided to explore the floodplain area near the present day inflow (Crooks Beck). This revealed extremely thick sediment sequences extending to depths of at least 14 metres. Further work revealed an extensive area of very thick Holocene sequences across the Raydale valley. These newly discovered deposits form the basis of Chapter 5. A heavy duty Giddings hydraulic piston corer was need to penetrate this thick deltaic/valley fill. Three Giddings coring sites (A, B and C) have been studied.

Each of the three Giddings cores has been characterised magnetically and changes in sediment density and lithostratigraphy with depth recorded. Detailed particle size measurements have also been undertaken on Giddings core A and a chronology established for each of the three Giddings cores using a combination of ^{14}C and pollen analysis. The thickness and lateral extent of sediments in the Raydale valley have also been determined using resistivity profiles. Surveying techniques have been employed to estimate the volume of sediment potentially eroded from gullies and rivers in the Semer Water catchment. In Chapter 8 the Raydale valley sediment data is combined with the lake sediment data of Chapter 4 to determine sediment influx and yields for the Semer Water catchment during the Holocene.

5.2 Core Collection

As described above having failed to obtain long sediment cores from the present lake Semer Water, gouge core investigations of the sediments in the Raydale valley bottom, upstream of the lake, were undertaken in May 1995. The gouge core survey indicated the presence of thick, extensive sediment sequences in the valley floor. The sediment was found to be in excess of 20 metres thick in places. Following the initial appraisal, seven transects of gouge cores were obtained (Figure 5.1). These include cores taken by students from the Universities of Liverpool and Edinburgh on undergraduate and postgraduate field courses. The depth profile information from the gouge core investigations is summarised in Figure 5.2. The gouge coring work demonstrated the presence of thick sequences of sediment extending up the Raydale valley towards Marsett covering an area of some 0.5 km^2.

Following the gouge core surveys a third phase of coring work was undertaken. Giddings cores were obtained from three locations in Raydale (Figure 5.1).

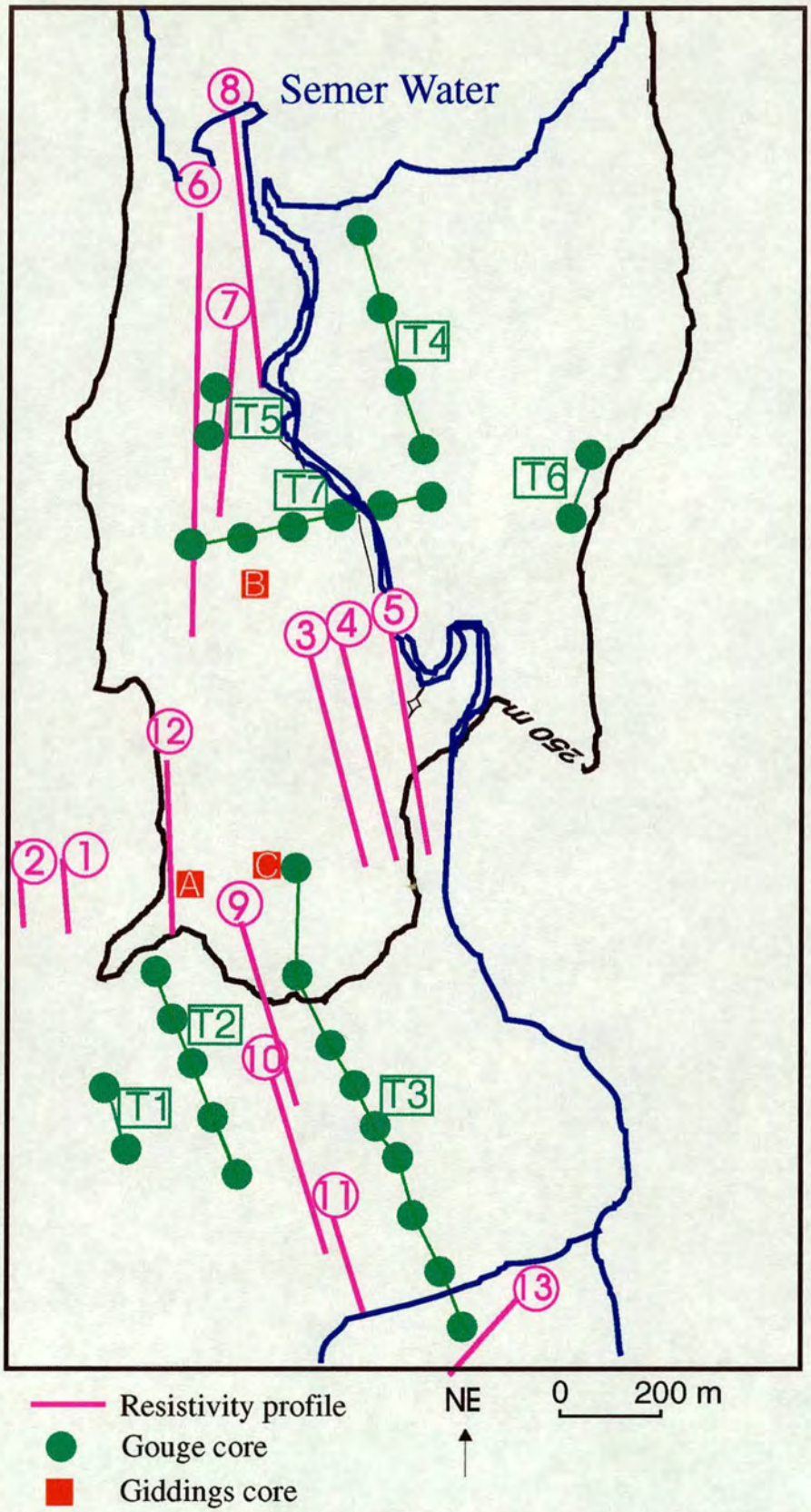

Figure 5.1 Location of resistivity profiles, gouge cores and Giddings cores at Raydale. Thirteen resistivity profiles have been obtained within the Raydale valley spanning both the old lake sediments and the surrounding bedrock. The resistivity results suggest that extensive thick lake sediment deposits occur within the area bounded approximately by the 250m contour. The gouge and giddings cores taken within the basin indicate that the sediments towards the centre of the basin, closest to the existing lake, comprise finer clays and silts than the more marginal cores which are characterised by silt and sand.

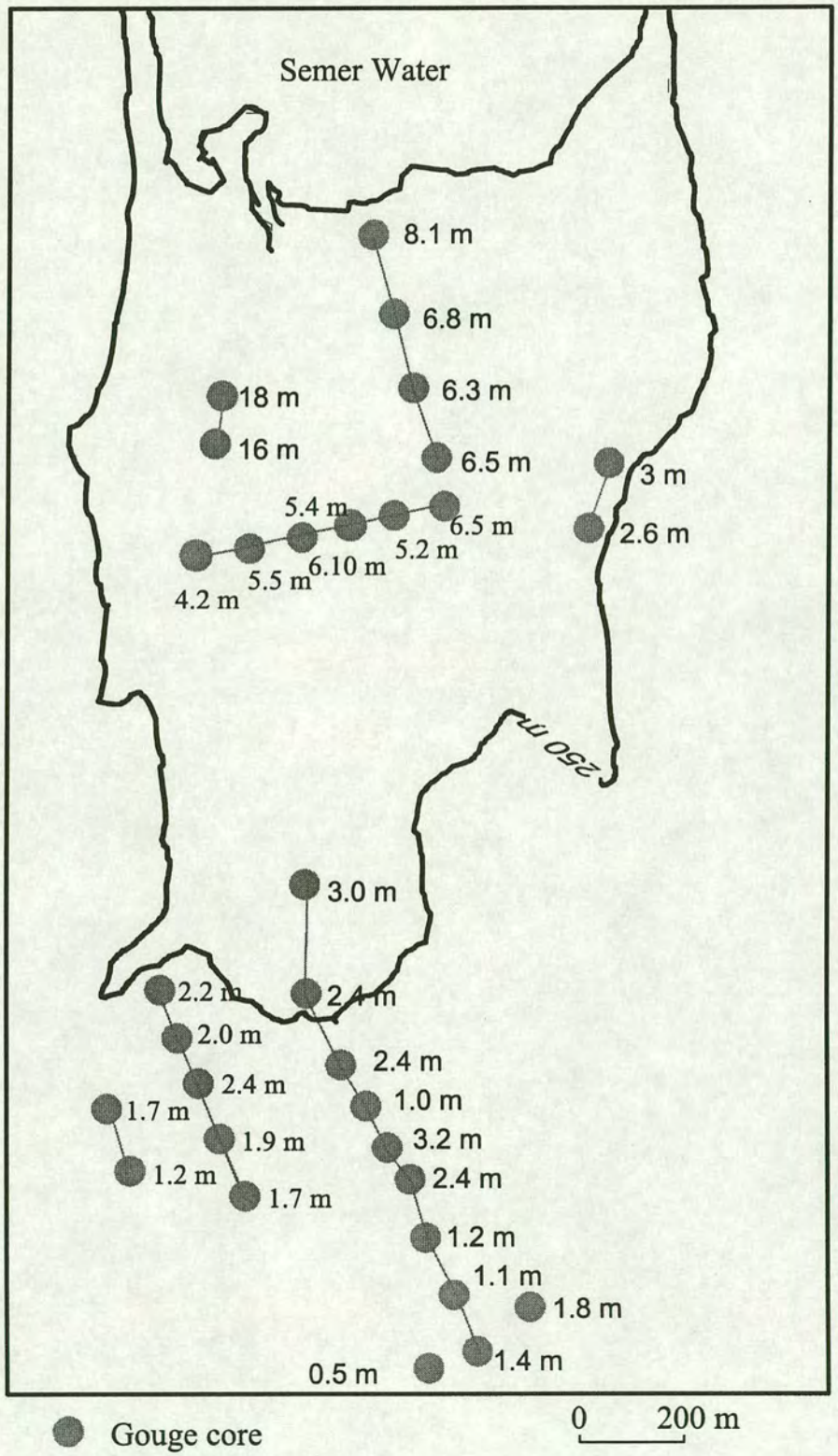

Figure 5.2 Sediment depth recovered from each Raydale gouge core. Only those two cores extending to depths of 16 and 18 m obtained within the 250 m contour reach the base of the lake sediment sequences. The upper sediment of cores obtained from the centre of the old lake basin comprises high proportion of clay, elsewhere the cores are dominated by a combination of silt and sand.

5.3 Lithostratigraphy

5.3.1 Giddings cores A, B and C

Significant variation in lithostratigraphy can be observed between Giddings cores A, B and C. Appendix I tabulates the stratigraphy of each of the three Giddings cores. In summary (as illustrated in Figure 5.4) the upper five metres of Giddings core A is dominated by clay and silt in roughly equal proportion and the lower three metres are dominated by silt and sand in approximately equal proportion. In parts of Giddings core A laminations, ranging from between 0.5 and 4 cm thick, were observed. The upper one and a half metres of Core B comprises a layer of silt (50%) and sand (50%) while the remainder of the core is dominated by clay (50%) and silt (50%) (Figure 5.4). In contrast core C is dominated by sand (50%) and silt (50%) throughout (Figure 5.4). Cores A, B and C have mean sediment densities of 1.21, 1.32 and 1.35 g cm^{-3} respectively. Considerable variation in densities occurs downcore, although no specific trends can be observed (Figure 5.5). In Giddings core A a sharp decrease in density occurs at a depth of c. 650 cm. This sudden change in sediment density may be indicative of either a change in the dominant source of sedimenting material or changes in the depositional environment resulting in an increase in the proportion of fine sediment being deposited at this site. Appendix H includes the complete sediment density data for Giddings cores A, B and C.

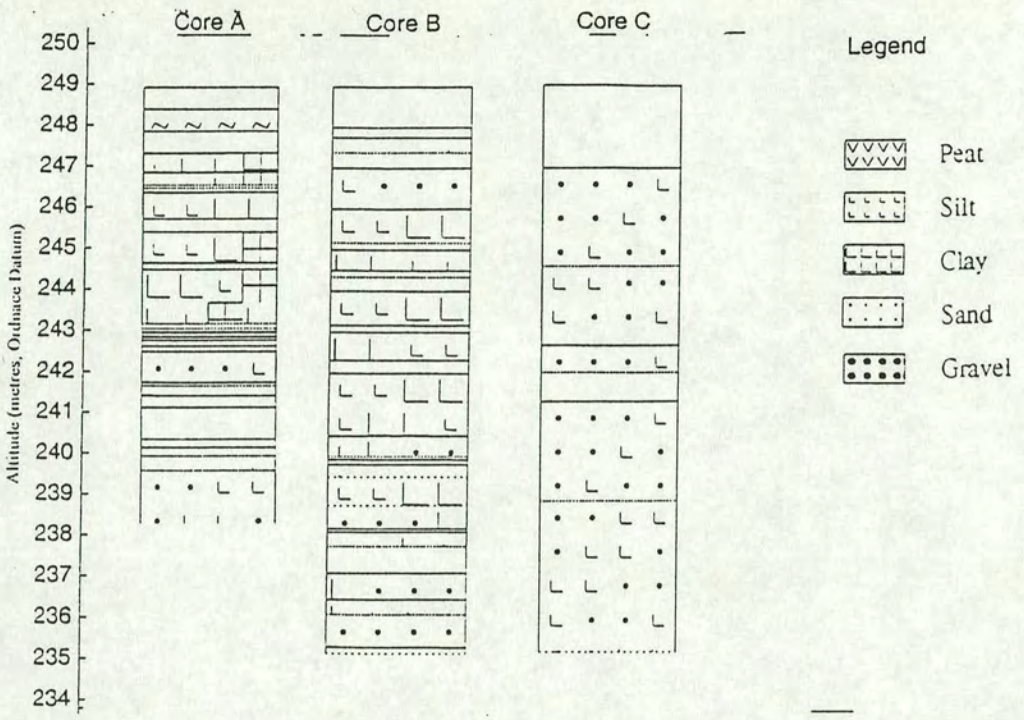

Figure 5.4 Changes in lithostratigraphy with depth in Raydale Giddings cores A, B and C recorded using the Troel Smith sediment classification index (refer to Section 3.3.7, Chapter 3).

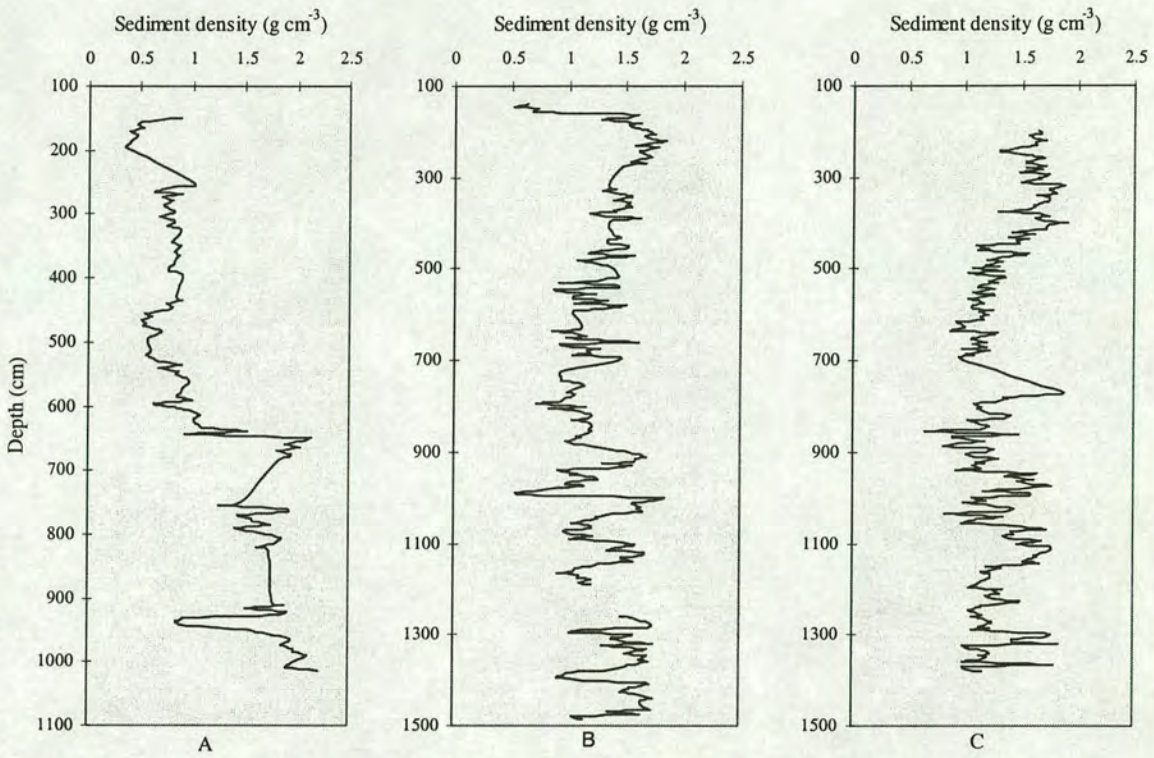

Figure 5.5 Changes in sediment density with depth in Raydale Giddings cores A, B and C.

5.3.2 Gouge Cores

Cores from transects T1 and T2 (Figure 5.2) comprise silt and clay material, similar to that identified in the upper five metres of Giddings core A. The uppermost sediment in cores taken along transect T3 is similarly dominated by silt and clay. However a particularly high proportion of clay dominates the upper sediment in cores collected from closest to the centre of the old lake basin (i.e. at the north east end of the transect). Sediment recovered from the lower part of the sequence of cores in T3 comprises coarser silt and sand, in agreement with the stratigraphy in Giddings Core C . Transects T4 and T5 are dominated by clay and silt material. However lenses of coarser material, principally sand and fine gravel, were also observed. The two cores recovered from transect T6 comprise sandy silt material and extend into glacial

boulder clay containing pebbles at depths of between c. 2.8 - 3 m. Figure 5.6 illustrates the changes in lithostratigraphy with depth in transect T7.

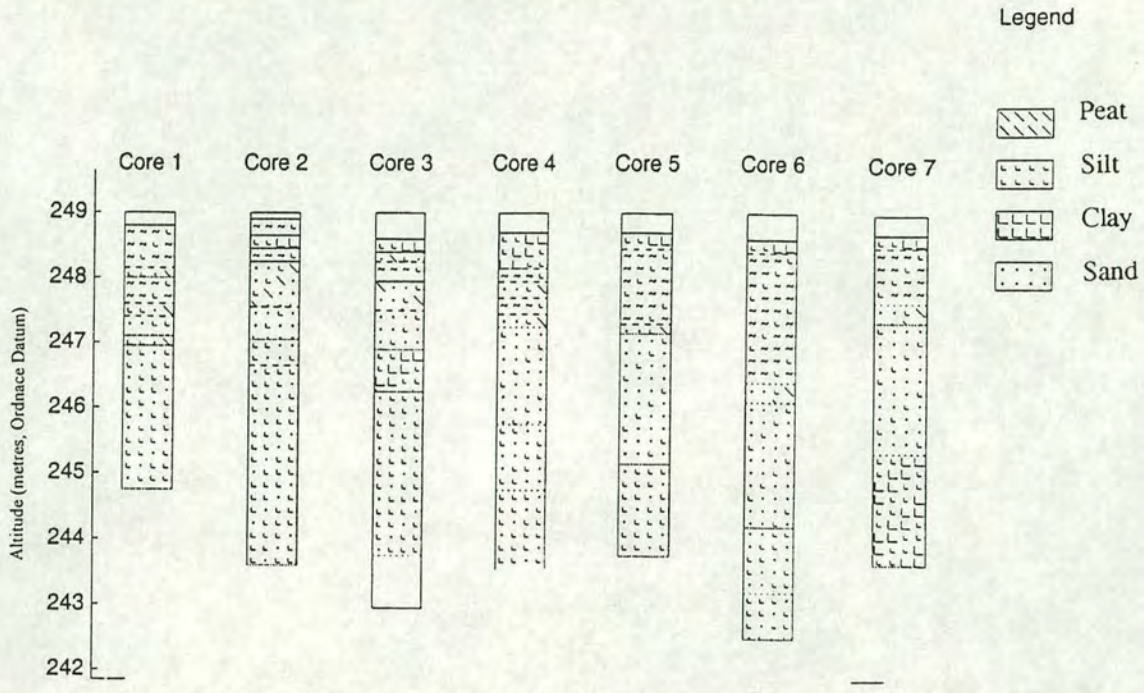

Figure 5.6 Lithostratigraphy of gouge cores from transect T7 in Raydale (based on a diagram from A.Plater, pers.comm.).

In summary, gouge cores obtained from a variety of locations in Raydale illustrate that the old lake sediments are found over an area of roughly 0.4 km^2, bounded approximately by the 250 m elevation contour. These lake sediments are dominated by a mixture of clay and silt, with an overlying layer of peat. They thicken towards the centre of the old lake near the intersection of transects T4 and T7.

5.4 Total Organic Carbon and Carbonate Content

The organic carbon and carbonate content of samples obtained Giddings A are given in Table 5.1.

Table 5.1 Organic carbon and carbonate content of samples taken from Giddings core A.

Depth (cm)	Organic (%)	Carbonates (%)
280	5.1	32.0
290	5.4	23.9
320	9.7	1.4
390	3.3	31.6
468	3.8	30.7
487	3.3	32.6
565	2.9	33.5
590	3.1	31.0
630	2.5	11.8
657	2.1	6.7
755	1.8	11.9
940	3.0	31.7
955	2.5	13.9
975	2.0	9.8
1000	2.3	4.1
Mean	3.5	20.4

The mean organic content in Giddings core A is 3.5% (std dev 1.9), while the mean carbonate content is typically c. 20% (std dev 11.7)

5.5 Chronology

5.5.1 ^{14}C Results

Thirteen samples from Raydale Giddings core C were submitted to the NERC laboratory at East Kilbride, Scotland for dating using AMS radiocarbon analysis. Table 5.2 summarises the results.

Table 5.2 A summary of the Raydale radiocarbon results

Sample	Core	Depth (m)	Composition	Publication Code	Radiocarbon age (BP± 1σ)	Calibrated age (yrs) (BP) (1σ range)
Raydale 1	Giddings C	2.25	wood	AA-25541	4,305 ± 65	4859 (4831-4872)
Raydale 2	Giddings C	3.80	wood	AA-25542	3,350 ± 60	3574 (3474-3681)
Raydale 3	Giddings C	4.55	wood	AA-25543	3,340 ± 60	3568 (3472-3633)
Raydale 4	Giddings C	5.00	wood	AA-25544	3,480 ± 65	3707 (3637-3833)
Raydale 5	Giddings C	5.80	wood	AA-25545	3,565 ± 55	3838 (3730-3912)
Raydale 6	Giddings C	7.95	wood	AA-25546	3,670 ± 60	3940 (3893-4085)
Raydale 7	Giddings C	8.05	wood	AA-25547	3,815 ± 95	4192 (3998-4403)
Raydale 8	Giddings C	8.30	wood	AA-25548	4,165 ± 65	4697 (4564-4830)
Raydale 9	Giddings C	8.55	macrofossil	AA-25549	3,885 ± 50	4331 (4158-4411)
Raydale 10	Giddings C	8.60	wood	AA-25550	3,725 ± 55	4022 (3939-4144)
Raydale 11	Giddings C	8.97	wood	AA-25551	3,785 ± 55	4101 (4009-4235)
Raydale 12	Giddings C	10.00	macrofossil	AA-25552	3,760 ± 50	4115 (3993-4222)
Raydale 13	Giddings C	10.17	wood	AA-25553	3,740 ± 65	4086 (3983-4221)

Notes:

i) Samples prepared to graphite at the NERC Radiocarbon Lab., East Kilbride and ^{14}C analysis by AMS carried out by the University of Arizona NSF AMS Facility.

The ^{14}C dates obtained for Giddings core C result in the depth-age trend displayed in Figure 5.7. As expected the overall depth-age trend is one of increasing age with depth, however some dates appear to be inverted. In particular the ^{14}C date of the uppermost sample results in a date which is apparently too old. These results are not an isolated example of an inverted ^{14}C sequence recorded in British Holocene sediments. Amongst others Mackereth (1971), O'Sullivan et al. (1973) and Pennington et al. (1976) have observed sediment profiles where, according to the ^{14}C dates, the age of the sediment towards the surface of the core increases rather than decreases. In most studies where an inverted ^{14}C sequence has been observed a

combination of pollen, chemical and sedimentological data have been used to illustrate that the input of old carbon can be attributed to human activity within catchments. The ^{14}C dates obtained on samples from Giddings core C thus indicate that some of the dated macrofossil and wood fragments are significantly older, perhaps up to 1000 years, than the sediments in which they have been deposited. One possible explanation for the good linear agreement between depth and age is that the dated macrofossils are contained within a single source which has been eroded at different times.

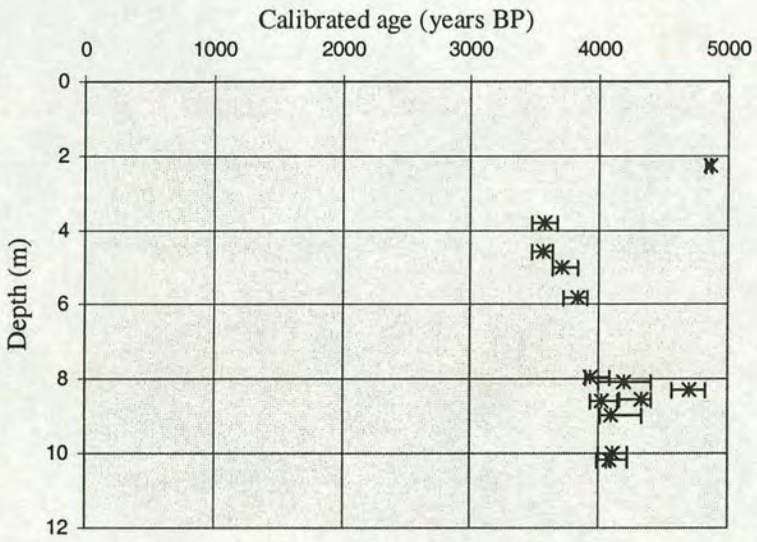

Figure 5.7 Depth-age trend determined from 13 ^{14}C dates from Raydale Giddings core C. The overall trend is one of increasing age with depth. The error bars represent errors calculated at the one sigma level.

The calibrated ^{14}C date determined at the base of core C is 4086 BP (range 3983 - 4221 BP) therefore it is assumed that the sediment deposited at site C can be no older than c. 4265 years old (4221 + (1994-1950)). The deposition of 10 metres of sediment in Giddings core C in this time corresponds to an average accumulation rate of 0.23 cm a^{-1}. The ^{14}C dates point to the extremely high accumulation rates that have taken place at Raydale, some ten to twenty times greater than those observed at many other British sites.

One alternative interpretation of the ^{14}C depth age profile, given the generally good linear agreement between depth and age, involves excluding a couple of dates including the uppermost date and taking the calibrated age of sediment at the top of the core of 3574 BP (range 3474 - 3681 BP) in order to calculate accumulation of 7.9 metres of sediment in c. 500 years (range 302-747). The deposition of 7.9 metres of sediment in Giddings core C in this time corresponds to an average accumulation rate of c. 1.6 cm a^{-1} (1.1-2.6 cm a^{-1}). The latter interpretation is deemed to be implausible. The author believes that such accumulation rates are unrealistic and the interpretation relies on a ^{14}C sequence which clearly includes some dates which, if not based on inwashed macrofossils, are erroneous.

5.5.2 Pollen Analysis

After pollen preparation in the Geography Department at Edinburgh University I made up and counted 30 slides from Raydale cores. The pollen analysis results of core A (Figure 5.8) show the *Alnus* rise at a sediment depth of between 5.80 and 6.00 m *Plantago* and *Gramineae* are present in low concentrations in the uppermost 6.55 m, though a notable increase in the concentration of *Gramineae* pollen can be observed in the uppermost four metres. *Corylus* is the dominant taxa throughout the profile. Its overall trend is one of decreasing concentration towards the surface. *Ulmus* pollen decreases from 25% of the total pollen count at a depth of 5.8 m to less than 5% at 4.45 m. *Quercus* and *Pinus* are present in low concentrations (c.10% of total pollen count) throughout the profile though Quercus increases in the uppermost sediments to 18% of the total pollen count.

Corylus occurs in significant quantities (25% of total pollen count) throughout sediment cores B and C and there is little variation in its concentration with depth in either core (Figures 5.9, 5.10). *Ulmus* is present in very low concentrations (max 5% of total pollen count) throughout cores B and C. *Alnus* decreases sharply from 40% of the total pollen count at a depth of 9.98 m to 5% at 6.7 m in core B. In contrast,

core C is characterised by high concentrations of *Alnus* pollen (c. 35% of total pollen) throughout the profile. In comparison to cores A and C, core B is characterised by particularly high concentrations of *Gramineae* (c. 20% of total pollen count) in the uppermost 6.7 m and, with the exception of horizons at depths of 8.5 and 9.98 metres, high concentrations (>20% of total pollen count) of *Plantago* throughout the core.

The alder rise, at a depth of between 5.80 - 6.00 m in Giddings core A, is dated to c. 7500 radiocarbon years BP in this area (Birks, 1989). By converting the dates from radiocarbon years to calendar years it is concluded that approximately six metres of sediment has been deposited since 8220 years BP (8174-8335 at 1σ). The elm decline, evident in core A, can be employed to illustrate that between 5.8 and 4.45 m of sediment has been deposited since 6294 BP (6280-6311 at 1σ). Birks (1989) demonstrates that the taxa *Corylus*, *Quercus* and *Pinus,* which are present throughout core A, arrived in the area at c. 8500 to 9500 years BP. Thus a minimum of 9.1 m of sediment has been deposited in the past 10513 years BP (10415-10798 years BP at 1σ) in Raydale. The extremely low concentrations of *Ulmus* throughout cores B and C indicate that the sediment has been deposited in the period since the elm decline of 6294 BP. This observation is confirmed by the occurrence of *Gramineae*, *Plantago* and high concentrations of *Alnus* throughout cores B and C which indicate that the sediment has been deposited since the alder rise of 8220 years BP (8174-8335 at 1σ). The age of sediment from the bottom of cores B and C (depths of 14.75 and 13.5 m respectively) therefore represents a maximum age of 6294 BP (6280-6311 at 1σ). Table 5.3 summarises the mean sediment accumulation rates in Giddings cores A, B and C determined from the results of pollen analysis

The maximum ^{14}C age of c. 4086 BP (range 3983 - 4221 BP) for a sample from a depth of 10.17 m in Giddings core C (Section 5.4.1) is thus in good agreement with the pollen determined chronology which suggests a maximum age of c.6300 years BP for sediment at a depth of 13.5 m.

Table 5.3 Sediment accumulation rates (cm a^{-1}) in cores A, B and C determined from pollen analysis results. The minimum and maximum accumulation rates are calculated using the 1σ errors associated with calibrating the radiocarbon dates into calendar years and, where given, using the depth ranges over which each of the significant dated changes in pollen assemblage occurs. For example the minimum and maximum accumulation rates in core A for the period 0-6294 are based on dates of 6280 and 6311 BP respectively and a sediment accumulation of 5.80 and 4.45 m during that period.

	Sediment accumulation rates (cm a^{-1})								
Time period (years BP)	0-6294			6294-8220			8200-10513		
	Min	Mean	Max	Min	Mean	Max	Min	Mean	Max
A	0.07	0.08	0.09	0	0.04	0.08	0.12	0.14	0.16
B	>0.23								
C	>0.21								

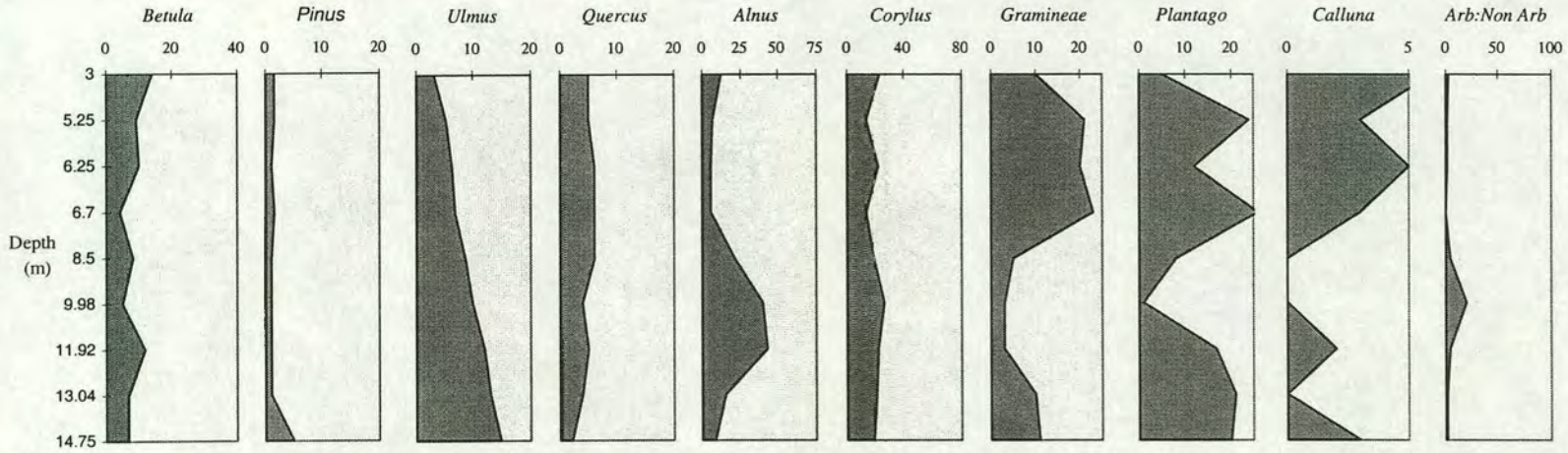

Figure 5.9 Summary pollen diagram for Raydale Giddings core B. The results are expressed as % of the total pollen count. 200 pollen grains were counted at each depth horizon. The very low concentrations of *Ulmus* in core B indicate that the sediment has been deposited since the elm decline of c. 6290 years BP.

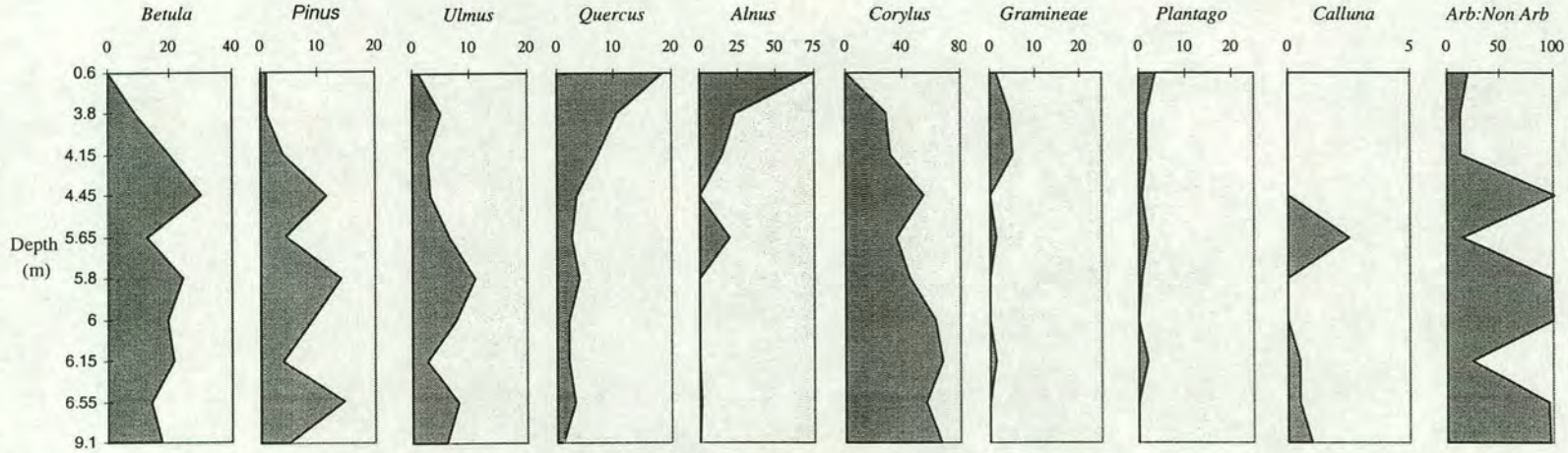

Figure 5.8 Summary pollen diagram for Raydale Giddings core A. The results are expressed as % of the total pollen count. 200 pollen grains were counted at each depth horizon. The well dated *Alnus* rise at a depth of between 5.80 and 6.00 m is very marked and can be used to indicate that approximately 6 m of sediment has been deposited since c. 8300 years BP.

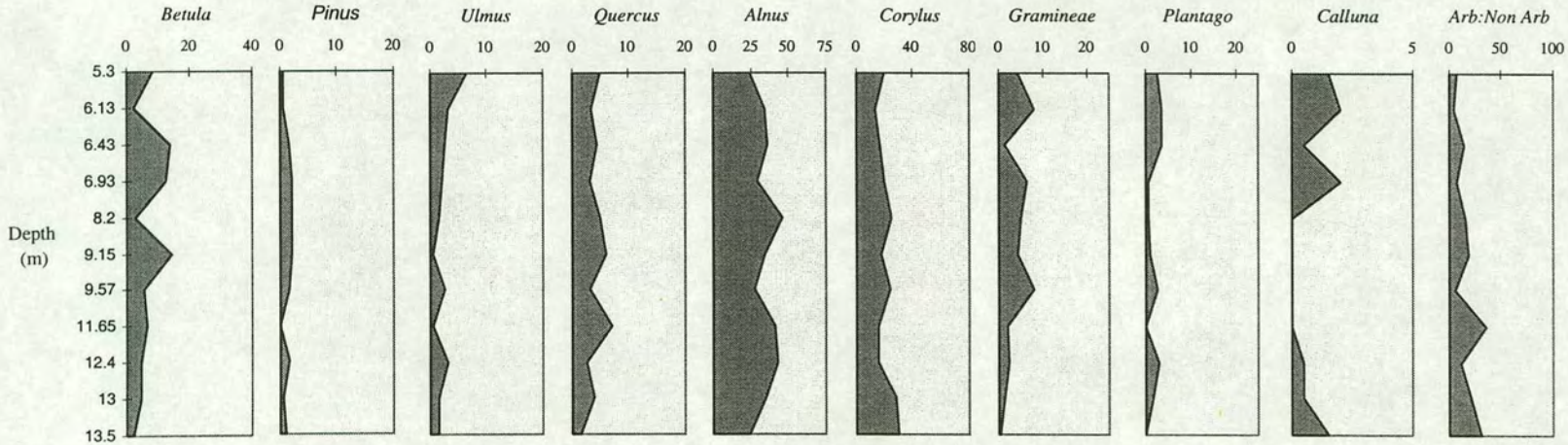

Figure 5.10 Summary pollen diagram for Raydale Giddings core C. The results are expressed as % of the total pollen count. 200 pollen grains were counted at each depth horizon. The high concentrations of *Alnus* and low concentrations of *Ulmus* indicate that the sediment has been deposited since 6290 years BP.

5.6 Particle Size Analysis

Particle size analysis has been undertaken on samples at five centimetre intervals throughout core A and a section of core C in Raydale. Based on the analysis of 126 samples, Figure 5.13 illustrates the heterogeneous nature of Giddings core A as shown by the variation in each of the five size components with depth. The core can be divided into three distinct zones on the basis of particle size data (Table 5.4).

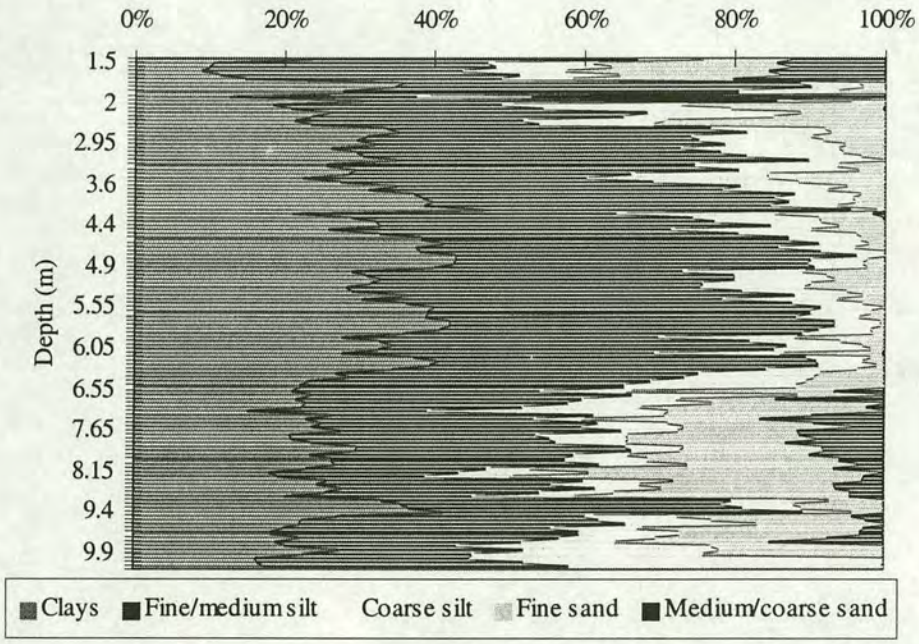

Figure 5.11 Changes in the proportion of clays, fine/medium silt, coarse silt, fine sand and medium/coarse sand with depth in Raydale Giddings core A. A significant medium/coarse sand component occurs in samples taken from between 1.5 and 2 m and between 7 and 9.5 m.

Table 5.4 Mean particle size (μm) for three distinct regions in Giddings core A

Depth range (cm)	Mean grain size (μm)
150-200	77.7
325-700	19.7
705-1010	65.5

The proportion of clays and fine/medium silt is greatest in the central part of the core whilst medium/coarse sand is only evident in the upper and lower section. At depths less than 200 cm the medium/coarse sand fraction constitutes, on average, 12% of the sediment mass compared to 0.2% in the central part of the core. Below 700 cm medium/coarse sand accounts for an average 5.6% of the sediment.

Core A contained numerous laminations often less than one cm thick. Whilst illustrating the heterogeneous nature of the sediment in Giddings core A the particle size analyses are unable to characterise the extent of variations existing on a much finer scale which can be visually observed in the core (Figure 5.12). In order to illustrate the variation within even a very narrow depth range within the core, and demonstrate the sharp boundaries between adjacent horizons, particle size analysis has been undertaken on three groups of adjacent samples (Table 5.5)

Table 5.5 Variations in particle size between adjacent samples from three zones in Giddings core A.

	Depth in core (cm)	Median particle size (μm)	Mean particle size (μm)
	722	19.4	44.4
Group 1	724	8.1	19.3
	725	19.5	30.5
Group 2	820	71.4	82.5
	821	26.2	67.9
Group 3	826	33.6	41.5
	827	71.5	69.7

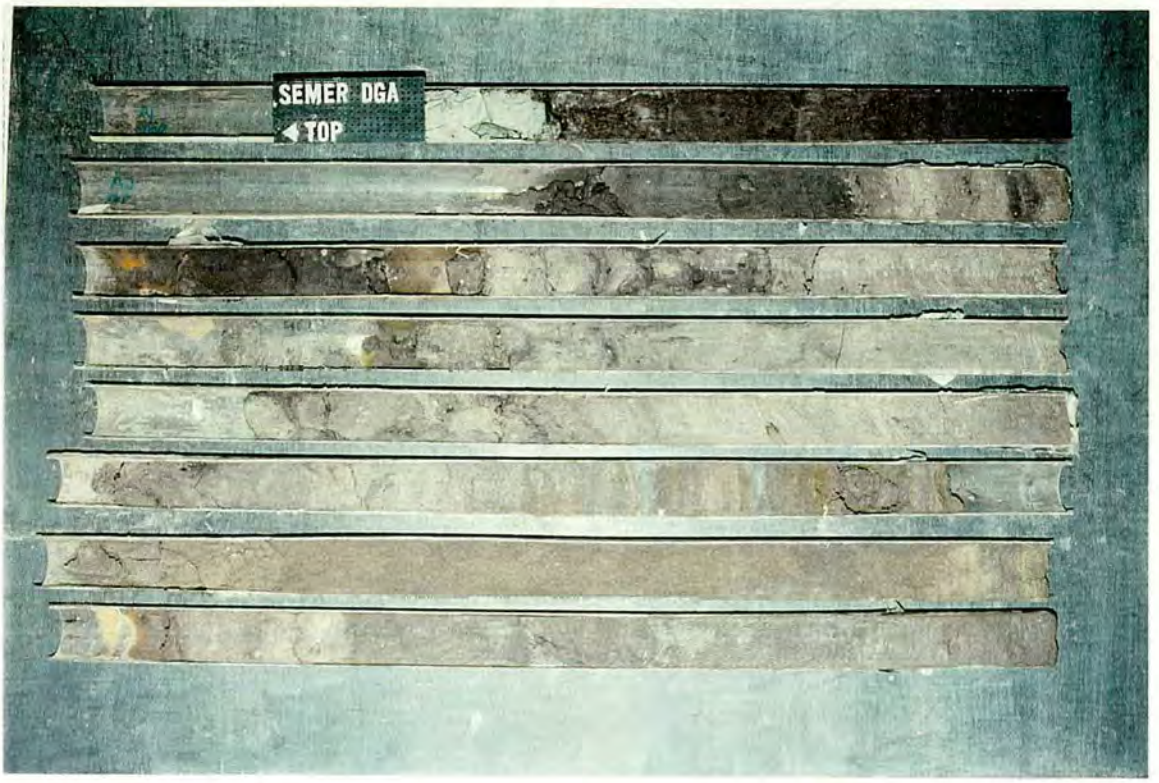

Figure 5.12 Laminations in Raydale Giddings core A.

The laminations of coarse material are interpreted as pulses of coarse eroded sediment brought into the lake by the Crooks Beck during storm events and deposited on reaching the delta. The catchment is well renowned for having a flashy hydrological regime and severe flooding events occur regularly, often depositing sediment sequences over the current Crooks Beck floodplain.

Core C is less heterogeneous than core A, it is composed primarily of sandy material. As illustrated in Figure 5.13 the proportion of fine/medium sand remains relatively constant downcore, averaging 57%. The only significant deviations from this trend occur where spikes of coarser sandy material have been identified, for example at depths of 220, 225 and 350 cm. A gradual increase in the clay component from 4% at the top of the profile to 19% at the bottom can be observed and this, excluding the

major spikes, corresponds to a decrease in the proportion of coarse sand within the core. The average grain size in the zone for which detailed particle size measurements were made (200 - 600 cm) is 157 μm. Below 600 cm particle size analysis was undertaken less frequently. Samples obtained at depths greater than 600 cm continued to be dominated by coarse sand and the remainder of the sediment core was homogeneous. Core C originates from the centre of the old lake deposits and does not record the laminations of fine and coarse material observed in the marginal Giddings core A.

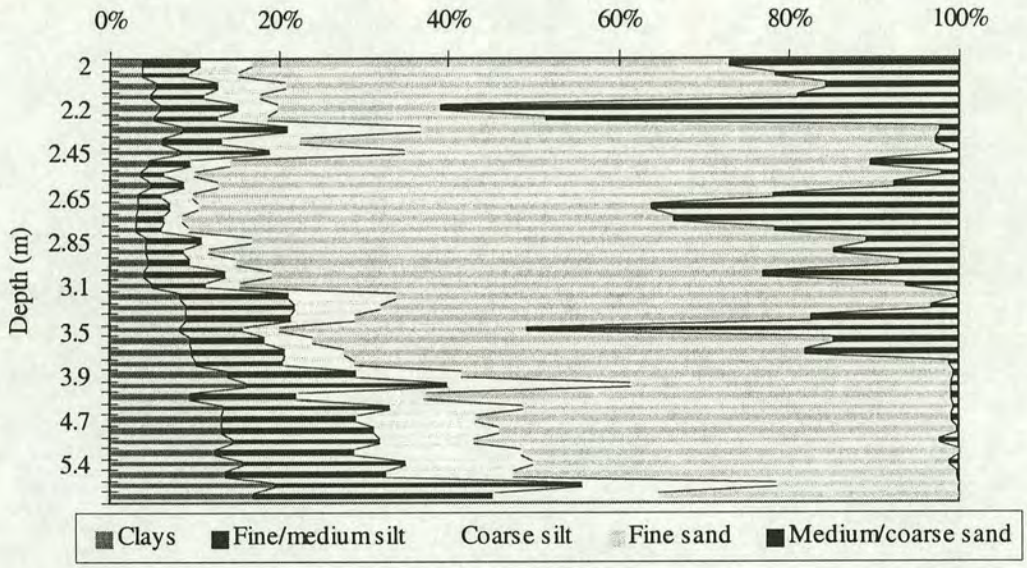

Figure 5.13 Changes in the proportion of clays, fine/medium silt, coarse silt, fine sand and medium/coarse sand with depth in a four metre section of Raydale Giddings core C. In general core C is characterised by an increase in the proportion of clay and silt with depth.

5.7 Raydale Electrical Resistivity Surveys

In October and November 1995 thirteen resistivity soundings were undertaken in the Raydale valley to compliment the results from gouge-core profiles and to help estimate the extent and lateral continuity of sedimentation in the basin. The location

of each sounding is indicated on Figure 5.1. The soundings extended from bedrock on the north west side of the valley onto the deep sediments in the centre of the valley. Soundings 1 and 2 were undertaken on the margin of the old lake basin, 1 was on a raised terrace and 2 very close to bedrock. Soundings 9 and 10 extend along the old lake sediment boundary and soundings 11 and 13 are on thin sequences of sand. Soundings 3, 4, 5, 6, 7 and 8 were undertaken over the thick sediment sequences as mapped by gouge- and Russian coring work. Figure 5.14 illustrates changes in apparent resistivity (ohms) with variation in electrode spacing (m) for two contrasting profiles from Raydale. Figure 5.14 A and 5.14 B show the results of soundings 6 and 10, undertaken on the thick lake sediment sequence and the old lake margin boundary respectively. Appendix K tabulates changes in apparent resistivity (ohms) with electrode spacing (m) for each of the thirteen soundings undertaken in Raydale. Profiles undertaken over the lake basin are, as expected, characterised by lower apparent resistivities than those obtained from the lake shore and bedrock.

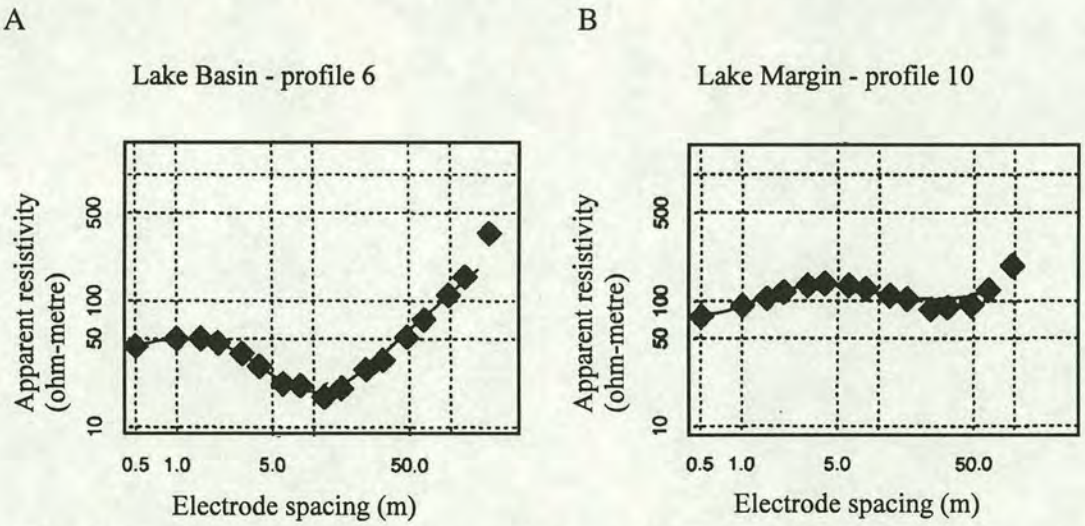

Figure 5.14 Changes in apparent resistivity with electrode spacing in representative profiles taken over the lake basin (A) and over the lake margin (B) in Raydale. Figure A shows three layers of differing resistivity, at close electrode spacing the resistivity is around 50 ohm-metre dropping to 15 ohm-metre at intermediate spacing and increasing to almost 500 ohm-metre at wide electrode spacing. Figure B, however, is characterised by little change in resistivity with electrode spacing indicative of just one resistivity layer.

The resistivity profiles made within the area of the old lake basin are characterised typically by a three layer structure. Profile 6 (Figure 5.14A) shows, at close electrode

spacings, resistivities of 50 ohm-metre to, 15 ohm-metre at intermediate electrode spacing and almost 500 ohm-metre at the greatest spacing (128 metres). The changing resistivities with electrode spacing can be interpreted in terms of changes in stratigraphy. A semi-resistive surface layer (overbank deposits) overlies a very conductive sediment layer (wet lake sediments). These two upper layers are underlain by a very resistive layer (either bedrock or glacial till). Profile 6 (Figure 5.14 A) is typical of all the surveys undertaken on the old lake basin. Profile 10 (Figure 5.14 B) undertaken outside the basin area only shows high till/bedrock values of over 50 ohm-metres.

Soundings undertaken on the marginal old shoreline area in Raydale (soundings 10, 11 and 13) and the suspected boulder clay adjacent to Carr End Farm (sounding 2) have resistivities of c. 100 ohm-metres. Sounding 1 undertaken on bedrock has a resistivity of c. 2500 ohm-metres (Figure 5.15). In order to estimate relative variations in sediment thickness across the old lake basin the resistivity data has been modelled assuming a constant resistance for both the lake sediments (15 ohm-metre) and the underlying till (100 ohm-metre) and bedrock (2500 ohm-metre). The resistivity of the upper layers was allowed to vary. In this way the inversion model is employed to calculate the resistivity of the surface layer and the thicknesses of all the layers.

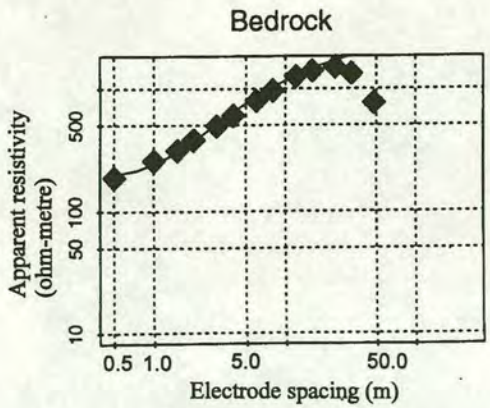

Figure 5.15 Changes in apparent resistivity with electrode spacing for a profile undertaken over bedrock. The high resistivity layer of 2500 ohm-metre represents the bedrock.

Figure 5.16 illustrates the interpreted resistivity data for profiles 6 and 10 while Appendix K lists the Davis-Merrick (constrained) inversion data for each sounding. The results indicate a strong contrast in conductivity in all profiles undertaken within the old lake basin at a relatively uniform depth across the valley floor. This contrast is interpreted as the boundary between the till/bedrock and the lake sediments. The resistivity data suggests that the whole of the old lake basin is underlain by a highly conductive layer of lake sediment deposits about 20 metres thick. The sequence of lake sediments is thickest at soundings site 4 and 5 with deposits of 33 and 28 metres respectively. In Chapter 8 the resistivity measurements are employed alongside gouge and Giddings core sediment data to determine the volume of Raydale Holocene sediment.

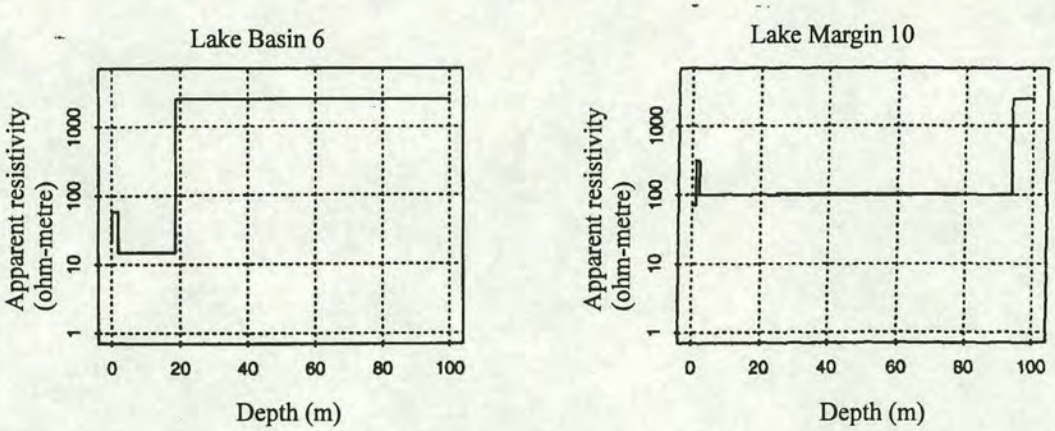

Figure 5.16 Interpreted resistivity data for profiles 6 and 10. Profile 6 shows the strong contrast between the lake sediments which are characterised by low resistivity values and the bedrock which is characterised by much higher resistivity values.

5.8 Raydale Magnetic Measurements

Measurement of χ, ARM, IRM_{100} and SIRM made on samples from 5 cm intervals down cores A, B and C. The four magnetic measurements made on each core are tabulated in Appendix J. Figure 5.17 illustrates changes in sediment density, χ, ARM, IRM_{100}, SIRM, ARM/SIRM, S_{100} and ARM/χ with depth for a representative Giddings core (A) from Raydale. As illustrated in Figure 5.17 variation in sediment

density with depth is minimal, although a sharp decrease occurs at a depth of c. 650 cm. Several very marked peaks in, ARM and IRM_{100} and SIRM can be observed in the uppermost 5.5 m. In mid core, between 5.5 and 8.0 m the magnetic signature is much weaker than in the uppermost 5.5 m and the lowermost 1 m. Table 5.6 summarises the magnetic characteristics of samples from Giddings cores A, B and C.

Table 5.6 A summary of the magnetic properties of Giddings cores A, B and C.

Core A

	χ ($\mu m^3 kg^{-1}$)	ARM ($mA\ m^2 kg^{-1}$)	IRM_{100} ($mA\ m^2 kg^{-1}$)	SIRM ($mA\ m^2 kg^{-1}$)	A/S	S_{100}	ARM/χ ($kA\ m^{-1}$)
Mean	0.050	0.085	0.547	0.733	0.109	0.699	1.547
St dev	0.030	0.094	0.618	0.790	0.044	0.124	1.267
Min	0	0.002	0.012	0.018	0.031	0.289	0.014
Max	0.163	0.457	3.156	3.967	0.222	0.917	4.670

Core B

Mean	0.044	0.026	0.287	0.445	0.070	0.666	1.183
St dev	0.033	0.022	0.278	0.406	0.032	0.113	1.231
Min	0.000	0.004	0.020	0.050	0.019	0.095	0.000
Max	0.133	0.137	2.404	2.952	0.189	1.031	7

Core C

Mean	0.042	0.012	0.200	0.375	0.040	0.524	0.384
St dev	0.024	0.001	0.176	0.308	0.031	0.129	0.370
Min	0.000	0.002	0.019	0.004	0.014	0.250	0.006
Max	0.176	0.045	0.899	1.352	0.167	0.849	2.3

As shown in Table 5.6 mean susceptibility values are low in all cores (typically 0.044 $\mu m^3 kg^{-1}$), a function of the weakly magnetic limestone bedrock underlying the catchment. Samples from Giddings cores A, B and C display a wide range of S_{100} ratios (from 0.095 to 1.031). As illustrated in Chapter 4 (Section 4.2.1) the catchment samples with particularly low S_{100} values are influenced by goethite rather than haematite and thus the magnetic signature within Giddings cores A, B and C can be concluded to arise from a mixture of magnetite and goethite.

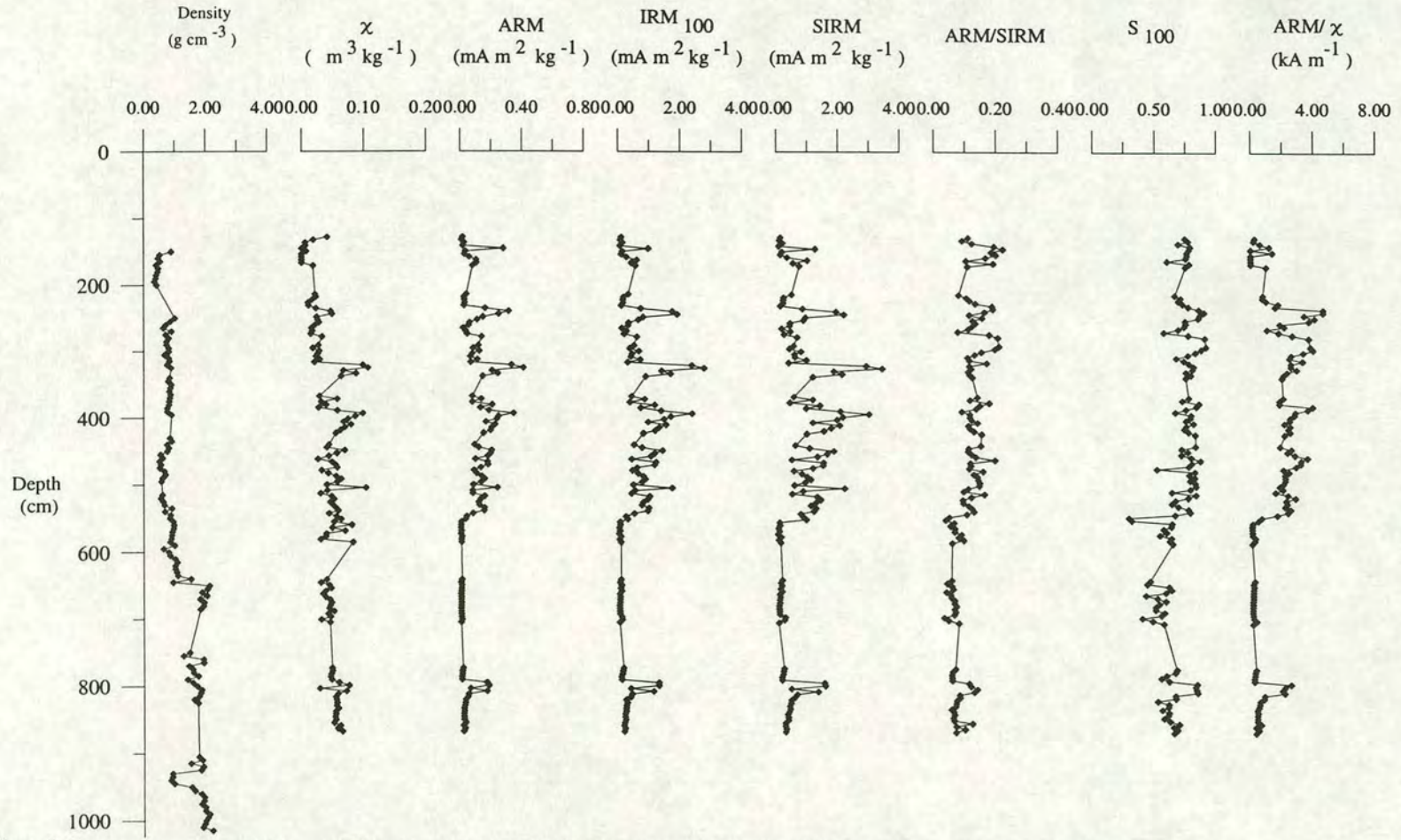

Figure 5.17 Changes in sediment density, χ, ARM, IRM_{100}, SIRM, ARM/SIRM, S_{100} and ARM/χ with depth in Raydale Giddings core A. A sharp decrease in sediment density can be observed at a depth of c. 650 cm, this coincides with an increase in the proportion of fine sediment. The uppermost 5.5 m and lowermost 1 m of core A are characterised by a more varied magnetic signature than central section. The uppermost 5.5 m includes several very prominent peaks in χ, ARM, IRM_{100} and SIRM, using these as indicators of magnetic concentration it is proposed that the variability in magnetic signature arises from variations in the particle size of sedimenting material.

As shown in Figure 5.18 the ARM signature in Giddings core C is both much weaker and less varied than that in Giddings A and B. In core C the average ARM is 0.012 mA m^2 kg^{-1} (standard deviation 0.008); this compares to values of 0.085 mA m^2 kg^{-1} (standard deviation 0.094) and 0.026 mA m^2 kg^{-1} (standard deviation 0.022) in cores A and B respectively. Corresponding variations in χ, IRM and SIRM are observed between Giddings cores A, B and C.

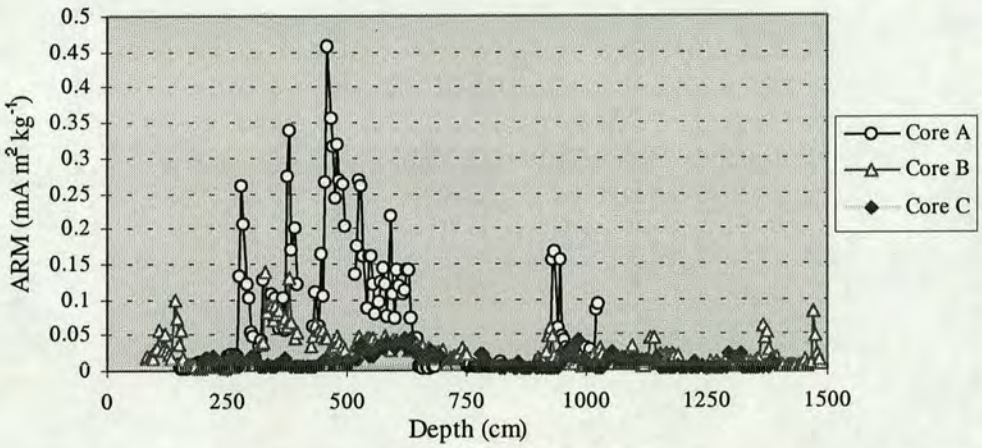

Figure 5.18 A comparison of ARM with depth in Raydale Giddings cores A, B and C. In general core A is characterised by considerably higher ARM values than cores B and C. The ARM signature is greatest in core A at depths between c. 250 -650 cm and 850-900 cm.

Figures 5.19 and 5.20 indicate where the samples, obtained from the Giddings cores, plot on biplots of (i) ARM/SIRM vs S_{100} and (ii) ARM/SIRM vs ARM/χ. The samples span a broader range of ARM/SIRM, S_{100} and ARM/χ ratios than those observed in the Semer Water lake samples. They can be interpreted to contain a mixture of the four magnetic components (i) bacterial magnetite, (ii) topsoil, (iii) goethite and (iv) detrital magnetite The magnetic signature of sediment samples from Giddings cores A and B are dominated by a mixture of, bacterial magnetite, detrital magnetite and topsoil derived magnetite. Giddings core C appears to have two distinct components. Most of the sediment samples display similar, low, ARM/SIRM ratios (0.02 - 0.05) and a range of S_{100} values (0.2 - 0.8) indicating the dominance of detrital magnetite and goethite in these samples. However, some

samples are characterised by increasing ARM/SIRM ratios (up to 0.17) and corresponding increases in S_{100} ratios. They fall on a mixing line between the two sources of goethite and topsoil/bacterial magnetite. As illustrated in Table 5.5, the ARM/χ ratios range between values of c. 0.1 and 7. The broad range of ARM/χ ratios indicates that the magnetic characteristics of some samples are dominated by the influence of detrital magnetite/topsoil whilst other samples are strongly dominated by the presence of magnetotactic bacterial magnetosomes.

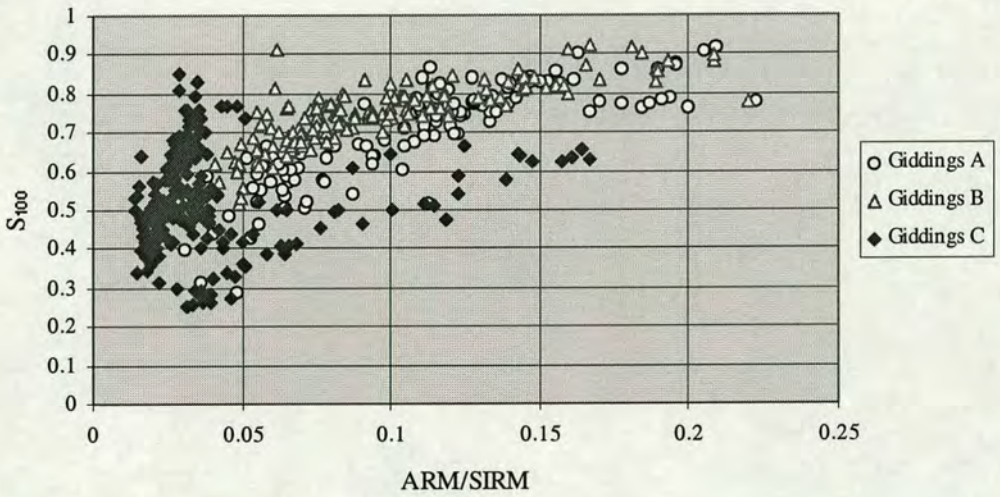

Figure 5.19 A comparison of ARM/SIRM and S_{100} ratios of samples from Raydale Giddings cores A, B and C. The biplot can be interpreted to indicate the origin of the magnetic signature within each of the Raydale cores (refer to Figure 3.6a, Chapter 3). Samples from Giddings core A and B are characterised by a range of ARM/SIRM ratios indicating that the magnetic mineralogy of these samples comprises a mixture of detrital magnetite and bacterial magnetite. Samples from Giddings core C contain comprise two components, most of them are characterised by a range of S_{100} ratios and low ARM/SIRM ratios indicating that they comprise a mixture of detrital magnetite and goethite. Some samples are characterised by increasing ARM/SIRM ratios and corresponding increases in the S_{100} ratio and thus form a mixing line between the two sources goethite and topsoil/bacterial magnetite.

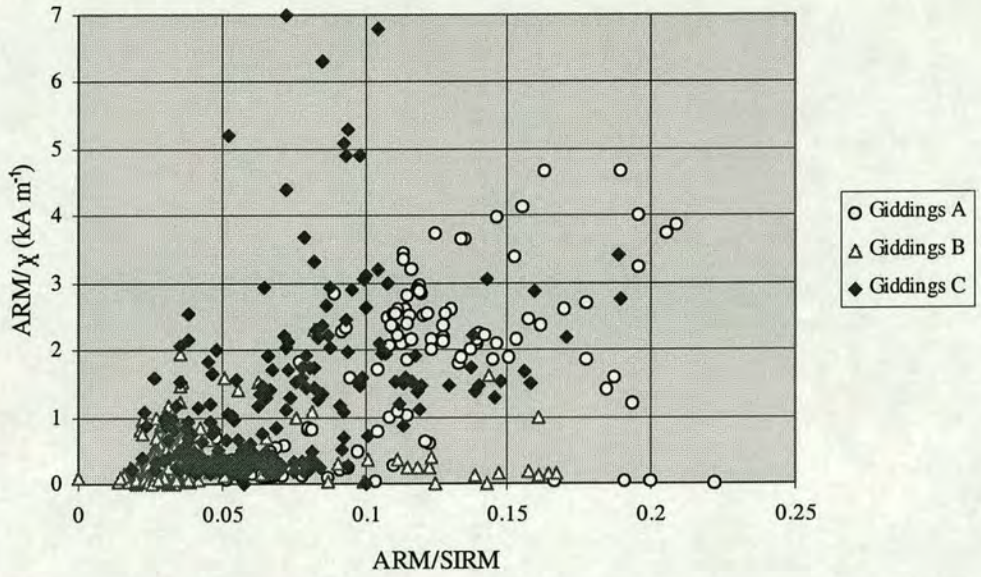

Figure 5.20 ARM/SIRM and ARM/χ ratios of samples from Raydale Giddings cores A, B and C. The biplot can be employed to distinguish between detrital/topsoil magnetic minerals, characterised by low ARM/χ ratios, and magnetotactic bacteria characterised by higher ARM/χ ratios (refer to Figure 3.6c, Chapter 3).

Figure 5.21 illustrates changes in ARM/χ ratio with depth in Giddings core A. Employing an ARM/χ ratio of 1 as a threshold between a topsoil dominated magnetic signature and a bacteria dominated magnetic signature, five distinct zones can be identified: (i) samples from a depth of between 150-260 cm, characterised by low ARM/χ values typical of topsoil (zone 1); (ii) samples from between 265-640 cm, characterised by high ARM/χ ratios indicative of bacteria (zone 2); (iii) samples from between 645-950 cm with low ARM/χ ratios (zone 3); (iv) samples from a depth of 950-965 cm with high ARM/χ ratios (zone 4) and finally; (v) samples from 975-1010 cm with low ARM/χ ratios (zone 5).

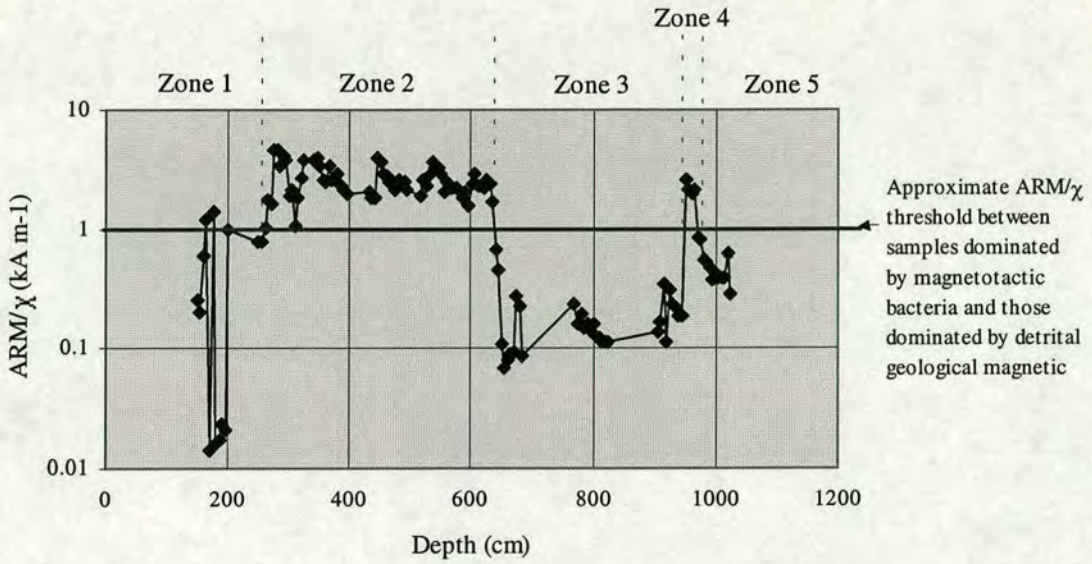

Figure 5.21 Changes in ARM/χ with depth in Raydale Giddings core A. An ARM/χ value of 1 kA m^{-1} has been used to identify five distinct zones separating a magnetic signature influenced by topsoil (ARM/χ <1 kA m^{-1}) from that arising from bacterial magnetosomes (ARM/χ >1 kA m^{-1}). Sediment samples from zones 2 and 4 are influenced by bacterial magnetosomes and samples from zones 1, 3 and 5 influenced more strongly by topsoil/detrital geological material.

5.9 Magnetics and Particle Size Relationships

The variability in magnetic signature in the Giddings cores has been interpreted in conjunction with particle size data. Using ARM as an indicator of magnetic mineral concentration, cores A and B (mean ARM values of 0.085 and 0.026 mA m^2 kg^{-1} respectively) are characterised by higher concentrations of magnetic minerals than core C (mean ARM of 0.012 mA m^2 kg^{-1}) (Figure 5.18). The differences in mean ARM values between cores A, B and C correspond with differences in particle size, as illustrated in Figures 5.11 and 5.13 (Section 5.5) detailed particle size analyses indicated that, whilst core A is characterised by a significant fine grained component, core C was dominated by much coarser material.

In order to study the relationship between the strength of magnetic signature and particle size multiple regression analysis was performed. Initially this was undertaken by regressing ARM with five particle size splits: clays, fine/medium silts,

coarse silts, fine sand and medium/coarse sand (Table 3.1, Section 3.3.3.3). A poor regression relationship was obtained between the clay content (%) and ARM. However stepwise multiple regression analysis performed on both ARM and SIRM and proportion of sediment of each particle size (output data from the laser Coulter Counter), i.e. column of % of material classed as 0.4 μm or 1.05 μm, produced a more significant positive correlation. A regression relationship between the percentage of sample of 1.05 μm size and ARM gives rise to an R^2 value of 65%, indicating that the step-wise procedure was able to predict variation in ARM well using the proportion of material of 1.05 μm size. The amount of sample falling in the 1.05 μm size category equates to a very small proportion of the total sediment group (0.3 to 2.3%), therefore regression analysis has been undertaken using sediment in the size range 0.5 - 1.6 μm. Regression of this data set vs ARM gives an R^2 value of 62% and is based on 3 - 20% of the total sample falling into this narrow particle size range (Figure 5.22). The regression analysis illustrates that 62% of the variation in ARM can be accounted for by variations in particle size.

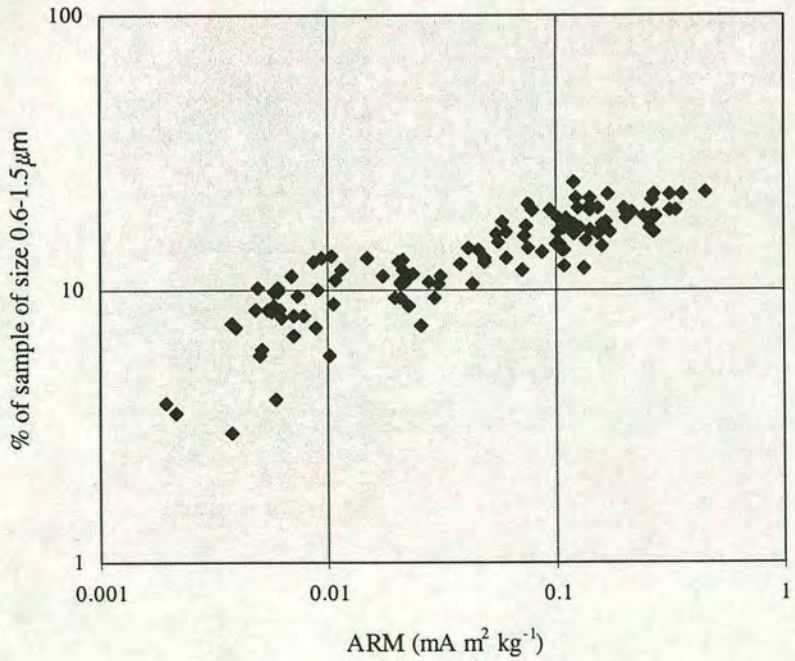

Figure 5.22 Correlation between the proportion of sample of size 0.6 to 1.5 μm and ARM in Raydale Giddings core A (R^2 value 62%). Increases in ARM are correlated with an increase in the proportion of very fine sediment (0.6-1.5 μm).

The changes in ARM are thus indicative of changes in grain size, especially changes in the amount of fine material, of size range 0.4 - 1.6 μm. Variations in grain size within the cores are interpreted as indicating either changes in the source of material within the catchment or changes in the depositional environment associated with either water level fluctuations or changes in the flow path of the inflowing Crooks Beck. The high ARM values, ARM/SIRM and ARM/χ ratios which characterise many of the sediment samples in Giddings core A indicate that the magnetic characteristics of these samples are dominated by bacteria. The relationship observed between fine grained material and magnetic concentration indicates that the bacteria lie in the fine-grained sediment.

In order to verify the relationship between the strength of magnetic signal and particle size in Giddings core A, a bulk sediment sample was obtained from a depth of 6.5 - 6.6 metres. This sample was split using the centrifuge technique outlined in Section 3.3.3, and χ, ARM, IRM and SIRM measurements obtained on each sample split (Table 5.7).

Table 5.7 Selected magnetic characteristics of Giddings core A size splits.

Particle size	ARM ($mA\ m^2\ kg^{-1}$)	SIRM ($mA\ m^2\ kg^{-1}$)	χ ($\mu m\ kg^{-1}$)	A/S	ARM/χ ($kA\ m^{-1}$)
0-2	0.1125	3.125	*	0.036	
2-10	0.099	1.048	0.081	0.094	1.22
10-63	0.057	0.438	0.026**	0.130	2.19
63-500	0.062	0.566	*	0.110	

* negative susceptibility - diamagnetic from plastic sample pot.

** probably lowered by diamagnetic contribution from plastic sample pot.

The magnetic results obtained on the particle size splits confirm the regression relationship between the strength of the ARM and SIRM signal and the proportion of sediment falling in the 0.5-1.6 μm fraction. The bulk sediment splits show that magnetic minerals are concentrated in the fine fractions of the sediment. The results indicate, however, that the 2-10 μm fraction contains significant concentrations of

magnetic minerals too. This observation may be attributed partly to the difficulties in separating the fine 0-2 μm particles completely from the coarser fractions.

A sample of sediment from the alluvial fan, i.e. contemporary sedimenting material, was also sub-divided into the above particle size fractions and magnetic measurements undertaken on each split. These results (Table 5.8) provide further evidence of the concentration of magnetic minerals in the fine fraction.

Table 5.8 Selected magnetic characteristics of alluvial fan sediment size splits.

Particle size	ARM ($mA\ m^2\ kg^{-1}$)	SIRM ($mA\ m^2\ kg^{-1}$)	χ ($\mu m\ kg^{-1}$)	A/S	ARM/χ ($kA\ m^{-1}$)
0-2	0.664	7.100	0.500	0.094	1.33
2-10	0.545	3.866	0.430	0.141	1.27
10-63	0.142	0.857	0.118	0.165	1.21
63-500	0.011	0.186	0.013**	0.058	0.83

** probably lowered by diamagnetic contribution from plastic sample pot.

Figure 5.23 illustrates the distribution of sample splits from Giddings material and alluvial fan material on the basis of ARM and SIRM information. As the diagram demonstrates, both the ARM and SIRM signature of the samples is significantly greater in the fine fraction. The strength of the ARM and SIRM signal decreases with increasing particle size in the alluvial fan samples. The core samples exhibit a similar trend. Surprisingly however, both the ARM and SIRM values appear to be slightly greater in the size fraction 63-500 than the size fraction 10-63.

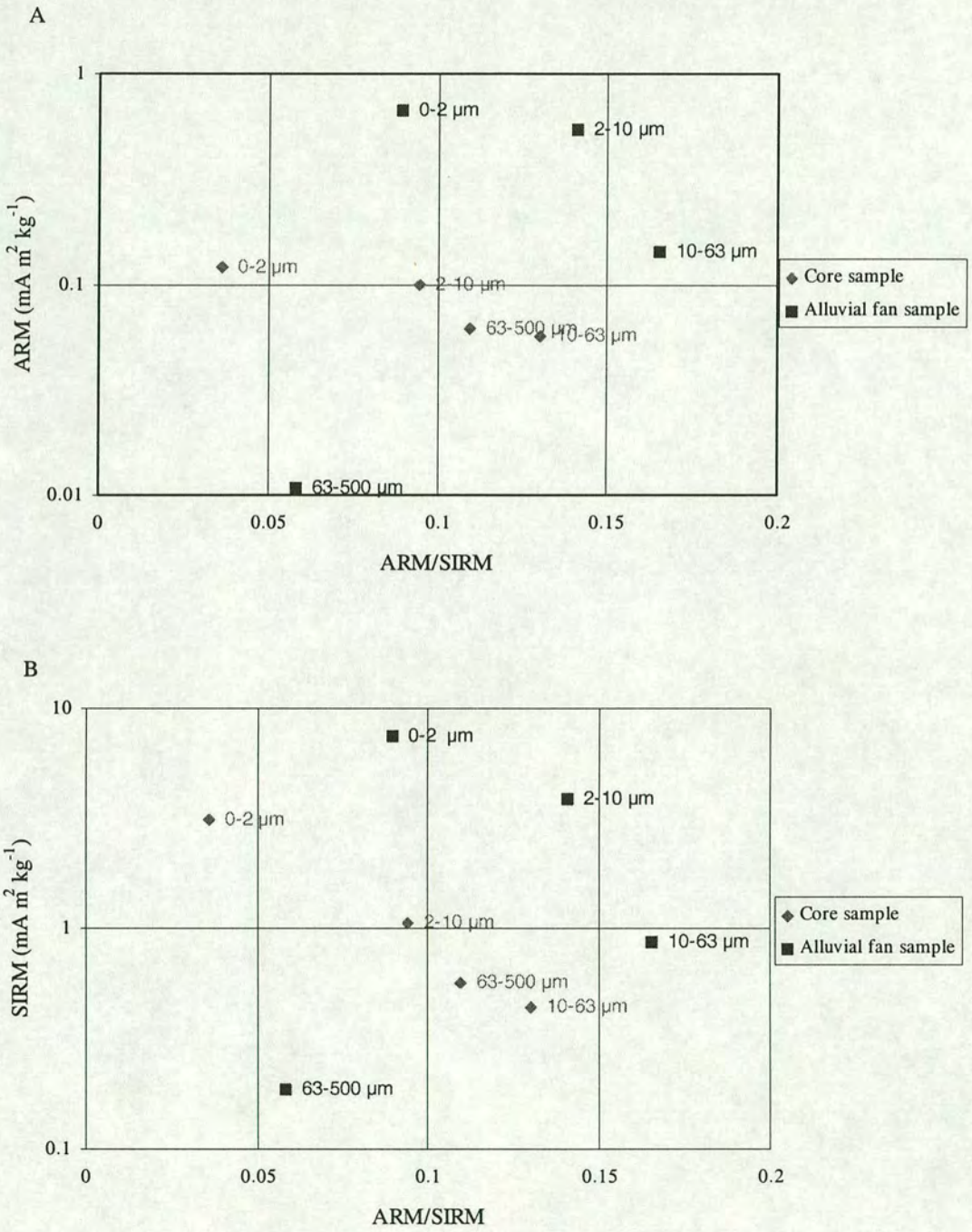

Figure 5.23 ARM/SIRM ratios plotted against ARM (A) and SIRM (B) for particle size splits from a bulk sample from Raydale Giddings core A and Semer Water alluvial fan deposits. The ARM and SIRM is greater in the fine sediment fraction of the alluvial fan sample. The sediment samples from the Raydale core display a similar trend of increasing ARM and SIRM values with decreasing sediment size, however they values appear to be slightly greater in the 65-500 µm size fraction than the 10-63µm size fraction.

A relationship between the strength of ARM, SIRM signature and particle size is observed in both contemporary sedimenting material in the delta and material deposited earlier in the Holocene (Giddings core A bulk sample). This observation suggests that high concentrations of magnetic minerals are present in the very fine material deposited in Giddings core A and in the alluvial fan samples. The high ARM/χ ratios in the fine fraction of the delta sample indicates that the magnetic signature results from magnetotactic bacteria. However the ARM/SIRM ratios for the 0-2 μm fraction in both the Giddings A and alluvial fan sediment splits are much lower than those typically associated with the presence of bacterial magnetosomes. Indeed the ARM/SIRM quotients are actually greater in the 2-10, 10-63 and 63-500 μm fractions of the core samples and in the 2-10 and 10-63 μm fractions of the alluvial fan sample than those quotients in the 0-2 μm fraction. Thus although the concentrations of magnetite are greatest in the fine fraction the extent of magnetic interaction appears to be greatest in the coarser 2-10 and 10-63 μm fractions.

In order to study the link between ARM/SIRM ratios and particle size, further stepwise regression analysis has been undertaken on the detailed particle size and magnetic measurements undertaken on Giddings core A. Stepwise regression indicated that no one particular sediment size or class of sizes yielded a strong relationship with the ARM/SIRM ratio. However, correlation between the ARM/SIRM ratio and a range of particle size classes indicates that the strongest positive correlation is observed between ARM/SIRM ratios and the proportion of sediment of 10-30 μm size (Table 5.9, Figure 5.24). A negative correlation between the ARM/SIRM ratio and the proportion of sediment of 50-70 and 70-500 μm is observed. The correlation coefficients obtained between the strength of the ARM/SIRM signal in samples from Giddings core A and the proportion of material of particular size fractions confirm the observed relationship between particle size and ARM/SIRM ratio in the bulk particle size splits. Increases in the ARM/SIRM quotients are influenced more strongly by increases in the proportion of material of 2-10 and 10-30 μm size than of 0-2 μm indicating weaker magnetic interactions in the 0-2 μm sized sediment that those present in the 2-30 μm fraction.

Table 5.9 Correlation between ARM/SIRM and particle size groups.

Size fraction (μm)	Correlation coefficient
0-2	0.22
2-10	0.38
10-30	0.47
30-50	0.03
50-70	-0.21
70-500	-0.41

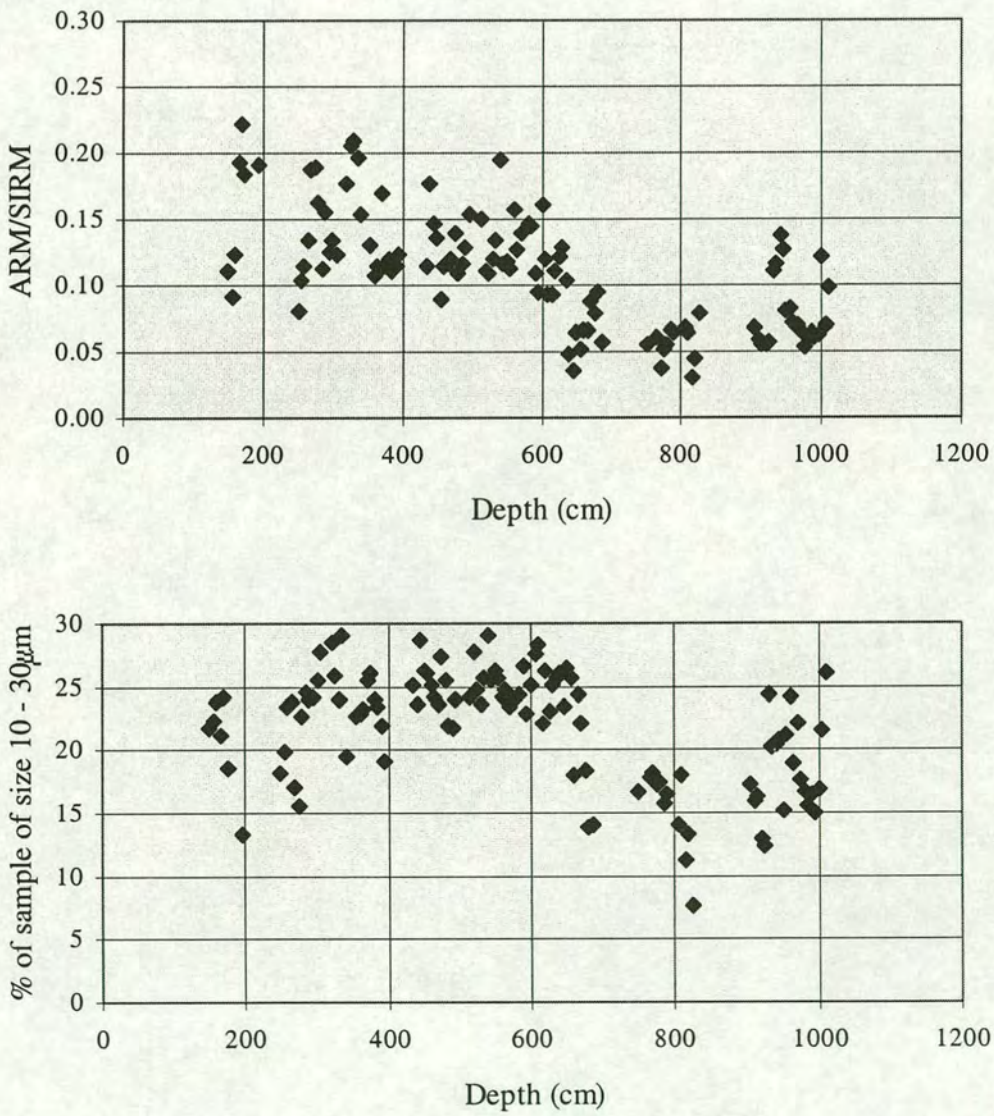

Figure 5.24 A comparison between ARM/SIRM ratio with depth and the proportion of sediment sample of 10 - 30 μm size with depth in Raydale Giddings core A. High ARM/SIRM ratios correspond with high proportions of sediment of sample size 10-30 μm in Giddings core A.

Given the relationship determined between ARM and particle size we can infer that core C must comprise a significant coarse component. Particle size results illustrated in Figure 5.14 confirm this. ARM values in core B fall in between those obtained on cores A and C. Values are particularly weak in the zone between 160 and 270 cm. The lithostratigraphy of this core (Figure 5.4) confirms that this section of the core comprises coarse sandy material.

5.10 Comparison of Raydale, Lake and Catchment Samples

Table 5.10 provides just one illustration of the variation in magnetic properties between the Raydale Giddings cores, Mackereth lake cores and catchment samples from Semer Water. Variation in the ARM/χ signal is greatest in Giddings core A and B. The average ARM/χ ratio is higher in the lake cores (SL1/SL2) than in the Giddings cores (A, B and C). The catchment samples are characterised by very low ARM/χ ratios.

Table 5.10 A comparison of ARM/χ quotients (kA m^{-1}) of samples from Raydale Giddings cores, Semer Water lake cores and the catchment samples.

	Giddings A	Giddings B	Giddings C	SL1	SL2	Catchment
Mean	1.54	1.60	0.37	2.11	1.90	0.25
St dev	1.26	1.35	0.37	0.40	0.21	0.17
Min	0.01	0.13	0.01	0.82	1.33	0.03
Max	4.67	6.8	2.3	2.89	2.46	0.84

The influence of bacterial magnetite on the magnetic signature recorded in Raydale, lake and catchment samples can also be studied using a bi-plot of ARM vs ARM/SIRM (Figure 5.25). The plot illustrates increasing significance of magnetic interactions along the horizontal axis and increasing concentration up the vertical axis. The biplot has a modal kind of distribution; many samples plot mid-way along the ARM/SIRM axis and high on the vertical ARM axis. As illustrated in Figure 5.26, the greatest concentration of magnetic minerals is observed in lake core

samples and in some samples from Giddings core A. These cores are characterised by high percentages of fine material, and a link between magnetic concentration and particle size has been found (Section 5.8).

The modal distribution displayed in Figure 5.25 may relate to differing degrees of preservation of bacteria chains. High ARMs, characteristic of the lake sediment samples, are perhaps indicative of high concentrations of broken bacterial chains whilst high ARM/SIRM ratios may result from lower concentrations of intact well preserved chains of bacteria, or vice versa.

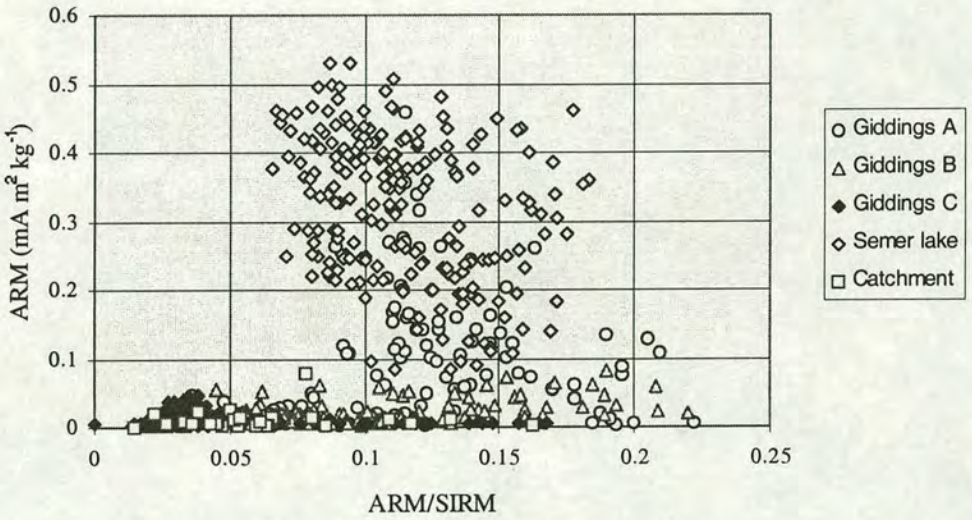

Figure 5.25 Biplot comparing ARM values and ARM/SIRM ratios for samples from Raydale Giddings cores A, B and C, Semer Water lake cores and the catchment (refer to Figure 3.6b, Chapter 3). Samples from Semer Water lake cores and some samples from Giddings core A are characterised by particularly high ARM values, perhaps indicative of high concentrations of broken bacterial chains.

5.11 Gully Surveys

Fifty five gullies have been identified in the Semer Water catchment (Figure 5.26). Each gully has been classed as either small, medium or large in cross-sectional area and the length measured. Appendix L tabulates the size class of each of the fifty five identified gullies in the Semer Water catchment. The cross-sectional areas of five surveyed gullies (A2, A3, B2, B3 and C2 on Figure 5.26) in the Semer Water catchment have been employed to estimate the average cross-sectional area of each of three size classes of gully (Table 5.11). The average cross-sectional area of each size class coupled to the length of each sized class gully in the Semer Water catchment is then used to determine the volume of material potentially eroded from all of the identified gullies within the catchment (Table 5.12). This worked out to be about four million cubic metres.

In order to take account of material potentially derived from river beds and river banks the length of the main river channels flowing into Semer Water (excluding those rivers flowing down gullies) has also been determined. It is similarly estimated at about four million cubic metres.

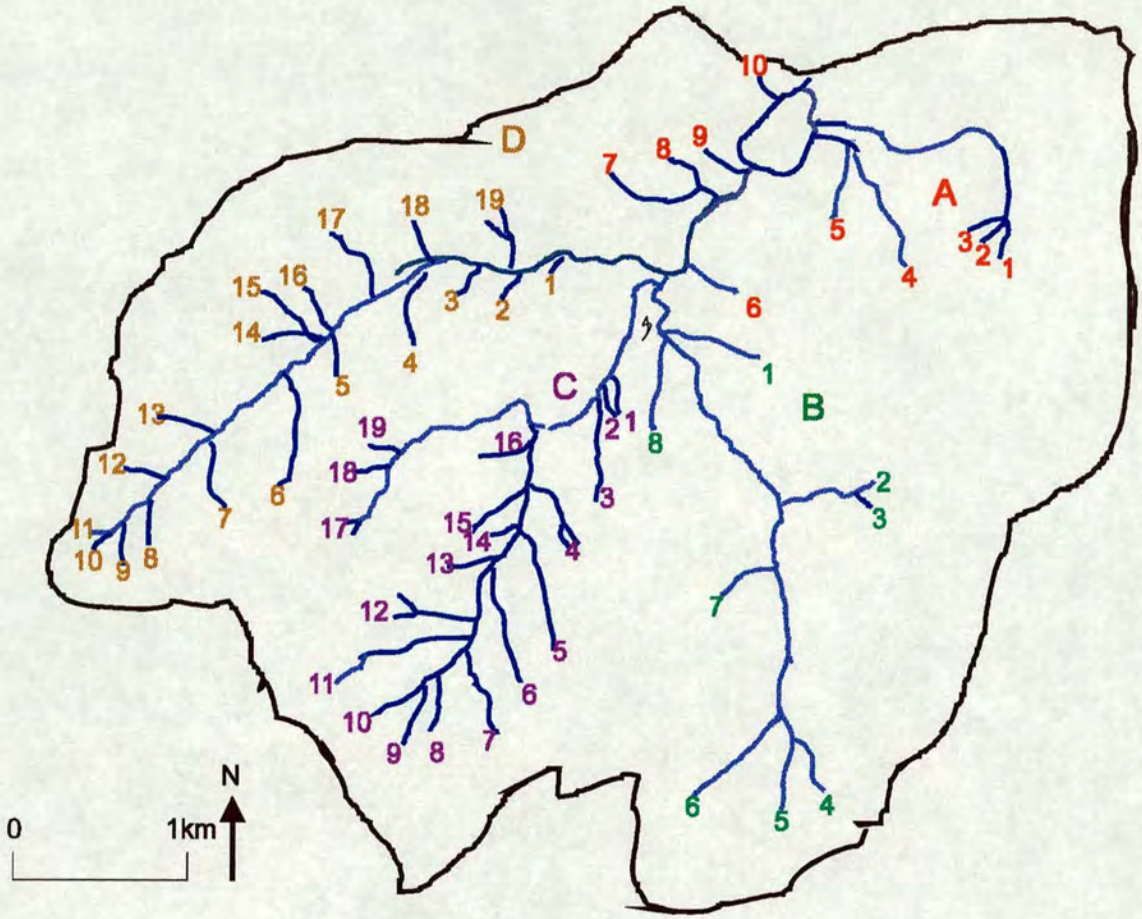

Figure 5.26 The location of gullies in the Semer Water catchment. Five gullies were surveyed in order to determine the mass of sediment potentially eroded from each one. Fifty five gullies identified in the Semer Water catchment were then classed into three size categories in order to estimate of the volume of material potentially produced during the Holocene from gully erosion within the Semer Water catchment.

Table 5.11 Cross sectional-area of surveyed gullies in the Semer Water catchment.

Gully	Cross-sectional area (m^2)	Code (Figure 5.26)	Category
Carpley Green Gully	246	A2	Small
Water Ling Gully	195	A3	Small
Shaw Gate Gill River	1737	B2	Large
Silky Gill Gully	444	B3	Small
Raydale Waterfall Gully	32	C2	Small

Table 5.12 Length of rivers and gullies, average cross-sectional area and volume of sediment potentially eroded from the gullies and rivers in the Semer Water catchment.

	Length (m)	Average cross-sectional area (m^2)	Volume ($10^6 m^3$)
Rivers	9875	400	3.9
Large gullies	8125	400	3.3
Medium gullies	4125	200	0.83
Small gullies	8275	25	0.20
Flood plain	2000	325	0.65
Total			8.8

Finally a rough estimate of material on the flood plain in the main Raydale valley (south west of the old lake basin) has been made. It is about 0.6 million cubic metres. It is therefore concluded that, potentially, in the region of nine million cubic metres of material may have been eroded during the Holocene from gullies in the Semer Water catchment. In Chapter 8 these volumes will be compared with those of the Semer Water lake sediments and then with Universal Soil Loss Equation estimates of erosion in the Semer Water catchment.

5.12 Summary

- Seven gouge core transects and three Giddings cores have been obtained from Raydale. The cores collected from the centre of the basin are characterised by silt and clay whilst the more marginal cores contain a higher sand content. Using a Giddings corer sediment cores in excess of 14 metres thick have been recovered from Raydale.

- Pollen is preserved in the Raydale cores. The *Alnus* rise and *Ulmus* decline, evident in Giddings core A, have been used to establish mean sediment accumulation rates of 0.08 and 0.04 cm a^{-1} for the time periods 0-6294 BP and 6294 - 8220 BP respectively in Giddings core A. Very low concentrations of

Ulmus and high concentrations of *Alnus, Plantago and Gramineaa* occur throughout cores B and C indicating that the sediment has been deposited since 6294 BP. The resulting sediment accumulation rates are 0.23 and 0.21 cm a^{-1} for Giddings cores B and C respectively.

- Detailed particle size analysis shows a variation from sand at the base of the core A, through fine silt in the centre and back to sand at the top of the core. In contrast core C is dominated by coarse sand and silt throughout.

- At Raydale changes in apparent resistivity with depth have been interpreted in terms of changes in stratigraphy. Thick lake sediment deposits have been identified over an area of 0.5 km^2.

- Surveying techniques shows that about eight million m^3 of material could, potentially have been eroded from the gullies and rivers in the Semer Water catchment during the Holocene.

Chapter 6

Gormire

6.1 Introduction

At Gormire both catchment samples and lake sediment cores have been collected and characterised magnetically. Variations in sediment density and lithostratigraphy have been noted. Magnetic techniques can be employed to correlate the uppermost section of the lake cores and hence to transfer the ^{210}Pb and ^{137}Cs chronology, determined by P.Appleby, to each core. Sediment accumulation rates and density have been used to calculate sediment influx and sediment yields within the Gormire catchment.

6.2 Catchment Samples

Catchment samples were collected from the six locations shown in Figure 6.1. The catchment samples included material from path erosion scars and topsoil (Table 6.1).

Table 6.1 The origin of catchment samples from the Gormire Catchment.

Samples	Origin
1, 3, 4	Exposed subsoil
2, 5, 6	Topsoil

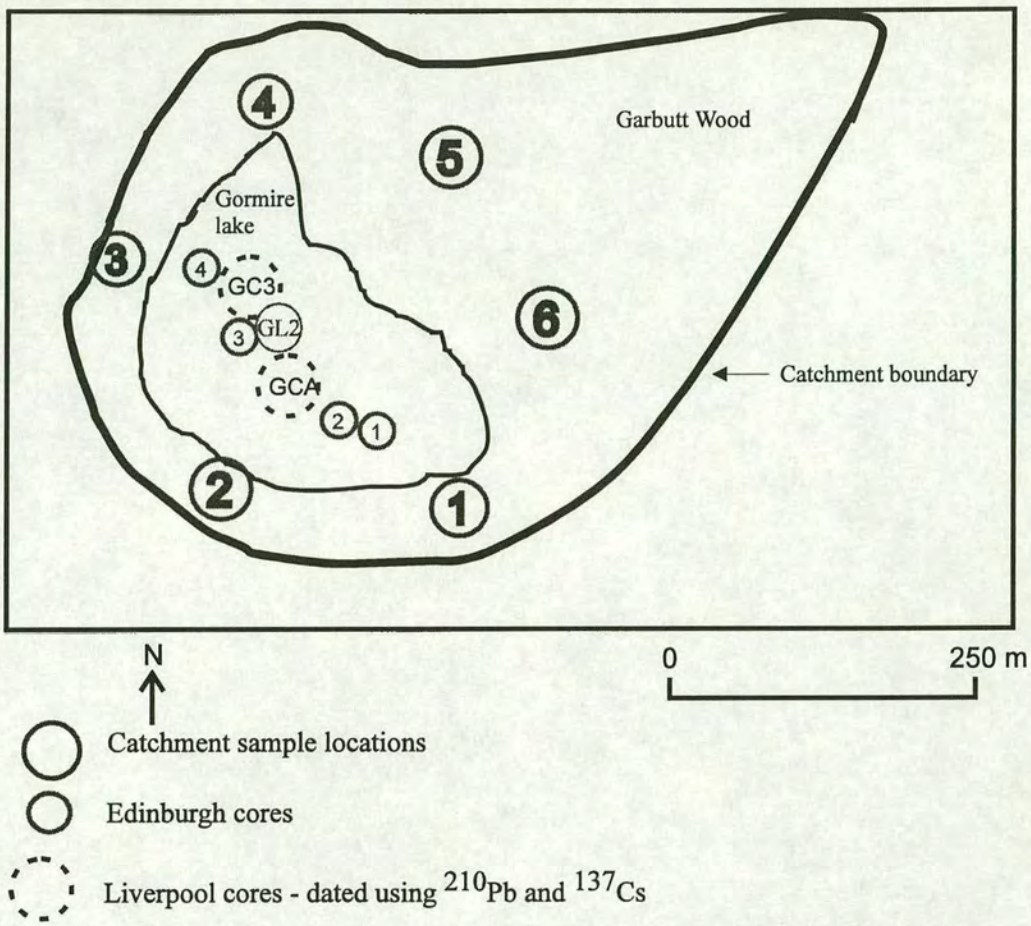

Figure 6.1 Location of seven Mackereth lake cores and six catchment samples at Gormire. Of the seven lake cores obtained five were collected by Edinburgh University and two by researchers at the University of Liverpool. The two cores from Liverpool have been dated by P.Appleby using ^{210}Pb and ^{137}Cs.

6.2.1 Magnetics of Catchment Samples

The magnetic properties of the six catchment samples collected from the Gormire catchment are summarised in Table 6.2.

Table 6.2 Magnetic properties of Gormire catchment samples.

Sample	χ ($\mu m^3 kg^{-1}$)	ARM ($mA\ m^2 kg^{-1}$)	IRM_{100} ($mA\ m^2 kg^{-1}$)	SIRM ($mA\ m^2 kg^{-1}$)	A/S	S_{100}	ARM/χ ($kA\ m^{-1}$)
1	0.065	0.025	0.34	0.61	0.041	0.558	0.387
2	0.200	0.059	1.62	2.81	0.021	0.578	0.293
3	0.051	0.007	0.07	0.18	0.039	0.407	0.134
4	0.184	0.055	1.03	1.72	0.032	0.597	0.301
5	0.222	0.051	0.81	1.25	0.041	0.649	0.228
6	0.063	0.019	0.39	0.66	0.029	0.584	0.307
Mean	0.131	0.036	0.71	1.20	0.034	0.562	0.275
St dev	0.072	0.018	0.48	0.81	0.007	0.069	0.072
Min	0.051	0.007	0.07	0.18	0.021	0.407	0.135
Max	0.222	0.059	1.62	2.81	0.041	0.649	0.387

Magnetically the samples exhibit varied behaviour. Samples 2, 4 and 5 are characterised by higher ARM, IRM_{100} and SIRM values than samples 1, 3 and 6. However the mean susceptibility value of 0.13 $\mu m^3 kg^{-1}$, and the narrow range of values, indicates that only small concentrations of magnetic minerals are present. The low S_{100} values of between 0.41 and 0.65 show the catchment samples to be dominated by a mixture of magnetite and haematite/goethite. Figure 6.2 illustrates how the Gormire catchment samples acquire IRM in fields up to 4T. All show rises of over 10% above 1T. Sample 3 acquires over half of its IRM in fields greater than 2T indicating the presence of goethite, rather than haematite in this sample.

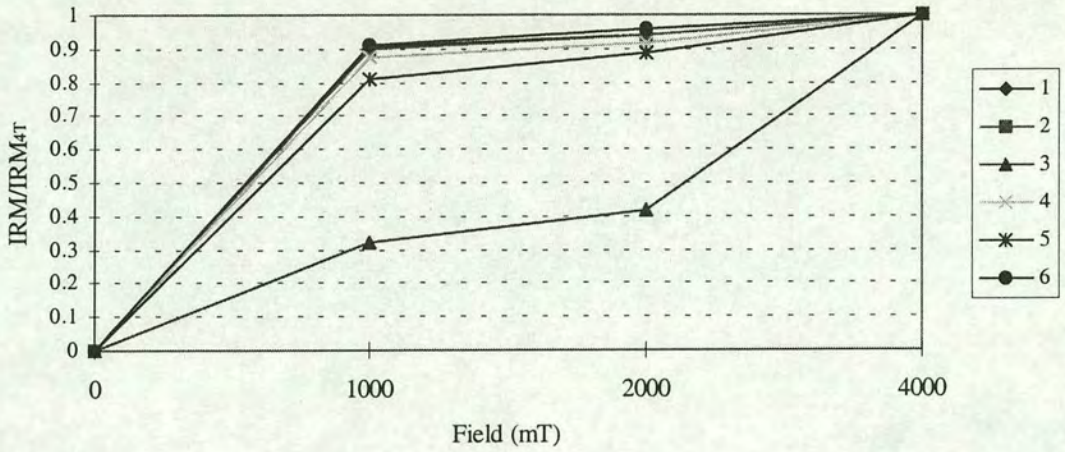

Figure 6.2 IRM acquisition curves for catchment samples 1-6 from Gormire. All show increases of over 10% above 1000 mT showing that haematite/goethite makes up over half of the minerals in the catchment samples. For sample 3 the magnetisation increases particularly significantly in fields above 2000 mT, indicating the dominance of goethite.

6.3 Sediment Cores

6.3.1 Core Collection

Six one-metre and two three-metre long Mackereth cores have been recovered from Gormire. The locations of the cores are shown in Figure 6.1.

6.3.2 Lithostratigraphy

The sediment cores obtained from Gormire display little variation in stratigraphy with depth. As observed at Semer Water and Hornsea Mere the cores are dominated by clay and silt. Fragments of partially decomposed organic matter, for example leaves, were observed.

Gormire cores display mean sediment densities of 0.353 g cm^{-3}. Variations in density of between 0.182 and 0.607 g cm^{-3} are observed and changes in density with depth in cores from Gormire are fairly gradual. Figure 6.3 illustrates changes in density with depth for a representative core from Gormire. The complete sediment density data for all 6 cores is provided in Appendix H.

6.3.3 Total Organic Carbon and Carbonate Content

Total organic carbon and carbonate content are being measured as part of a collaborative project with Liverpool University. Fisher (pers.comm., January 1998) reports the following total organic carbon (TOC) and carbonate content in a Gormire long core (G3).

	TOC (%)	Carbonates (%)
Zone IV	11	16
Zone III	11	14
Zone II	20	11
Zone I	25	16

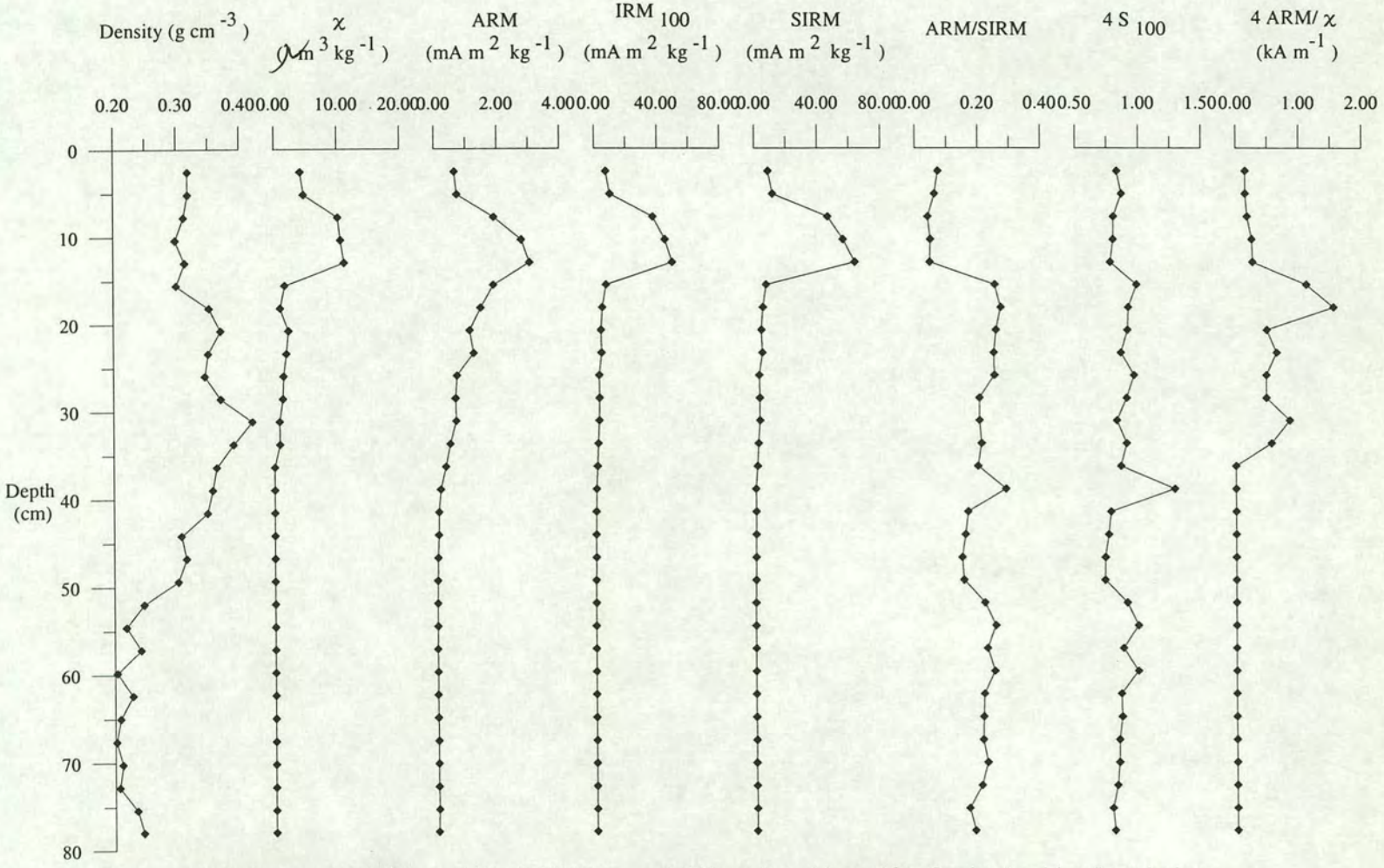

Figure 6.3 Changes in sediment density, χ ARM, IRM_{100}, SIRM, ARM/SIRM, S_{100} and ARM, χ with depth in core 4 from Gormire. A peak in sediment density can be observed towards the centre of core 4 and peaks in χ ARM, IRM_{100} and SIRM occur in the uppermost 20 cm of the sediment core. The prominent peak is attributed to the presence of the magnetic sulphide greigite.

6.3.4 Gormire Chronology

Appleby (1998) has determined a chronology for two cores from Gormire, GCA and GC3, using ^{210}Pb and ^{137}Cs. Appleby (1988) estimates sediment accumulation rates of 0.25 (st dev 0.20) and 0.24 (st dev 0.13) cm a^{-1} for cores GCA and GC3 respectively.

Blackham *et al.* (1981) collected central and marginal cores from Gormire. They identified the alder rise at a depth of about 5 m and the onset of forest cover at about 6 m. Dating these events to 8220 BP and 12 000 BP results in accumulation rates of 0.06 and 0.03 cm a^{-1} for the period since 8220 BP and between 8220 and 12 000 BP.

6.3.5 Lake Sediment Magnetic Measurements

As at all sites measurements of χ, ARM, IRM_{100} and SIRM were made on every sample taken at 2 cm intervals down each of six cores. The results of these magnetic measurements are tabulated in Appendix J. Figure 6.3 illustrates changes in sediment density χ, ARM, IRM_{100}, SIRM, ARM/SIRM, S_{100} and ARM/χ for a representative core (4) from Gormire. A peak in sediment density can be observed towards the centre of core 4 and peaks in ARM, IRM_{100} and SIRM occur in the uppermost 20 cm of the sediment core.

ARM is chosen as representative of changes in magnetic concentration in the Gormire sediments. Figure 6.4 shows how ARM varies in the six cores studied. It shows very low magnetic concentrations in the lowermost part of the core followed by an increase in the centre which rises to a peak in the uppermost half of the core. Following the peak ARM values fall to values approximately mid-way between those at the base of the core and those at the peak. Excluding core 1 lake cores obtained from Gormire can be divided into four depth zones which display distinctly different magnetic characteristics. The magnetic zone boundaries are illustrated on Figures 6.4 and 6.5, which plot changes in ARM and ARM/SIRM ratio with depth. Table 6.3

tabulates the depths employed to define the boundaries between the zones. Table 6.4 sets out the mean, minimum and maximum of the χ, ARM and SIRM values for each zone and Table 6.5 summarises the magnetic characteristics of each zone.

Table 6.3 Approximate depth (cm) of each magnetic zone boundary.

	Core							Age
Boundary	1	2	3	4	GCA	GC3	GL2	
III/IV	*	*	5	15	15	15	7	1935
II/III	10	15	16	27	27	25	27	#
I/II	40	44	42	39	41	49	41	#

* III/IV boundary not evident

Sediment too old to data using ^{210}Pb

Table 6.4 A comparison between the mean χ, ARM and SIRM values for samples from zones I, II, III and IV in cores 2, 3, 4 and GL2.

		Zone I	Zone II	Zone III	Zone IV
χ	Mean	0.000	0.065	0.518	0.445
($\mu m^3 kg^{-1}$)	Min	0.000	0.000	0.124	0.419
	Max	0.000	0.225	1.117	0.471
ARM	Mean	0.065	0.695	1.604	0.690
($mA\ m^2\ kg^{-1}$)	Min	0.041	0.055	0.478	0.653
	Max	0.112	2.174	3.041	0.727
SIRM	Mean	0.441	3.031	23.0	10.3
($mA\ m^2\ kg^{-1}$)	Min	0.261	0.284	4.26	8.86
	Max	1.121	8.68	63.8	11.7

Table 6.5 Selected magnetic characteristics of each zone in Gormire cores 2, 3, 4, GL2, GCA and GC3.

	ARM	SIRM	Hardness of ARM	ARM/SIRM	χfd	ARM/χ	SIRM/χ
Zone I	low	low	soft	medium	zero	high	
Zone II	rising	rising	hard	med/high	zero	high	
Zone III	medium/high	high	hard	low	high	low	high
Zone IV	low/medium	high/med	hard	low, rising	high	low	medium

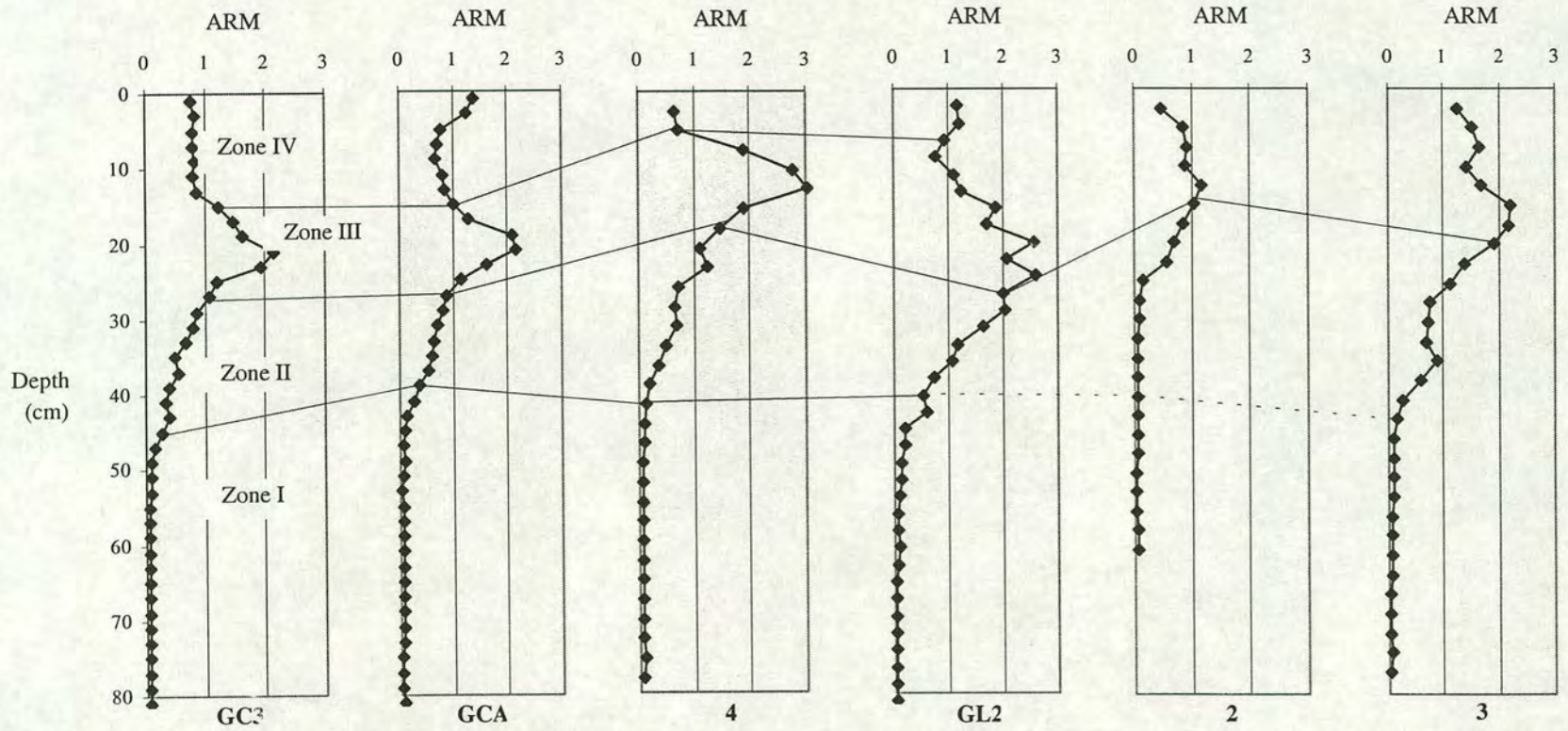

Figure 6.4 Changes in ARM with depth in cores 2, 3, 4, GL2, GCA and GC3 from Gormire. Four distinct magnetic zones have been identified in each of these cores. Cores 2, 3, 4 and GL2 ARM (mA m^2 kg^{-1}) Edinburgh measurements. Cores GCA and GC3 ARM (arbitary units) Liverpool measurements. Zone III is characterised by a prominent peak in ARM which is attributed to the presence of the authigenic iron sulphide greigite, however without more information about the biogenic or chemical processes operating within the lake or sediment no explanation is offered for the presence of this marked peak.

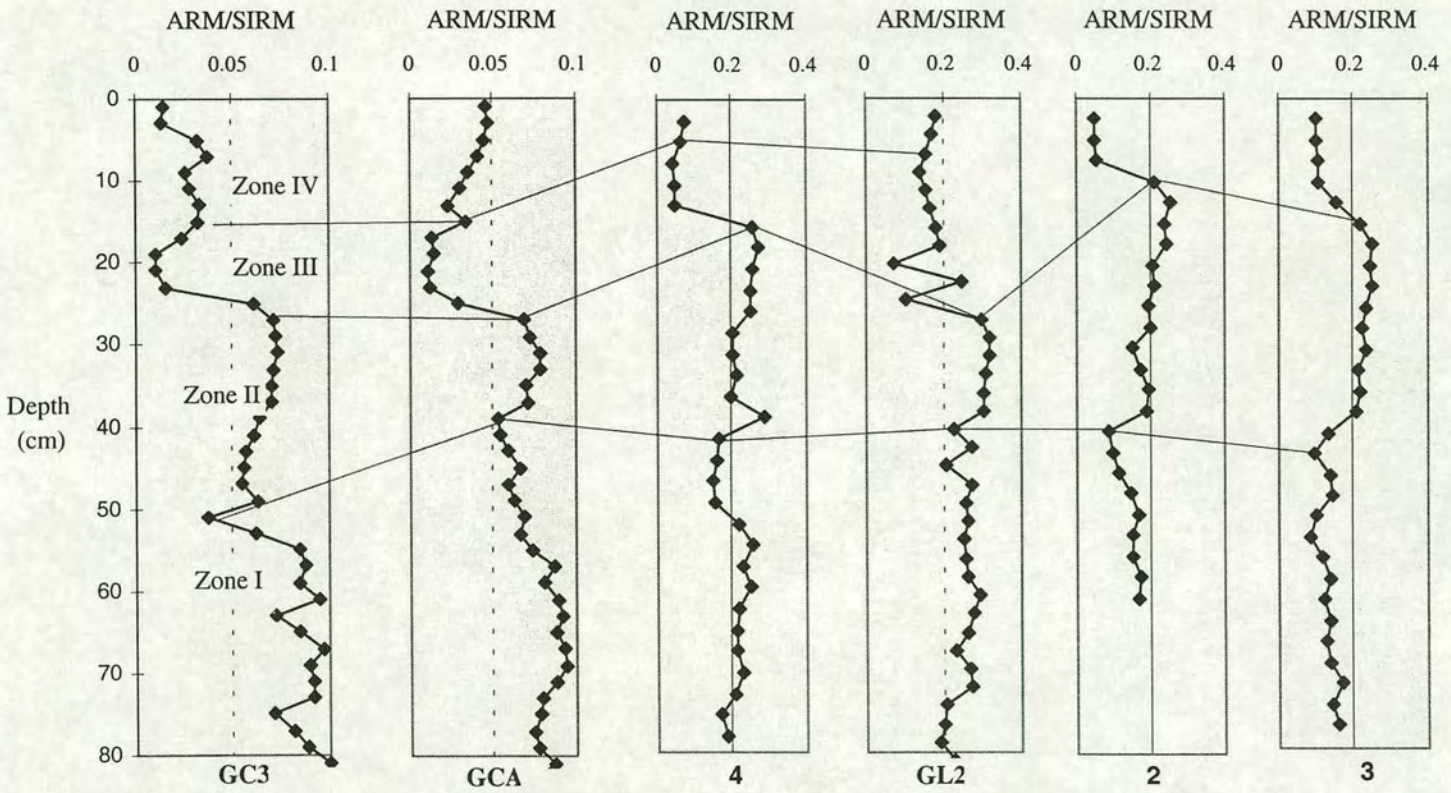

Figure 6.5 Changes in ARM/SIRM with depth in cores 2, 3, 4, GL2, GCA and GC3 from Gormire. Four distinct magnetic zones have bee identified in each of these cores. Cores 2, 3, 4 and GL2 ARM/SIRM Edinburgh measurements. Cores GCA and GC3 ARM/SIRM (arbitary units) Liverpool measurements.

Zone I is characterised by a weak magnetic remanence. It also has zero frequency dependency of susceptibility and ARM/SIRM ratios of around 0.15. Zone II displays rising magnetic values, high ARM/χ and ARM/SIRM ratios and again no frequency dependency. Zones III and IV are characterised by much stronger magnetisations. They also have high frequency dependent values (between 5 and 10%), low ARM/χ and low ARM/SIRM values. Zone IV displays lower ARM and SIRM values than Zone III. As illustrated in Figures 6.4 and 6.5 the trends in magnetic properties in cores 2, 3, 4, GL2, GCA and GC3 can be employed for core correlation.

Figures 6.6 and 6.7 illustrate the magnetic distinction between samples from Zones I, II, III and IV in terms of ARM, S_{100} and ARM/SIRM. The very low ARM values of samples from Zone I are indicative of very small concentrations of magnetic minerals. With ARM/SIRM ratios ranging from 0.08 to 0.26 the samples are characterised by magnetic minerals of topsoil or bacterial origin. As observed in Table 6.5, Zone I samples do not display any frequency dependency, and have high ARM/χ ratios indicating that the magnetic signature in this zone is dominated by bacterial magnetosomes. Zone II samples are characterised by high ARM/SIRM ratios up to 0.28, a range of ARM values up to 2.2 mA m^2 kg^{-1}, high ARM/χ ratios and no frequency dependency of susceptibility. These magnetic characteristics indicate high concentrations of magnetic minerals of bacterial origin. With ARM/SIRM ratios of 0.03 to 0.15, low ARM/χ ratios and a high degree of frequency dependency, sediment samples from zones III and IV have a magnetic signature attributable to topsoil. Three samples from zone III are characterised by significantly higher ARM/SIRM ratios than other samples within this zone. This may be indicative of the influence of intact magnetotactic bacterial magnetosome chains in these samples. The peak in remanence observed in Figure 6.6 towards the top of the Gormire cores cannot be attributed to the input of atmospheric spherules because the peak in ARM (18-20 cm and 20-22 cm in cores GCA and GC3 respectively), has been dated to between c. 1860 and 1900 in cores GCA and GC3 (Section 6.2.4), predating the period of significant atmospheric deposition in Britain (N.Rose, pers.comm).

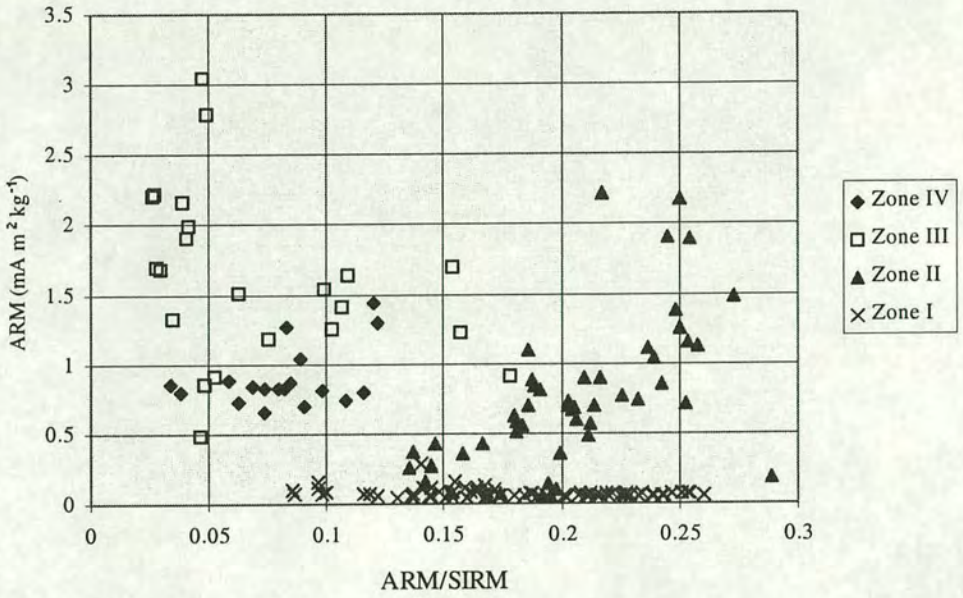

Figure 6.6 Biplot of ARM versus ARM/SIRM for samples from zones I, II, III and IV from Gormire cores 2, 3, 4, GL2, GCA and GC3. The biplot can be interpreted to indicate changes in the concentration and origin of the magnetic signature within samples from each zone at Gormire (refer to Figure 3.6c, Chapter 3). Zone 1 is characterised by low ARM values and medium to high ARM/SIRM ratios indicating low concentrations of bacterial magnetite. Samples from zone II have ARM values which extend up to 2.2 mA m^2 kg^{-1} and high ARM/SIRM values indicative of high concentrations of magnetic minerals of bacterial origin. Samples from zones III and IV are characterised, in general, by lower ARM/SIRM ratios than samples from zones I and II, when coupled to the low ARM/χ ratios this suggests that the magnetic signature within these samples derived from topsoil.

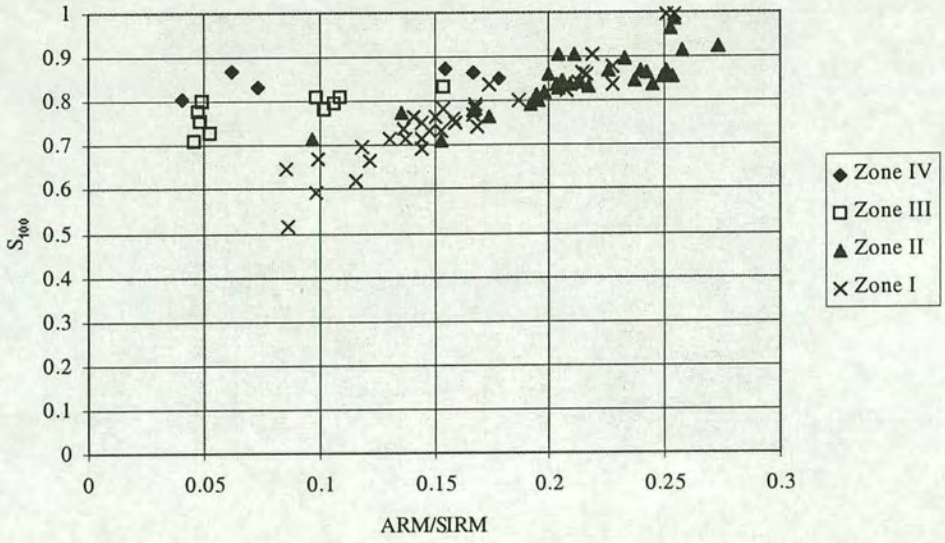

Figure 6.7 Biplot of ARM/SIRM versus S_{100} for samples from zones I, II, III and IV from Gormire cores 2, 3, 4, and GL2.. The biplot can be interpreted to indicate the origin of the magnetic signature within samples from each zone at Gormire (refer to Figure 3.6a, Chapter 3 and Figure 6.6 above). The samples from zones I-IV span a range of ARM/SIRM ratios (as discussed in the caption to Figure 6.8) and are characterised by generally high S100 ratios indicating that magnetite is the dominant magnetic mineral in these samples. Samples from cores GCA and GC3 have not been included as S_{100} measurements are unavailable for these cores.

Figure 6.8 shows the variation in the ratio SIRM/χ down core 4. Samples from zone III are characterised by high SIRM/χ ratios (c. 50 kA m^{-1}) which, when combined with the low ARM/SIRM values in zone III, indicate that the remanence peak may be attributable to the presence of greigite.

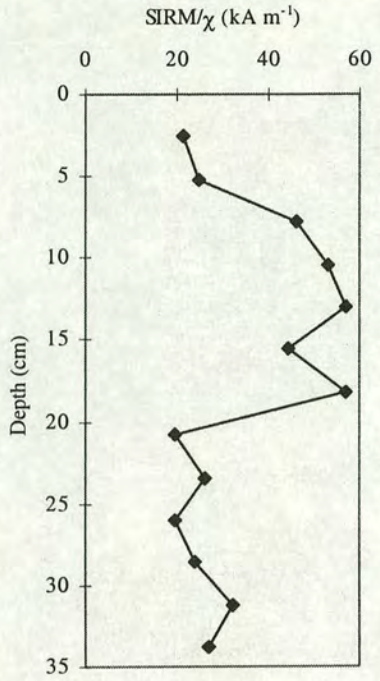

Figure 6.8 Variation in SIRM/χ with depth in core 4 from Gormire. With SIRM/χ ratios of c. 50 kA m^{-1}. The remanence peak at a depth of between c. 8 - 20 cm can be attributed to the presence of the greigite.

6.4 Comparison of Catchment Sample and Lake Sample Magnetic Data

As shown in Figure 6.9 the catchment samples display noticeably weaker remanence signatures than the majority of lake sediment samples, especially those from zones III and IV, and thus contain much smaller concentrations of magnetic minerals. However some of the lake samples from zones I and II are characterised by lower ARM and SIRM values than all but one of the catchment samples. The weaker remanence values observed in the lake sediment samples is interpreted to indicate lower concentrations of magnetic minerals in these lake samples than in five of the six catchment samples. The reduced magnetic mineral concentrations in these samples may be indicative of dissolution in the lowermost lake sediment. Table 6.6 summarises the source of the magnetic signature within samples from each zone in the Gormire lake sediment cores.

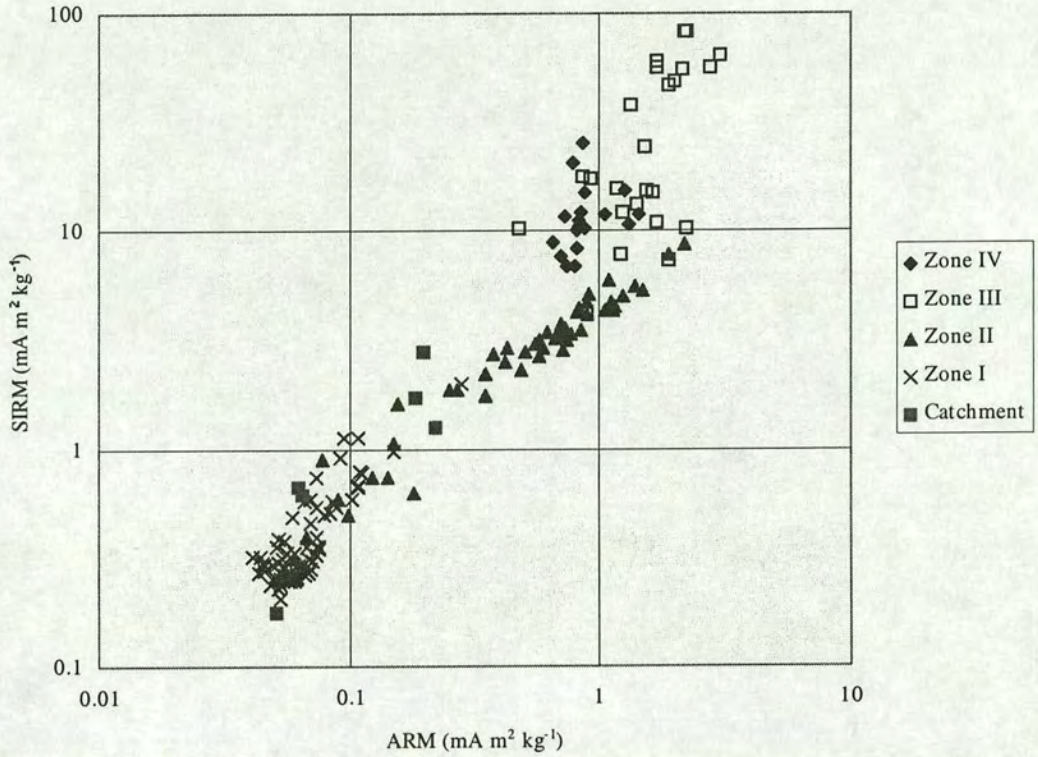

Figure 6.9 A comparison of ARM versus SIRM for catchment and lake sediment samples from Gormire. The biplot illustrates changes in magnetic mineral concentrations in samples from zones I, II, III and IV from Gormire cores. The lowest ARM and SIRM values, indicating the lowest concentrations of magnetic minerals, are found in samples from zones I and II and the catchment samples.

Table 6.6 The origin of the magnetic signature in Gormire lake sediments

Zone	Origin of magnetic signature
IV	Topsoil
III	Greigite, topsoil
II	Bacterial magnetosomes
I	Dissolution

6.5 Summary

- The magnetic signature of catchment samples from Gormire arises from a combination of detrital magnetite, goethite and haematite.

- The Gormire lake cores are composed of approximately 50% clay and 50% silt.

- Magnetic characterisation of lake cores from Gormire shows the magnetic signature to be dominated by the influence of bacterial magnetite, topsoil and dissolution.

- The uppermost 50 cm of the lake cores can be correlated using the variation in ARM/SIRM ratio with depth.

- Based on radionuclide data Appleby (1998) reports mean sediment accumulation rates of 0.25 (st dev 0.20) and 0.24 (st dev 0.13) cm a^{-1} for cores GCA and GC3 since 1853 and 1890 respectively.

Chapter 7

Hornsea Mere

7.1 Introduction

As described in Section 3.1.3 Hornsea Mere lies in the coastal lowlands in a predominantly arable agricultural catchment. At Hornsea Mere catchment samples and lake sediment cores have been collected and characterised magnetically. The cores have been correlated using changes in magnetic signature with depth. Variations in sediment density and lithostratigraphy have been noted. Appleby (1998) has used ^{210}Pb and ^{137}Cs radionuclide data to establish a chronology and determine sediment accumulation rates for several lake sediment cores.

7.2 Catchment Samples

Catchment samples were collected from six locations (illustrated in Figure 7.1) within the Hornsea Mere catchment. The origin of each catchment sample is listed in Table 7.1).

Table 7.1 The origin of catchment samples within the Hornsea Mere catchment.

Sample	Origin
1	Hornsea subsoil shoreline
2	Stream bank, Hornsea
3	Rabbit hole - Hornsea, pasture field
4	Ploughed field - Seaton
5	Cornfield, Stud Farm, Hornsea
6	Hornsea - till on shoreline

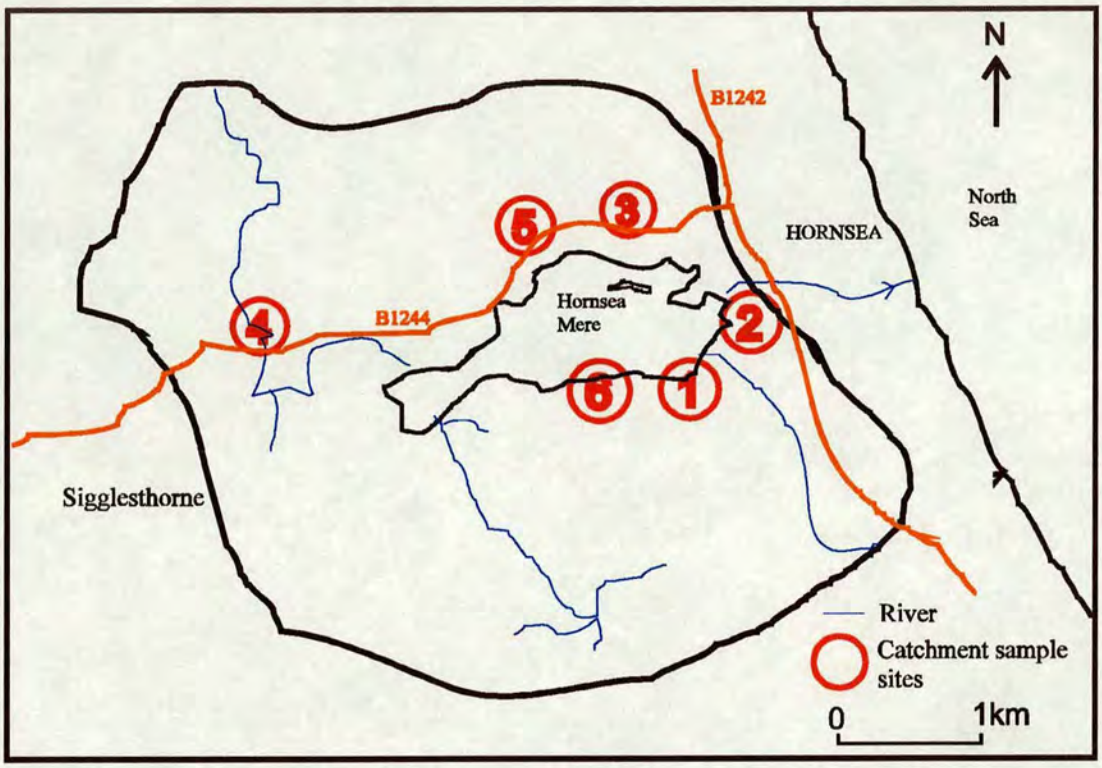

Figure 7.1 Location of 6 sampling sites in the Hornsea Mere catchment. Also shown are the three inflowing rivers and the outflow to the North Sea.

7.2.1 Magnetics of Catchment Samples

Table 7.2 summarises the magnetic characteristics of the Hornsea Mere catchment samples. The catchment samples are characterised by a mean susceptibility 0.34 μm^3 kg^{-1}, indicative of low concentrations of magnetic minerals. As illustrated in Figure 7.2, the catchment samples, with a mean ARM/SIRM ratio of 0.031 and S_{100} ratio of 0.67, are characterised by a mixture of magnetite and haematite/goethite. The particularly low S_{100} ratio of 0.42 in catchment sample 1 indicates that haematite/goethite are the dominant magnetic minerals in this sample, rather than magnetite. Figure 7.3 illustrates how catchment sample 1 acquires IRM in fields up to 4000 mT. A significant increase in magnetisation occurs in fields between 2000 and 4000 mT indicating that the mineralogy of this sample is dominated by goethite rather than haematite.

Table 7.2 A summary of the Hornsea Mere catchment sample magnetic results.

	χ ($\mu m^3 kg^{-1}$)	ARM ($mA\ m^2 kg^{-1}$)	IRM_{100} ($mA\ m^2 kg^{-1}$)	SIRM ($mA\ m^2 kg^{-1}$)	A/S	S_{100}	ARM/χ ($kA\ m^{-1}$)
1	0.13	0.032	0.74	1.77	0.018	0.42	0.24
2	0.37	0.107	4.04	5.88	0.018	0.69	0.29
3	0.29	0.125	2.18	2.66	0.047	0.82	0.43
4	0.68	0.343	6.37	8.38	0.041	0.76	0.51
5	0.40	0.164	2.77	3.97	0.041	0.70	0.41
6	0.14	0.037	1.23	1.96	0.019	0.63	0.26
Mean	0.34	0.135	2.89	4.10	0.031	0.67	0.36
St dev	0.18	0.104	1.89	2.37	0.012	0.13	0.09
Min	0.13	0.032	0.74	1.77	0.018	0.42	0.24
Max	0.68	0.343	6.37	8.38	0.047	0.82	0.51

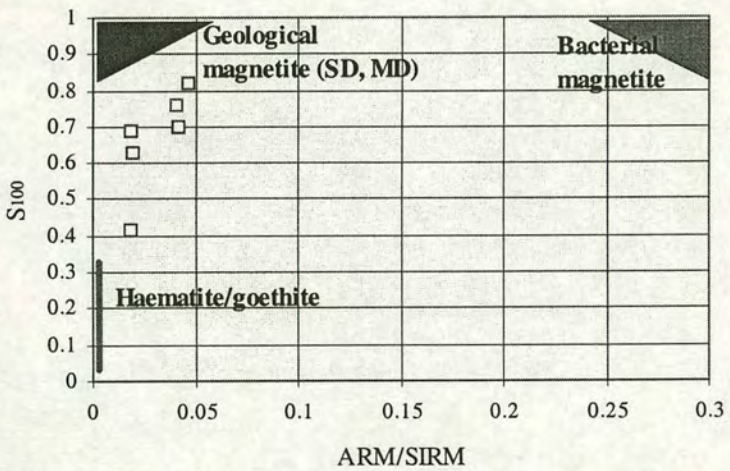

Figure 7.2 Biplot of ARM/SIRM and S_{100} ratios of Hornsea Mere catchment samples. The biplot can be interpreted to indicate the magnetic mineralogy and hence the origin of the magnetic signature within the samples. Detrital magnetite plots in the top left corner, haematite/goethite towards the bottom left and bacterial magnetosomes towards the top right corner (refer to Figure 3.6a, Chapter 3).

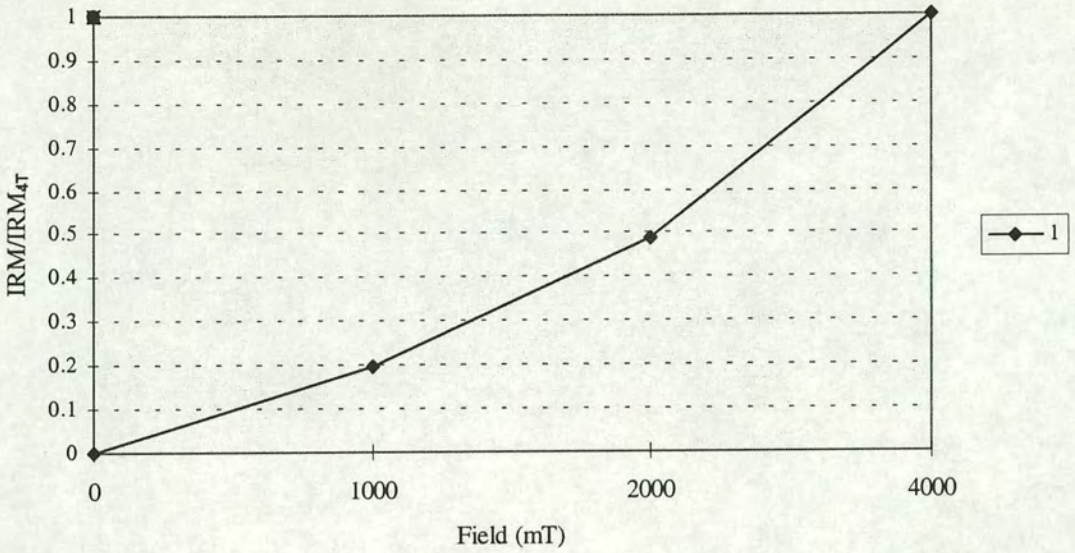

Figure 7.3 IRM acquisition curve for catchment sample 1 from Hornsea Mere. The magnetisation of catchment sample 1 increases significantly in fields above 2000 mT, indicating the dominance of goethite in this sample.

7.3 Sediment Cores

7.3.1 Hornsea Mere Core Collection

A transect of ten one-metre Mackereth cores was obtained from Hornsea Mere running east to west along the axis of the lake as shown in Figure 7.4. The lake is very shallow (c. 1 metre) and thus the use of three and six-metre Mackereth corers was not possible.

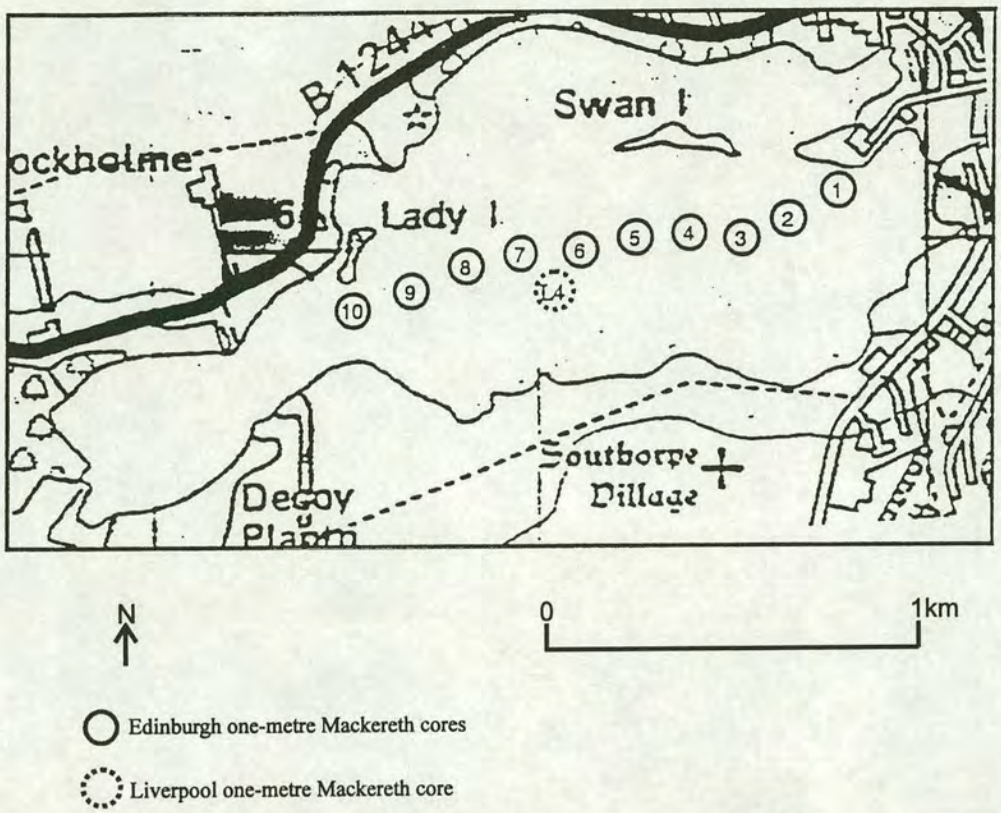

Figure 7.4 The location of cores at Hornsea Mere.

7.3.2 Lithostratigraphy

The sediment cores obtained from Hornsea Mere display little variation in lithology with depth. Hornsea Mere cores are composed of fine grained material of clay/silt size. The average sediment density in Hornsea Mere cores (1-10) is 0.389 g cm^{-3} and little between core variation in density is found. A slight decrease in density from an average 0.385 g/cm^3 in the lowermost sample to 0.326 g cm^{-3} in the uppermost sample occurs. Changes in density with depth in cores from Hornsea Mere are fairly gradual. Figure 7.5 illustrates changes in density with depth for one representative core (8) from Hornsea Mere. The complete sediment density data for each core is provided in Appendix H.

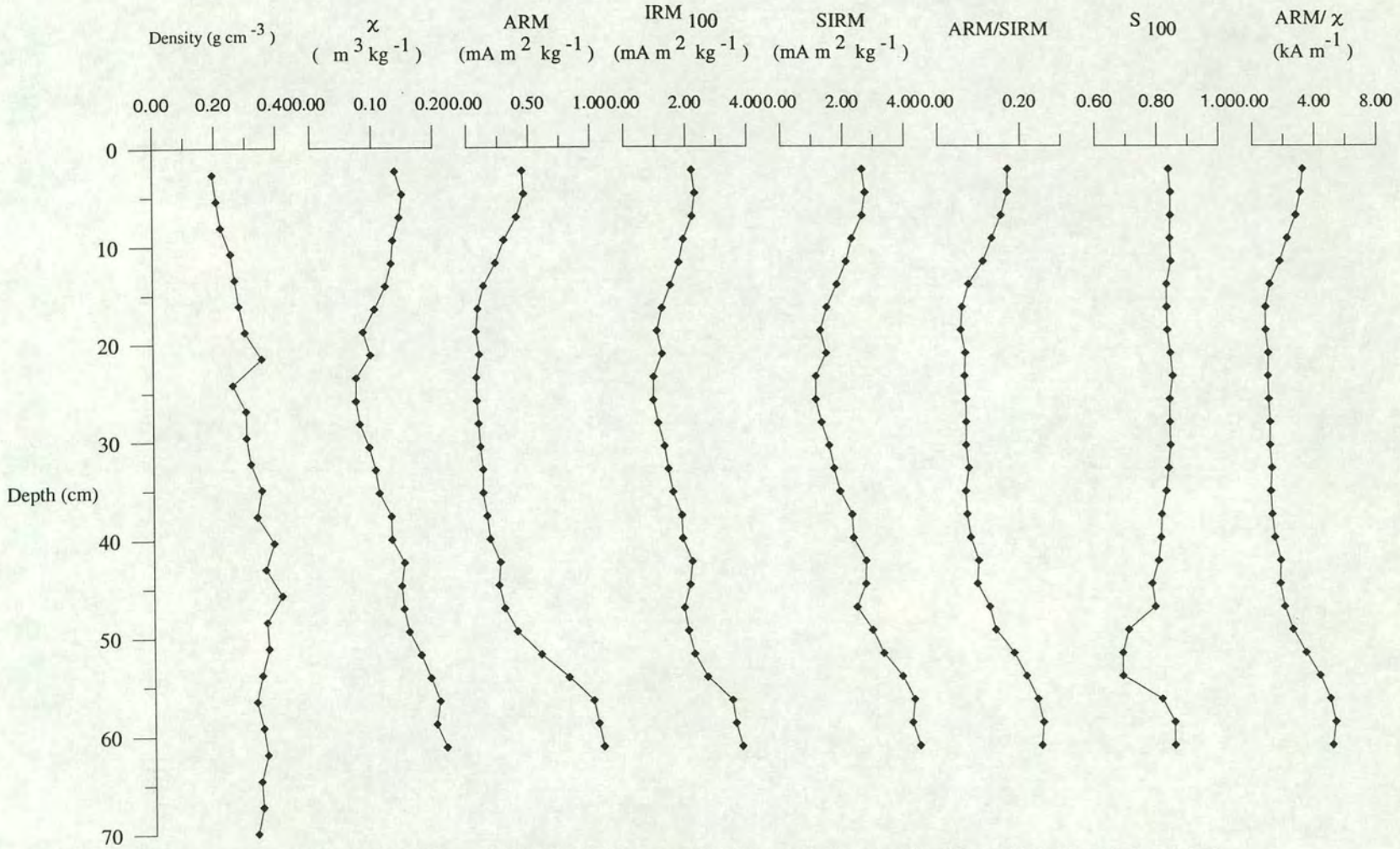

Figure 7.5 Changes in sediment density, χ ARM, IRM $_{100}$, SIRM, ARM/SIRM, S $_{100}$ and ARM/ χ with depth in core 8 from Hornsea Mere. Core 8 is characterised by higher magnetic remanence values in the lower most and upper most parts and lowest values in the centre of the core. This indicates that the concentrations of magnetic minerals are weakest in the centre of the core.

7.3.3 Total Organic Carbon and Carbonate Content

As for Gormire total organic carbon and carbonate content are being measured at Liverpool University. Fisher (pers.comm., January 1998) reports the following average TOC and carbonate content results in Hornsea Mere lake core L4.

Depth (cm)	TOC (%)	Carbonates (%)
Zone III	5	38
Zone II	3.5	29
Zone I	3.0	16

7.3.4 Chronology

Based on radionuclide data Appleby (1998) reports mean sediment accumulation rates of 0.38 (st dev 0.23) and 0.48 (st dev 0.24) cm a^{-1} in cores L4 and 8 respectively.

7.3.5 Lake Sediment Magnetic Measurements

As for the other lake cores studied in this thesis the four magnetic parameters χ, ARM, IRM_{100} and SIRM have been measured on samples at 2 cm intervals down all ten cores 1-10 collected from Hornsea Mere. Table 7.3 summarises these magnetic characteristics. Figure 7.5 illustrates changes in sediment density, χ, ARM, IRM_{100}, S_{100}, ARM/SIRM and ARM/χ with depth in one representative core (8).

Three magnetic mineral assemblage zones can be observed. The magnetic zone boundaries are shown in Figures 7.6. Zones I and III are characterised by a higher ARM/χ ratio and high ARM, SIRM and χ values whilst zone II has a much weaker remanence signal. Table 7.5 illustrates the mean χ, ARM and SIRM values of

samples from the three zones (I, II and III) in Hornsea Mere cores. The greatest concentration of magnetic minerals occurs in Zone I.

Table 7.3 Range and mean of χ, ARM and SIRM values in zones I, II and III in Hornsea Mere cores 4 to 9.

		Zone I	Zone II	Zone III	Catchment samples
χ	Mean	0.232	0.150	0.141	0.335
($\mu m\ kg^{-1}$)	Min	0.122	0.056	0.124	0.131
	Max	0.255	0.174	0.170	0.677
ARM	Mean	0.880	0.247	0.372	0.135
($mA\ m^2\ kg^{-1}$)	Min	0.096	0.056	0.260	0.032
	Max	1.174	0.475	0.462	0.343
SIRM	Mean	4.402	2.433	2.525	4.103
($mA\ m^2\ kg^{-1}$)	Min	1.665	0.809	2.210	1.773
	Max	5.165	3.576	2.774	8.383

The lake sediment samples are characterised by very high ARM/χ ratios, ranging up to 5.59 kA m^{-1}, and averaging 2.34 kA m^{-1}. Individual ARM values range from 0.054 to 1.17 mA m^2 kg^{-1}, averaging 0.37 mA m^2 kg^{-1}. As illustrated in Section 2.2 such values have been associated with the presence of bacterial magnetosome chains. In order to confirm the potential presence of magnetosome chains in the Honrsea Mere lake sediments a sample from a depth of 5 cm in core 7 was analysed by Marianne Hanzlik at the Institut für Allgemeine und Angewandte Geophysik und Geophysikalisches Observatorium der Ludwig-Maximilians-Universität München, using a TEM. Her analysis confirmed the presence of chains of bacterial magnetosomes.

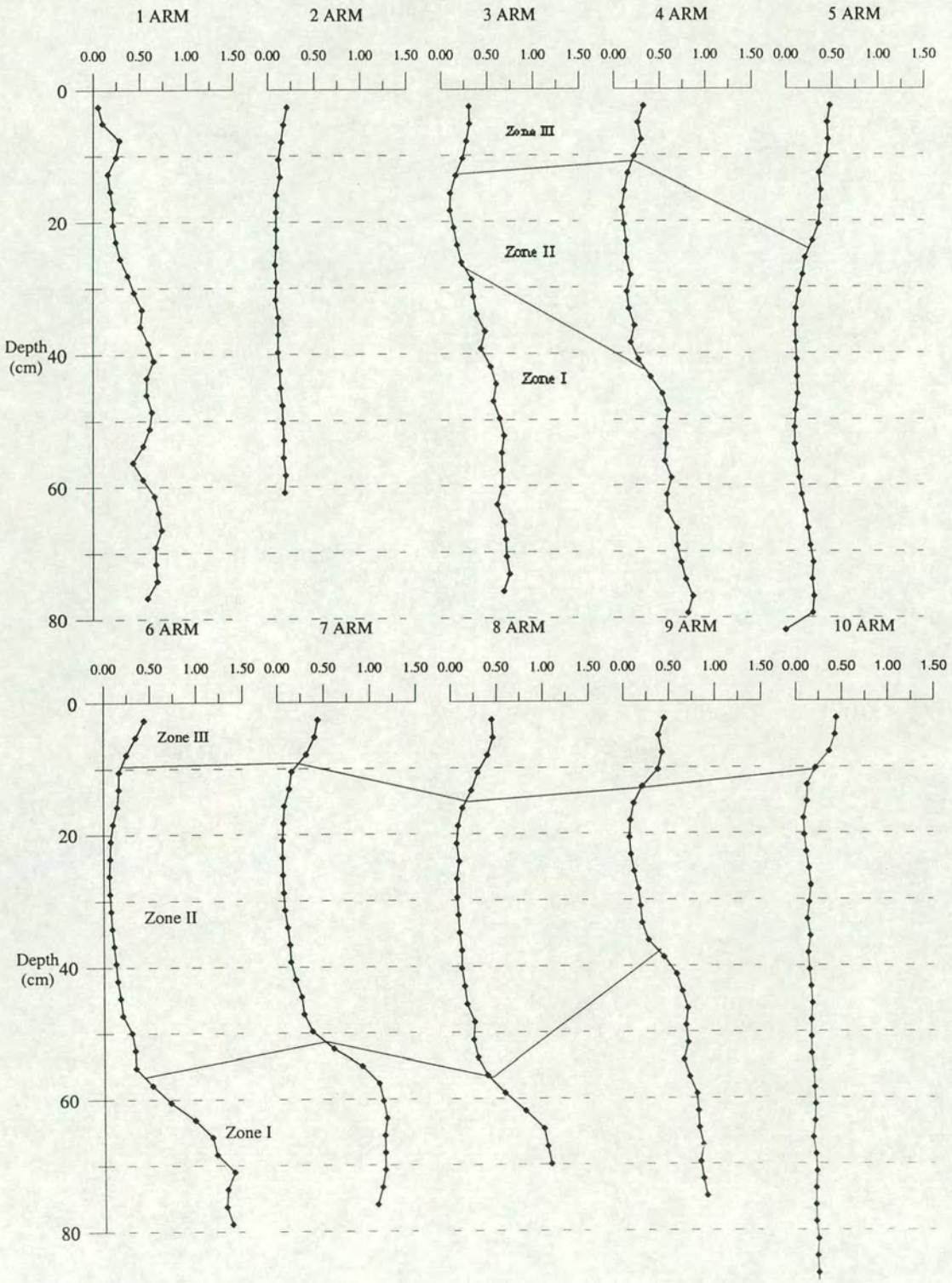

Figure 7.6 Changes in ARM (mA m2 kg-1) with depth in Hornsea Mere cores 1-10. Three magnetic mineral assemblage zones have been identified. Zones I and III are characterised by higher ARM values than Zone II. Tentative Zone boundaries have been plotted.

Figure 7.7 shows a complete chain of magnetite crystals found in the sample and the well preserved crystals inside the cells. S_{100} values average 0.80 kA m^{-1} within the sediment cores, and thus provide further evidence that magnetite is the dominant magnetic mineral within the sediments.

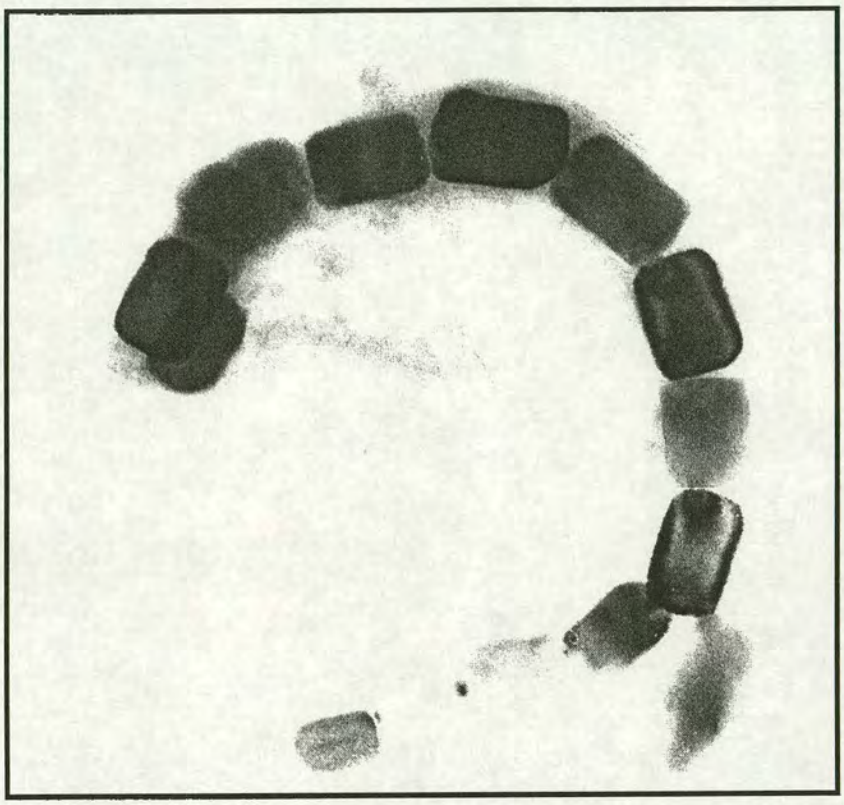

Figure 7.7 TEM image of a chain of magnetotactic bacteria in a sediment sample from core 7 at Hornsea Mere. (TEM image courtesy of M. Hanzlik, Institut für Allgemeine und Angewandte Geophysik und Geophysikalisches Observatorium der Ludwig-Maximilians-Universität München).

Magnetic characterisation has enabled the Hornsea Mere cores to be correlated using the ratio ARM/χ (kA m^{-1}). As demonstrated in Figure 7.8, eight of the ten cores can be linked, with cores six through to nine correlating particularly well. The two cores that do not match are from the ends of the core transect near to the inflow and outflow.

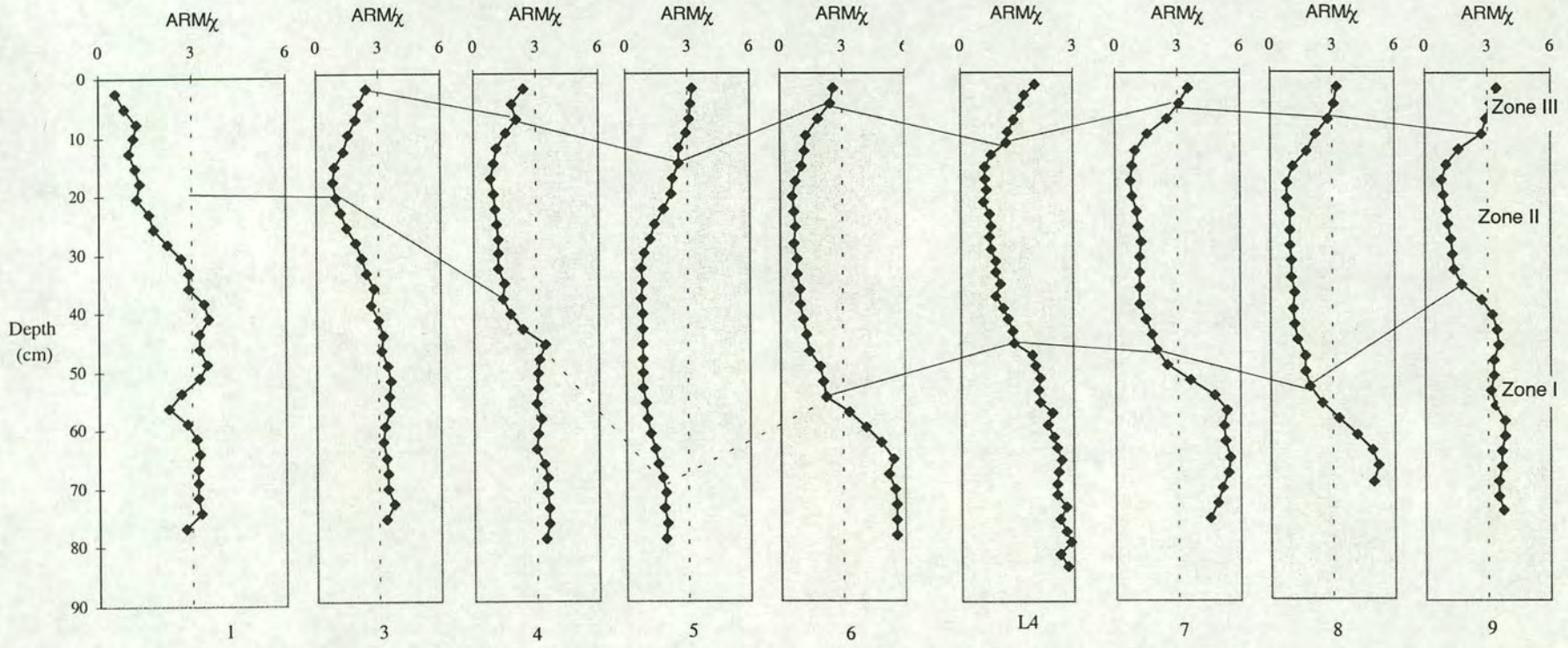

Figure 7.8 Correlation of cores from Hornsea Mere using ARM/ χ ratio. Cores 1, 3-9 ARM/χ (kA m^{-1}) Edinburgh measurements. Core L4 ARM/ χ (arbitrary units) Liverpool measurements. The correlations proposed are only the authors suggestion. The Figure indicates increasing sediment accumulation in in zone II towards the centre of the lake (cores 4-7).

7.4 Comparison of Catchment and Lake Samples

By comparing Table 7.2 and 7.3 it can be seen that ARM/SIRM ratios, ARM/χ ratios and ARM values of the catchment samples are considerably lower than those of the lake sediments. The S_{100} ratio is also markedly less in the catchment samples.

With a mean ARM value of 0.135 mA m^2 kg^{-1} the catchment samples are characterised by considerably weaker ARM values than those found in Hornsea Mere lake sediments (mean 0.368 mA m^2 kg^{-1}). The comparatively low ARM values recorded in the catchment samples indicate that the ARM signature within the lake samples is enhanced. As illustrated on Figure 7.9 the lake samples are characterised by ARM/χ values greater than 1 kA m^{-1}, indicating that the magnetic material in the lake is dominated by bacterial magnetite which overrides the detrital magnetic signature present.

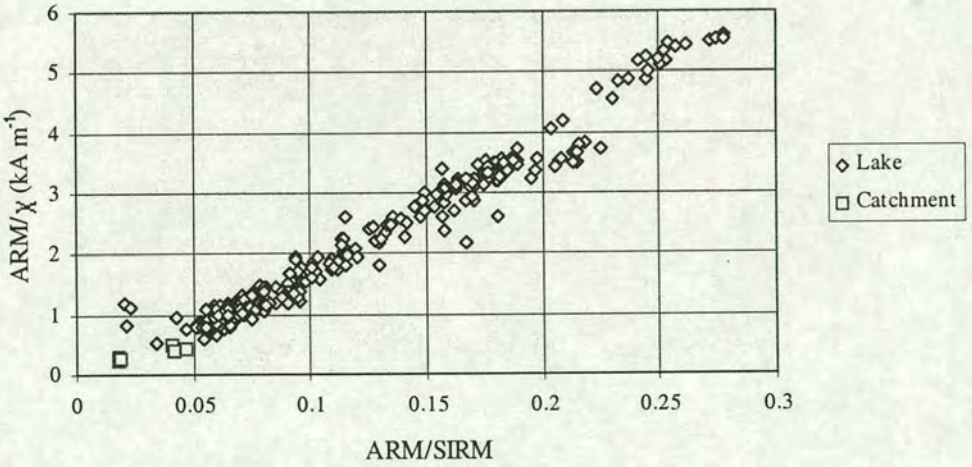

Figure 7.9 A comparison between lake and catchment samples from Hornsea Mere using ARM/χ and ARM/SIRM ratios. The biplot can be employed to distinguish between detrital/topsoil magnetic minerals and magnetotactic bacteria (refer to Figure 3.6b, Chapter3). The array of points can be viewed on a mixing line between catchment detrital material (which plot in the lower left corner) and sediment dominated by intact bacterial magnetosomes (which plot towards the top right corner).

The average S_{100} value of lake samples are considerably higher than that of the catchment samples (Figure 7.10). This indicates a secondary source of low-coercivity magnetic material within the lake which is not present in the detrital catchment material. The mean ARM of the lake samples is nearly three times that of the catchment samples and thus, coupled with the S_{100} information, can be attributed to chains of bacterial magnetite in the lake sediment samples.

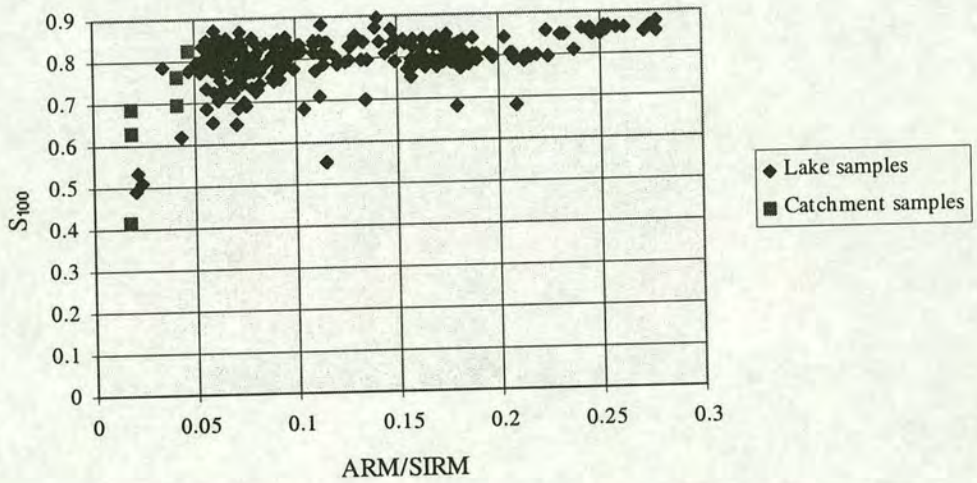

Figure 7.10 A comparison between lake and catchment samples from Hornsea Mere using S_{100} and ARM/SIRM ratios. The biplot can be interpreted to indicate the origin of the magnetic signature of samples from Hornsea Mere cores (refer to Figure 3.6a, Chapter 3). A triangular spread of points can be viewed as a three component mixture of (i) low goethite catchment samples, (ii) higher magnetite catchment samples and (iii) bacterial magnetosomes.

Figure 7.9 illustrates the strong relationship between the ratios ARM/χ and ARM/SIRM. Increases in ARM/χ values corresponds to increases in the ARM/SIRM ratio which indicates increases, either in the extent of magnetic (grain/cell) interactions, or in magnetic mineral concentration. The correlation coefficient of this relationship is 0.98. As expected, the catchment samples plot in the bottom left corner of the diagram, indicating the absence of magnetotactic

bacteria in these samples. At Hornsea Mere the strong correlation between ARM and ARM/χ of 0.97 enables Figure 7.8 (correlation of cores using ARM/χ) to be interpreted in terms of changes in bacterial magnetite concentration. Zones I and III record higher concentrations of bacterial magnetosomes than zone II.

In this site we conclude that the magnetic signature of the lake samples are dominated by bacterial magnetite, and that the changes in the concentrations of magnetotactic bacteria with depth can be inferred from the ARM values.

7.5 Summary

- Catchment samples obtained from Hornsea Mere have been characterised magnetically. The catchment magnetic signature is shown to arise from a combination of magnetite and haematite.

- Hornsea Mere lake cores are composed of clay/silt size material.

- Magnetic characterisation of lake cores from Hornsea Mere shows the magnetic signature to be dominated by the influence of bacterial magnetosomes. TEM analysis confirms the presence of chains of bacterial magnetosomes in sediments from Hornsea Mere.

- The lake cores have been successfully correlated using the variation in ARM/χ ratio with depth.

- Appleby (1998) reports mean sediment accumulation rates of 0.38 (st dev 0.23) and 0.48 (st dev 0.24) cm a^{-1} in cores L4 and 8 respectively.

Chapter 8

Sediment Flux Modelling

8.1 Introduction

As discussed in Section 3.3.10 lake sediment studies can be employed to estimate the flux of material from a catchment to a lake. A theoretical mean sediment yield may be determined, based on the area of the catchment contributing sediment to the lake and the mass of sediment accumulated on the lake bed. Section 8.2 uses this approach to determine sediment flux and yield for Semer Water, Gormire and Hornsea Mere. At Semer Water sediment flux since c. 1950, using accumulation rates determined from radionuclide data, can be compared with sediment flux during the Holocene as determined from sediment accumulation rates in cores from Raydale which are based on pollen and ^{14}C analysis. At Gormire and Hornsea Mere the estimates of sediment flux are based purely on accumulation rates determined from radionuclide data and cover only the more recent time period since c. 1630 and 1730 at Gormire and Hornsea Mere respectively. Uncertainties in accumulation rates, the thickness of sediment deposits and the area of sedimentation have been estimated in order to estimate minimum and maximum sediment fluxes at each site. Section 8.3 goes on to study the relationship between catchment characteristics and sediment flux for 30 British lake and reservoir catchments including Semer Water, Gormire and Hornsea Mere. Using a second approach to estimating sediment flux, sediment yields have been predicted for each of the 30 catchments. This approach involves the Universal Soil Loss Equation (USLE) coupled to a sediment delivery ratio. These two independent approaches to sediment flux estimates are then compared. In addition stepwise regression techniques were used to construct an empirical model, predicting sediment flux on the basis of land use and catchment characteristics.

8.2 Sediment Flux and Yields at Semer Water, Gormire and Hornsea Mere

Following the methodology outlined in Section 3.3.10, estimates of sediment flux and yield have been determined for Semer Water, Gormire and Hornsea Mere. The method hinges on using multiple core studies to determine the mass of sediment deposited in the lake bed over specific time intervals.

8.2.1 Semer Water

Estimates of sediment flux at Semer Water over three time zones have been obtained by calculating (i) flux to the existing lake and (ii) flux into old lake sediments deposited in Raydale.

8.2.1.1 Sediment Flux Into Existing Lake Semer Water

As noted in Chapter 4 (Section 4.3.5) correlation of Semer Water lake sediment cores was not possible using magnetic techniques. This study therefore uses accumulation rates, reported by Appleby (1998), for three dated cores (6, T3 and SEM95) to establish a mean sediment accumulation rate in Semer Water for the recent period (Table 8.1)

Table 8.1 Mean sediment accumulation rate in three Semer Water cores

Depth (cm)	Core	Time period	Accumulation rate (cm a^{-1})*
0-60	6	1950-1994	0.9
0-8	T3	1979-1994	0.60
0-18	SEM95	1947-1995	0.37
Mean			**0.62**

*standard deviation not given.

The mean sediment accumulation rate at Semer Water since c. 1950 has been 0.62 cm a^{-1}. The radiocarbon date obtained on sample Semer Water 18 from core SL2 results in a mean accumulation rate of 0.34 cm a^{-1} (range: 0.32-0.37 cm a^{-1}) since 1441 AD. The sediment accumulation rate data for Semer Water is limited (based on only three $^{210}Pb/^{137}Cs$ profiles and one ^{14}C determination), it indicates an increase in the rate of sedimentation in the most recent period (post 1950) as compared to that since 1441 AD.

Obtaining an estimate of the area of active sedimentation at Semer Water is made difficult by (i) the discontinuous nature of sedimentation as observed in the ^{137}Cs and ^{210}Pb profiles of cores T3 and SEM95, and (ii) the varied bathymetry (Figure 4.6, Chapter 4). Whilst the majority of Semer Water is very shallow, a deep trench (kettle hole) extends south-west to north-east (Barlow 1994). The dated cores are from a variety of water depths spanning the shallow and deep areas of sediment accumulation in Semer Water (Figure 4.5, Section 4.3.1). On the basis of a combination of bathymetric information and of observations of regions of sediment accumulation, obtained when coring the lake, the active sediment accumulation area within Semer Water has been estimated at 90 000 m^2 (Figure 8.1). Sediment density, organic and carbonate content and the area of active sedimentation have been combined with the accumulation rate data (Table 8.1) to calculate sediment flux for Semer Water (Table 8.2). These calculations result in a mean annual sediment flux of 270 t (270 x 10^3 kg) for the period since 1950. This flux of sediment, when combined with catchment area, converts to a mean sediment yield of 8.0 t km^{-2} a^{-1}.

Minimum and maximum sediment fluxes and yields have been estimated using the standard deviations associated with the sediment accumulation rate (Table 8.1), density, organic and carbonate content data (Section 4.3, Chapter 4). A minimum and maximum area of sedimentation has also been estimated using a combination of information gained during coring and bathymetric data. The minimum area of sedimentation is taken as that area within the 6 metre water depth contour (Figure 4.5), this is the approximate area of the deep trench and equates to c. 60 000 m^2. The

maximum area of sedimentation is taken as that area within the 2 metre water depth contour (Figure 4.6), this area covers approximately 120 000 m^2.

Table 8.2 Semer Water lake sediment flux estimates.

	Time period 1950-1994 AD
Number of cores	3
Mean annual accumulation (cm a^{-1} ± st dev)	0.62 (0.40 - 0.84)
Mean density (kg m^{-3} ± st dev)	592 (504 - 680)
Mean organic content (% ± st dev)	11 (9.9 - 12.1)
Mean biogenic silica content (%) #	4
Mean carbonate content (% ± st dev)	2.1 (1.4 - 2.8)
Sedimentation area/range (km^2)	0.09 (0.06 - 0.12)
Sediment mass/range (t)	N/A*
Annual flux/range (t a^{-1})	330 (121 - 685)
C,CO_3, Si content/range (%)	17.1 (15.3 - 18.9)
Annual minerogenic flux/range (t a^{-1})	274 (102 - 555)
Yield/range (t km^{-2} a^{-1})	6.3 (2.4 -12.8

*Mass of sediment has not been calculated, the average sediment accumulation rates are based on cores spanning a range of timescales.
Estimated. Foster *et al.* (1985) report values of 4% in the uppermost sediment at Merevale lake, UK.

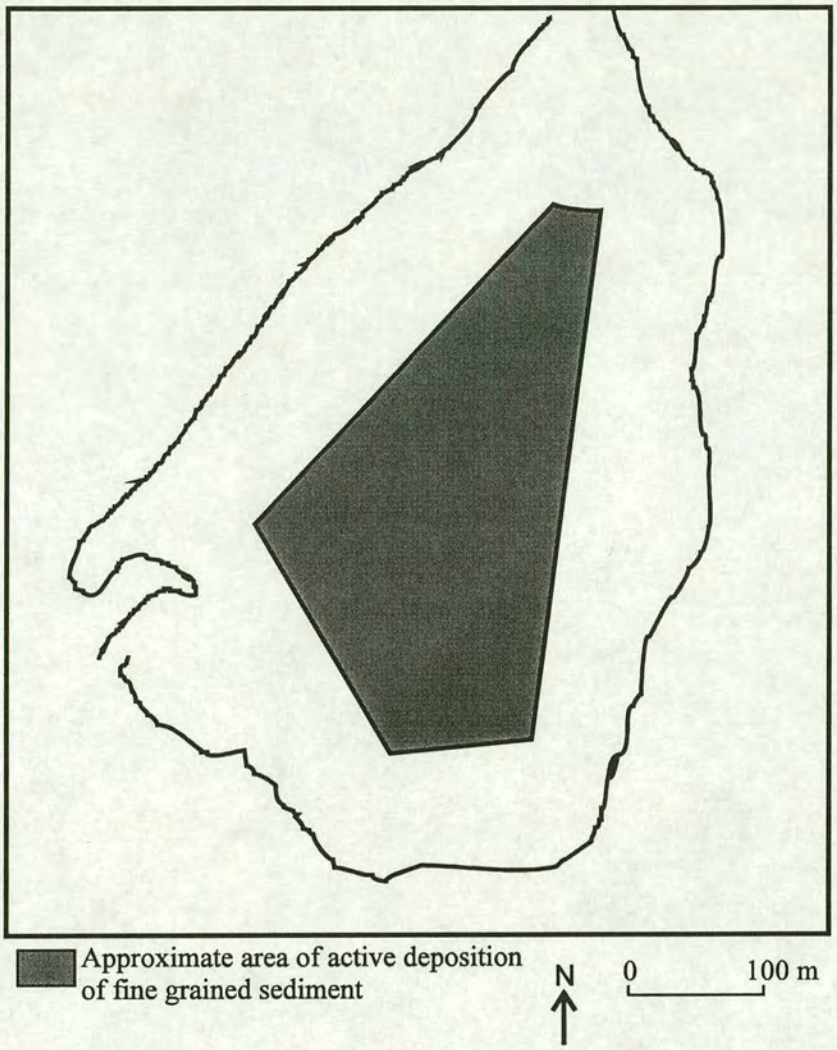

Figure 8.1 Approximate area of active deposition of fine grained sediment at Semer Water.

8.2.1.2 Sediment Flux Into the Old Lake Deposits in Raydale

The pollen and ^{14}C chronology (Table 8.3) allows sediment accumulation rates in Giddings cores A, B and C to be calculated for a range of time periods (Table 8.4). The area of deposition has been mapped using resistivity profiles and gouge cores (Sections 5.2 and 5.7). So once again the combination of accumulation rate data and depositional area can be used to estimate sediment flux.

Table 8.3 Pollen and ^{14}C determined chronology for Giddings cores A, B and C.

Core	Depth (m)	Age (range 1σ) (years BP)	^{14}C age (range 1σ) (years BP)
A	4.45	6294 (6280-6311)	
A	5.80	8220 (8174-8335)	
A	9.10	10513 (10415-10798)	
B	14.75	6294 (6280-6311)	
C	13.50	6294 (6280-6311)	
C	10.17		4086 (3983-4221)

Table 8.4 Accumulation rates in Giddings cores A, B and C (refer to Table 5.3 for explanation of the determination of minimum, mean and maximum accumulation rates.

	Sediment accumulation rates (cm a^{-1})			
	Time period (years BP)			
	0-4086	0-6294	6294-8220	8200-10513
	Mean (Range)	Mean (Range)	Mean (Range)	Mean (Range)
A		0.08 (0.07-0.09)	0.04 (0-0.08)	>0.14
B		>0.23		
C	0.24 (0.23-0.25)	>0.21		
Mean		**0.17**		
Std dev		**0.06**		

The mean sediment accumulation rate is considerably lower in the marginal core A than in either of the central lake basin cores, B and C, which show remarkably similar rates of sedimentation. In Giddings core A the sediment accumulation rate is markedly higher in the period 8220-10513 years BP than in both the 0-6294 and 6294-8220 years BP periods.

By assuming that sediment deposition rates were the same in the earlier part of the Holocene as in that period represented by each of the Giddings cores, sedimentation rates can be employed to estimate the thicknesses of Holocene sediment at Giddings-core locations A, B and C (Table 8.5). It should be noted however that sediment accumulation rates in Giddings core A for the early Holocene period (8220-10513

BP) are more than twice those of the later Holocene period (Table 8.4). Therefore if the decrease in sediment accumulation since 8220 BP recorded in Giddings core A is representative of the rest of the Raydale basin the extrapolated Holocene sediment thickness for Giddings core B will be an underestimate, it is based on the sediment accumulation rate in the post 6294 BP period.

Table 8.5 Estimation of the thickness of Holocene sediments in Raydale from core data.

Site	Lake sediment thickness (m)	Estimated age of base of core (BP)	Estimated depth of Holocene base from coring/dating accumulation rates (m)
A	9.10	max 10513	9.1
B	14.75	max 6294	25
B	14.75	max 6294	25
C	13.50	max 6294	23
Gouge core	>18.0	*	*

* Age not known, base of Holocene sequence not reached.

Resistivity profiles 3,4,5,6,7,8 and 9, taken in the centre of the basin, have very similar conductivity structures suggesting that cores B and C are representative sequences for the majority of the basin. The thickness of Raydale lake sediments deposits can thus be used to calculate a mean Holocene sediment accumulation rate. Furthermore as shown in Table 8.6 the total thickness of lake sediments determined from constrained Davis-Merrick resistivity inversions is in reasonable agreement with that from the coring studies.

A scaling factor can be determined to enable the mean thickness of the high conductivity layer to be converted into an estimate of sediment thickness over the whole of the basin. Rather that relying on just three Giddings cores a mean sediment thickness over the entire basin can be calculated using seven resistivity profiles. The resistivity determined estimates of the thickness of the high conductivity layer are converted into a sediment thickness using the scaling factor calculated by comparing

resistivity estimates of sediment thickness taken adjacent to the Giddings core sites with sediment thickness determined from the coring data (Table 8.6).

Table 8.6 Comparison of lake sediment thickness in Raydale using resistivity and coring techniques

Resistivity sounding	Thickness of high conductivity layer (m)	Estimated depth of Holocene base from coring/dating accumuation rates (m)	Scaling factor
3	20	25	1.3
6	19	25	1.3
9	22	23	1.0
12	7.8	9.1	1.2
Mean			**1.2**

The depth of the highly conductive layer has been estimated to be between 19-33 m over the basin. An average thickness of the high conductivity layer within the old lake bed (west of Crooks Beck) of 24 m (st dev 4.6 m) can be calculated (Table 8.7). The variability in the sediment thickness determined from resistivity measurements is attributed to noise rather than real variation in sediment thickness.

Table 8.7 Average thickness of lake basin deposits determined from resistivity soundings

Sounding	Lake sediment thickness (m)
3	20
4	33
5	28
6	19
7	22
8	25
9	22
Average	24 m
St dev	4.6

Multiplying the mean thickness of the high conductivity layer in Raydale by the scaling factor of 1.2 results in a mean sediment thickness over the basin of 29 m (23-34 m).

The extent of sedimentation to the east of Crooks Beck is less well known than that to the west. Access to this area is much more difficult, hampering efforts to obtain resistivity profiles. Although attempts were made to undertake resistivity profiles in this area, equipment failure prevented reliable data collection. The depth of sediment deposited within the old lake basin east of Crooks Beck can be estimated from a combination of gouge cores and the assumption that the uniform sediment thickness of to the west of Crooks Beck are also representative of the depth of sediments deposited within the 250 metre contour to the eastern side of Crooks Beck. Gouge-cores obtained from this area revealed sediments sequences in excess of 10.0 metres. Only at the south eastern edge of the basin did the corer reach the base of the Holocene penetrating into boulder clay. Elsewhere the cores did not reach the bottom of the sediment sequence.

The 250-metre contour is taken to delineate the area of 29 metre thick lake sediment deposits in Raydale. This gives an area of sedimentation of 0.31 km^2. A mean sedimentation area for the Holocene period of 0.4 (0.37 - 0.43) km^2 has been calculated by adding the Semer Water sedimentation area (Section 8.2.1.1) to the Raydale sedimentation area of 0.31 km^2.

An average depth of sediment of 29 metres and a sediment deposition area of 0.4 km^2 results in a volume of 11600000 m^3 of sediment deposited during the Holocene. Using average sediment density of 1280 kg m^{-3} the total mass of sediment deposited in Raydale is estimated to be 15 million tonnes. By taking account of the organic, carbonate and biogenic silica content a mean Holocene sediment yield of minerogenic matter of 28 t km^{-2} a^{-1} has been determined (Table 8.8).

Thinner sequences of sediment, observed from resistivity surveys and gouge core transects, further up into Raydale towards Marsett, have not been included in calculating the volume of old lake sediments in Raydale, thus suggesting that the lake sediment flux estimates may be conservative. The Raydale flux estimates are based on the thick sediment sequences within the 250 m contour which, as indicated by the resistivity profiles, are taken to be relatively uniform in thickness.

Table 8.8 Sediment flux and yield in the Raydale catchment determined from lake sediment deposits in Raydale.

	Time period	
	Present - 6294 BP	Present - 10513 BP
Number of cores	3	NA*
Mean annual accumulation (cm a^{-1} ± st dev)	0.17 (0.11-0.23)	0.27 (0.22 - 0.32)
Mean density (kg m^{-3} ± st dev)	1280 (920 - 1640)	1280 (920-1640)
Mean organic content (% ± st dev)	3.5 (1.6 - 5.4)	3.5 (1.6 - 5.4)
Mean biogenic silica content (%) #	2	2
Mean carbonate content (% ± st dev)	20 (8.3 - 31.7)	20 (8.3 - 31.7)
Sedimentation area/range (km^2)	0.40 (0.37 - 0.43)	0.40 (0.37-0.43)
Annual flux/range (t a^{-1})	870 (374 - 1620)	1380 (750-2260)
C,CO_3, Si content/range (%)	25.5 (11.9 - 39.1)	25.5 (11.9 - 39.1)
Annual minerogenic flux/range (t a^{-1})	650 (330 - 990)	1215 (661 - 1370)
Yield/range (t km^{-2} a^{-1})	15 (7.6 -23)	28 (15 - 32)

* Resistivity, Giddings and gouge core data employed to determine sediment thickness.

Estimated. Foster *et al.* (1985) and Foster and Walling (1994) report decreasing biogenic silica values with depth in lake sediment, therefore the biogenic silica content in these deeper sediments is taken to be 2% (half of that employed in the post 1950 sediment at Semer Water).

8.2.1.3 Combined Semer Water and Raydale Sediment Flux Results

Table 8.9 compares the minerogenic sediment flux and sediment yields for three time periods within the Semer Water catchment. Sediment flux and yields for the 1950-1980 year period are based on the accumulation rate data from three cores in Semer Water (Section 8.2.1.1). The flux and yield data for the periods present to 6294 years BP and present to 10513 years BP have been calculated using the core and resistivity

data from the Raydale lake deposits (Section 8.2.1.2). Table 8.9 shows that the recent flux of sediment into Semer Water of 274 (102-555) t a^{-1} is considerably lower than average sediment flux into Raydale during the Holocene of about 1200 (661 - 1370) t a^{-1}.

Table 8.9 Sediment flux and yield in the Semer Water catchment

Time period	Annual minerogenic sediment flux (t a^{-1})	Minerogenic sediment yield (t km^{-2} a^{-1})
1950-1994 AD	274	6.3
0-5500 BP	650	15
0-10 000 BP	1215	28

8.2.2 Gormire

At Gormire sediment flux has been studied during three time periods; 1630-1889, 1889-1949 and 1949-1994. By transferring the ^{210}Pb and ^{137}Cs chronologies of cores GCA and GC3, as determined by Appleby (1998), to cores G2, G3, G4 and GL2 using ARM correlations average accumulation rates can be calculated. Figure 8.2 illustrates the ARM correlations extrapolation of the ^{210}Pb and ^{137}Cs chronologies determined on cores GCA and GC3 to cores G2, G3, G4 and GL2. Cores GC3 and GCA date the zone III/IV boundary (Section 6.2.3, Figure 6.4) as 1949 and 1944 respectively. The peak in ARM in core GC3 is dated to 1889. In core GCA the sample immediately preceding the ARM peak is dated to 1856 and thus 1889 is taken as a date for the ARM peak. The average accumulation rate determined for the oldest part of the dated sediment sequence can be used to estimate approximate dates for the deeper sediments which cannot be dated using radiometric methods. In cores GC3 and GCA the average accumulation rates in the lower sediment are 0.11 cm a^{-1} and 0.09 cm a^{-1} respectively (P.Appleby, pers.comm.). They can be used to estimate approximate dates for the zone I/II boundary of 1632 and 1625 in cores GC3 and GCA respectively. The mean accumulation rates in the 6 Gormire cores for the

periods 1630-1889, 1889-1949 and 1949-1994 are 0.08 (st dev 0.01), 0.11 (st dev 0.03) and 0.23 (st dev 0.07) cm a^{-1} respectively.

Accumulation rates are fairly homogeneous in the six cores collected. Observations on sediment accumulation and water depth obtained whilst coring, coupled to the bathymetric data of (Blackham *et al.* 1981) who report that central part of the lake bottom is relatively flat, have been employed to estimate an area of active sedimentation in Gormire of 45 000 m^2 (Figure 8.3).

By using the total organic carbon and carbonate data reported in Section 6.2.3, an estimate of the biogenic silica component of 4% and the sediment density data of Appendix H, sediment flux and yields can be calculated for the three time periods in Gormire (Table 8.10). Minimum and maximum sediment fluxes and yields have been estimated using the standard deviation associated with the sediment accumulation rate. A minimum and maximum area of sedimentation has also been estimated using a combination of information gained during coring and bathymetric data. A minimum sedimentation area is estimated to be 20 000 m^2 which is the area with a water depth in excess of 4 m (Figure 8.4). A maximum area of sedimentation is estimated to be the entire lake area (70 000 m^2) less a strip 10 m wide around the perimeter of the lake where the water depth shallows. As given in Appendix F the perimeter is 1000 m and thus a maximum sedimentation area of 60 000 m^2 can be employed.

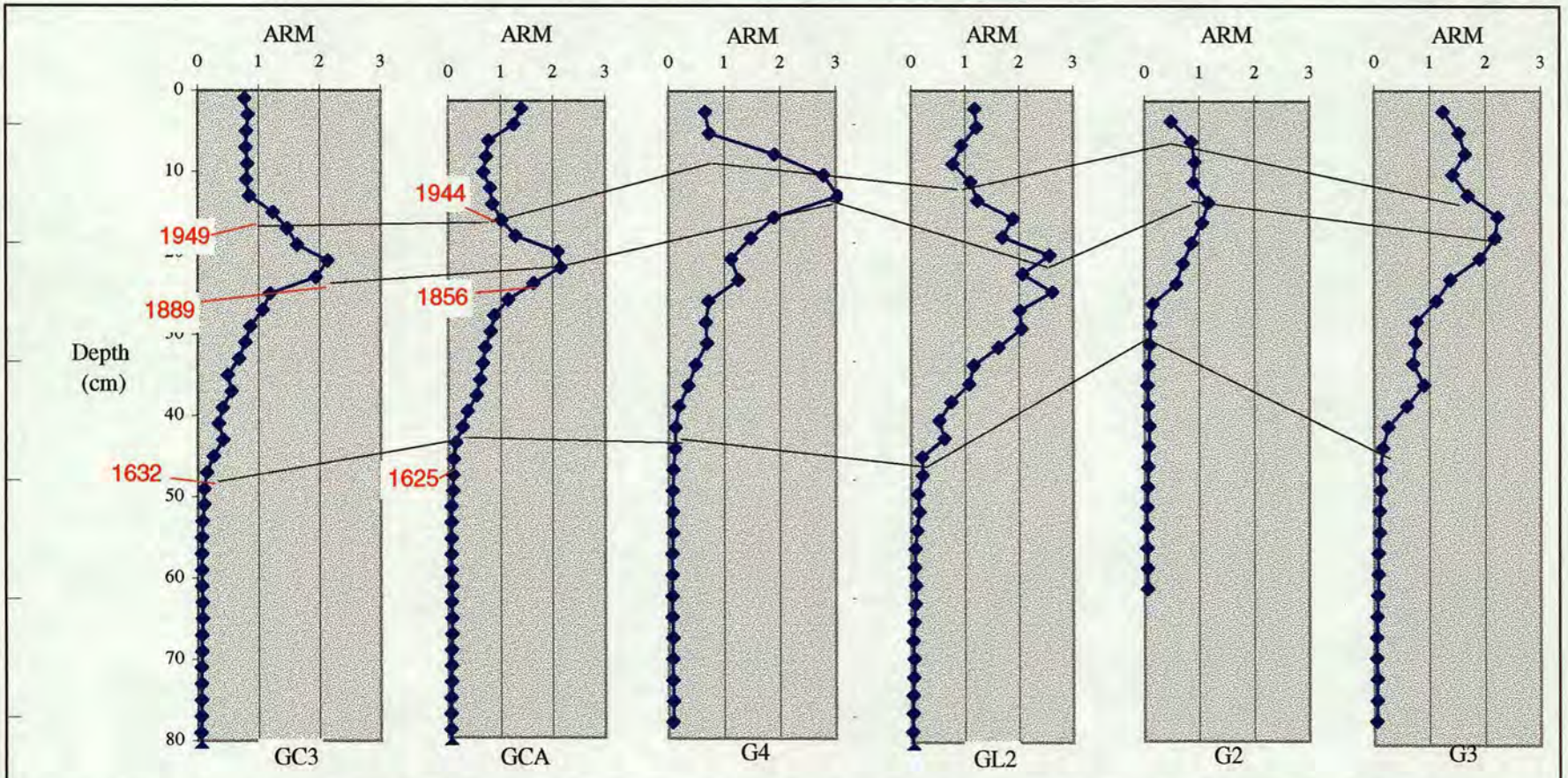

Figure 8.2 Core correlation at Gormire based on changes in ARM values with depth. Cores 2, 3,4 and GL2 Edinburgh measurements (mA m^2 kg^{-1}), cores GC3 and GCA Liverpool measurements (arbitrary units). The upper two correlation lines have been dated using the ^{210}Pb and ^{137}Cs chronologies established for cores GC3 and GCA by Appleby (1998). The lower correlated line is dated to 1630 AD by extrapolation of accumulation rate in the lowermost sediment in each of cores GC3 and GCA.

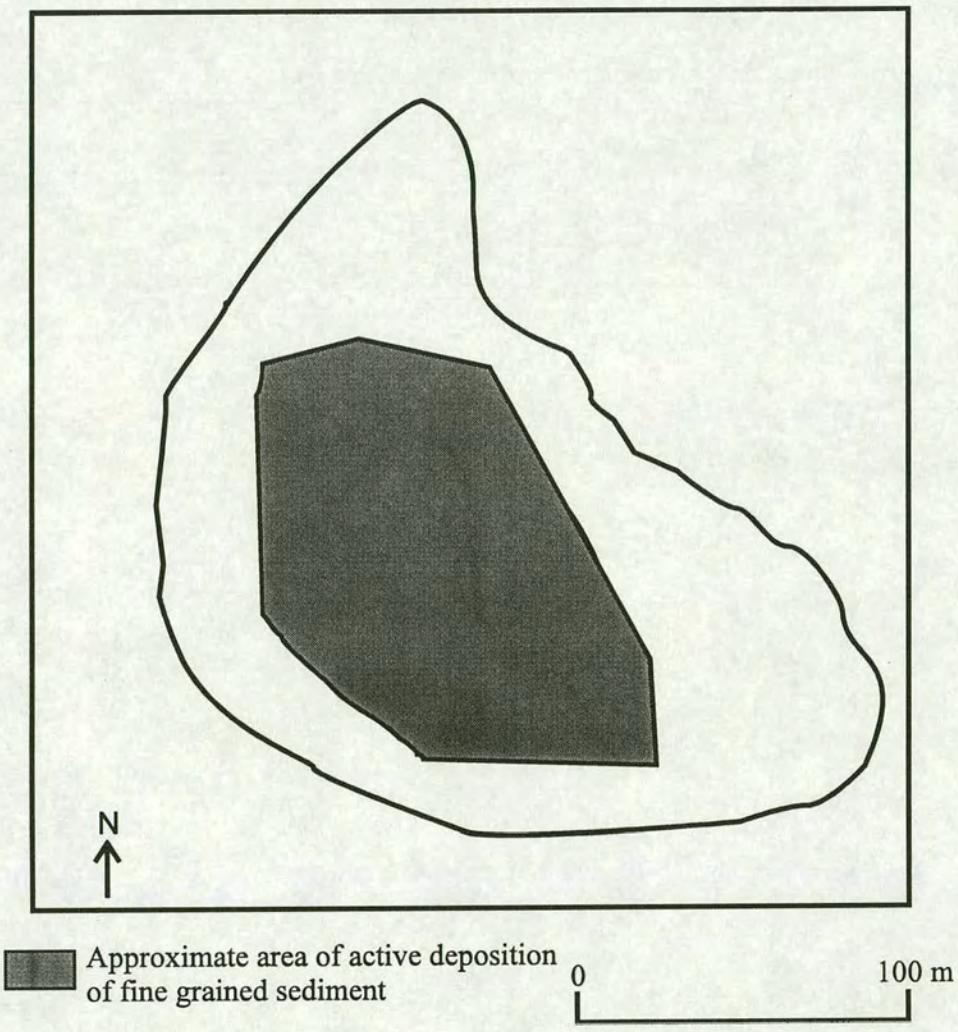

Figure 8.3 Approximate area of active deposition of fine grained sediment at Gormire.

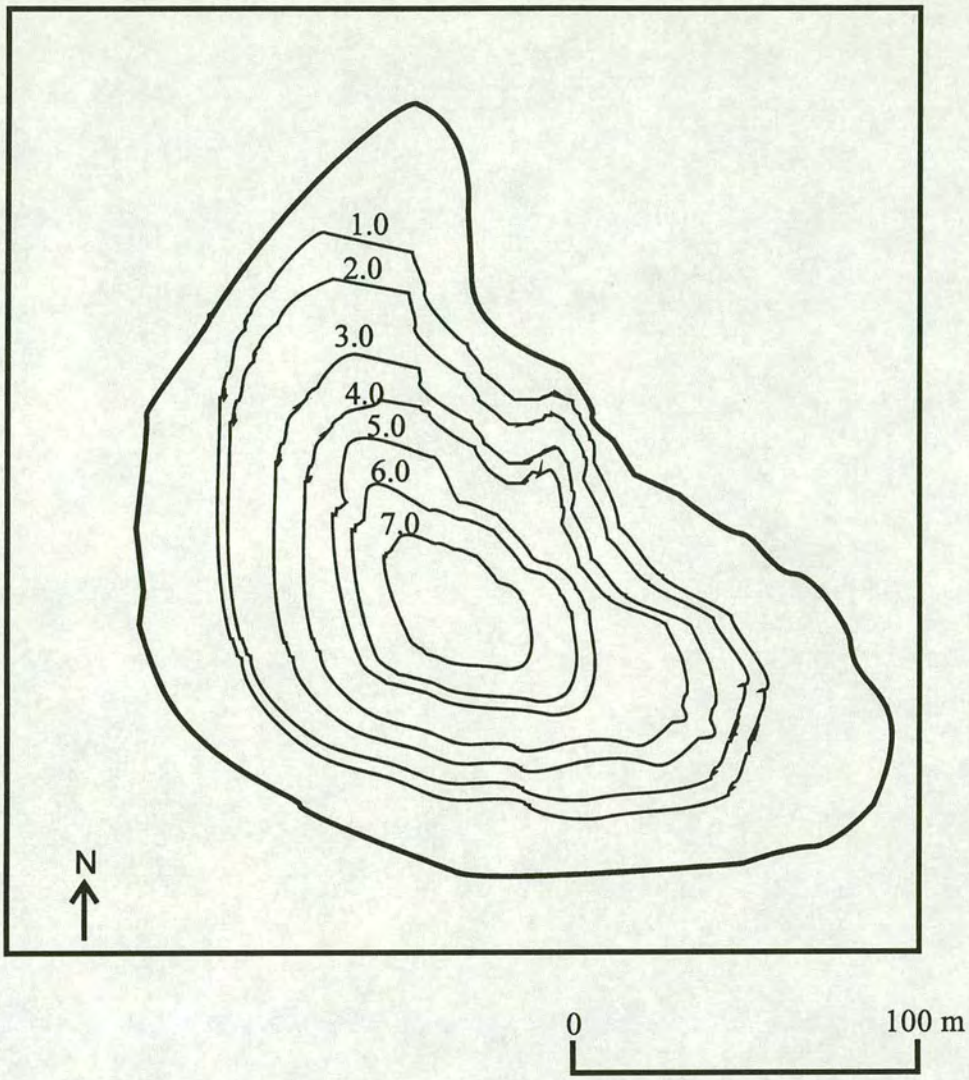

Figure 8.4 Bathmetry of Gormire. All water depths are in metres. Simplified from B.Wake (pers.comm).

Table 8.10 Sediment flux and yields at Gormire

	Time period		
	1949-1994	1889-1949	1630-1889
Number of cores	6	6	6
Mean annual accumulation (cm a^{-1} ± st dev)	0.23 (0.16-0.30)	0.11 (0.08-0.14)	0.08 (0.07-0.09)
Mean density (kg m^{-3} ± st dev)	305(205-405)	331 (211-451)	400 (300-500)
Mean organic content (% ± st dev)	10	20	20
Mean biogenic silica content (%) #	4	4	4
Mean carbonate content (% ± st dev)	16	14	14
Sedimentation area/range (km^2)	0.045 (0.02-0.06)	0.045 (0.02-0.06)	0.045 (0.02-0.06)
Annual flux/range (t a^{-1})	32 (6.6-73)	16 (3.4-38)	14 (4.2-27)
C,CO_3, Si content/range (%)	30	30	30
Annual minerogenic flux/range (t a^{-1})	22 (4.6-51)	11 (2.4-27)	9.8 (2.9-19)
Yield/range (t km^{-2} a^{-1})	78 (16-180)	39 (1.7-19)	35 (10.4-68)

Estimate. Foster *et al.* (1985) report a mean biogenic silica content of 4% in the upper sediments of Merevale lake, UK.

It is found that sediment yields have increased significantly from a mean of 35 t km^{-2} a^{-1} in the period 1640-1889 to 78 t km^{-2} a^{-1} in the period 1949-1994.

Using the pollen analysis results of Blackham *et al.* (1981), obtained on a six metre sediment core from Gormire, sediment accumulation rates have been used to calculate theoretical sediment flux and yields for the post *Alnus* rise and Holocene period (Table 8.11). The sediment flux and yield data calculated in Table 8.10 assume that the area of active sedimentation, sediment density, organic, biogenic silica and carbonate content are the same as those determined and used in this study. The accumulation rate data indicates that sediment accumulation in the earlier Holocene period was much lower than in the more recent time. Mean sediment accumulation rates have increased from 0.03 cm a^{-1} for the period 11000-7500 to 0.07 cm a^{-1} since 7500 BP to values between 0.08-0.23 cm a^{-1} in the period post 1640 AD.

As shown in Table 8.11 sediment yields of 25 and 16 t km^2 a^{-1} for the periods 8220 years BP to present and 11000 to 8220 years BP have been calculated. These yields

are considerably lower than those calculated for the more recent period (Table 8.9). The sediment flux and yield estimates in Table 8.11 are also based on accumulation in just one core and thus they should be interpreted with some caution.

Table 8.11 Holocene sediment flux and yields at Gormire

Period AD	No Cores	Accumulation Total (cm)	Annual (cm a^{-1})	Density (kg m^{-3})	Organic (%)	Carbonate (%)	Biogenic silica # (%)
Since 8220	1	500	0.06	400*	20*	15*	0
11000 - 8220	1	100	0.04	400*	20*	15*	0

Sedimentation area (m^2)	Annual flux (t a^{-1})	C, CO3, Si (%)	Minerogenic flux t a^{-1}	Yield (t km^{-2} a^{-1})
45000	11	35	7	25
45000	7	35	4.5	16

* Estimated (Values from Table 8.9 used)
# Assumed to be zero.

8.2.3 Hornsea Mere

As at Gormire sediment fluxes at Hornsea Mere have been determined using the rate and area of sediment accumulation, sediment density, organic carbon, carbonate and biogenic silica content. Sediment flux has been determined for three time periods at Hornsea Mere; 1730-1963, 1963-1979 and 1979-1994.

Figure 8.5 illustrates the correlation of cores at Hornsea Mere using the ratio ARM/χ. The ^{210}Pb and ^{137}Cs chronology of cores L4 and 8, as determined by Appleby (1998), date as 1979 that point immediately following the rise in ARM/χ ratio in the uppermost part of the core (sediment depths of 12 cm and 8 cm in cores L4 and 8 respectively). The base of the trough in ARM/χ is dated to 1963 (sediment depths of 16 cm and 20 cm in cores L4 and 8 respectively). The average accumulation rate determined for the oldest part of the dated sediment sequence is used to estimate an approximate date of sediment deeper in the lake which cannot be dated using radiometric methods. In core L4 the average accumulation rate in the lower sediment is 0.15 cm a^{-1} (1901-1927) (Table 7.3, Section 7.2.4). The base of the trough in

ARM/χ ratio, at a depth of 45 cm in core L4, can be thus dated to 1754. The average accumulation rate in the lower sediment in core 8 is 0.18 cm a^{-1} (1906-1928) and thus the base of the trough in ARM/χ ratio can be dated to 1764. In this study a date of 1760 is taken to represent the base of the trough in ARM/χ ratio in cores 3-9.

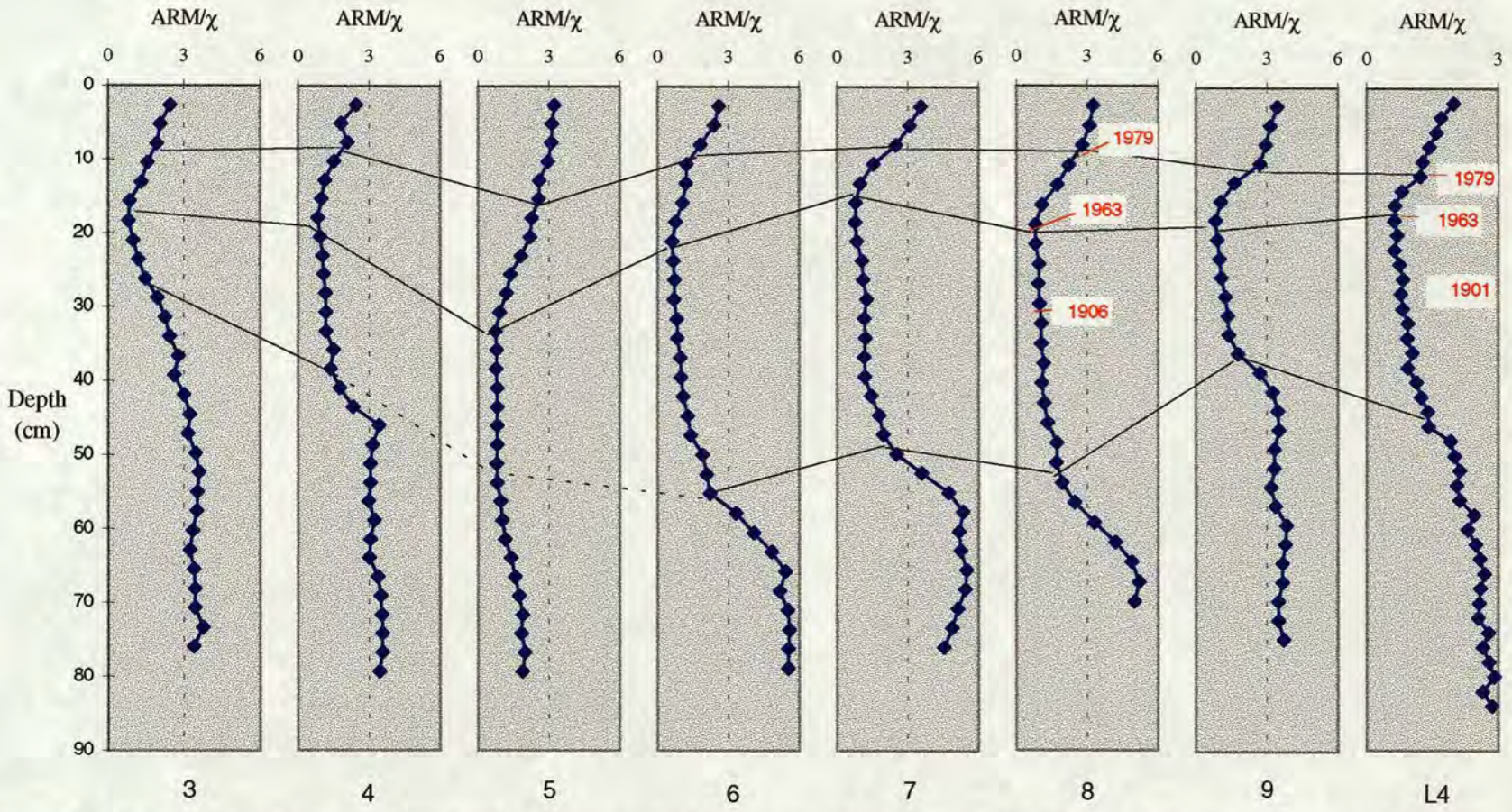

Figure 8.5 Core correlation at Hornsea Mere based on changes in the ARM/χ ratio with depth. Cores 3-9 ARM/χ Edinburgh measurements (kA m^{-1}), core L4 Liverpool measurements (arbitrary units). The dates 1979 and 1963 in cores L4 and 8 have been determined from the ^{210}Pb and ^{137}Cs chronologies of Appleby (1998). The lower correlated line is dated to 1760 AD by extrapolation of accumulation rate in the lowermost sediment in each of cores L4 and 8.

Rates of sedimentation are roughly uniform along the linear extent of Hornsea (Figure 8.5). The lake is shallow with a roughly uniform water depth of 1 metre. Therefore an area of active sedimentation of 0.7 km^2 (Figure 8.6) has been employed. Using TOC and carbonate data reported in Section 7.3.3, an estimate of the biogenic silica component of 4% and sediment density data reported in Appendix H sediment yields and flux can be constructed for three time periods of 1730-1963, 1963-1979 and 1979-1994 (Table 8.12).

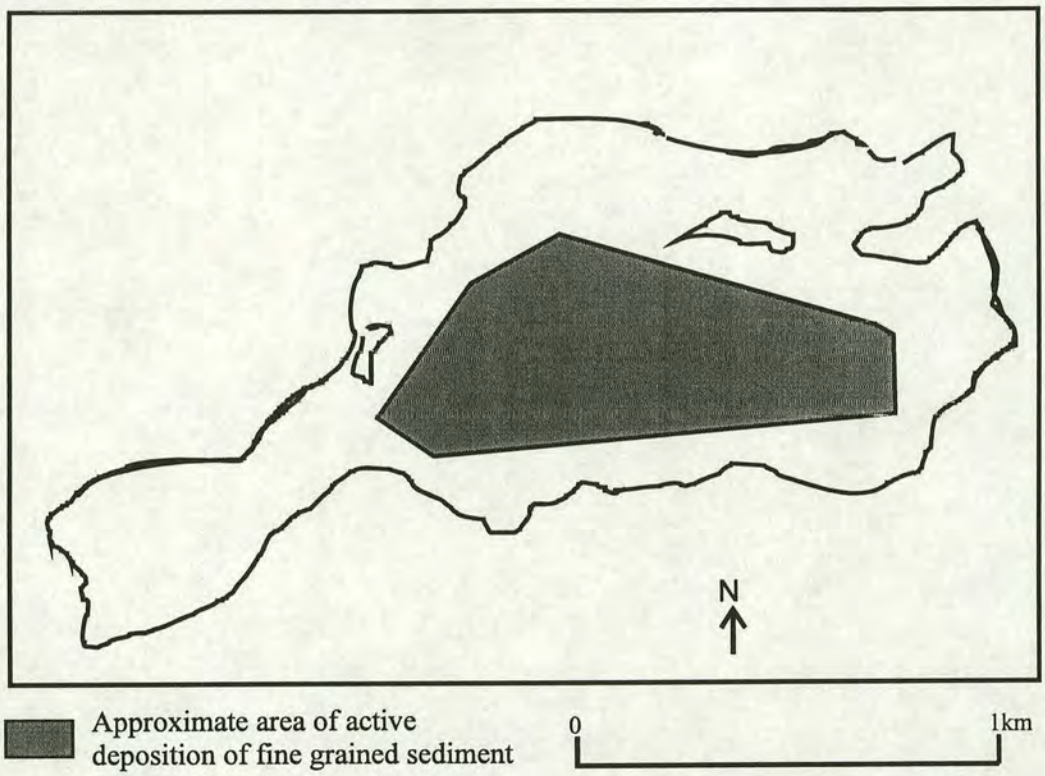

Figure 8.6 Approximate area of active deposition of fine grained sediment at Hornsea Mere.

Minimum and maximum sediment fluxes and yields have been estimated using the standard deviations associated with the sediment accumulation rate and density. A minimum and maximum area of sedimentation has also been estimated. The lake is very shallow and of roughly uniform depth (1 m). The minimum area of sedimentation is taken to be the length of the core transect (c. 1250 m) multiplied by 200 m wide strip either side of the transect (1200 x 200) which results in a sedimentation area of 480 000 m^2. The maximum area of sedimentation is estimated to be the lake area (1200 000 m^2) less a strip 100 m wide around the edge of the lake, where the lake is especially shallow. With a lake perimeter of 2800 m (Appendix F)

this maximum area of sedimentation is estimated to be 920 000 m^3 (1200 000 m^3 – 280 000 m^3).

Table 8.12 Sediment flux and yields at Hornsea Mere

	Time period		
	1979-1994	1963-1979	1730-1963
Number of cores	8	8	8
Mean annual accumulation (cm a^{-1} ± st dev)	0.62 (0.46-0.78)	0.51(0.30-0.72)	0.11(0.08-0.14)
Mean density (kg m^{-3} ± st dev)	265(200-325)	339(288-391)	357(312-402)
Mean organic content (% ± st dev)	5	3.5	3.5
Mean biogenic silica content (%) #	4	4	4
Mean carbonate content (% ± st dev)	38	29	29
Sedimentation area/range (km^2)	0.7 (0.48-0.92)	0.7 (0.48-0.92)	0.7 (0.48-0.92)
Annual flux/range (t a^{-1})	1150 (644-2330)	1210 (605-2590)	275 (120-520)
C,CO_3, Si content/range (%)	47	36.5	36.5
Annual minerogenic flux/range (t a^{-1})	610 (340-1330)	770 (385-1645)	175 (76-330)
Yield/range (t km^{-2} a^{-1})	41 (23-90)	52 (26-112)	12 (5.2-22)

Estimate. Foster *et al.* (1985) report a mean biogenic silica content of 4% in the upper sediments of Merevale lake, UK.

Sediment yields are found to increase dramatically from 12 t km^{-2} a^{-1} in the period 1730-1963 to 52 t km^{-2} a^{-1} between 1963 to 1979, but then to decline again to 41 t km^{-2} a^{-1} in the most recent period 1979-1994.

8.3 Modelling Sediment Flux in British Catchments.

In order to investigate links between physical catchment and land use characteristics and sediment flux I have compiled a database of 30 catchments for which sediment yield data is available (Appendix F). Twenty catchment and land use characteristics have been determined for each of the 30 lake and reservoir sites in Britain. Table 8.13 summarises the parameters determined within each catchment, the potential influence of each parameter on sediment flux and the source of the data. The catchments are characterised by a very broad range of land uses, soil types, altitudes, stream lengths and lake and catchment areas and thus are taken to constitute a representative cross-section of British sites. Appendix F includes records of sediment yield and flux determined from each lake/reservoir study and USLE estimates of sediment yields for each site.

With the exception of the Round Loch of Glenhead, Loch Valley and Loch Enoch the sediment yields at each site have been based on multiple core studies or reservoir surveys. At the Round Loch of Glenhead, Loch Valley and Loch Enoch sediment yield has been calculated from accumulation rate in one core (Flower *et al.* 1987). The area of active sediment accumulation and extent of sediment focusing (expressed as a percentage of the lake area) has been estimated by R.Flower at the Environmental Change Research Centre, University College, London (pers.comm). The records of sediment yield are averages over long time periods, generally of at least the past 100 years. Using average sediment yields over such time periods eliminates the short term flux variability encountered in stream monitoring estimates of sediment flux. At Loe Pool (O'Sullivan *et al.* 1982) exceptionally high sediment yields associated with intensive mining activity in the catchment in the period 1860-1938 are reported. Rather than using these sediment yields in the model sediment yields in just the period 1938-1981 have been employed. Agriculture is reported to be the dominant catchment activity during this period.

Table 8.13 Parameters employed in regression analysis and their potential influence on sediment flux.

Parameter	Relationship to sediment flux	Source of data
Mean annual precipitation	Soil loss closely related to rainfall through (i) detaching power when raindrops strike surface (ii) rainfall contribution to runoff	2
Maximum mean monthly precipitation	Employed to determine p^2/P	2
p^2/P	Indicates concentration of rainfall in one month, gives measure of rainfall intensity	1
Lake perimeter	Significance of lake bank erosion	1
Catchment area	Area of potential erosion	3
Log catchment area	Area of potential erosion. The log accounts for the effect of storage in larger catchments which results in a reduction in sediment yield with increasing area	1
Lake area	Area of sediment deposition	1
Catchment:lake ratio	Frequently plotted against sediment yield in the literature	4
River lengths	Indicate significance of lake bank erosion	1
Lake altitude	Influence on rainfall and vegetation	1
Mean catchment altitude	Influence on rainfall and vegetation Perhaps related to slope gradient/catchment area?	1
Soil erodibility	Resistance of soil to (i) detachment and (ii) transport	1
Catchment soil erosion susceptibility	Soil erodibility factor multipled by catchment area	1
Vegetation	Soil protection offered by vegetation cover	1
Slope gradient	Velocity of surface runoff	1
Length of slope	Volume of surface runoff	1
Mean annual erosivity	Indicative of erosion intensity	1
USLE Sediment yield	Surface erosion, assuming no sediment storage	1
LS	USLE combined slope length/gradient factor	1
R	USLE rainfall erosivity factor	1

Sources:

1 Determined for this study, refer to Section 3.4.
2 Climate Research Unit, University of East Anglia
3 Published and unpublished sources, refer to Appendix F
4 Refer to section 8.3

Sections 2.3.2 summarised a selection of studies by, amongst others, Brune (1950), Flaxman and Hobba (1955), and Schumm (1958) which linked catchment characteristics to sediment yield. The simplest relationships often investigated by these authors was between sediment yield and (i) catchment to lake ratio (Dearing and Foster 1993) or (ii) sediment yield and catchment area (Duck and McManus 1987, Butcher et al. 1993). Figures 8.7 and 8.7 illustrate these two relationships for the 30 lake catchments I have studied (Appendix F). A very poor relationship between catchment to lake ratio and sediment yield, and between catchment area and sediment yield is found.

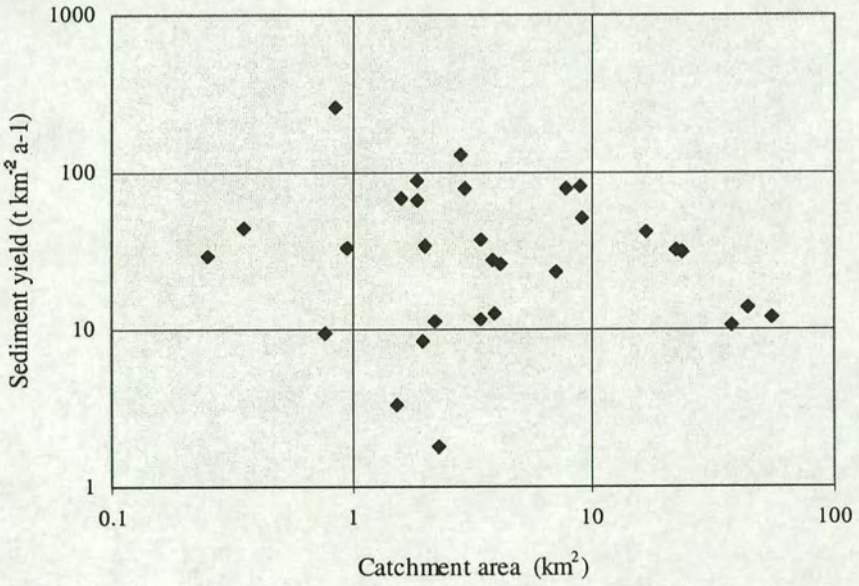

Figure 8.7 The relationship between sediment yield and catchment area for 30 British lake and reservoir sites. The data is very scattered and thus it is difficult to identify any specific trend in sediment yield with catchment area.

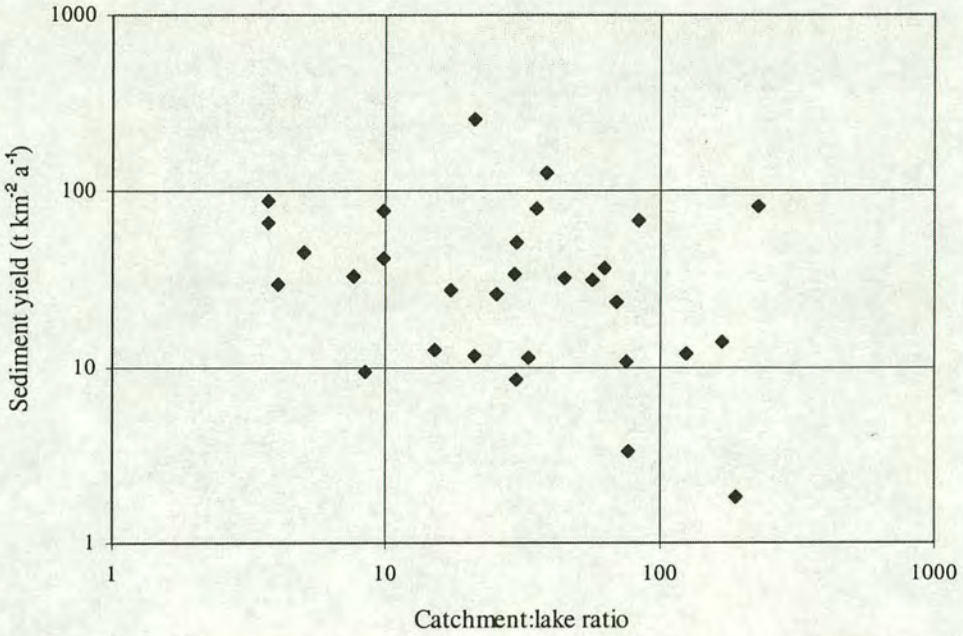

Figure 8.8 The relationship between sediment yield and catchment to lake ratio (CLR) for 30 British lake and reservoir sites. The relationship between sediment yield and catchment to lake ratio is poor and no specific trends can be observed.

The terms 'catchment to lake ratio' or 'sediment yield' do have limitations. Although the catchment to lake ratio tends to be dominated by catchment area it is a rather unuseful term. As illustrated in Figure 8.9, which plots the relationship between catchment area and lake area for the 30 data sets employed in this study, the two variables are not highly correlated. The relationship between catchment to lake area has an R^2 value of only 14%. Sediment yield (t km^{-2} a^{-1}) is not an ideal term to employ in studies comparing sediment yields in different catchments. Expressed as yields, a uniform rate of erosion over the whole of the catchment is assumed, an assumption which is misleading. In this study the flux of sediment to a lake is presented (t a^{-1}) in preference to yield, and this parameter has been employed to study the variation in the mass of material delivered from a catchment for a range of land use and catchment characteristics, and investigate the link between sediment delivery and catchment area.

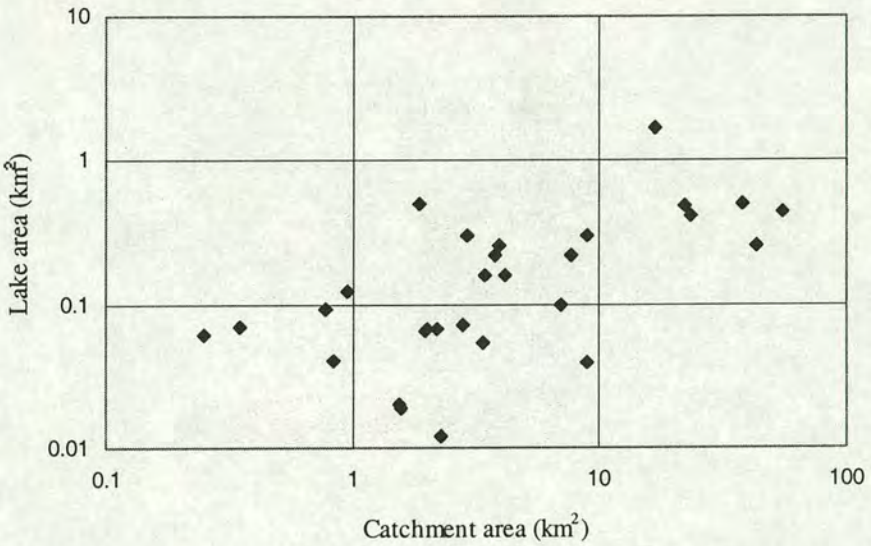

Figure 8.9 The relationship between catchment area and lake area for 30 British catchments. The Figure shows that lake area and catchment area are not necessarily highly correlated. Consequently plotting sediment yield or flux against catchment to lake ratio, as has frequently been done in the literature, is not a very useful relationship with which to investigate the relationship between catchment area and sediment yield.

Sediment flux has also been estimated by multiplying USLE determined erosion rates by the catchment area and applying a sediment delivery ratio. Figure 8.10 illustrates predicted sediment flux for each of the 30 catchments studied using the (i) Universal Soil Loss Equation alone and (ii) the Universal Soil Loss Equation estimate multiplied by a sediment delivery ratio of the A.S.C.E (1975) (Section 2.3.1). Figure 8.9 also compares sediment fluxes predicted using the USLE with flux estimates observed from lake sediment studies. The USLE estimates of sediment flux alone are, with two exceptions (Snailsden and Loch Enoch), considerably greater than the lake sediment flux estimates. The difference between USLE predicted sediment flux lake sediment records of sediment flux can be attributed to the effect of sediment storage in catchments. The USLE estimate of sediment flux is calculated simply by multiplying the USLE determined erosion rate by the catchment area, assuming no sediment storage occurs. Multiplying the USLE sediment flux estimate by the

sediment delivery term makes the USLE flux estimates more comparable with those determined from lake sediment studies. At some sites there is considerable disagreement between the yield estimates obtained from lake sediment and those predicted using the Universal Soil Loss Equation. In particularly the USLE.SDR sediment flux estimates are greater than the lake sediment determined flux records for the seven largest catchments in the database. The discrepancy between USLE predicted sediment flux and lake sediment flux at Lambieltham is particularly marked. Duck and McManus (1987) suggest that the low sediment yield from the Lambieltham catchment results from reservoir management practises. A bypass channel has prevented water and sediment reaching the reservoir. The relationship between the USLE coupled to the sediment delivery ratio estimate of yield and the lake sediment estimate of yield has an R^2 value 34%.

Traditional methods of estimating sediment flux to lakes, involving the use of catchment area, catchment to lake ratio, or the USLE appear to be of limited value in UK studies of sediment flux. In an attempt to predict sediment flux into British lakes and reservoirs more accurately stepwise regression techniques have been employed to construct simple empirical models of sediment flux using catchment and land use characteristics.

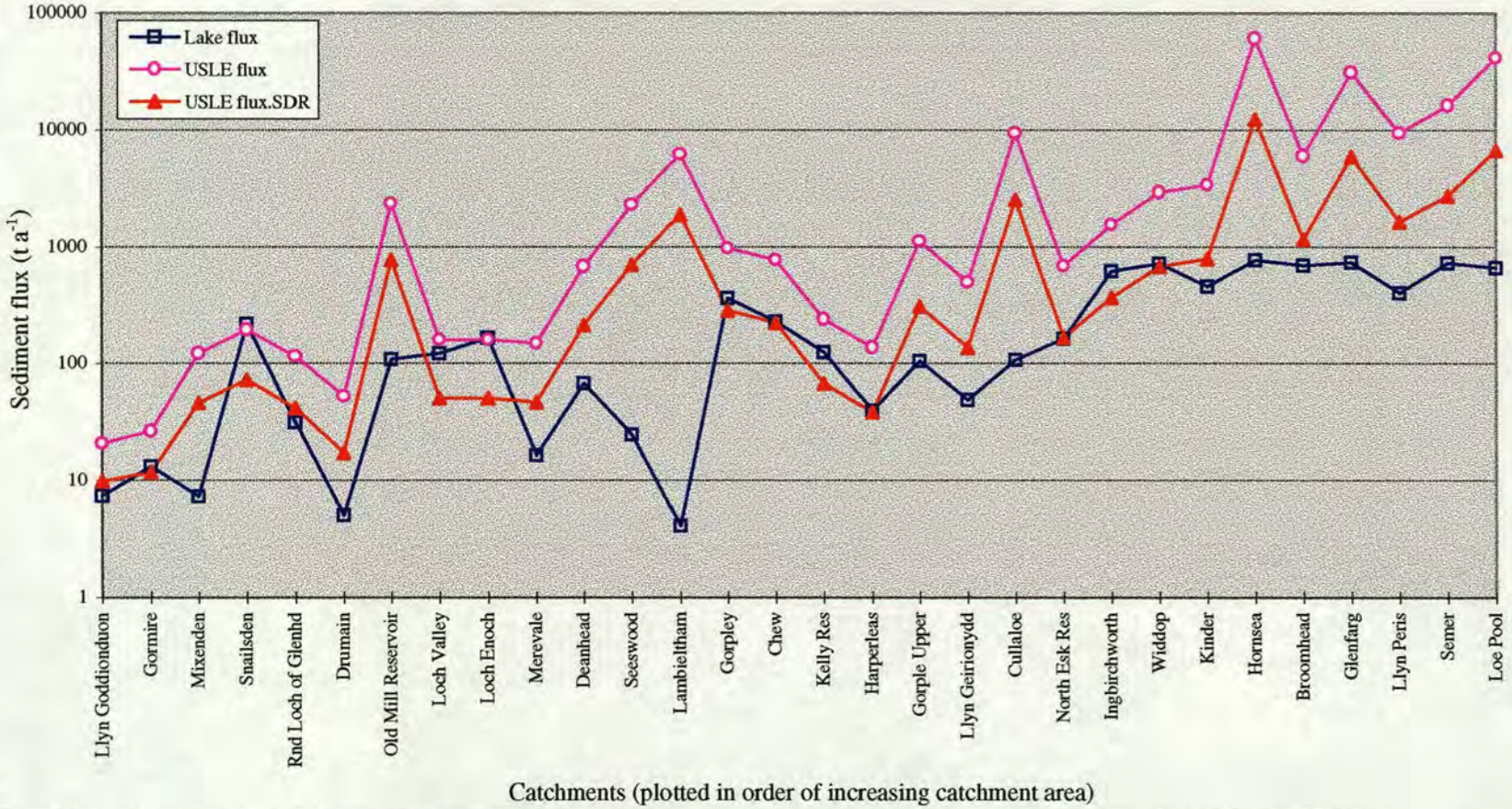

Figure 8.10 A comparison of sediment flux to 30 British lakes/reservoirs using (i) the USLE alone, (ii) the USLE multiplied by the US Soil Conservation Service sediment delivery ratio and (iii) the lake/reservoir estimates of sediment flux. The lake sediment flux estimates are generally lower than those obtained using the USLE multiplied by the US Soil Conservatin Service sediment delivery ratio.

As a precursor to further studies Figure 8.11 demonstrates the poor relationship between sediment flux and catchment area for each of the 30 sites in the database. The relationship is weak, having an R^2 value of 52%.

The regression equation is

Flux = 18.5(catchment area)

Stepwise regression analysis of all the land use and catchment characteristics, including those derived for inclusion in the Universal Soil Loss Equation, listed in Appendix L has been performed. Table 8.14 compares the variables employed in the Universal Soil Loss Equation with the additional catchment and land use characteristics factors determined for each of the 30 sites.

Table 8.14 Summary table comparing and distinguishing the model parameters employed in the Universal Soil Loss Equation with the additional ones determined for regression analysis.

Universal Soil Loss Equation factors	Equivalent catchment characteristic factors
Rainfall erosion factor (R)	Mean precipitation (P) or Mean maximum monthly precipitation (p) or p^2/P
Crop management factor (C)	Vegetation index or Catchment altitude
Soil erodibility factor (K)	Soil erodibility factor (K)
Slope factor (LS)	Catchment area or Mean catchment slope
Erosion control measures (P)	Not applicable
Not applicable	Stream length
Not applicable	Lake perimeter or lake area

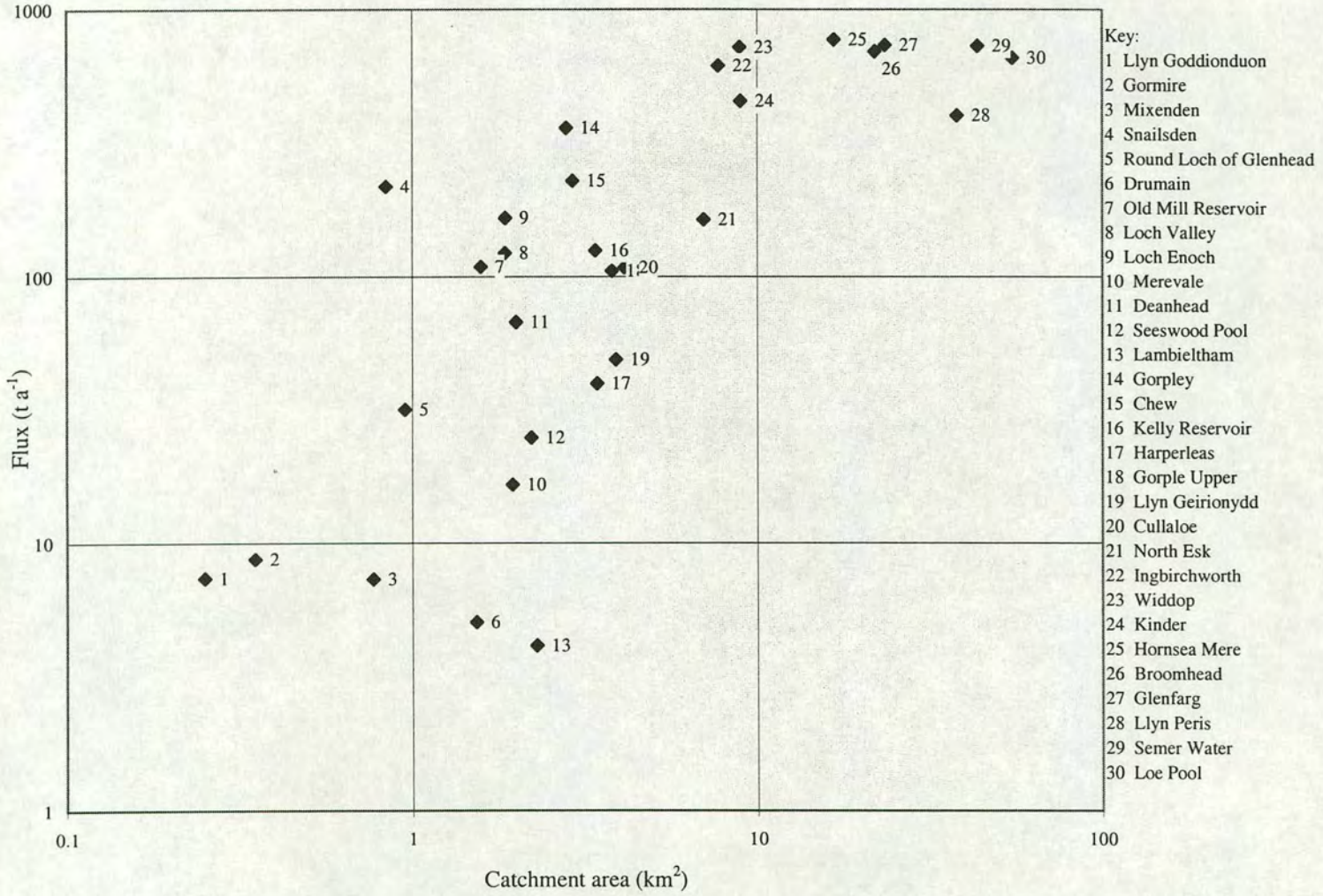

Figure 8.11 The relationship between sediment flux and catchment area for 30 British sites. An increase in sediment flux with increasing catchment area can be observed, however the relationship has an R2 value of only 52% and is thus relatively weak.

Stepwise regression analysis studies the F-statistic of any variable in the equation. A K value is set to determine, depending on the F-statistic, whether any variables are removed from the equation. Where any variable has an F value below K the variable with the smallest F-statistic is removed from the equation. Minitab uses a default F-value of 4.

Table 8.15 summarises the abbreviations used to denote each physical catchment parameter in each of the regression equations which follow and the respective units.

Table 8.15 Abbreviations and units of the parameters employed in the regression models.

Abbreviation	Parameter	Units
LCA	Log of catchment area	log10 (km^2)
S	USLE slope length factor	dimensionless
KA	Catchment soil erodibility susceptibility	dimensionless.km^2
LP	Lake perimeter	km
LA	Lake altitude	m
UF	Predicted USLE sediment yield.catchment area	$t\ a^{-1}$

Stepwise regression analysis determines sediment flux using the following equation

$$\text{Flux} = 92.5 + 25.2\ KA + 0.023\ UF + 135\ LA \qquad (8.2)$$

Figure 8.12 illustrates the relationship between the fits of these variables and flux. The relationship observed has an R^2 value of 65% and correlation coefficient of 80%. Reducing the F value to 3 does not affect the regression equation.

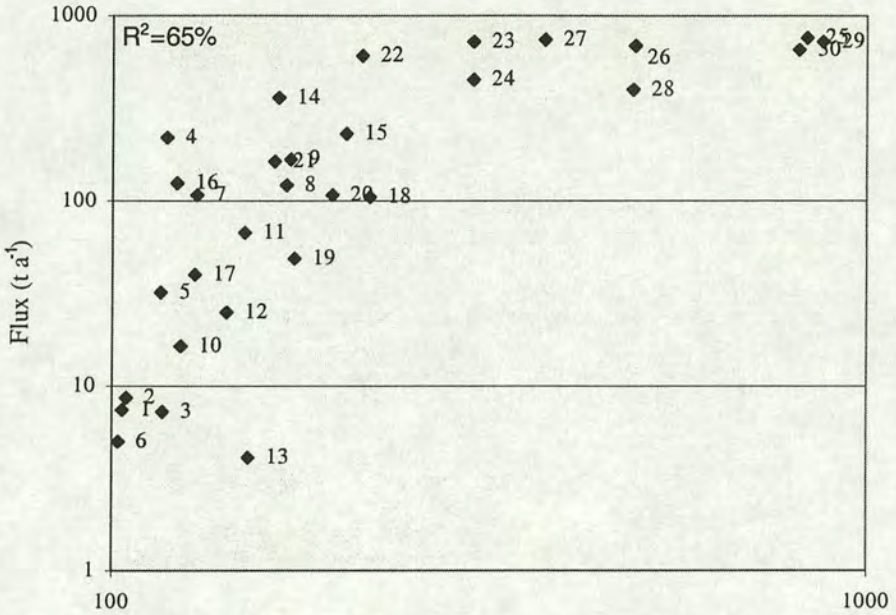

Figure 8.12 The multiple regression relationship between sediment flux and a catchment soil erosion susceptibility factor, USLE determined sediment flux and lake altitude produced using a stepwise regression analysis. Refer to Figure 8.11 for key to catchments. The relationship is good, resulting in an R^2 value of 65%.

As noted in Section 2.3.2 (Figures 2.13, 2.14) a variety of authors have reported decreases in sediment yield with increasing catchment area. In an attempt to improve on the simple relationship between catchment area and sediment flux (Figure 8.10) and account for the progressive increase in sediment storage in catchments as the catchment area increases I have determined the log of catchment area and related it to sediment flux. As shown in Figure 8.13, I have found that the relationship between log of catchment area and sediment flux is significantly stronger than that observed between catchment area and sediment flux. The following regression relationship is obtained between log of catchment area and sediment flux resulting in an R^2 value of 66% and correlation coefficient of 81%:

$$\text{Flux} = 39.8 + 381\ \text{LCA} \qquad (8.3)$$

When the log of catchment area is added to the step-wise regression analysis and an F value of 4 employed log of catchment area is the only variable to be selected and regression equation 8.3 is produced.

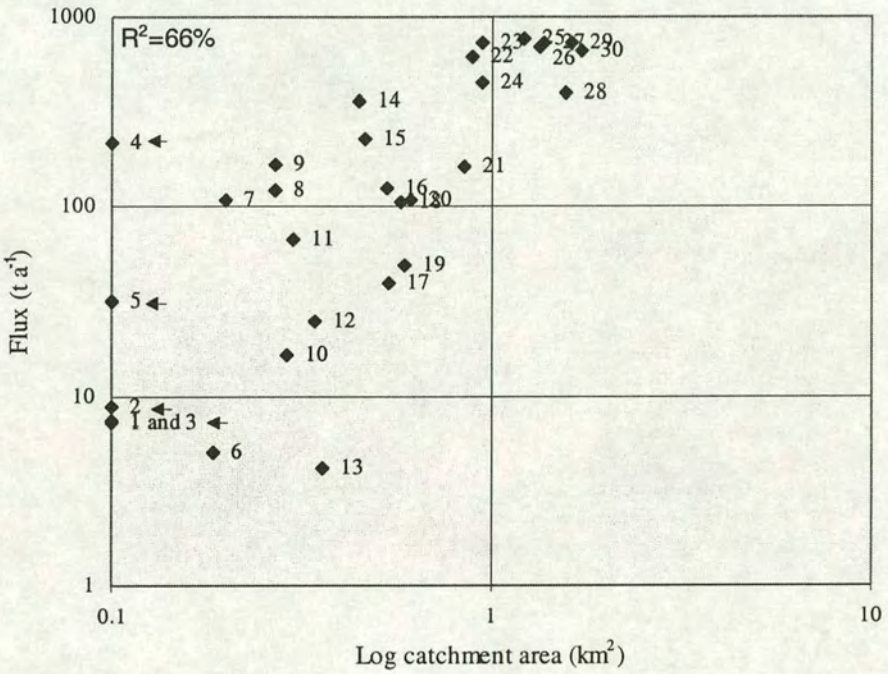

Figure 8.13 The relationship between log of catchment area and sediment flux for 30 British lake and reservoir sites. Refer to Figure 8.11 for key to catchments. With an R^2 value of 66% the relationship between log of catchment area and sediment flux is considerably greater than that obtained using catchment area. This implies that the log of catchment area incorporates the effect of sediment deposition in catchments.

If the F value is reduced to 3 fewer parameters are removed from the regression analysis and the following regression equation produced

$$\text{Flux} = 696 + 400\,\text{LCA} - 249\,\text{S} + 246\,\text{KA} \qquad (8.4)$$

The relationship between sediment flux and the best fit values of the variables log of catchment area, USLE slope length and soil erodibility (Equation 8.4) has an R^2 value of 80% and correlation coefficient of 89% (Figure 8.14).

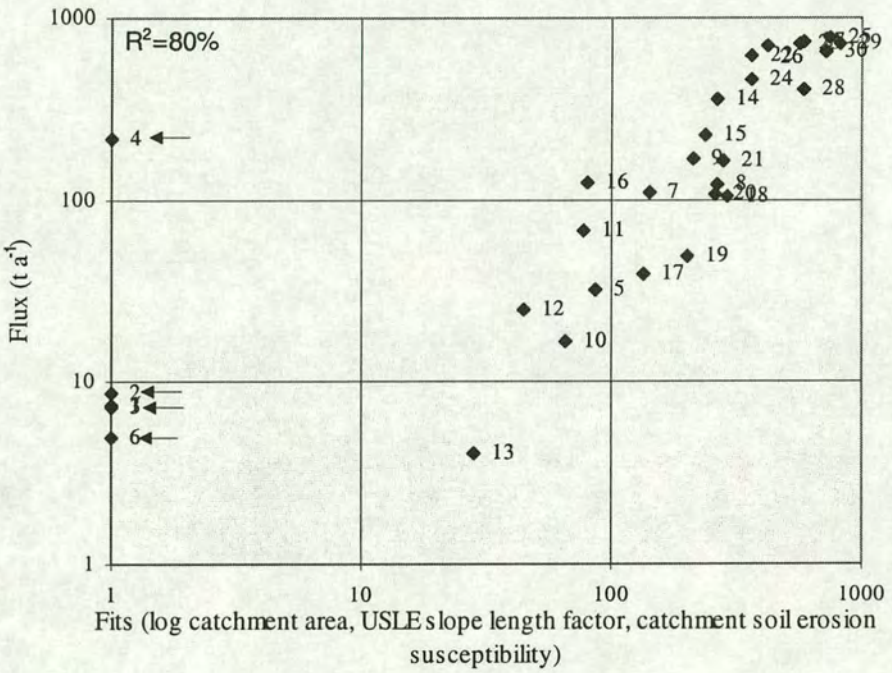

Figure 8.14 The regression relationship between sediment flux and the log of catchment area, the USLE slope length factor and the catchment soil erosion susceptibility factor as produced using a stepwise regression analysis. Refer to Figure 8.11 for key to catchments. A strong regression relationship (R^2 80%) results from this stepwise regression analysis.

Reducing the F value to 2 results in the following regression equation:

$$\text{Flux} = 709 + 466\ \text{LCA} - 261\ \text{S} + 26.1\ \text{KA} - 32.2\ \text{LP} + 0.273\ \text{LA} \qquad (8.5)$$

This relationship results in an R^2 value of 83% and correlation coefficient of 91% (Figure 8.15).

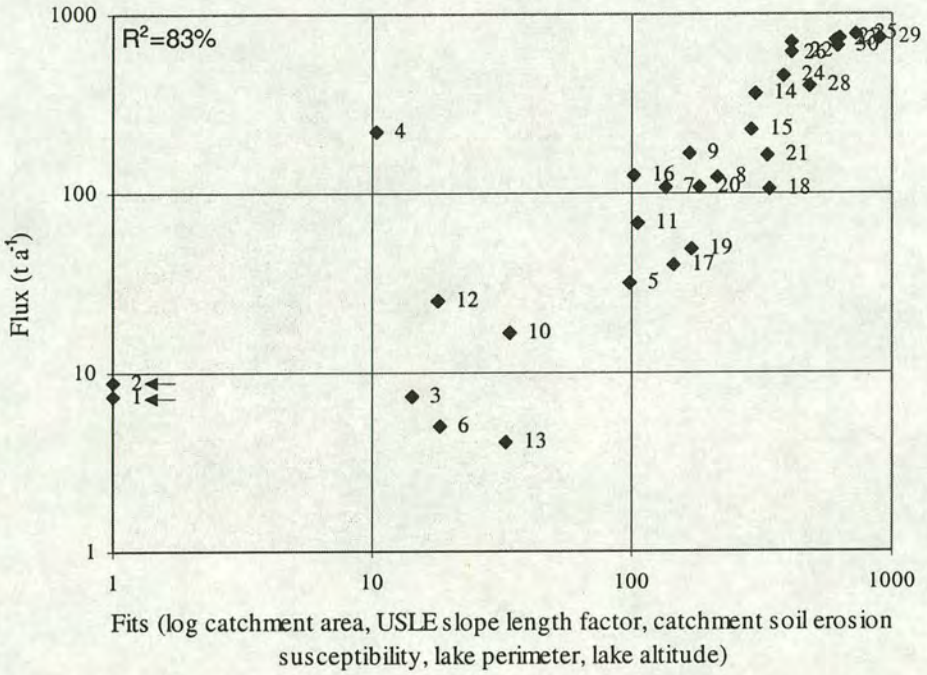

Figure 8.15 The regression relationship between sediment flux and the log of catchment area, the USLE slope length factor, the catchment soil erosion susceptibility factor, lake perimeter and lake altitude as produced using a stepwise regression analysis. Refer to Figure 8.11 for key to catchments. Relating these five parameters to sediment flux using stepwise regression results in an R^2 value of 83%.

Table 8.16 summarises the R^2 and correlation coefficient values which result from employing various combinations of catchment characteristics to determine sediment flux. In selecting the most appropriate regression equation to estimate sediment fluxes a balance between a strong correlation and a simple empirical model is sought. Balancing an acceptable accuracy with simplicity the regression relationship between sediment flux and log of catchment, soil erodibility of the A horizon and lake area is the most suitable applicable model. However the more simple model employing log of catchment area alone provides a reasonable account of sediment flux where other catchment characteristics are not obtainable.

Table 8.16 Summary of the R^2 and correlation coefficients obtained from each of the regression analyses

R^2 value	Correlation coefficient (%)	Variables
83	91	Log catchment area USLE slope length factor Soil erodibility factor x catchment area Lake perimeter Lake altitude
80	89	Log catchment area Soil erodibility factor x catchment area USLE slope length factor
65	80	Soil erodibility factor x catchment area USLE sediment yield x catchment area Lake altitude
66	81	Log catchment area
50	70	Catchment area

8.4 Summary

- Since 1950 sediment yields at Semer Water have averaged 6.3 t km^{-2} a^{-1}, approximately one quarter of the mean Holocene sediment yield of 28 t km^{-2} a^{-1} for the Raydale valley.

- At Gormire sediment yields of 35, 39 and 78 t km^{-2} a^{-1} have been determined for the periods 1640-1889, 1889-1949 and 1949-1994 respectively.

- At Hornsea Mere sediment yields 12 t km^{-2} a^{-1} and 52 t km^{-2} a^{-1} and 41 t km^{-2} a^{-1} have been found for the periods 1730-1963, 1963-1979 and 1979-1994 respectively.

- The optimum relationship to predict sediment influx from catchment and land use characteristics in British sites is

  Flux = 696 + LCA - 249 S + 246 KA

Chapter 9

Discussion

9.1 Magnetic Characterisation of Lake Sediments

This study has demonstrated a range of different sources of magnetic minerals which contribute to the magnetic signature within lake sediments. The magnetic characteristics of sediment cores from Semer Water and Raydale are influenced by a combination of topsoil, geological material and bacterial magnetosomes. At Gormire the magnetic signature is dominated by topsoil and bacterial magnetite. There is also evidence of dissolution in the sediment at Gormire. TEM studies and magnetic analysis show that the magnetic characteristics of lake sediments from Hornsea Mere are dominated by the influence of bacterial magnetosomes. In summary the study demonstrates that the magnetic signature in upland and lowland lake sediments may not arise solely from the input of detrital catchment material. The detrital model of Thompson *et al.* (1975) which links the magnetic signature recorded in Holocene lake sediments to the inwash of catchment material via erosion is not always applicable.

The influence of magnetotactic bacteria upon the magnetic signature is significant at all three sites studied, especially at Hornsea Mere. Semer Water, Gormire and Hornsea Mere are situated in areas where the underlying sedimentary geology results in a very weak detrital magnetic signature. Consequently the magnetic signature arising from magnetotactic bacteria can easily overprint such a weak background signature. At sites such as Hornsea Mere, where magnetotactic bacteria are present in the lake sediment in sufficient quantity to overprint the detrital magnetic signal completely, magnetic techniques cannot be employed to trace the source of deposited sediment and discriminate between, for example, channel bank and top soil erosion.

Magnetic techniques are better applied to sediment tracing studies in catchments underlain by rocks characterised by high concentrations of magnetic minerals. The studies at the Lough Neagh (Dearing and Flower 1982) and Lough Frisa (Dearing 1979) catchments, underlain by basalts, are good examples.

The magnetic characteristics of sediment cores from Raydale are strongly influenced by particle size. The high correlation between ARM and the proportion of fine material 0.4-1.6 μm in Giddings core A is confirmed by magnetic measurements made on particle size splits from bulk sediment samples (i) Giddings core A sediment and (ii) Semer Water alluvial fan material.

It follows that a brief appraisal of a lake's sediment magnetic characteristics is a worthwhile precursor to lake sediment source provenance studies which use magnetic techniques. Magnetic measurements made on just one surface sediment sample would indicate (i) the concentration of magnetic minerals and (ii) the presence of any magnetotactic bacteria. Based on results from Hornsea Mere, Semer Water and Gormire ARM/SIRM and ARM/χ ratios of greater than 0.15 and 1 kA m^{-1} respectively can be employed to indicate the presence of magnetotactic bacteria.

9.2 Multicore Lake Sediment Studies

In this multicore study of lake sediments from Semer Water, Gormire and Hornsea Mere the correlation of cores with magnetic measurements has been met with mixed success. Eight of the ten cores collected from Hornsea Mere correlate very well. The correlation is based on changes in ARM/χ ratio which is attributed to downcore variations in the concentration/preservation of bacterial magnetosomes. At Semer Water core correlation has proved very difficult using magnetic techniques. The occurrence of sediment hiatuses and complex sediment deposition environment prevents core correlation. Although down core magnetic measurements have proved unsuccessful in correlating cores from Semer Water, coupled to variations in

sediment density they have nevertheless served as a useful tool for identifying a core (6) without a hiatus i.e. the most appropriate core for establishing a ^{210}Pb and ^{137}Cs chronology. The uppermost magnetic zones (III and IV) at Gormire have also been correlated successfully using ARM and ARM/SIRM ratio.

In any study of sediment yield there is a trade off between basing a study on accumulation rate in just one core and using a multicore study. Although magnetic characterisation of samples is a very rapid technique, sub-sampling cores is an extremely time consuming process. The researcher must choose between sub-sampling many cores from one lake site, or one core from many lake sites. In choosing between these two options the researcher must prioritise the study's objectives. If the aim is to study relative changes in sediment flux with time, then perhaps it is sufficient to assume that variations in sediment accumulation in one core are representative of those variations in the whole lake or reservoir basin. For example in their study of Braeroddach at in north east Scotland, Edwards and Rowntree (1980) were able to relate significant differences in sediment accumulation during the Holocene to vegetation change associated with climatic warming following the Late-glacial and to Neolithic agricultural activity in the latter half of the Holocene. However many studies including that at Llyn Goddionduon (Bloemendal *et al.* 1979) have clearly demonstrated, not only that sedimentation patterns vary spatially in a lake basin but also that they change with time. Therefore it is potentially inaccurate to relate changes in accumulation rate in just one core to changes in sediment delivery from a catchment. Where quantitative estimate of sediment flux and changes in flux with time are required multicore studies are essential. Multicore studies also provide information on the area of active sedimentation within a lake basin. Without such knowledge it is hard even to guess what the active sedimentation area may be.

Even in these multicore studies I have reservations about the accuracy of estimating areas of active sedimentation at Semer Water, Gormire and Hornsea Mere and believe that it is likely to be the biggest source of inaccuracy in calculating sediment

fluxes to each site. Table 9.1 compares the lake area with that of the active sedimentation area at each of Semer Water, Gormire and Hornsea Mere and illustrates the potential error if the lake area had been employed to calculate sediment flux rather than the area of active sedimentation.

Table 9.1 A comparison of lake area, area of active sedimentation and the associated error in using lake area rather than active sedimentation area when calculating sediment flux.

Site	Lake area (km^2)	Area of active sedimentation (km^2)	Flux overestimate in using lake area rather than active sedimentation area (%)
Semer Water	0.27	0.09	+300
Gormire	0.07	0.045	+156
Hornsea Mere	1.2	0.70	+171

In summary I believe that multi-core studies are essential in attempts to derive quantitative estimates of sediment flux.

9.3 Sediment Yields

9.3.1 Semer Water

At Semer Water mean sediment yields of just 6.3 t km^{-2} a^{-1} have been recorded since 1950. In comparison to average rates of soil erosion proposed by Morgan (1995, Table 1) of between 10 - 50 t km^{-2} a^{-1} under natural conditions, and 10 - 200 t km^{-2} a^{-1} under cultivated land, the sediment yields at Semer Water are low, especially for the recent period. The sediment yields are also very low in comparison to suspended sediment yields of British rivers which are typically between 50 and 100 t km^{-2} a^{-1} (Walling 1990). Sediment yields at Semer Water fall towards the lower end of the range of values reported by Butcher *et al.* (1993), who observed sediment yields of between 2.9 and 289 t km^{-2} a^{-1} in their study of sedimentation in 28 reservoirs in the Pennines. These differences remain difficult to explain. They may, in part, derive from sediment storage in the large Semer Water catchment which results in low

sediment deliveries. However such strange sites need to account for over 10 million m^3 of eroded sediment and yet have not been identified

Wass (1996) as a separate research project within the Rivers, Atmosphere, Estuaries and Coasts Study (RACS) component of the Land Ocean Interaction Study has measured the concentration of suspended solids in four rivers within the Humber catchment and in combination with river discharge data estimated sediment flux in sub-catchments of the Humber. Table 9.2 shows the sediment load and sediment yield for his four rivers.

Table 9.2 Sediment yield determined for four rivers for the period October 1994 to September 1995 (Wass 1996).

River	Monitoring site	Total load (kg)	Sediment yields ($t\ km^{-2}\ a^{-1}$)
Swale	Lecby	71,803, 809	53.2
Ure	Westwich	48,258,698	52.8
Nidd	Cowthorpe	19,956,631	28.2
Ouse	Skelton	120,042,747	36.2.
Total		**132,863,137**	

Semer Water falls within the Ure drainage basin and both the Rivers Ure and Swale drain upland, largely rough grazing/grassland catchments. Sediment flux estimates of 52.8 t km^{-2} a^{-1} and 53.2 t km^{-2} a^{-1} recorded for the Rivers Ure and Swale are considerably greater than the lake sediment based estimate of flux at Semer Water of 6.3 t km^{-2} a^{-1}. Aside from the effect of sediment storage, another possible explanation for the low sediment yields at Semer Water could be that the lake is not a particularly efficient sediment trap and thus significant quantities of sediment may escape as suspended sediment through the outflow. In order to assess the significance of sediment loss through the outflow, river discharge and suspended sediment concentrations would need to be monitored.

9.3.2 Raydale

Surprisingly, the mean sediment yields for the Holocene period of 28 t km^{-2} a^{-1}, recorded from sediment deposits in the Raydale valley, are over three times greater than those recorded in the more recent lake sediment record. Thus a decrease in sediment yield with time in the recent period has occurred rather than the expected increase caused by human activies in the catchment. The changes in Holocene sediment yields at Raydale can be compared with those determined from other sites in Britain. At Llyn Geirionydd, North Wales, an increase in sediment yield from 2 to 5 t km^{-2} a^{-1} was observed in the Holocene (Snowball and Thompson 1992). A similar increase has been recorded at Lough Catherine, Northern Ireland (Snowball and Thompson 1990). Sediment yields ranged from 0.05 t km^{-2} a^{-1} in the period 7000 - 10000 BP to t km^{-2} a^{-1} for the period 250-1500 BP, although a peak of 1.5 t km^{-2} a^{-1} is observed in the period 1500 - 4000 BP. Bloemendal (1982) reported a much more dramatic increase in sediment yield during the Holocene at Llyn Goddionduon, North Wales. Inorganic sediment yields of 2.8 t km^{-2} a^{-1} were found for 10400-800 BP increasing to 9.9 t km^{-2} a^{-1} for the period 800 BP - 1951 AD and 18.3-22.6 t km^{-2} a^{-1} for the period 1951-1977 AD. Based on changes in accumulation rate in one core from Braerodach, north east Scotland, Edwards and Rowntree (1980) observed an overall increase in sediment accumulation during the Holocene with two particularly significant increases in sediment accumulation occurring, one at 5390 BP and the most significant at 370 BP. So marked was the increase at 370 BP that subsequent sediment deposition accounts for approximately 25% of the total sediment deposited during the Holocene.

The Holocene sediment yields determined at Raydale are therefore very different from other published Holocene records from British sites. Firstly, the Holocene sediment yield of 28 t km^{-2} a^{-1} is considerably greater than that observed in Holocene records elsewhere in Britain. Secondly the decrease in sediment yields in the more recent period is in contrast to the pattern of an overall increase in sediment yield during the Holocene displayed at other British sites.

The high mean Holocene sediment yields may in part arise from gully erosion in the catchment. As illustrated in Chapter 5 (Section 5.11) an estimated nine million cubic metres of sediment (11 million tonnes) could, potentially, have been eroded from gullies during the Holocene. The mass of minerogenic sediment deposited in the Semer Water and Raydale deposits is similarly estimated to be 11 million tonnes. This suggests that the gully erosion could have been a very significant source of sediment for the extensive Holocene deposits in Raydale.

The Holocene sediment record does not record changes in yields with time in sufficient detail to identify specific periods during which erosion has been particularly high. The record is based on only three cores, limited pollen analysis and ^{14}C dates from just one core. However ^{14}C dates, with ages ranging from 3340 to 4305 years BP, from samples from Giddings core C span a period of less than 1000 years and indicate that 10 metres of sediment have accumulated since c. 4000 years BP. Indeed it would seem that about 8 metres of sediment was deposited in less than 1000 years. These sediments may well indicate a period of intense gully erosion.

Harvey *et al.* (1981) studied the age of gully formation at Middle Langdale in the Howgill fells, Cumbria, a site c. 30 km north west of Semer Water. The large gullies, cut through periglacial material, but are now stabilized and inactive. ^{14}C dates have been determined for a buried soil horizon under the debris cone produced by the eroding gully. Dates range from 2580+- 55 yrs BP at the base of the organic horizon to 940 +- 95 years BP for fossil rootlets in the uppermost organic layer immediately below the overlying debris cone. Harvey *et al.* (1981) suggested that the increase in soil erosion, gully development and debris cone deposition at Middle Langdale may have been a response to the Scandinavian introduction of sheep farming in the tenth century A.D. in this area. Comparing the ^{14}C evidence for gully erosion at Middle Langdale with that at Semer Water indicates either that (i) gully erosion at Semer Water occurred at an earlier date, of between 3500 and 4200 years BP, or (ii) the thick sediment sequences in Raydale are a result of gully erosion in the tenth century

and that the ^{14}C dated macrofossils deposited Raydale represent inwashed older material. Future work could include obtaining ^{14}C dates from soils beneath the alluvial fan at the base of selected gullies in Raydale and so to date the onset of gullying.

9.3.3 Gormire

At Gormire mean sediment yields of between 35 and 78 t km^{-2} a^{-1} are recorded for the time period 1640-1994. These sediment yields are much greater than those recorded at Semer Water. The higher yields may be due, in part, to the fact that the Gormire catchment is very small and steep, providing fewer opportunities for sediment storage and thus resulting in a high sediment delivery ratio. Sediment yields at Gormire are comparable with yields in other small upland British catchments. These are typically between 30 t km^{-2} a^{-1} (Walling and Webb 1981) and 50 t km^{-2} a^{-1} (Newson 1986). A progressive increase in sediment yield since 1640 is observed at Gormire. The increase coincides with evidence for forest clearance as suggested by a steady decline in tree pollen and an increase in cereal and grassland species (B.Wake, Unpublished pollen diagram). Although based on sediment accumulation rate in just one core sediment yields during the Holocene at Gormire appear to have increased significantly in the most recent period. Indeed they have increased by a factor of over 20 since the early Holocene. This finding is in agreement with the rapid increases in sediment yields in the latter part of the Holocene which have been reported at Llyn Goddionduon (Bloemendal 1982), Llyn Geirionydd (Snowball and Thompson 1992) and Lough Catherine (Snowball and Thompson 1990).

9.3.4 Hornsea Mere

In comparison to Semer Water and Gormire, sediment yields recorded at Hornsea Mere are very varied. Yields of between 12 and 52 t km^{-2} a^{-1} are found in the period since 1730, with the highest yields occurring between 1963 and 1979.

The highest sediment yield at Hornsea Mere occurs in the period 1963-1979 and could be attributed to a number of factors. Appleby (1998) reports that since 1963 ^{210}Pb fluxes in the Hornsea sediments increase towards levels considerably greater than atmospheric flux. Thus the increase in sediment flux since 1963 may be partly attributable to a shift in the pattern of sediment focusing. A second possible explanation for the increase in sediment yield would be changes in the catchment boundary and thus the source area contributing sediment to the lake. The watershed at Hornsea Mere boundary is very hard to define as the catchment is very low lying and a number of artifical drainage channels have been constructed which may have been responsible for altering the catchment area with time.

One possible explanation for the decline in sediment yields in the period since 1979 is that although originally designated as a Site of Special Scientific Interest (SSSI) in 1951, in 1983 the boundary of the SSSI around the edge of the lake was altered. The exact details are not documented (L.Homes, English Nature, pers.comm.) but it seems probable that they included increasing the extent of a strip of uncultivated land around the lake which may be acting to reduce the flux of sediment into the Mere in the recent period.

9.4 Converting sediment yields into rates of erosion at Semer Water, Gormire and Hornsea Mere.

Using sediment yield data alone to compare rates of erosion in different catchments is of limited value. Sediment yields calculated from lake sediment flux studies are a function of both the rate of erosion in a catchment and the efficiency with which the sediment is transported to the lake (i.e. the sediment delivery ratio). In an attempt to

relate sediment flux to sediment erosion in the Semer Water, Gormire and Hornsea Mere catchments the sediment delivery ratio of the A.S.C.E. (1975) has been employed (Table 9.3);

$SDR = 0.36A^{-0.2}$, where A is catchment area km^2 (Section 2.3.1)

Table 9.3 A comparison of lake sediment yields and erosion rates using both the Barlow sediment delivery ratio and the American A.S.C.E sediment delivery ratio at each of Semer Water, Gormire and Hornsea Mere.

	Lake sediment yield estimate ($t\ km^{-2}\ a^{-1}$)	Erosion rate using A.S.C.E. SDR ($t\ km^{-2}\ a^{-1}$)
Semer Water		
1950-1994 AD	6.3	47
0-10000 BP	28	136
Gormire		
1949-1994 AD	78	94
1889-1949 AD	39	63
1630-1889 AD	35	46
7500-0 BP	11	10
11000-7500 BP	7	4
Hornsea Mere		
1979-1994 AD	41	255
1963-1979 AD	52	440
1730-1963 AD	12	52

Estimates of erosion for each of Semer Water, Gormire and Hornsea Mere, obtained by combining lake sediment yield estimates with a sediment delivery ratio, compare much more closely with mean soil erosion estimates in Britain summarised by Morgan (1995, Table 1):

Natural conditions	Cultivated land	Bare soil
10 - 50 $t\ km^{-2}\ a^{-1}$	10 - 200 $t\ km^{-2}\ a^{-1}$	100 - 2000 $t\ km^{-2}\ a^{-1}$

By virtue of the large catchment area at Hornsea Mere the sediment delivery ratio is low and hence the already high sediment yields in the post 1963 period at Hornsea Mere translate into exceptionally large rates of erosion. Although high rates of erosion in the Hornsea Mere catchment are not particularly surprising given that it is dominated by arable land, and hence the land is likely to be highly susceptible to topsoil erosion especially when bare. As for Hornsea Mere the large catchment area at Semer Water results in a low predicted sediment delivery ratio and hence predicted mean rates of erosion during the Holocene period at Semer Water are exceptionally high (Table 9.3).

9.5 Sediment Flux Modelling

9.5.1 The Universal Soil Loss Equation

The Universal Soil Loss Equation (USLE) is the most widely used soil erosion model available, and remains one of the simplest to use. However this study has illustrated that estimates of sediment erosion determined for British catchments using the USLE tend to be considerably greater than those from the lake sediment studies. The USLE only estimates surface sheet erosion, it does not include gully or channel erosion and consequently it might be expected to underestimate erosion. One of the major limitations of the USLE is that it was designed for small plot studies rather than lake catchments, consequently the slope length factor term was not designed to accommodate the downhill slope lengths observed in catchments. Indeed Hickey *et al.* (1994) state that '....the largest problem in using the USLE' has been the calculation of the cumulative downhill slope length factor.

In summary it is difficult to ascertain whether the high USLE flux estimates result from (i) overestimates of sediment erosion obtained using the USLE, or (ii) underestimates of the sediment delivery ratio.

Turning to other parts of the world a variety of studies employing the USLE to estimate soil erosion have found the USLE determined erosion rate are higher that those obtained using other techniques. For exampe Busaca *et al.* (1993) compared estimates of erosion in an agricultural watershed in Idaho, America using the Revised Universal Soil Loss Equation (RUSLE) with estimates determined using ^{137}Cs as a sediment tracer. They found that the RUSLE significantly overestimated erosion. Similarly Harden (1993), working on an agricultural drainage basin in Andean Ecuador, noted that upland soil erosion estimates determined using the USLE were consistently higher than estimates extrapolated from rainfall simulation experiments. Kusumandari and Mitchell (1997) compared rates of erosion determined using the USLE with those determined using the Agricultural Non-Point Source Pollution (AGNPS) model in a forested basin in West Java, Indonesia. The rate of erosion determined using the AGNPS model was found to be about half that predicted by the USLE. All these results further suggest that rates of erosion predicted using the USLE in UK catchments may be too high.

9.5.2 Sediment Delivery Ratios

Semer Water

In order to test how realistic the delivery ratios determined for Semer Water are, the theoretical volume of material stored in sediment sinks in the catchment can be calculated. By combining the predicted sediment delivery ratio with the volume of sediment observed in the Raydale and Semer Water deposits an estimate of the volume of sediment stored within the catchment can be obtained. The sediment volume can be converted into a mean sediment thickness over the whole of the catchment (Table 9.4),

Table 9.4 Theoretical volume of sediment stored within the Semer Water catchment.

	Sediment volume in Raydale (m^3)	Volume of sediment in sediment sinks using A.S.C.E SDR (m^3)	Mean sediment thickness over entire catchment using the A.S.C.E. SDR (m)
Semer Water	8800000	52000000	1.2

Using the delivery ratio of the American A.S.C.E eroded sediment which has been deposited elsewhere in the catchment before reaching the Raydale and Semer Water deposits would constitute a mean sediment thickness of 1.2 metres over the entire Semer Water catchment. It seems impossible that between 1 and 2 metres of sediment could overlay the entirety of the Semer Water catchment. Semer Water lies in a fairly steep catchment and although there are some areas where sediment accumulation may occur, it seems highly improbable that these are sufficient to result in mean sediment thickness of between 1 and 2 metres over the entire catchment. This would appear to be very unreaslistic, and thus either (i) significant quantities of sediment are being lost through the outflow, or (ii) the sediment delivery ratios underestimate the proportion of sediment entering into the lake. In order to test the first hypothesis suspended sediment concentrations could be monitored at the inflow and outflow. Monitoring would have to take place over a reasonable length of time and must include monitoring during storm events. Wass (1996) reports that 89% of the annual suspended sediment flux determined at Westwick on the Ure during the year October 1994 to September 1995 occurred during December 1994 and January 1995. Consequently sediment flux should be monitored over a period of at least one year.

Gormire

At Gormire steep slopes drain almost exclusively straight into the lake and thus there is virtually no scope for sediment storage. Delivery ratios of 0.46 and 0.57 determined using the American A.S.C.E. sediment delivery equation and that

calculated in Section 8.3 would appear to be unrealistic, a value of nearer 1 is deemed more suitable. On balance it seems highly probable that the sediment delivery ratios determined using the A.S.C.E. equation underestimates sediment delivery.

Future studies could use a combination of gouge cores transects and resistivity surveys at Semer in an attempt to map the extent of sediment sinks within the catchment. At Gormire, gouge core transects over the area immediately surrounding the lake, and in the two small fields which fall within the catchment, could be employed to assess the depth of sediments deposited. The Gormire catchment may also be an ideal catchment in which to use ^{137}Cs to trace sediment movement and thus determine a sediment delivery ratio, since the catchment is extremely small, the boundary very well defined and there is no outflow.

I conclude that (i) the USLE estimates of sediment erosion within each catchment are too great and, (ii) the sediment delivery ratios are too small. Sediment delivery remains as an extremely complex and limiting factor in relating lake sediment fluxes to erosion rates in catchments. Whilst lake sediment flux estimates are an ideal way of determining the mass of material reaching a given point, insufficient data on rates of erosion in British catchments prevents the determination of more accurate estimates of sediment delivery. Consequently any attempts to develop our understanding of the factors which influence the delivery ratio, and quantify the importance of different factors, are limited.

9.5.3 A Sediment Delivery Model

Simpler models, which can be more readily and easily applied to catchments, are very desirable. Such models enable the identification of catchments where further more detailed studies may be warranted in order to test hypothesis relating for

example sediment delivery to slope lengths or gradients. The models linking sediment flux to various physical catchment characteristics constructed in Section 8.2 do not require the addition of sediment delivery ratio, thus avoiding additional uncertainties in selecting an appropriate value. The regression models developed in Section 8.2 represent the first attempt to devise a model of sediment flux in British catchments on the basis of physical land use and catchment characteristics that can be readily obtained or determined. The optimum regression equation determined relates sediment flux to the log of catchment area, catchment soil erosion susceptibility and a slope length factor. The regression equation has an R^2 value of 79%. The model thus indicates that the log of catchment area is more strongly related to sediment flux than catchment area alone, presumably becuase it incorporates a measure of sediment storage in catchments. The slope length factor is similarly related to the size of the catchment and thus is strongly related to sediment flux. The model indicates that the soil type within a catchment has a significant impact on its tendency to erode. The fact that other catchment variables have not been selected by the stepwise regression procedure for incorporation into the model does not preclude their potential influence on sediment flux, but rather indicates that they play a less significant role in determining the extent of sediment flux within British catchments. Using the USLE to estimate sediment flux in each catchment, combined with the A.S.C.E. (1975) sediment delivery ratio, the R^2 value is only 34%. Therefore the regression model developed in this thesis represents a considerable improvement in estimating sediment flux to catchments in Britain. The lake and reservoir determined sediment fluxes used to develop the regression model are averages over time periods over a minumum of one hundred and fifty years and therefore the problems associated with short term sediment flux variability, encountered using river flux estimates, are avoided.

The model has potential to be employed in the water industry to estimate reservoir infilling rates which are critically important with regard to the operation and lifetime of the reservoir. Such models could also be employed to estimate the soil and nutrient load associated with sediment flux to a particular site, whether it be a river, lake or

reservoir. The modelling approach is considerably less time consuming and cheaper than undertaking lake or reserovoir studies using coring or reservoir survey techniques. The regression models developed could also be used to direct future lake and reservoir sediment studies. Using the predicted sediment flux at a given site hypotheses could be tested for example where modelling indicates that the flux is notably small or large lake sediment studies could be used to confirm or disprove this and attempts made to quantify the storage of sediment in a catchment in an attempt to improve our understanding of the links between sediment flux and rates of erosion.

9.6 Sediment Flux to the Humber Estuary

As a component of the NERC Land Ocean Interaction Study one of the initial aims of this project was to determine an estimate of the flux of sediment into the Humber. It should be noted however that the potential problems of extrapolating data for a few small areas to a considerably larger catchment results in significant potential errors. The most likely source of error arises from the difficulties in determining the sediment delivery ratio.

Using the American A.S.C.E. (1975) $SDR = 0.36A^{-0.2}$ where A is catchment area in km^2 and taking the Humber catchment area as 24240 km^2 (A. Parkes, pers.comm.), the sediment delivery ratio to the Humber is found to be 0.048. Four methods have been employed to estimate the annual flux of sediment to the Humber estuary and are described below.

Method 1: Small Reservoirs and Lakes

A mean sediment yield from published and unpublished reservoir and lake sediment studies undertaken on sites within the Humber catchment has been used. Using just those sites with a small catchment area, of less than 3 km^2 a sediment delivery of 1

assumed (Table 9.5). The mean sediment yield determined can then be multiplied by the area of the Humber catchment and coupled to a sediment delivery ratio.

Table 9.5 Sediment yield estimates from small lake and reservoirs catchments in the Humber catchment.

Site	Catchment area (km^2)	Sediment yield ($t\ km^{-2}\ a^{-1}$)
Gormire	0.35	51
Chew	2.92	78.5
Deanhead	2	33.7
Gorpley	2.8	129.1
Mixenden	0.77	9.5
Snailsden	0.84	260.2
Mean		**93.7**

The mean sediment yield at six lake and reservoir sites within the Humber catchment is 93.7 $t\ km^{-2}\ a^{-1}$. When multiplied by the Humber catchment area and combined a sediment delivery ratio of 4.8% the flux of sediment into the Humber is estimated to be 109000 $t\ a^{-1}$.

Method 2: Semer Water and Gormire Sediment Yield Estimates

An average sediment yield determined for each of Gormire and Semer Water of 30 $t\ km^{-2}\ a^{-1}$ has been used as a representative sediment yield for the Humber catchment. At Gormire the storage of sediment within the catchment is believed to be minimal, and thus a sediment delivery ratio of one has been assumed. At Semer Water a delivery ratio of 0.5 has been estimated in preference to the figure of 0.17 determined from the relationship of the American A.S.C.E. (1975). The mean sediment yield of 30 $t\ km^{-2}\ a^{-1}$ has been multiplied by the area of the Humber catchment and a sediment delivery ratio of 4.8% and used to determine a mass of 35000 tonnes of sediment which enters the Humber estuary each year. Estimates of sediment yield for Hornsea Mere have not been included in calculating a mean sediment yield for the Humber catchment using this method because it is a large, low

lying catchment where the sediment storage is likely to be significant and hence the delivery ratio is likely to be low.

Method 3: Universal Soil Loss Equation

A mean USLE estimate of sediment yield of 573 t km^{-2} a^{-1} has been determined from USLE estimates at each of 15 sites that lie in the Humber catchment. This sediment delivery has been multiplied by the Humber catchment area and a sediment delivery ratio of 0.048 to produce an estimated flux of sediment into the Humber estuary from the Humber catchment of 667000 t a^{-1}.

Method 4 Simple Regression Model

The model linking sediment flux to the log of catchment area, determined in Section 8.3 has been employed. Using the equation

Flux = 40.2 + 378(log of catchment area)

sediment flux to the Humber estuary is estimated to be 1700 t a^{-1}.

Table 9.6 Estimated sediment flux to the Humber and a comparison with values of G.Leeks and P.Wass (pers.comm) and J.Hardisty (pers.comm).

Method	Sediment influx into Humber (t a^{-1})
Reservoirs/lake sediment studies in the Humber catchment	109000
Semer Water/Gormire sediment yields	35000
USLE	667000
Regression model using catchment area	1700
Leeks and Wass estimate	177000
Hardisty estimate	300000

9.7 Summary

The USLE estimate of sediment flux to the Humber is discarded, as discussed in Section 9.4 the USLE appears to overestimate sediment flux considerably. Method 4, using the log of catchment area model results in what appear to be unrealistically low estimates of sediment flux. This very simple model is based on catchments considerably smaller in size (up to 60 km^2) than the Humber catchment (24240 km^2) and thus it is not appropriate to apply this model over such a large area. Using the estimates of sediment flux obtained from the mean yields at six lake and reservoir sites in the Humber catchment and the mean yields from Semer Water and Gormire in the period post 1950 AD the flux of sediment to the Humber estuary is estimated to be between 40 000 and 110 000 t a^{-1}. These flux estimates are slightly lower than estimates of sediment flux to the Humber proposed by Leeks and Wass (pers.comm) and Hardisty (pers.comm). of between 170 000 and 300 000 t a^{-1}. Hardisty and Rouse (1995) report that each flood and ebb tide transports 80-160 and 90-160 x 10^3 tonnes of sedment respectively. In comparison to the mass of material transported by each flood and ebb tide the mass of material entering the Humber estuary from the Humber catchment represents an insignificant sediment source.

I conclude that it is very difficult to use sediment flux estimates in a few small catchments to estimate the flux of sediment on a much larger scale, for example to the Humber. I believe that estimating the significance of sediment storage, and thus an appropriate sediment delivery ratio, is the single most limiting factor. However the estimated sediment flux to the Humber, obtained using mean sediment yields at Semer Water and Gormire, is comparable with fluvial estimates of suspended sediment from rivers in the Humber catchment (Wass 1986) and likely to provide a more accurate longer term average than those obtained from fluvial suspended sediment concentrations over time periods of just a few years.

Chapter 10

Conclusions

1) In lake studies of sediment flux it is important to investigate areas outwith the present day lake area as they may contain significant quantities of eroded sediment.

2) At Semer Water changes in sediment yield through the Holocene imply that a significant decrease in erosion has occurred in the most recent period. A mean Holocene sediment yield of 28 t km^{-2} a^{-1} has been found at Semer Water.

3) At Gormire sediment yields have increased from 35 t km^{-2} a^{-1} to 78 t km^{-2} a^{-1} in the period since 1640.

4) Sediment yields of between 12 and 52 t km^{-2} a^{-1} have been determined at Hornsea Mere since 1730. The highest sediment yields occur during the period 1963-1979.

5) Bacterial magnetosomes can contribute significantly to the magnetic signature in upland and lowland sites in northern Britain. They are found in the finest grain sediments and have distinctive high ARM/SIRM and ARM/χ ratios.

6) A strong relationship (R^2 = 80%) has been found between sediment flux and catchment area, catchment soil erosion susceptibility and a slope length factor for 30 British sites.

7) The sediment delivery ratio remains one of the most poorly understood and quantified concepts in studies of sediment erosion.

8) Sediment flux to the Humber estuary from the Humber catchment is estimated to be between 40 000 and 110 000 t a^{-1}.

Bibliography

A.S.C.E. (American Society of Civil Engineering), 1975. Sedimentation engineering. Am. Soc. Civ. Eng., New York. Manuals and reports on engineering practises, No. 54.

Aaby, B. and Berglund, B.E. (1986) Characterization of peat and lake deposits. Chapter 12 in *Handbook of Holocene Palaeoecology and Palaeohydrology* (B.E.Berglund, ed.). London: John Wiley and Sons Ltd. 231-246.

Al-Ansari, N.A., Al-Jabbari, Al., McManus, J. (1977) The effect of farming upon solid transport in the River Almond, Scotland. *Int. Assoc. Hydrol. Sci. Publ.* **122**, 118-125.

Anderson and Rippey (1988). Diagenesis of magnetic minerals in the recent sediments of a eutrophic lake. *Limnology and Oceanography*, **33**, 1476-1492.

Anderson, N.J., Patrick, S.T., Appleby, P.G., Oldfield, F. Rippey, B., Richardson, N., Darley, J. and Battarbee, R.W. (1988). An Assessment of the use of Reservoir Sediments in the Southern Pennines for Reconstructing the History and Effects of Atmospheric Pollution. Working Papers No. 30. Palaeoecology Research Unit, Department of Geography, University College London, 26 Bedford Way, London WC1H OAP.

Appleby, P. (1998) Radiometric dating of sediment cores from Gormire, Semer Water and Hornsea Mere (HULAP project). Unpubl. report.

Appleby, P.G. and Oldfield, F. (1978) The calculation of lead-210 dates assuming a constant supply of unsupported ^{210}Pb to the sediment. *Catena*, **5**, 1-8.

Appleby, P.G. and Oldfield, F. (1984) A combined radiometric and mineral magnetic approach to recent geochronology in lakes affected by catchment disturbance and sediment redistribution. *Chemical Geology*, **44**, 67-83.

Avery, B.W. (1990) *Soils of the British Isles*. CAB International, Wallingford.

Barlow, D. (1994) Eutrophication in a small upland lake: The case of Semer Water. Unpubl. B.Sc thesis. University of Plymouth.

Barrow, C.J. (1991) *Land Degradation*. Cambridge University Press, Cambridge.

Battarbee, R.W. (1978) Observations on the recent history of Lough Neagh and its drainage basin. *Phil. Trans. R. Soc. Lond. B* **281**, 303-345.

Beckett, S. (1981) Pollen diagrams from Holderness, North Humberside. *Journal of Biogeography* **8**, 177-198.

Bengtsson, L and Enell, M. (1981) Chemical analysis. Chapter 21 in *Handbook of Holocene Palaeoecology and Palaeohydrology* (B.E.Berglund, ed.). London: John Wiley and Sons Ltd. 231-246.

Bennett, H.H. (1939) *Soil Conservation*. New York, McGraw-Hill.

Birks, H.J.B (1989) Holocene isochrone maps and patterns of tree-spreading in the British Isles. *Journal of Biogeography* **16**, 503-540.

Blackham, A., Davies, C. and Flenley, J. (1981) *Evidence for Late Devensian Landslipping and Late Flandrian Forest Regeneration at Gormire Lake, North Yorkshire.* In Essays, reviews and original work on the Quaternary (J.Neale and J.Flenley eds.). Pergamon Press.

Blakemore, R. (1975) Magnetotactic Bacteria. *Science* **190**, 377-379.

Bloemendal, J. (1982) The quantification of rates of total sediment influx to Llyn Goddionduon, Gwynedd. Unpubl. PhD thesis. University of Liverpool.

Bloemendal, J., Oldfield, F. and Thompson, R. (1979) Magnetic measurements used to assess sediment influx at Llyn Goddionduon. *Nature* **280**, 50 -53.

Borman, F.H. and Likens, G.E. (1969) The watershed-ecosystem concept and studies of nutrient cycles. *The ecosystem concept in natural resource management.* G.M. Van Dyne (ed).

Boyce, R.C. (1975) Sediment routing with sediment delivery ratios, in present and prospective technology for predicting sediment yields and sources. USDA Agriculture Research Service, publication ARS-S40, 61-65.

Brown, C.B. (1948) Perspectives on sedimentation-purpose of conference. In*: Proceedings of the First Federal Interagency Sedimentation Conference.* U.S. Dep. Inter., Bur. Reclam.

Brune, G.M. (1950) The dynamic concept of sediment sources. *Trans. Am. Geophys. Union* **31** (4), 587-594.

Busacca, A.J., Cook, C.A. and Mulla, D.J. (1993) Comparing landscape-scale estimation of soil-erosion in the Palouse using Cs-137 and RUSLE. *J. Soil and Water Conservation* **48** (4) 361-367.

Butcher, D.P, Labadz, J.C., Potter, A.W.R. and White, P. (1993). Reservoir Sedimentation Rates in the Southern Pennine Region, UK. Chapter 6 *in Geomorphology and Sedimentology of Lakes and Reservoirs* (J. McManus and Duck,R.W eds.). John Wiley & Sons Ltd. 73-92.

Canfield, D.E. and Berner, R.A. (1987) Dissolution and pyritisation of magnetite in anoxic marine sediment. *Geochemica et Cosmicha Acta* **51**, 645-659.

Chikazumi, (1964) *Physics of Magnetism*, Wiley, New York.

Cisowski, S. (1981) Interacting vs. Non-interacting single-domain behaviour in natural and synthetic samples. *Phys. Earth Planet. Inter.* **26**, 77-83.

Collinson, D.W. (1968). An Estimate of the Haematite Content of Sediment by Magnetic Analysis. *Earth and Planet. Sci. Lett.* **4**, 417-421.

Crick, M.I. (1985). Investigation into the relationship between sediment accumulation in the Lower Ley, Slapton, and spatial patterns of erosion within its catchment, using magnetic measurements. Unpublished BSc dissertation, Plymouth Polytechnic.

Cummins, W.A. and Potter, H.R. (1972) Rate of erosion in the catchment area of Cropston reservoir, Charnwood Forest, Leicestershire. *Mercian Geologist*, **6** 149-157.

Davis, M.B. (1976) Erosion Rates and Land-use History in Southern Michigan. *Environmental Conservation* **3** (2), 139-148.

Davis, M.B. and Ford, M.S. (1982). Sediment focusing in Mirror Lake, New Hampshire. *Limnol. Oceanogr.*, **27** (1), 137-150.

Dearing, J.A. (1979) The applications of magnetic measurements to studies of particulare flux in lake-watershed ecosystems. Unpubl. PhD thesis. University of Liverpool.

Dearing, J.A. (1986). Core correlation and total sediment influx. Chapter 13 *in Handbook of Holocene Palaeoecology and Palaeohydrology* (B.E. Berglund ed.) London: John Wiley & Sons Ltd. 247-270.

Dearing, J.A. (1992). Sediment Yields and Sources in a Welsh Upland Lake-Catchment During the Past 800 Years. *Earth Surface Processes and Landforms* **17**, 1-22.

Dearing, J.A., Elner, J.K. and Happey-Wood, C.M. (1981) Recent Sediment Flux and Erosional Processes in a Welsh Upland Lake-catchment Based on Magnetic Susceptibility Measurements. *Quaternary Research* **16**, 356-372.

Dearing, J.A. and Flower, R.J. (1982) The magnetic susceptibility of sedimenting material trapped in Lough Neagh, Northern Ireland, and its erosional significance. *Limnol. Oceanogr.* **27** (5), 969-975.

Dearing, J.A. and Foster, I.D.L (1986) Lake sediments and palaeohydrological studies. Chapter 2 in *Handbook of Holocene Palaeoecology and Palaeohydrology* (B.E. Berglund ed.) London: John Wiley & Sons Ltd. 247-270.

Dearing, J.A., Alström, Bergman, A, Regnell, J and Sandgren, P. (1990) Recent and Long-term Records of Soil Erosion From Southern Sweden. Chapter 12 in *Soil Erosion on Agricultural Land*, (J.Boardman, I.D.L. Foster and J.A. Dearing, eds.). London: John Wiley & Sons Ltd. 173-191.

Dearing, J.A. and Foster, I.D.L. (1993) Lake Sediments and Geomorphological Processes: Some Thoughts. Chapter 2 in *Geomorphology and Sedimentology of Lakes and Reservoirs*, (J.McManus and R.W. Duck eds.). London: John Wiley & Sons Ltd.

Dickinson, W.T. , Wall, G.L and Rudra, R.P. (1990) Model building for predicting and managing soil erosion and transport. Chapter 27 in *Soil Erosion on Agricultural Land*, (J.Boardman, I.D.L. Foster and J.A. Dearing, eds.). London: John Wiley & Sons.

Douglas, I. (1967) Man, vegetation and the sediment yields of rivers, *Nature* **215**, 25-28.

Duck, R.W. and McManus, J. (1985) Sediment yield estimated from reservoir siltation in the Ochil Hills, Scotland. *Earth Surface Processes and Landforms* **10**, 193-200.

Duck, R.W. and McManus, J. (1987) Sediment yields in lowland Scotland derived from reservoir surveys, *Trans Royal Soc Edinburgh; Earth Sciences* **78**, 369-377.

Duck, R.W. and McManus, J. (1990). Relationships between Catchment Characteristics, Land Use and Sediment Yield in the Midland Valley of Scotland. Chapter 18 in *Soil Erosion on Agricultural Land*, (J.Boardman, I.D.L. Foster and J.A. Dearing, eds.). London: John Wiley & Sons Ltd.

Dunlop, D.J. (1972). Magnetic Mineralogy of Unheated and Heated Red Sediments by Coercivity Spectrum Analysis. *Geophys. J. R. Astr. Soc.* **27**. 37-55.

Dunlop, D.J. (1986) Coercive forces and coercivity spectra of submicron magnetites, *Earth Planet. Sci. Lett.* **78**, 288-295.

Edwards, K.J. and Rowntree, K.M. (1980) Radiocarbon and palaeoenvironmental evidence for changing rates of erosion at a Flandrian stage site in Scotland in *Timescales in geomorphology*, (R.A. Cullingford, D.A. Davison and J.Lewis eds.).

Ferguson, R.I. and Stott, T.A. (1987) Forestry effects on suspended sediment and bedload yields in the Balquhidder catchments, Central Scotland. *Trans. Royal Soc. Edin.: Earth Sciences*, **78,** 379-384.

Findlay, D.C., Colborne, G.J.W., Cope, D.W. Harrod. T.R., Hogan, D.V. and Staines, S.J. (1984) Soils and their use in South West England. Soil Survey of England and Wales, Bulletin no 14. London: Harpenden.

Finlayson, B.L. (1977). Runoff contributing areas and erosion. Res. Paper 18, School of Geography, University of Oxford.

Flaxman, E.M. and Hobba, R.L. (1955) Some factors affecting rates of sedimentation in the Columbia River basin. *Trans. Am. Geophys. Union*. **38**(2), 293-303.

Fleming, G.,(1969) Sediment Balance of the Clyde Estuary. *Proceedings of the American Society of Civil Engineers, Hydraulics Division 96*, HY11, 2219-2230.

Flower, R.J., Battarbee, R.W., and Appleby, P.G. (1987) The recent palaeolimnology of six acid lakes in Galloway, south-west Scotland. Diatom analysis, pH trends, and the role of afforestation. *Journal of Ecology* **75**, 797-824.

Folk, R.L. (1974) *Petrology of sedimentary rocks*. Austin, Texas: Hemphill Publishing Company.

Foster, G.R. (1982) Modeling the erosion process in *Hydrologic Modeling of Small Watersheds* (C.T. Hann, H.P. Johnson and D.L. Brakensiek eds.). Amer. Soc. of Agric. Engr., St Joseph, Michigan, 297-382.

Foster, I.D.L, Dearing, J.A., Simpson, A.D. and Appleby, P.G. (1985) Lake catchment based studies of erosion and denudation in the Merevale catchment, Warwickshire, UK. *Earth Surface Processes and Landforms* **10,** 45-68.

Foster, I.D.L., Dearing, J.A. and Appleby, P.G. (1986) Historical trends in catchment sediment yields: a case study in reconstruction from lake-sediment records in Warwickshire, UK. *Hydrological Sciences-Journal-des Sciences Hydrologiques* **31** (3), 427-443.

Foster, I.D.L, Dearing, J.A. and Grew, R. (1988). Lake-catchments: an evaluation of their contribution to studies of sediment yield and delivery processes. Sediment Budgets (Proceedings of the Porto Alegre Symposium, December 1988). *IAHS Publication* **174**, 1988.

Foster, I., Grew, R. and Dearing, J. (1990A) Magnitude and Frequency of Sediment Transport in Agricultural Catchments: A Paired Lake-catchment Study in Midland England. Chapter 11 in *Soil Erosion on Agricultural Land*, (J.Boardman, I.D.L. Foster and J.A. Dearing, eds.). London: John Wiley & Sons Ltd. 153-171.

Foster, I.D.L., Dearing, J.A., Grew, R. and Orend. K. (1990B). The sedimentary data base: an appraisal of lake and reservoir sediment based studies of sediment yield. Erosion, Transport and Deposition Processes (Proceedings of the Jerusalem Workshop, March-April 1987). *IAHS Publication* **189**, 19-43

Foster, I.D.L. and Walling, D.E. (1994). Using reservoir deposits to reconstruct changing sediment yields and sources in the catchment of the Old Mill Reservoir, South Devon, UK, over the past 50 years. *Hydrological Sciences-Journal-des Sciences Hydrologiques* **39**, (4) 347-368.

Fournier, F. (1960) *Climat et érosion: la relation entre l'érosion du sol par l'eau et les précipitations atmosphériques*. Paris: Presses Universitaires France.

Francis, I..S. (1990). Blanket peat erosion in a mid-Wales catchment during two drought years. *Earth Surface Processes and Landforms* **12**, 95-104.

Frankel, R.B., Blakemore, R.P. and Wolfe, R.S. (1979) Magnetite in Freshwater Magnetotactic Bacteria. *Science* **203**, 1355-1356.

Gavish, E. and Friedman, G.M (1973) Quantitative analysis of calcite and Mg-calcite by X-ray diffraction: effect of grinding on peak height and peak area. *Sedimentology* **20**, 437-444.

Geikie, A. (1868). On Denudation Now in Progress. *The Geological Magazine* **V** (XLVIII), 249-254.

Goudie, A. (1995) *The Changing Earth*. Oxford: Blackwell.

Gregory, K.J. and Walling, D.E. (1973) *Drainage basin form and process*. London: Edward Arnold.

Haan, C.T. , Barfield, B.J. and Hayes, J.C. (1994) *Design Hydrology and Sedimentology for Small Catchments*. London: Academic Press

Hall, D.G. (1967) The pattern of sediment movement in the River Tyne. *Int. Assoc. Sci. Hydrol.* **75**, 117-142.

Harden, C.P. (1993) Upland erosion and sediment yield in a large Andean drainage basin. *Physical Geography* **14** (3), 254-271.

Hardisty, J. and Rouse, H.L. (1995). The Humber Observatory: Monitoring, modelling and management for the coastal environment. *J. Coastal Research* **12** (3) 683-690.

Harvey, A.M., Oldfield, F. and Baron, A.F. (1981), Dating of post-glacial landforms in the central Howgills. *Earth Surface Processes and Landforms* **6**, 401-412.

Hickey, R., Smith, A. and Jankowski, P. (1994) Slope length calculations from a DEM within ARC/INFO grid. *Computers, environment and urban systems* **18** (5) 365-380.

Higgitt, S.E. (1985) The palaeoecology of the Lac d'Annecy and its drainage basin. Unpubl. PhD thesis. University of Liverpool.

Higgitt, S.R., Oldfield, F. and Appleby, P.G. (1991). The record of land use changes and soil erosion in the Late Holocene sediments of the Petit Lac d'Annecy, eastern France. *The Holocene* **1** (1), 14-28.

Hilton, J. (1990). Greigite and the magnetic properties of sediments. *Limnol. Oceanogr.* **35**, 497-508.

Hilton, J and Lishman, J.P. (1985) The effect of redox change on the magnetic susceptibility of sediments from a seasonally anoxic lake. *Limnol. Oceanogr.* **30**, 907-909.

Hilton, J., Lishman, J.P. and Allen, P.V. (1986). The dominant processes of sediment distribution and focusing in a small, eutrophic, monomictic lake. *Limnol.Oceanogr.* **31**, 125-133.

HMSO (1954). *British Regional Geology: The Pennines and Adjacent areas*. 3rd Edition London: HMSO.

Hutchinson, S. M. (1995). Use of Magnetic and Radiometric Measurements to Investigate Erosion and Sedimentation in a British Upland Catchment. *Earth Surface Processes and Landforms* **20**, 293-314.

Imeson, A.S.(1970) Variation in sediment production from three East Yorkshire catchments. In *The role of water in agriculture* (J.A. Taylor ed.), 39-56. Oxford: Pergamon Press.

Jackson, W.L., Gebhardt, K. and Van Haveren, B.P (1986) Use of the Modified Universal Soil Loss Equation for average annual sediment yield estimates on small rangeland drainage basins. In: Drainage basin sediment delivery, (Proceedings of the International Symposium on Sediment Delivery, Albuquerque, New Mexico, August 1986). *IAHS Publication* **159**. 413-422.

Jarvis, R.A., Bendelow, V.C., Bradley, R.I., Furness, D.M., Kilgour, I.N.L. and King, S.J. (1984). *Soils and their Use in Northern England.* Soil Survey of England and Wales, Bulletin No 10. London: Harpenden.

Jiles, D. (1991) Introduction to magnetism and magnetic materials, Chapman and Hall.
Karlin, R. and Levi, S. (1983) Diagenesis of magnetic minerals in recent haemipelagic sediments. *Nature* **203** (5915), 327-330.

Kearey, P and Brooks, M. (1984) *An introduction to geophysical exploration.* London: Blackwell

Kendall, P.F. and Wroot, H.E. (1924) Geology of Yorkshire. Reprint, 1972, Menston, Yorks.

Kerfoot, W.C. (1974) Net accumulation rates and the history of cladoceran communities. *Ecology* **55**, 51-61.

Kirkby, M.J. (1967) Measurements and theory of soil creep. *The Journal of Geology* **75** (4) 359-378.

Kusumandari, A. and Mitchell, B. (1997) Soil erosion and sediment yield in forest and agroforestry areas in West Java, Indonesia. *J. Soil and Water Conservation* (**52**) 5 376-380.

Labadz, J.C. (1988) Run-off and sediment production in blanket peat moorland: studies in the southern Pennines. Unpubl. PhD thesis, Huddersfield Polytechnic.

Labadz, J.C., Burt, T.P and Potter, A.W.R. (1991) Sediment yield and delivery in the blanket peat moorlands of the southern Pennines. *Earth Surface Processes and Landforms* **16**, 255-271.

Langbein, W.B. and Schumm, S.A. (1958) Yield of sediment in relation to mean annual precipitation. *Trans. Am. Geophys. Union* **39**, 1076-1084.

Le Borgne, E. (1955) Susceptibilité Magnétique Anormale Du Sol Superficiel. *Ann. Geophys.* **11**, 399-419.

Le Borgne, E. (1960) Influence du feu sur les propriétés magnétiques du sol et du granite. *Ann. Geophys.* **16**, 159-195.

Ledger, D.C. , Lovell, J.P.B and McDonald, A.T. (1974) Sediment Yield Studies in Upland Catchment Areas in South-East Scotland. *J. Appl. Ecol.* **11,** 201-206.

Ledger, D.C., Lovell, J.P.B. and Cuttle, S.P. (1980) Rate of sedimentation in Kelly Reservoir, Strathclyde. *Scot. J. Geol.* **16**, 281-285.

Lewin, J. (1981) (Ed.). *British Rivers.* London: Goerge, Allen & Unwin.

Likens, G.E and Davis, M.B. (1975) Post-glacial history of Mirror Lake and its watershed in New Hampshire, U.S.A.:an initial report. *Verhandlungen der International Vereinigung für Theoretische und Angewandte Limnologie*, **19**, 982-993.

Loughran, R.J., Campbell, B.J. and Wallind, D.E. (1987) Soil erosion and sedimentation indicated by caesium-137: Jackmoor Brook catchment, Devon, England. *Catena* **14**, 201-212.

Lovell, J.P.B., Ledger, D.C., Davies, I.M. and Tipper, J.C. (1973) Rate of sedimentation in the North Esk Reservoir, Midlothian. *Scott. J. Geol* **9**, (1). 57-61.

Macaulay Institute for Soil Research, Aberdeen (1984) 1:250 000 Soil survey of Scotland maps, Sheets 5, 6 and 7.

Macaulay Institute for Soil Research, Aberdeen (1994) 1:250 000 Land use capability maps sheets 5, 6 and 7.

Mackereth (1958). A portable core sampler for lake deposits. *Limnol. Oceanogr.* **3**, 181-191.

Mackereth (1959). A short core sampler for subaqueous deposits. *Limnol. Oceanogr.* **14,** 145-151.

Mackereth (1971). On the variation in direction of the horizontal component of remanence magnetisation in lake sediments. *Earth Planet. Sci. Lett.* **12**, 332-338.

Maher (1988) Magnetic properties of some synthetic sub-micron magnetites. *Geophys. J.* **94**, 83-96.

McManus, J. (1986). Land-derived sediment and solute transport to the Forth and Tay estuaries, Scotland. *Journal of the Geological Society, London* **143,** 927-934.

McManus, J. and Duck, R.W. (1985). Sediment Yield Estimated from Reservoir Siltation in the Ochil Hills, Scotland. *Earth Surface Processes and Landforms* **10**, 193-200.

Meade, R.H. (1982). Sources, sinks and storage of river sediment in the Atlantic Drainage of the United States. *J. Geol.* **90**, 235-252.

Milson, J. (1996) *Field Geophysics*. John Wiley and Sons, London.

Ministry of Agriculture, Fisheries and Food (MAFF), (1977) Agricultural land classification in England and Wales, (1:250 000 maps), sheets 1-6.

Ministry of Agriculture, Fisheries and Food (MAFF), (1982). *Environment Matters: The Pennine Dales ESA: Guidelines for Farmers*. HMSO, London.

Moore, P.D., Webb, J.A. and Collinson, M.E. (1991) *Pollen Analysis*. 2nd edition. Oxford: Blackwell Scientific Publications.

Morgan, R.P.C. (1980). Soil erosion and conservation in Britain. *Progress in Physical Geography* **4**, 24-47.

Morgan, R.P.C. (1995) *Soil Erosion and conservation*. 2nd edition. Harlow: Longman Scientific and Technical.

Moore, R.J. and Newson, M.D. (1986) Production, storage and output of coarse upland sediments: natural and artificial influences as revealed by research catchment studies. *Journal of the Geological Society, London* **143**, 921-926.

Moskowitz, B., Frankel, R.B. and Bazylinski, D.A. (1993) Rock magnetic criteria for the detection of biogenic magnetite. *Earth and Planet. Sci. Lett.* **120** 283-300.

Mullins, C.E. (1977) Magnetic suceptibility of the soil and its significance in Soil Science: a review. *J. Soil Sci.* **28**, 223-246.

Mullins, C.E. and Tite, M.S. (1973). Magnetic Viscosity, Quadrature Susceptibility, and Frequency Dependance of Susceptibility in Single-Domain Assemblies of Magnetite and Maghemite. *Journal of Geophysical Research* **78**, (5). 804-809.

Myers, N. (1993) *Gaia: An Atlas of Planet Management* (Anchor and Doubleday: New York).

Nature Conservancy Council (1985) unpubl. Gormire SSSI designation notes.

NERC (1994) Land Ocean Interaction Study (LOIS). Implementation Plan for a Community Research Project. Natural Environment Research Council.

Newson, M.D. (1986) River basin engineering - fluvial geomorphology. *J. Inst. Wat. Eng. Scient.*, **40** (4) 307-324.

O'Neill, P. (1991) *Environmental Chemistry*. London: Chapman and Hall.

O'Reilly, W. (1984) *Rock and mineral magnetism*. Glasgow: Blackie.

O'Sullivan, P.E. (1979) The Ecosystem-watershed concept in the environmental sciences - a review. *J. Environ. Sci.* **13**, 273-281.

O'Sullivan, P.E., Oldfield, F. and Battarbee, R.W. (1973) Preliminary studies of Lough Neagh sediment. 1. Stratigraphy, chronology and pollen analysis. In *Quaternary Plant Ecology* (H.J.B. Birks and R.G.West eds.). Oxford: Blackwell.

O'Sullivan, P.E., Coard, M.A. and Pickering, D.A. (1982). The use of laminated sediments in the estimation and calibration of erosion rates. Recent Developments in the Explanation and Prediction of Erosion and Sediment Yield (Proceedings of the Exeter Symposium, July 1982). *IAHS Publication* **137**, 385-396.

Oldfield, F. (1977). Lakes and their drainage basins as units of sediment-based ecological study. *Progress in Physical Geography* **1,** 460-504.

Oldfield, F. (1990) Magnetic measurements of recent sediments from Big Moose Lake, Adirondack Mountains, N.Y., U.S.A. *J. Paleolimnol.*, **15** 529-553.

Oldfield, F. (1991) Environmental Magnetism - A Personal Perspective. *Quaternary Science Reviews* **10,** 73-85.

Oldfield, F. (1994). Toward the discrimination of fine-grained ferrimagnets by magnetic measurements in lake and near-shore marine sediments. *J. of Geophys. Res.* **99** (B5), 9045-9050.

Oldfield, F., Rummery, T.A., Thompson, R. and Wallind, D.E. (1979). Identification of Suspended Sediment Sources by Means of Magnetic Measurements: Some Preliminary Results. *Water Res. Res.* **15**, (2), 211-218.

Oldfield, F. and Maher, B. (1984) A mineral magnetic approach to erosion studies. In *Report of conference on Drainage Basin Erosion and Sedimentation*, Newcastle, N.S.W., Australia, May 1984.

Oldfield, F. and Richardson, N. (1990). Lake sediment magnetism and atmospheric deposition. *Phil. Trans. R. Soc. Lond. B* **327**, 325-330.

Omernik. J. and Griffith, G. (1991) Ecological regions versus hydrologic units: Frameworks for managing water quality. *J. Soil and Water Cons.* **Sept-Oct**, 334-340.

Owens, P.N. (1990) Valley sedimentation at Slapton, South Devon, and its implications for the estimation of lake sediment-based erosion rates. Chapter 13 in *Soil Erosion on Agricultural Land*, (J.Boardman, I.D.L. Foster and J.A. Dearing, eds.). London: John Wiley & Sons Ltd. 193-211.

Oxley, N.C. (1974) Suspended sediment delivery rates and solute concentration of stream discharge in two Welsh catchments. In *Inst. Br. Geogs Sp. Publ.* **6**, 141-153.

Parry, L.G. (1965). Magnetic Properties of Dispersed Magnetite Powders. *Philosophical Magazine* **11** (110) 303-312.

Peart, M.R. and Walling, D.E. (1982). Particle size characteristics of fluvial suspended sediment. Recent Developments in the Explanation and Prediction of Erosion and Sediment Yield (Proceedings of the Exeter Symposium, July 1982). *IAHS Publication* **137**, 397-407.

Peart, M.R. and Walling, D.E. (1988) Fingerprinting sediment source: The example of a drainage basin in Devon, UK. In R.F. Hadley (ed) Drainage Basin Sediment Delivery. *IAHS Publication* **159**, 41-55.

Peirson, D.H. and Salmon, L. (1959). Gamma-radiation from deposited fall-out. *Nature* **184**, 1678-1679.

Pennington, W. (1978) The impact of man on some English lakes: rates of change. *Polskie Archiwum Hydrobiologia* **25** (1/2), 429-437.

Pennington, W. (1981) Records of a lake's life in time: the sediments. *Hydrobiologia* **79**, 197-219.

Pennington, W. Cambray, R.S. and Harkness, D.D. (1976) Radionuclide dating of the recent sediments of Blelham Tarn. *Freshwater Biology* **6**, 317-331.

Penny, L.F. (1974). Quaternary. Chapter 9 In *The Geology and Mineral Resources of Yorkshire* (D.H. Rayner and J.E. Hemingway, eds.).

Peters, C. (1995). Unravelling magnetic mixtures in sediments, soils and rocks. Unpubl. Ph.D. Thesis. University of Edinburgh.

Pigott, C.D. and Pigott, M.E. (1963) Late-glacial and post-glacial deposits at Malham, Yorkshire. *New Phytologist* **62**, 317-334.

Pimental, D (1976) Land degradation: effects on food and energy resources. *Science* **194**, 149-155.

Pimentel, D. Harvey, C, Resosudarmo, P, Sinclair, K., Kurz, D., McNair, M., Crist, S., Shpritz, L., Fitton, L., Saffouri, R and Blair, R. (1995) Environmental and Economic Costs of Soil Erosion and Conservation Benefits. *Science* **267**, 1117-1123.

Radhakrishnamurty, C. Likhite, S.D., Amin, B.S. and Somayajulu, B.L.K. (1968) Magnetic susceptibility in ocean sediment cores. *Earth Planet. Sci. Lett.* **4**, 464-468.

Ragg, J.M. Beard, G.R., George, H., Heaven, F.W., Hollis, J.M., Jones, R.J.A., Palmer, R.C., Reeve, M.J., Robson, J.D. and Whitfield, W.A.P. (1984) *Soils and their use in Midland and Western England.* Soil Survey of England and Wales, Bulletin no 12. London: Harpenden.

Richardson, N. (1986) The mineral magnetic record in recent ombrotrophic peat synchronised by fine resolution pollen analysis. *Phys. of the Earth and Plan. Int.* **42**, 48-56.

Robinson, M and Blyth, K. (1982) The effect of forest drainage operations on upland sediment yields: a case study. *Earth Surface Processes and Landforms*, **7**, 85-90.

Rodda, J.C. (1970) Rainfall excesses in the United Kingdom. *Transaction of the British Geographers* **49**, 49-60.

Rodda, J.C. (1976) Systematic hydrology. London: Newnes-Butterworth.

Rudeforth, C.C., Hartnup, R., Lea, J.W., Thompson, T.R and Wright, P.S (1984) *Soils and their use in Wales*. Soil Survey of England and Wales, Bulletin no 11. London: Harpenden.

Sandgren, P. and Fredskild, B. Magnetic measurements recording Late Holocene man-induced erosion in S. Greenland. *Boreas* **20**, 315-331.

Schumm, S.A (1963) The disparity between present rates of denudation and orogeny. US Geological Survey Professional Paper, 454-H, 1-13.

Shankar, R., Thompson, R and Galloway, R.B. (1994) Sediment source modelling: Unmixing of artificial magnetisation and natural radioactivity measurements. *Earth and Plan. Sci. Lett.* **126**, 411-420.

Smith, C.T. (1969) The drainage basin as an historical basis for human activity. *In Introduction to Geographical Hydrology* (R. Chorley ed). Methuen and Co., London, Eng 20-29.

Snowball, I.F. (1993) Geochemical control of magnetiite dissolution in subarctic lake sediments and the implications for environmental magnetism. *Journal of Quaternary Science* **8** (4), 339-346.

Snowball, I.F. (1994). Bacterial magnetite and the magnetic properties of sediments in a Swedish lake. *Earth and Plan. Sci. Lett.* **126,** 129-142.

Snowball, I. and Thompson, R. (1988) The occurrence of Greigite in sediments from Loch Lomond, *Journal of Quaternary Science* **3** (2), 121-125.

Snowball, I. and Thompson, R. (1990) A mineral magnetic study of Holocene sedimentation in Lough Catherine, Northern Ireland. *Boreas* **19**, 127-146.

Snowball, I. and Thompson, R. (1992). A mineral magnetic study of Holocene sediment yields and deposition patterns in theLlyn Geirionydd catchment, north Wales. *The Holocene* **2** (3), 238-248.

Soil Survey of England and Wales (1983) Soil Survey maps (1:250 000), Sheets 1-6.

Speth, J.G. (1994) Towards an effective and operational international convention on desertification Internation Negotiating Committtee, Internation Convention on Desertification, United Nations, New York. New York: United Nations.

Squance, M.A. (1980) Survey of Lake Semerwater and adjacent Wetland Vegetation. Unpubl. internal report, Nature Conservancy Council.

Stott, A.P. (1985) Reservoir sedimentation and landuse change in N.W. England, Unpubl. PhD thesis, University of Manchester.

Stott, T.A., Ferguson, R.I., Johnson,R.C. and Newson, M.D. (1986) Sediment budgets in forested and unforested basins in upland Scotland (Hadley, R.F. ed.)., Drainage Basin Sediment Delivery, Proc symposium Albuquerque 1986. *IAHS Publication*, **159**, 57-68.

Strakhov, N.M. (1967). *Principles of Lithogenesis*. Vol. 1. Consultants Bureau, New York.

Stuiver, M. and Reimer, P.J. (1993) Radiocarbon calibration program. *Radiocarbon* **35**, 215-230.

Tarling, D.H. (1983). *Palaeomagnetism*. London: Chapman and Hall.

Thompson, R. (1973) Palaeolimnology and palaeomagnetism. *Nature* **242**, 182-184.

Thompson, R. (1978). Resistivity Investigation of an Infilled Kettle Hole. *Quaternary Research* **9**, 231-237.

Thompson, R. (1986) Modelling magnetisation data using SIMPLEX. *Phys. Earth Planet Int.* **42**, 113-127.

Thompson, R., Battarbee, R.W., O'Sullivan, P.E. and Oldfield, F. (1975) Magnetic Susceptibility of Lake Sediments. *Limnol. and Oceanogr.* **20** (5), 687-698.

Thompson, R. and Morton, D.J. (1979) Magnetic susceptibility and particle-size distribution in recent sediments of the Loch Lomond Drainage Basin, Scotland. *Journal of Sedimentary Petrology* **49** (3), 801-812.

Thompson, R. and Oldfield, F. (1986) *Environmental Magnetism*. Allen & Unwin, London, UK.

Trimble, S.W. (1981) Changes in sediment storage in the Coon Creek Basin, Driftless area, 1853-1975. *Science* **214**, 181-183.

Troake, R.P. and Walling, D.E. (1973). The hydrology of the Slapton Wood stream. *Field Studies* **3**, 719-740.

Vali, H., Förster, O., Amarantidis, G. and Petersen, N. (1987) Magnetotactic bacteria and their magnetofossils in sediments. *Earth and Planet. Sci. Lett.* **86,** 389-400.

van der Post, K.D., Oldfield, F., Haworth, E.Y., Crooks, P.R.J. and Appleby, P.G. (1997) A record of accelerated erosion in the recent sediments of Blelham Tarn in the English Lake District. *J.Paleolimnology* **18**, 103-120.

Vanoni, V.A. (Ed) (1975) Sediment engineering (American Socity of Civil Engineering manuals and reports on engineering practises, No 54). ASCE, New York.

Walling, D.E. (1978) Suspended sediment and solute response characteristics of the River Exe, Devon, England. In *Research in fluvial systems*, R. Davidson-Arnott and W. Nickling (eds), 169-197. Norwich: Geobooks.

Walling, D.E. (1983) The sediment delivery problem. *J. Hydrol.* **65**, 209-237.

Walling, D.E. (1988) Erosion and sediment yield research - some recent perspectives. *J. Hydrol.* **100**, 113-141.

Walling, D.E. and Webb (1981) Water quality, in *British Rivers* (J.Lewin, ed.), London: George Allen and Unwin, 126-169.

Wass, P. (1996) Suspended sediment fluxes and dynamics in RACS Rivers. LOIS meeting conference proceedings.

White, P. (1993) The reliability of sediment yield estimates from reservoir studies: an appraisal of variability in the southern Pennines of the UK. Unpubl PhD thesis. University of Huddersfield.

Williams, J.R. and Berndt, M.O. (1972). Sediment yield with Universal equation. *J. Hydraul. Div., Proc. ASCE.* **HY12**, 2087-2098.

Williams, M. (1992) Evidence for the Dissolution of Magnetite in Recent Scottish Peats. *Quaternary Research* **37**, 171-182.

Wischmeier, W.H. and Smith, D.D (1958) Rainfall energy and its relationship to soil loss. *Trans.Am. Soc. Am. Geophys. Union* **39** (2), 285-291.

Wischmeier, W.H., Johnson, C.B, and Cross, B.V. (1971) A soil erodibility nomograph for farmland and construction sites. *J. Soil. Wat. Cons.* **26**, 189-193.

Wischmeier, W.H. and Smith, D.D. (1978) Predicitng rainfall erosion losses. USDA Agricultural Research Service Handbook 537.

Wolman, M.G. (1977). Changing Needs and Opportunities in the Sediment Field. *Water Resources Research* **13** (1) 50-54.

Young, A. (1958). A Record of the rate of erosion on Millstone Grit. *Proceedings of the Yorkshire Geological Society* **31** (2), 149-156.

Yu, L. and Oldfield, F. (1989) A multivariate mixing model for identifying sediment soruces from magnetic measurements. *Quaternary Research* **32**, 168-181.

Yu, L. and Oldfield, F. (1993) Quantitative sediment source ascription using magnetic measurements in a reservoir-catchment system near Nijar, S.E. Spain. *Earth Surface Processes and Landforms* **18**, 441-454.

Appendix A

Suspended Sediment Loads in a Range of British Rivers

Catchment	Area (km^2)	Period of record	Suspended sediment load ($t\ km^{-2}\ a^{-1}$)	Source
Almond	176	1972-74	59	Al-Ansari *et al.* (1977)
Earn	-	1972-74	97	
Tyne	2159	1959-1961	61	Hall (1967)
Hodge Beck	18.9	1966-68	488	Imeson (1970)
Ebyr N.	0.07	1971	1.1	Oxley (1974)
Ebyr S.	0.09	1971	0.8	
Creedy	262	1972-74	53	Walling (1978)
Dart	46	1975	91	
Exe	601		24	
East Devon catchments				
1	0.11	1967-8	9.5	Walling (1977)
2	0.47	1967-8	37	
3	0.78	1967-8	50	
4	4.97	1967-8	46	
5	6.4	1967-8	56	
Sid	39.3	1967-8	47	
Slapton Wood	0.94	1971-2	8.4	Troake and Walling (1973)
Coalburn	3.1		3.0-25.0	Robinson and Blyth (1982)
Monachyle, Balquhidder	7.7		38.0	Stott *et al* (1986)
Kirton, Balquihidder	6.85		54.0	Ferguson and Stott (1987)
Cyff Plymlimon	3.1		6.0	Moore and Newson (1986)
Tanllwyth Plynlimon	0.9		38.0	Moore and Newson (1986)
Upper Severn Plynlimon	0.94		66.0	Francis (1987)
Wesl	0.0042		55.0	Labadz (1988)

Appendix B

Sediment Yields Determined for a Range of British Catchments using Reservoir Surveys

Site	Sediment yield ($t\ km^{-2}\ a^{-1}$)	Source
Strines Reservoir, South Pennines. Mixed forest and moorland. No sedi dens given	113	Young (1958)
Recalculated by McManus and Duck (1985) Inorganic only: Total	 39.4 52.5	
Recalculated by Walling and Webb (1981) using 82 % shrinkage on drying and s.g 2.1 (i.e. figures of Ledger *et al.* 1974)	49.7	
Cropston Reservoir, Leicestershire. Recalculated by McManus and Duck (1985). Inorganic only.	25.4	Cummins and Potter (1967) and (1972)
Recalculated by Walling and Webb (1981). Assumed 82% shrinkage, sg 2.1.	45.6	
Catcleugh Reservoir, Northumberland. Heather moorland and conif plantation. No sediment density given.	$114\ m^3\ km^{-2}\ a^{-1}$	Hall (1967)
Recalculated by Walling and Webb (1981) Assumed 82% shrinkage, s.g. 2.1	43.1	
North Esk and Hopes Reservoir, SE Scotland Deeply dissected moorland, podsolic soils and peats.	25	Ledger *et al.* (1974)
Deep Hayes Reservoir, Staffordshire. Lowland, mostly arable. Some decid woodland.	4.4	Rodda *et al.* (1976)
Recalc by Walling and Webb (1981). Assumed 82% shrinkage and s.g. 2.1	6.7	
Kelly Reservoir, Strathclyde. Inorg only	41	Ledger *et al.* (1980)
Merevale, Warwickshire. Deciduous woodland, lowland.	4.71-14.23	Foster *et al.* (1985)
Trentabank Reservoir, Macclesfield Forest S.Pennine upland	34.5-49.3	Stott (1985)
Glenfarg and Glenquey reservoirs, S.Scotland. Arable with patches of woodland, grazed moorland on higher ground and some areas of peat. Glenfarg only: Combined catchment:	9 26.3-31.3	McManus and Duck (1985)

Site		Sediment yield ($t\ km^{-2}\ a^{-1}$)	Source
Four reservoirs in the Scottish midland valley. Mostly rough moorland grazing, some mixed arable.			
Lambieletham	total	2.1	Duck and McManus (1987)
(lowland)	inorganic only	1.8	
Harperleas	total	13.8	
	inorganic only	11.5	
Drumain	total	3.9	
	inorganic only	3.3	
Cullaloe	total	30.8	
(lowland)	inorganic only	26.2	
Wessenden Valley, Pennines. Rough moorland			Labadz *et al.* (1991)
Four reservoirs	total	203.7	
	organic only	38.8	
Five reservoirs in the Scottish midland valley. Rough moorland.			
Pinmacher	total	50.9	Duck and McManus (1990)
	inorganic only	45.6	
Holl	total	72.3	
	inorganic only	61.7	
Earlsburn (peat upland)	total	68.2	
North Third (peat upland)	total	205.4	
Carron Valley (peat upland).	total	141.9	
Selected reservoirs in the Pennines			
Broomhead		31.8	Butcher *et al.* (1993)
Chew		78.5	
Deanhead		33.7	
Gorple Upper		27.6	
Gorpley		129.1	
Ingbirchworth		79.8	
Kinder		50.9	
Mixenden		9.5	
Silsden		195.9	
Snailsden		260.2	
Strines		83.8	
Widdop		81.1	

Appendix C

Sediment Yields Determined for a Range of British Catchments using Multiple Coring Techniques

Site	Time period	Inorganic sediment yield ($t\ km^{-2}\ a^{-1}$)	Source
Merevale, Warwickshire	1964-1982 AD	10	Foster *et al.* (1985)
	1954-1964	5.5	
	1942-1954	6.0	
	1936-1942	1.4	
	1922-1937	1.1	
	1915-1922	1.5	
	1906-1914	1.4	
	1879-1906	5	
	1861-1879	6.5	
Llyn Geirionydd, North Wales.	1961-1985 AD	15.3	Dearing (1992)
	1926-1961	17.6	
	1903-1926	15.7	
	1830-1903	8.1	
	1795-1830	9.9	
	1765-1795	13.9	
	1670-1765	5.8	
	1595-1670	6.4	
	1530-1595	8.2	
	1470-1530	6.6	
	1405-1470	5.8	
	1345-1405	7.9	
	1270-1345	8.2	
	1190-1270	8	
	150-1500 BP	5	Snowball and Thompson (1992)
	1500-4000 BP	5	
	4000 - 7000 BP	3	
	7000 - 10000 BP	2	
Old Mill Reservoir,	1942-1991 AD	54/69	Foster and Walling Devon. (1994)
Howden Reservoir, Derbyshire.	1912-1987 AD	96.4	Hutchinson (1995)
Loe Pool, Cornwall	1938-1981 AD	12	O'Sullivan (1982)
	1937-1938	361	
	1930-1936	421	
	1860-1920	174	
Llyn Goddionduon, North Wales	1951-1977 AD	26-33	Bloemendal (1982)
	800 BP -1951AD	12	
	10400-800 BP	3.6	

Seeswood Pool,	1978-1982 AD	36.2	Foster *et al.* (1986)
Warwickshire	1973-1977	18.3	
	1948-1964	12	
	1934-1947	12.8	
	1926-1933	16.1	
	1920-1925	21.6	
	1903-1919	9.6	
	1881-1902	8.1	
	1854-1880	12.2	
	1765-1853	7	
Llyn Peris,	1976-1965.5 AD	41.65	Dearing *et al.* (1981)
North Wales.	1965.5-1952	11.8	
	1952-1931	7.65	
	1931-1920.5	14.1	
	1920.5-1901.5	7.5	
	1901.5-1895.5	14.75	
	1895.5-1885.5	5.95	
	1885.5-1878.5	8.9	
	1878.5-1864.5	3.95	
	1864.5-1856	2.9	
	1856-1847	4.35	
Semer Water,	1950-1994 AD	8	Chapter 8
West Yorkshire.	10 000-0 BP	23	
Gormire,	1949-1994 AD	43	Chapter 8
North Yorkshire	1889-1949 AD	29	
	1640-1889 AD	21	
Hornsea Mere	1979-1994 AD	54	Chapter 8
Humberside	1963-1979 AD	93	
	1730-1963 AD	11	

Appendix D

Particle Size Splits Obained Using Centrifuge Techniques

0-2 μm

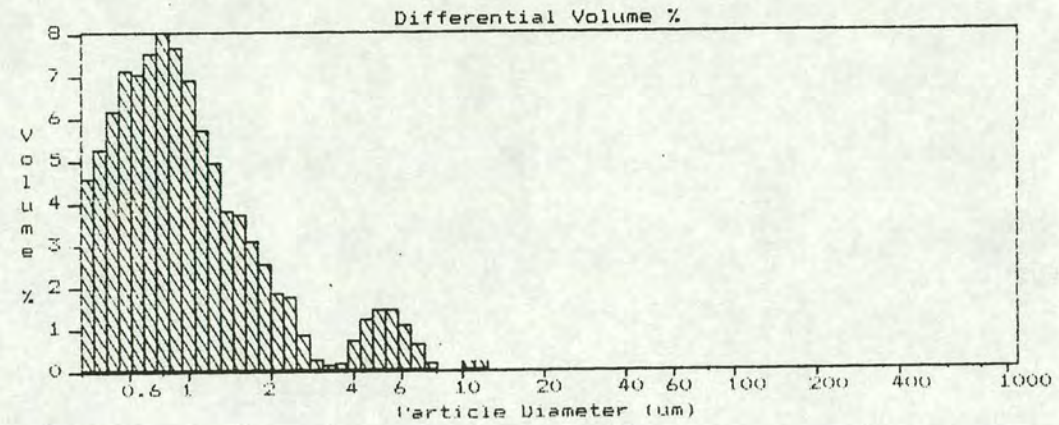

2-10 μm

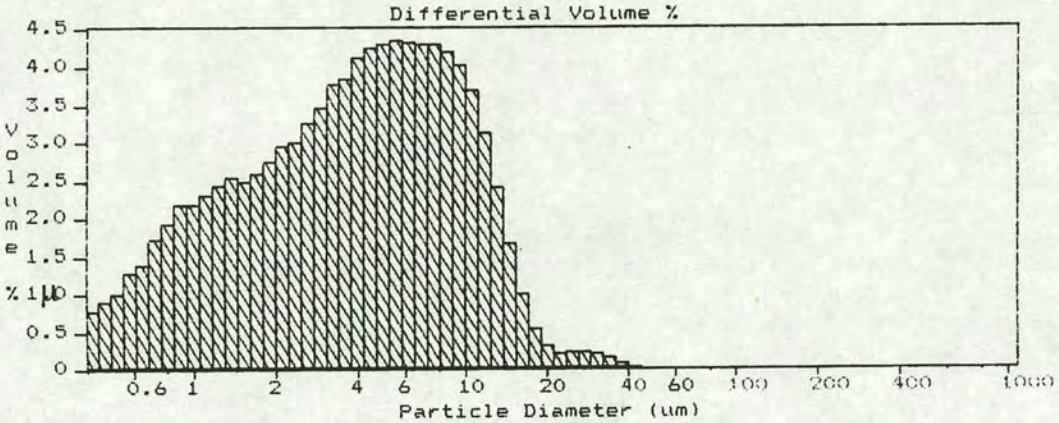

10-63 μm

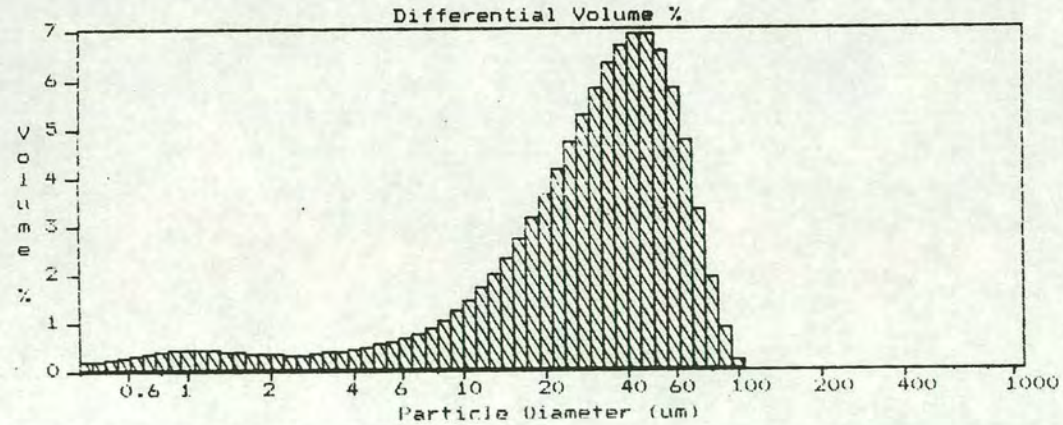

Appendix E

Calculation of C and K Values for Incorporation in the USLE and Sediment Flux Model.

Table 1 - Determination of a C value for each sites in the database

Lake	Land use (%)				C value				
	Forest	Grass land	Rough grazing	Arable	Forest	Grass land	Rough grazing	Arable	Catch-ment
North Esk	10	0	90	0	0.000	0.000	0.009	0.000	0.009
Semer	5	25	70	0	0.000	0.005	0.007	0.000	0.012
Gormire	80	20	0	0	0.001	0.004	0.000	0.000	0.005
Glenfarg	30	0	20	50	0.000	0.000	0.002	0.125	0.127
Loe Pool	7	71	10	10	0.000	0.014	0.001	0.025	0.040
Glenhead	0	0	100	0	0.000	0.000	0.010	0.000	0.010
Loch Valley	0	0	100	0	0.000	0.000	0.010	0.000	0.010
Loch Enoch	0	0	100	0	0.000	0.000	0.010	0.000	0.010
Merevale	85	15	0	0	0.001	0.003	0.000	0.000	0.004
L.Geirionydd	40	5	55	0	0.000	0.001	0.006	0.000	0.007
L.Goddionduon	100	0	0	0	0.001	0.000	0.000	0.000	0.001
Seeswood	0	70	0	30	0.000	0.014	0.000	0.075	0.089
Old Mill	12	28	40	20	0.000	0.006	0.004	0.050	0.060
Kelly	0	0	100	0	0.000	0.000	0.010	0.000	0.010
Llyn Peris	10	0	90	0	0.000	0.000	0.009	0.000	0.009
Lambieltham	0	0	0	100	0.000	0.000	0.000	0.250	0.250
Harperleas	10	0	90	0	0.000	0.000	0.009	0.000	0.009
Drumain	0	0	100	0	0.000	0.000	0.010	0.000	0.010
Cullaloe	30	0	0	70	0.000	0.000	0.000	0.175	0.175
Hornsea	0	10	0	90	0.000	0.002	0.000	0.225	0.227
Broomhead	9	29	62	0	0.000	0.006	0.006	0.000	0.012
Chew	0	25	75	0	0.000	0.005	0.008	0.000	0.013
Deanhead	0	25	75	0	0.000	0.005	0.008	0.000	0.013
Gorple Upper	0	4	96	0	0.000	0.001	0.010	0.000	0.010
Gorpley	0	10	90	0	0.000	0.002	0.009	0.000	0.011
Ingbirchworth	0	96	4	0	0.000	0.019	0.000	0.000	0.020
Kinder	0	25	75	0	0.000	0.005	0.008	0.000	0.013
Mixenden	12	34	54	0	0.000	0.007	0.005	0.000	0.012
Snailsden	0	5	95	0	0.000	0.001	0.010	0.000	0.011
Widdop	0	4	96	0	0.000	0.001	0.010	0.000	0.010

Reference C values (after Wischmeier and Smith 1978)

Forest	0.001
Rough grazing	0.01
Arable	0.25
Grassland	0.02

Table 2 - C values Corrected for Precipitation Variation in Catchments with Arable Land

English sites		% annual rainfall				Weighted C value			
	C value	Seeswood Pool	Old Mill Reservoir	Hornsea Mere	Loe Pool	Seeswood Pool	Old Mill Reservoir	Hornsea Mere	Loe Pool
January	0.25	0.086	0.120	0.089	0.121	0.022	0.030	0.022	0.030
February	0.25	0.088	0.098	0.063	0.096	0.022	0.025	0.016	0.024
March	0.25	0.078	0.089	0.078	0.089	0.020	0.022	0.020	0.022
April	0.25	0.077	0.058	0.074	0.056	0.019	0.014	0.018	0.014
May	0.25	0.083	0.062	0.081	0.060	0.021	0.016	0.020	0.015
June	0.25	0.088	0.058	0.081	0.056	0.022	0.014	0.020	0.014
July	0.25	0.077	0.051	0.075	0.055	0.019	0.013	0.019	0.014
August	0.25	0.096	0.073	0.092	0.066	0.024	0.018	0.023	0.016
September	1	0.082	0.077	0.081	0.077	0.082	0.077	0.081	0.077
October	0.6	0.078	0.092	0.086	0.098	0.047	0.055	0.052	0.059
November	0.6	0.087	0.102	0.100	0.112	0.052	0.061	0.060	0.067
December	0.25	0.099	0.120	0.101	0.113	0.025	0.030	0.025	0.028
Annual C factor						**0.379**	**0.387**	**0.384**	**0.394**

Scottish sites		% annual rainfall			Weighted C value		
	C value	Lamb'm	Cullaloe	Glenfarg	Lamb'm	Cullaloe	Glenfarg
January	0.6	0.089	0.088	0.112	0.054	0.053	0.067
February	0.6	0.062	0.065	0.075	0.037	0.039	0.045
March	0.6	0.079	0.075	0.086	0.047	0.045	0.051
April	0.6	0.066	0.062	0.056	0.040	0.037	0.033
May	0.6	0.077	0.072	0.070	0.046	0.043	0.042
June	0.25	0.075	0.075	0.069	0.019	0.019	0.017
July	0.25	0.083	0.080	0.069	0.021	0.020	0.017
August	0.25	0.098	0.098	0.083	0.024	0.025	0.021
September	1	0.098	0.103	0.094	0.098	0.103	0.094
October	0.6	0.096	0.093	0.098	0.058	0.056	0.059
November	0.6	0.092	0.097	0.094	0.055	0.058	0.056
December	0.6	0.085	0.092	0.099	0.051	0.055	0.059
Annual C factor					**0.550**	**0.552**	**0.563**

Calculation assumptions:

Scotland

C value assumed to 0.25 when crop cover is maximum (June-August), soil bare in September hence a C value of 1 is assumed. Following the planting of spring barley in October a mid-range C value of 0.6 is assumed, i.e. the crop cover is somewhere between that of bare soil and the maximum. (R.Hood, pers.comm. Scottish Agricultural College, Edinburgh).

England

Wheat dominant arable crop in England, C value of 0.25 assumed when crop cover is at maximum (June-August). C value of 1 assumed in September after harvesting. Planting of winter crop in October and November - partial crop cover - C value of 0.6 assumed, reducing to 0.25 during spring months.

Table 3 K values for each soil series. Mean values calculated from over 60 published descriptions of soil series.

Soil type	Soil map code	Silt & very fine sand (%)	Sand (%)	Organic content (%)	Soil strucutre	Permeab-ility	K
Humic rankers rankers	311	60.0	26.0	10.4	2.5	3	0.48
Gleying brown calc earths	512	41.5	53.5	2.9	2.5	3.5	0.3
Typical brown earths	541	56	39.2	3.4	2.5	1	0.35
Typical brown podzolic soils	611	61.5	40.5	2	2.5	1	0.48
Humic brown podzolic soils	612	42	50	11	2.5	1	0.15
Iron-pan stagnopodzols	651a	67.3	23.5	12.25	2.5	2	0.45
Humus Iron pan stagnopodzols	651b	43	71.5	6	2.5	2	0.45
Ferric stagnopodzols	654	63	43.6	11.2	2.5	3	0.47
Typical stagnogley soils	711	66.1	25.1	3.1	2.5	5	0.52
Pelo stagnogley soils	712	50	7	3.6	2.5	5	0.27
Cambic stagnogley soils	713	8.7	26	1.7	2.5	5	0.17
Cambic stagno-humic gley soils	721	63.5	44	5.8	2.5	5	0.58
Peat	1011			v.high			1
Non calcareous gleys	360, 446	66	25	3	2.5	3	0.25
Brown forest soils	446	55	40	3.5	2.5	1	0.27
Brown forest soils with gleying	287, 445 447	40	30	4	2.5	2	0.2
Peaty podzols	126, 153	35	30	5	2.5	3	0.15
Peaty gleys	360, 119,	42	25	3.6	2.5	5	0.3
Sub-alpine soils	236	60	25	10	2.5	3	0.35
Humus iron podzols	227, 115	67	23.5	12	2.5	5	0.45

Catchment	Soil Types	K value
North Esk	40% 447, 40% 466, 20% 444	0.307
Semer	60% 721, 20% 711, 10% 1011b, 10% 541r	0.624
Gormire	100% 712a	0.32
Glenfarg	100% 337	0.15
Loe Pool	65% 541, 15% 611, 20% 612	0.364
Glenhead	80% 126, 20% 129	0.26
Loch Valley	70% 126, 30% 129	0.25
Loch Enoch	65% 126, 20% 129, 10% 4	0.323
Merevale	50% 711, 20% 541	0.435
L.Geirionydd	100% 654	0.47
L.Goddionduon	100% 654	0.47
Seeswood	70% 711, 25% 541	0.435
Old Mill	100% 27	0.4
Kelly	50% 360, 50% 287	0.243
Llyn Peris	10% 651, 30% 612, 15% 311	0.307
Lambieltham	90% 445, 10% 444	0.226
Harperleas	20% 446, 40% 147, 20% 153, 20% 341	0.16
Drumain	20% 446, 40% 147, 20% 153, 20% 341	0.16
Cullaloe	60% 445, 40% 147	0.215
Hornsea	80% 711, 20% 512	0.574
Broomhead	70% 721, 15% 541, 15% 1010	0.57
Chew	100% 1011	1
Deanhead	80% 1011, 20% 721	0.87
Gorple Upper	100% 1011	1
Gorpley	30% 651, 20% 721, 50% 1011	0.83
Ingbirchworth	80% 541, 20% 721	0.44
Kinder	20% 541, 10% 311, 40% 651, 30% 1011	0.69
Mixenden	100% 721	0.6
Snailsden	90% 1011, 10% 721	0.916
Widdop	30% 651, 70% 1011	0.835

Appendix F Catchment Parameters Determined for 30 British Catchments

Lake	Source of flux data*	Grid reference	Mean annual precipitation (mm)	Max mean monthly precipitation (mm)	p^2/P	Lake perimeter (km)
North Esk Reservoir	1	NT155582	1077	116	12.49	1.8
Semer Water	2	SD918874	1375	161	18.85	2.4
Gormire	3	SE 505833	825	82	8.15	1.0
Glenfarg	4	NO16110	969	108	12.04	4.0
Loe Pool	5	SW648250	1032	125	15.14	6.0
Round Loch of Glenhead	6	NX450805	2360	267	30.21	1.2
Loch Valley	7	NX445817	2360	267	30.21	4.0
Loch Enoch	8	NX445851	2360	267	30.21	4.8
Merevale	9	SP300970	639	63	6.21	1.6
Llyn Geirionydd	10	SH605763	2555	329	42.36	2.8
Llyn Goddionduon	11	SH753586	2555	329	42.36	1.2
Seeswood	12	SP327905	639	63	6.21	1.6
Old Mill Reservoir	13	SX850522	1090	131	15.74	0.4
Kelly Reservoir	14	NS223685	1767	200	22.64	1.0
Llyn Peris	15	SH570620	2330	310	41.24	6.4
Lambieltham	16	NO502134	738	72	7.02	0.5
Harperleas	17	NO212053	949	93	9.11	1.8
Drumain	18	NO223043	949	93	9.11	0.4
Cullaloe	19	NT188875	796	82	8.45	3.6
Hornsea Mere	20	TA190447	652	66	6.68	2.8
Broomhead	21	SK260960	980	104	11.04	3.6
Chew	22	SE040020	1604	168	17.60	2.2
Deanhead	23	SE0404150	1357	151	16.80	1.2
Gorple Upper	24	SE920315	1478	164	18.20	1.6
Gorpley	25	SE910230	1512	166	18.23	1.2
Ingbirchworth	26	SE215060	1006	109	11.81	1.6
Kinder	27	SK055883	1175	119	12.05	2.6
Mixenden	28	SE060290	1087	116	12.38	0.4
Snailsden	29	SE135040	1542	177	20.32	1.2
Widdop	30	SD930330	1326	144	15.64	2.4

* Source of sediment yield/flux estimates

1 Lovell *et al.* (1973)
2, 3, 20 Chapter 8
4 McManus and Duck (1985)
5 O'Sullivan *et al.* (1982)
6,7,8 Flower *et al.* (1987)
9 Foster et al. (1985)
10 Snowball and Thompson (1992) and Dearing (1982)
11 Bloemendal (1982)
12 Foster *et al.* (1986)
13 Foster and Walling (1994)
14 Ledger *et al.* (1980)
15 Dearing *et al.* (1981)
16-19 Duck and McManus (1987)
21-30 Butcher *et al.* (1993)

Lake	Lake perimeter (km)	Catchment area (km^2)	Lake area (km^2)	Catchment: lake ratio	Stream length (km)	Slopes %	Lake Altitude (m)	Average catchment altitude (m)
North Esk	1.8	7	0.10	70.0	16.0	14.7	340	462
Semer Water	2.4	43.6	0.26	167.7	96.6	7.5	248	532
Gormire	1.0	0.3	0.07	4.3	0.0	22.5	160	228
Glenfarg	4.0	23.5	0.41	58.0	11.6	9.0	497	572
Loe Pool	6.0	55	0.44	125.0	47.6	4.1	5	99
Round Loch of Glenhead	1.2	1	0.125	7.6	1.6	19.6	300	370
Loch Valley	4.0	1.86	0.501	3.7	1.6	18.1	330	385
Loch Enoch	4.8	1.86	0.500	3.7	1.8	12.1	500	545
Merevale	1.6	1.95	0.065	30.0	4.4	5.2	110	150
Llyn Geirionydd	2.8	3.90	0.26	150.0	6.0	10.4	190	479
Llyn Goddionduon	1.2	0.25	0.062	4.0	0.4	17.1	244	367
Seeswood	1.6	2.21	0.067	32.9	4.0	2.0	125	145
Old Mill	0.4	1.58	0.019	85.4	2.4	22.1	45	160
Kelly	1.0	3.40	0.054	63.0	12.0	5.2	200	262
Llyn Peris	6.4	38.00	0.500	76.0	70.0	22.0	100	594
Lambieltham	0.5	2.29	0.012	189.3	3.6	1.5	102	127
Harperleas	1.8	3.44	0.162	21.2	6.8	9.8	259	360
Drumain	0.4	1.53	0.020	75.7	2.6	4.4	231	278
Cullaloe	3.6	4.13	0.162	25.5	4.0	6.8	89	144
Hornsea Mere	2.8	16.70	1.200	13.8	12.0	2.4	0	13
Broomhead	3.6	21.96	0.485	45.3	65.6	10.3	180	419
Chew	2.2	2.92	0.30	17.8	16.4	5.2	490	522
Deanhead	1.2	2.00	0.068	29.4	10.0	11.0	305	410
Gorple Upper	1.6	3.80	0.219	17.4	4.0	9.5	350	411
Gorpley	1.2	2.80	0.072	38.9	9.2	16.5	260	354
Ingbirchworth	1.6	7.72	0.217	35.6	4.4	5.3	260	308
Kinder	2.6	8.95	0.300	29.8	23.6	18.1	280	517
Mixenden	0.4	0.77	0.092	8.4	0.4	6.3	260	311
Snailsden	1.2	0.84	0.040	21.0	4.0	5.4	420	452
Widdop	2.4	8.90	0.039	228.2	4.4	15.2	320	408

Lake	K (A)	Catchment soil erosion susceptibility	Vegetation	Lake sediment yield ($t\ km^{-2}\ a^{-1}$)	Lake sediment flux ($t\ a^{-1}$)	Length of slope (m)	LS	R
North Esk	0.31	2.118	0.010	23.400	163.800	1100	5.4240	931.6
Semer Water	0.62	27.050	0.012	13.800	730.000	4267	5.6809	1189.4
Gormire	0.32	0.090	0.005	44.600	8.700	278	6.5697	713.6
Glenfarg	0.15	3.464	0.563	31.300	735.550	860	4.0597	838.2
Loe Pool	0.36	19.860	0.394	12.000	660.000	3760	5.0910	892.7
Round Loch of Glenhead	0.26	0.215	0.010	33.292	31.661	430	5.9443	2041.4
Loch Valley	0.25	0.339	0.010	66.092	122.733	300	5.2599	2041.4
Loch Enoch	0.32	0.439	0.010	89.380	166.247	420	4.0443	2041.4
Merevale	0.44	0.820	0.007	8.470	16.517	940	3.6190	552.7
Llyn Geirionydd	0.47	1.711	0.007	12.490	48.711	960	4.3998	2210.1
Llyn Goddionduon	0.47	0.088	0.005	29.500	7.375	232	4.8239	2210.1
Seeswood	0.44	0.932	0.379	11.230	24.818	1140	3.5087	552.7
Old Mill	0.40	0.624	0.387	69.000	109.020	540	6.9067	942.9
Kelly	0.24	0.811	0.010	36.900	125.460	1320	3.9492	1528.5
Llyn Peris	0.31	11.513	0.010	10.600	402.800	2470	8.3805	2015.5
Lambieltham	0.23	0.515	0.550	1.800	4.122	1200	3.5254	638.4
Harperleas	0.16	0.524	0.010	11.500	39.560	1040	4.3693	820.9
Drumain	0.16	0.242	0.010	3.300	5.049	1020	3.6095	820.9
Cullaloe	0.22	0.853	0.552	26.200	108.206	700	3.5552	688.5
Hornsea Mere	0.57	8.610	0.384	41.960	770.000	540	2.8829	564.0
Broomhead	0.57	12.241	0.011	31.800	698.328	3240	5.7465	847.7
Chew	1.00	2.620	0.012	78.500	229.220	720	3.3823	1387.5
Deanhead	0.87	1.681	0.012	33.700	67.400	1000	4.5484	1173.8
Gorple Upper	1.00	3.581	0.010	27.600	104.880	780	4.0557	1278.5
Gorpley	0.83	2.264	0.011	129.100	361.480	580	5.3061	1307.9
Ingbirchworth	0.44	3.301	0.017	79.800	616.056	940	3.6303	870.2
Kinder	0.69	5.969	0.012	50.900	455.555	1380	6.5291	1016.4
Mixenden	0.60	0.407	0.012	9.500	7.315	592	3.3519	940.3
Snailsden	0.92	0.733	0.010	260.200	218.568	712	3.3956	1333.8
Widdop	0.84	7.399	0.010	81.100	721.790	668	5.0951	1147.0

Lake	USLE slope length factor	USLE sediment erosion ($t\ km^{-2}\ a^{-1}$)	USLE erosion x by catchment area ($t\ a^{-1}$)	Sediment delivery ratio (SDR)	USLE erosion x SDR ($t\ km^{-2}\ a^{-1}$)	USLE sediment flux ($t\ a^{-1}$)	Time period of lake sediment flux record (AD)
North Esk	3.2279	99.91	689.4	0.244	24.378	168.2	1850-1971
Semer Water	4.8478	373.28	16181.7	0.169	63.084	2734.7	c.1730-1994
Gormire	2.1366	94.60	26.5	0.444	42.002	11.8	1889-1994
Glenfarg	2.9982	1348.21	31130.2	0.191	257.508	5945.9	1926-1982
Loe Pool	4.6673	758.02	41357.6	0.162	122.799	6699.9	1938-1991
Round Loch of Glenhead	2.4353	139.10	114.9	0.364	50.632	41.8	1821-1981
Loch Valley	2.1860	118.35	160.5	0.318	37.635	51.0	1861-1981
Loch Enoch	2.4181	117.39	159.7	0.318	37.330	50.8	1772-1982
Merevale	3.0792	79.11	149.1	0.315	24.920	47.0	1861-1964
Llyn Geirionydd	3.0988	137.10	499.0	0.274	37.565	136.7	1830-1985
Llyn Goddionduon	2.0237	110.53	20.8	0.475	52.502	9.9	1951-1977
Seeswood	3.2627	1070.99	2295.1	0.307	328.794	704.6	1854-1982
Old Mill	2.6075	1497.97	2338.3	0.329	492.832	769.3	1942-1991
Kelly	3.4094	71.83	240.3	0.282	20.256	67.8	1850-1978
Llyn Peris	4.1145	250.85	9406.9	0.174	43.648	1636.8	1847-1976
Lambieltham	3.3133	2721.52	6199.6	0.305	830.064	1890.9	1900-1985
Harperleas	3.1741	41.95	137.5	0.281	11.788	38.6	1875-1983
Drumain	3.1556	34.65	52.3	0.331	11.469	17.3	1867-1984
Cullaloe	2.8186	2361.88	9371.9	0.271	640.069	2539.8	1876-1986/ 1908-1980
Hornsea Mere	2.6075	4035.82	60537.3	0.205	827.343	12410.1	1730-1994
Broomhead	4.4634	279.20	5995.8	0.194	54.165	1163.2	1929-1988
Chew	2.8425	294.77	772.3	0.291	85.778	224.7	1914-1987
Deanhead	3.1369	352.43	680.9	0.313	110.311	213.1	1840-1986
Gorple Upper	2.9116	313.31	1122.0	0.276	86.474	309.7	1934-1989
Gorpley	2.6640	355.08	968.7	0.293	104.038	283.8	1905-1990
Ingbirchworth	3.0792	206.06	1546.1	0.239	49.248	369.5	1868-1990
Kinder	3.4552	392.62	3396.2	0.232	91.088	787.9	1912-1987
Mixenden	2.6804	180.25	122.2	0.379	68.315	46.3	1873-1989
Snailsden	2.8330	242.14	193.7	0.373	90.318	72.3	1899-1990
Widdop	2.7793	328.65	2912.2	0.233	76.575	678.5	1878-1978

Appendix G

Semer Water Catchment Sample Magnetic Results

Sample	χ	ARM	IRM_{100}	SIRM		
	$\mu\ m^3\ kg^{-1}$	$mA\ m^2\ kg^{-1}$	$mA\ m^2\ kg^{-1}$	$mA\ m^2\ kg^{-1}$		
1	0.010	0.125	3.807	5.687		
2	0.003	0.017	0.083	0.242		
3	0.007	0.070	3.225	3.642		
4	0.012	0.092	3.678	5.239		
5	0.011	0.094	3.957	5.005		
6	0.009	0.100	1.408	2.096		
7	0.003	0.045	0.180	0.284		
8	0.016	0.114	3.479	3.953		
9	0.016	0.121	4.042	4.776		
10	0.018	0.187	4.377	5.776		
11	0.004	0.041	1.278	1.661		
12	0.024	0.379	6.642	10.075		
13	0.038	0.008	0.129	0.254		
14	0.048	0.016	0.329	0.534		
15	0.142	0.008	0.099	0.318		
16	0.009	0.003	0.043	0.099		
17	0.023	0.003	0.048	0.133		
18	0.137	0.005	0.073	0.344		
19	0.038	0.003	0.035	0.054		
20	0.048	0.013	0.132	0.216		
21	0.087	0.012	0.327	0.542		
22	0.010	0.004	0.070	0.100		
23	0.047	0.007	0.239	0.413		
24	0.040	0.010	0.260	0.400		
25	0.053	0.014	0.344	0.563		
26	0.000	0.006	0.087	0.116		
27	0.038	0.012	0.134	0.193		
28	0.023	0.003	0.021	0.029		
29	0.055	0.004	0.033	0.190		
30	0.032	0.014	0.151	0.220		
31	0.047	0.002	0.013	0.034		
32	0.072	0.008	0.044	0.243		
33	0.053	0.024	0.345	0.617		
34	0.880	0.743	5.135	6.270		
35	0.012	0.004	0.036	0.062		
36	0.042	0.008	0.075	0.171		
37	0.039	0.005	0.088	0.112		
38	0.046	0.006	0.071	0.147		
39	0.164	0.078	0.613	0.990		
40	0.053	0.026	0.266	0.511		
41	0.001	0.000	0.010	0.016		
42	0.060	0.021	0.495	0.959		

Appendix H

Down Core Sediment Density Data

	Semer Water core 1			Semer Water core 2			Semer Water core 3		
Sample	Depth (cm)	Dry weight (g)	Density (g cm^{-3})	Depth (cm)	Dry weight (g)	Density (g cm^{-3})	Depth (cm)	Dry weight (g)	Density (g cm^{-3})
1	2.60	6.06	1.01	2.60	2.99	0.17	2.70	12.56	0.55
2	5.20	7.21	1.20	5.20	3.62	0.20	5.40	12.01	0.54
3	7.80	7.93	1.32	7.80	3.89	0.22	8.10	10.93	0.38
4	10.40	6.52	1.09	10.40	4.47	0.18	10.80	12.35	0.66
5	13.00	6.72	1.12	13.00	3.81	0.19	13.50	12.19	0.59
6	15.60	7.05	1.18	15.60	3.99	0.20	16.20	12.44	0.68
7	18.20	8.37	1.40	18.20	4.13	0.23	18.90	12.07	0.65
8	20.80	7.77	1.30	20.80	4.64	0.22	21.60	12.11	0.63
9	23.40	6.53	1.09	23.40	4.85	0.18	24.30	12.30	0.68
10	26.00	6.32	1.05	26.00	4.19	0.18	27.00	12.06	0.71
11	28.60	8.48	1.41	28.60	4.97	0.24	29.70	12.03	0.73
12	31.20	9.48	1.58	31.20	4.88	0.26	32.40	12.77	0.78
13	33.80	7.83	1.31	33.80	4.85	0.22	35.10	12.20	0.70
14	36.40	8.75	1.46	36.40	4.85	0.24	37.80	13.00	0.88
15	39.00	8.49	1.42	39.00	5.05	0.24	40.50	12.48	0.74
16	41.60	7.45	1.24	41.60	4.72	0.21	43.20	12.14	0.75
17	44.20	8.42	1.40	44.20	4.96	0.23	45.90	11.24	0.76
18	46.80	8.92	1.49	46.80	4.64	0.25	48.60	12.08	0.79
19	49.40	8.23	1.37	49.40	4.66	0.23	51.30	12.66	0.79
20	52.00	8.89	1.48	52.00	4.52	0.25	54.00	12.21	0.76
21	54.60	8.25	1.38	54.60	4.56	0.23	56.70	11.30	0.73
22	57.20	9.54	1.59	57.20	4.23	0.27	59.40	12.80	0.78
23	59.8	9.79	1.63				62.1	11.55	0.76
24	62.4	8.27	1.38				64.8	12.02	0.69
25	65	7.21	1.20				67.5	9.1	0.70
26	67.6	6.82	1.14				70.2	12.02	0.73
27	70.2	6.11	1.02				72.9	11.85	0.75
28	72.8	5.62	0.94				75.6	12	0.74
29	75.4	6	1.00						

Sample	Depth (cm)	Dry weight (g)	Density (g cm^{-3})	Depth (cm)	Dry weight (g)	Density (g cm^{-3})	Depth (cm)	Dry weight (g)	Density (g cm^{-3})
	Semer Water core 4			**Semer Water core 5**			**Semer Water core 6**		
1	2.70	3.04	0.51	2.25	1.75	0.29	2.25	1.75	0.29
2	5.40	3.00	0.50	4.50	2.30	0.38	4.50	2.05	0.34
3	8.10	3.59	0.60	6.75	2.32	0.39	6.75	2.28	0.38
4	10.80	3.51	0.59	9.00	2.78	0.46	9.00	2.18	0.36
5	13.50	3.34	0.56	11.25	2.46	0.41	11.25	2.49	0.42
6	16.20	3.50	0.58	13.50	2.31	0.39	13.50	2.57	0.43
7	18.90	3.72	0.62	15.75	2.50	0.42	15.75	2.87	0.48
8	21.60	3.67	0.61	18.00	2.51	0.42	18.00	2.96	0.49
9	24.30	4.22	0.70	20.25	2.29	0.38	20.25	2.80	0.47
10	27.00	4.50	0.75	22.50	2.59	0.43	22.50	2.70	0.45
11	29.70	4.30	0.72	24.75	2.55	0.43	24.75	2.76	0.46
12	32.40	4.58	0.76	27.00	2.57	0.43	27.00	2.77	0.46
13	35.10	4.24	0.71	29.25	2.63	0.44	29.25	2.49	0.42
14	37.80	4.65	0.78	31.50	2.57	0.43	31.50	2.14	0.36
15	40.50	4.40	0.73	33.75	2.79	0.47	33.75	2.61	0.44
16	43.20	4.70	0.78	36.00	2.54	0.42	36.00	2.91	0.49
17	45.90	4.53	0.76	38.25	2.44	0.41	38.25	2.69	0.45
18	48.60	4.44	0.74	40.50	2.85	0.48	40.50	2.61	0.44
19	51.30	4.22	0.70	42.75	3.08	0.51	42.75	2.73	0.46
20	54.00	4.58	0.76	45.00	3.34	0.56	45.00	2.76	0.46
21	56.70	4.56	0.76	47.25	3.14	0.52	47.25	2.59	0.43
22	59.40	4.20	0.70	49.50	2.60	0.43	49.50	2.58	0.43
23	62.10	4.34	0.72	51.75	2.92	0.49	51.75	2.93	0.49
24	64.80	4.61	0.77	54.00	2.54	0.42	54.00	2.46	0.41
25	67.50	4.40	0.73	56.25	2.07	0.35	56.25	2.71	0.45
26	70.20	3.97	0.66	58.50	2.58	0.43	58.50	2.71	0.45
27	72.90	4.42	0.74	60.75	2.52	0.42	60.75	2.75	0.46

Sample	Depth (cm)	Dry weight (g)	Density (g cm^{-3})	Depth (cm)	Dry weight (g)	Density (g cm^{-3})	Depth (cm)	Dry weight (g)	Density (g cm^{-3})
	Semer Water core 7			**Semer Water core 8**			**Semer Water core 9**		
1	2.80	2.90	0.48	2.60	3.04	0.51	2.90	4.20	0.70
2	5.60	3.10	0.52	5.20	3.95	0.66	5.80	5.13	0.86
3	8.40	3.47	0.58	7.80	3.95	0.66	8.70	4.83	0.81
4	11.20	3.69	0.62	10.40	3.71	0.62	11.60	4.58	0.76
5	14.00	3.71	0.62	13.00	3.76	0.63	14.50	4.56	0.76
6	16.80	4.00	0.67	15.60	4.13	0.69	17.40	4.46	0.74
7	19.60	4.05	0.68	18.20	3.85	0.64	20.30	4.07	0.68
8	22.40	3.90	0.65	20.80	4.14	0.69	23.20	4.52	0.75
9	25.20	5.47	0.91	23.40	3.98	0.66	26.10	4.68	0.78
10	28.00	5.76	0.96	26.00	4.03	0.67	29.00	4.80	0.80
11	30.80	7.18	1.20	28.60	4.11	0.69	31.90	4.40	0.73
12	33.60	8.76	1.46	31.20	4.68	0.78	34.80	4.29	0.72
13	36.40	8.14	1.36	33.80	5.82	0.97	37.70	4.53	0.76
14	39.20	6.92	1.15	36.40	5.50	0.92	40.60	4.52	0.75
15	42.00	6.86	1.14	39.00	6.36	1.06	43.50	2.33	0.39
16	44.80	5.95	0.99	41.60	6.95	1.16	46.40	3.11	0.52
17	47.60	5.41	0.90	44.20	6.93	1.16	49.30	5.26	0.88
18	50.40	5.57	0.93	46.80	6.30	1.05	52.20	5.58	0.93
19	53.20	8.38	1.40	49.40	6.00	1.00	55.10	6.82	1.14
20	56.00	9.81	1.64	52.00	6.63	1.11	58.00	7.11	1.19
21	58.80	8.01	1.34	54.60	6.96	1.16	60.90	6.24	1.04
22	61.60	6.47	1.08	57.20	7.86	1.31	63.80	6.42	1.07
23	64.40		21.25	59.80	7.08	1.18	66.70	6.30	1.05
24	67.20		0.97	62.40	6.89	1.15	69.60	7.21	1.20
25				65.00	8.15	1.36	72.50	6.45	1.08
26				67.60	8.14	1.36	75.40	6.59	1.10
27				70.20	7.97	1.33			

Sample	Depth (cm)	Dry weight (g)	Density (g cm^{-3})	Depth (cm)	Dry weight (g)	Density (g cm^{-3})	Depth (cm)	Dry weight (g)	Density (g cm^{-3})
	Semer Water core 10			**Semer Water core 11**			**Semer Water core 12**		
1	2.60	6.36	1.06	2.90	2.76	0.46	2.70	2.63	0.44
2	5.20	6.35	1.06	5.80	2.88	0.48	5.40	3.07	0.51
3	7.80	7.72	1.29	8.70	3.60	0.60	8.10	3.80	0.63
4	10.40	8.31	1.39	11.60	3.48	0.58	10.80	4.01	0.67
5	13.00	7.74	1.29	14.50	3.68	0.61	13.50	4.30	0.72
6	15.60	7.29	1.22	17.40	4.03	0.67	16.20	4.24	0.71
7	18.20	7.96	1.33	20.30	4.22	0.70	18.90	4.24	0.71
8	20.80	7.30	1.22	23.20	4.56	0.76	21.60	4.10	0.68
9	23.40	7.38	1.23	26.10	5.03	0.84	24.30	4.37	0.73
10	26.00	8.01	1.34	29.00	4.81	0.80	27.00	4.18	0.70
11	28.60	7.40	1.23	31.90	4.43	0.74	29.70	4.02	0.67
12	31.20	8.40	1.40	34.80	4.42	0.74	32.40	4.00	0.67
13	33.80	9.54	1.59	37.70	4.22	0.70	35.10	4.27	0.71
14	36.40	9.17	1.53	40.60	4.31	0.72	37.80	4.78	0.80
15	39.00	7.95	1.33	43.50	4.07	0.68	40.50	4.31	0.72
16	41.60	8.61	1.44	46.40	4.13	0.69	43.20	4.51	0.75
17	44.20	9.59	1.60	49.30	4.37	0.73	45.90	4.38	0.73
18	46.80	8.66	1.44	52.20	4.56	0.76	48.60	4.06	0.68
19	49.40	8.88	1.48	55.10	4.53	0.76	51.30	3.89	0.65
20	52.00	9.04	1.51	58.00	4.57	0.76	54.00	4.23	0.71
21	54.60	9.23	1.54	60.90	4.56	0.76	56.70	4.16	0.69
22	57.20	9.35	1.56	63.80	4.34	0.72	59.40	4.29	0.72
23	59.80	8.76	1.46	66.70	4.42	0.74	62.10	4.52	0.75
24	62.40	7.88	1.31	69.60	4.46	0.74	64.80	4.43	0.74
25	65.00	6.13	1.02	72.50	4.16	0.69	67.50	4.40	0.73
26	67.60	6.62	1.10	75.40	4.45	0.74	70.20	4.53	0.76
27	70.20	6.54	1.09	78.30	4.40	0.73	72.90	4.93	0.82
28	72.80	6.72	1.12	81.20	4.44	0.74	75.60	5.69	0.95
29	75.40	5.99	1.00	84.10	4.50	0.75	78.30	4.88	0.81
30	78	6.09	1.02			20.40	81.00	4.84	0.81
31	80.6	6.88	1.15			0.70	83.70	4.68	0.78

Sample	Depth (cm)	Dry weight (g)	Density (g cm^{-3})	Depth (cm)	Dry weight (g)	Density (g cm^{-3})	Depth (cm)	Dry weight (g)	Density (g cm^{-3})
	Semer Water core 13			**Semer Water core 14**			**Semer Water core 15**		
1	2.50	4.84	0.81	2.60	7.25	1.21	2.70	3.13	0.52
2	5.00	3.96	0.66	5.20	7.08	1.18	5.40	2.96	0.49
3	7.50	5.34	0.89	7.80	7.46	1.24	8.10	3.80	0.63
4	10.00	5.71	0.95	10.40	6.79	1.13	10.80	3.61	0.60
5	12.50	6.03	1.01	13.00	6.71	1.12	13.50	3.76	0.63
6	15.00	6.10	1.02	15.60	6.30	1.05	16.20	4.09	0.68
7	17.50	6.40	1.07	18.20	6.16	1.03	18.90	4.32	0.72
8	20.00	6.65	1.11	20.80	5.72	0.95	21.60	4.57	0.76
9	22.50	6.46	1.08	23.40	5.80	0.97	24.30	4.69	0.78
10	25.00	7.69	1.28	26.00	6.18	1.03	27.00	4.62	0.77
11	27.50	7.88	1.31	28.60	6.18	1.03	29.70	4.68	0.78
12	30.00	7.39	1.23	31.20	6.10	1.02	32.40	4.50	0.75
13	32.50	6.20	1.03	33.80	6.16	1.03	35.10	4.26	0.71
14	35.00	7.80	1.30	36.40	6.48	1.08	37.80	4.19	0.70
15	37.50	8.34	1.39	39.00	6.60	1.10	40.50	4.17	0.70
16	40.00	7.92	1.32	41.60	6.93	1.16	43.20	4.32	0.72
17	42.50	8.35	1.39	44.20	7.22	1.20	45.90	4.40	0.73
18	45.00	9.38	1.56	46.80	6.92	1.15	48.60	4.28	0.71
19	47.50	7.87	1.31	49.40	6.98	1.16	51.30	4.60	0.77
20	50.00	6.30	1.05	52.00	7.03	1.17	54.00	4.62	0.77
21	52.50	6.00	1.00	54.60	7.21	1.20	56.70	4.43	0.74
22	55.00	6.23	1.04				59.40	4.48	0.75
23	57.50	6.12	1.02				62.10	4.18	0.70
24	60.00	8.04	1.34				64.80	4.47	0.75
25	62.50	6.04	1.01				67.50	4.13	0.69
26							70.20	4.29	0.72
27							72.90	4.38	0.73
28							75.60	4.50	0.75
29							78.30	4.37	0.73
30							81.00	4.28	0.71
31							83.70	4.26	0.71

Sample	Depth (cm)	Dry weight (g)	Density (g cm^{-3})	Depth (cm)	Dry weight (g)	Density (g cm^{-3})
	Semer Water core SL1			**Semer Water core SL2**		
1	2.19	2.08	0.35	2.36	2.97	0.50
2	4.38	2.65	0.44	4.72	3.00	0.50
3	6.56	2.53	0.42	7.08	3.35	0.56
4	8.75	2.66	0.44	9.44	3.34	0.56
5	10.94	3.00	0.50	11.80	3.36	0.56
6	13.13	2.91	0.49	14.16	3.19	0.53
7	15.32	2.92	0.49	16.52	3.15	0.53
8	17.50	2.90	0.48	18.88	3.07	0.51
9	19.69	2.84	0.47	21.24	3.00	0.50
10	21.88	2.75	0.46	23.60	3.15	0.53
11	24.07	2.68	0.45	25.96	3.17	0.53
12	26.26	2.66	0.44	28.32	3.11	0.52
13	28.44	1.88	0.31	30.68	3.13	0.52
14	30.63	2.50	0.42	33.04	3.13	0.52
15	32.82	2.30	0.38	35.40	3.16	0.53
16	35.01	2.57	0.43	37.76	2.91	0.49
17	37.20	2.92	0.49	40.12	3.02	0.50
18	39.38	2.62	0.44	42.48	2.76	0.46
19	41.57	2.83	0.47	44.84	3.15	0.53
20	43.76	2.53	0.42	47.20	3.13	0.52
21	45.95	2.69	0.45	49.56	3.25	0.54
22	48.14	2.59	0.43	51.92	3.09	0.52
23	50.32	2.86	0.48	54.28	3.18	0.53
24	52.51	2.73	0.46	56.64	3.26	0.54
25	54.70	2.55	0.43	59.00	3.07	0.51
26	56.89	2.40	0.40	61.36	3.07	0.51
27	59.08	2.78	0.46	63.72	3.29	0.55
28	61.26	2.48	0.41	66.08	3.06	0.51
29	63.45	3.02	0.50	68.44	3.13	0.52
30	65.64	3.24	0.54	70.80	2.95	0.49
31	67.83	2.72	0.45	73.16	3.12	0.52
32	70.02	2.88	0.48	75.52	3.24	0.54
33	72.20	2.97	0.50	77.88	3.26	0.54
34	74.39	3.17	0.53	80.24	3.36	0.56
35	76.58	2.53	0.42	82.60	3.16	0.53
36	78.77	2.76	0.46	84.96	3.18	0.53
37	80.96	2.55	0.43	87.32	3.45	0.58
38	83.14	2.80	0.47	89.68	3.41	0.57
39	85.33	2.17	0.36	92.04	3.48	0.58
40	87.52	2.45	0.41	94.40	3.83	0.64
41	89.71	2.48	0.41	96.76	3.94	0.66
42	91.90	2.21	0.37	99.12	3.78	0.63
43	94.08	1.41	0.24	101.48	3.66	0.61
44	96.27	2.90	0.48	103.84	3.76	0.63
45	98.46	3.77	0.63	106.20	3.40	0.57
46	100.65	4.05	0.68	108.56	3.51	0.59
47	102.84	3.89	0.65	110.92	3.51	0.59
48	105.02	4.11	0.69	113.28	3.40	0.57
49	107.21	3.94	0.66	115.64	3.54	0.59
50	109.40	3.56	0.59	118.00	3.79	0.63

Sample	Depth (cm)	Dry weight (g)	Density (g cm^{-3})	Depth (cm)	Dry weight (g)	Density (g cm^{-3})
51	111.59	3.66	0.61	120.36	3.70	0.62
52	113.78	3.59	0.60	122.72	3.54	0.59
53	115.96	3.58	0.60	125.08	3.44	0.57
54	118.15	3.06	0.51	127.44	3.57	0.60
55	120.34	3.44	0.57	129.80	3.32	0.55
56	122.53	3.57	0.60	132.16	3.46	0.58
57	124.72	3.83	0.64	134.52	3.21	0.54
58	126.90	4.12	0.69	136.88	3.12	0.52
59	129.09	4.16	0.69	139.24	3.26	0.54
60	131.28	4.39	0.73	141.60	3.06	0.51
61	133.47	4.17	0.70	143.96	2.99	0.50
62	135.66	3.47	0.58	146.32	3.01	0.50
63	137.84	2.83	0.47	148.68	3.31	0.55
64	140.03	3.25	0.54	151.04	3.06	0.51
65	142.22	4.28	0.71	153.40	3.32	0.55
66	144.41	4.28	0.71	155.76	3.33	0.56
67	146.60	4.77	0.80	158.12	3.29	0.55
68	148.78	4.17	0.70	160.48	3.26	0.54
69	150.97	3.96	0.66	162.84	3.64	0.61
70	153.16	4.21	0.70	165.20	3.58	0.60
71	155.35	3.50	0.58	167.56	3.53	0.59
72	157.54	3.63	0.61	169.92	3.41	0.57
73	159.72	3.96	0.66	172.28	3.39	0.57
74	161.91	4.17	0.70	174.64	3.39	0.57
75	164.10	4.44	0.74	177.00	3.37	0.56
76	166.29	4.00	0.67	179.36	3.59	0.60
77	168.48	4.17	0.70	181.72	3.75	0.63
78	170.66	3.23	0.54	184.08	3.58	0.60
79	172.85	4.26	0.71	186.44	3.67	0.61
80	175.04	5.57	0.93	188.80	3.72	0.62
81	177.23	5.53	0.92	191.16	3.87	0.65
82	179.42	5.42	0.90	193.52	3.63	0.61
83	181.60	5.49	0.92	195.88	4.28	0.71
84	183.79	4.75	0.79	198.24	4.32	0.72
85	185.98	4.73	0.79	200.60	4.08	0.68
86	188.17	4.23	0.71	202.96	3.95	0.66
87	190.36	4.09	0.68	205.32	4.49	0.75
88	192.54	4.14	0.69	207.68	4.56	0.76
89	194.73	4.96	0.83	210.04	4.60	0.77
90	196.92	4.84	0.81	212.40	4.59	0.77
91	199.11	4.62	0.77	214.76	4.87	0.81
92	201.30	4.87	0.81	217.12	4.96	0.83
93	203.48	5.12	0.85	219.48	5.00	0.83
94	205.67	5.77	0.96	221.84	4.66	0.78
95	207.86	5.42	0.90	224.20	4.87	0.81
96	210.05	4.88	0.81	226.56	4.61	0.77
97	212.24	4.03	0.67	228.92	4.46	0.74
98	214.42	4.03	0.67	231.28	4.46	0.74
99	216.61	4.34	0.72	233.64	4.17	0.70
100	218.80	4.61	0.77	236.00	4.49	0.75
101	220.99	4.73	0.79	238.36	4.20	0.70
102				240.72	3.98	0.66

Giddings core A				Giddings core B			Giddings core C		
Sample	Depth (cm)	Dry weight (g)	Density (g cm^{-3})	Depth (cm)	Dry weight (g)	Density (g cm^{-3})	Depth (cm)	Dry weight (g)	Density (g cm^{-3})
1	150	5.32	0.89	140	9.50	0.64	200	9.87	1.65
2	155	3.10	0.52	145	9.21	0.52	205	10.04	1.67
3	160	2.77	0.46	150	10.05	0.73	210	9.39	1.57
4	165	3.18	0.53	155	9.72	0.68	215	9.86	1.64
5	170	2.38	0.40	160	12.12	1.22	220	10.24	1.71
6	175	2.81	0.47	165	13.56	1.58	225	9.68	1.61
7	180	2.71	0.45	170	13.03	1.46	230	9.76	1.63
8	185	2.39	0.40	175	12.01	1.28	235	9.34	1.56
9	190	2.31	0.38	180	12.98	1.62	240	7.86	1.31
10	195	2.07	0.34	185	12.43	1.53	245	7.81	1.30
11	200	2.48	0.41	190	12.28	1.57	250	9.51	1.59
12	250	6.00	1.00	195	13.31	1.69	255	9.69	1.62
13	255	5.15	0.86	200	13.27	1.68	260	10.23	1.71
14	260	4.26	0.71	205	13.63	1.76	265	9.22	1.54
15	265	3.76	0.63	210	13.00	1.65	270	9.16	1.53
16	270	5.35	0.89	215	13.45	1.73	275	10.31	1.72
17	275	4.22	0.70	220	14.22	1.84	280	9.23	1.54
18	280	4.83	0.81	225	13.95	1.81	285	10.08	1.68
19	285	4.37	0.73	230	12.34	1.58	290	8.84	1.47
20	290	4.42	0.74	235	13.93	1.78	295	10.45	1.74
21	295	4.83	0.80	240	12.86	1.62	300	9.87	1.65
22	300	4.81	0.80	245	12.90	1.62	305	10.01	1.67
23	305	4.01	0.67	250	13.57	1.70	310	8.98	1.50
24	310	4.81	0.80	255	13.90	1.73	315	10.49	1.75
25	315	4.96	0.83	260	13.68	1.67	320	11.26	1.88
26	320	4.52	0.75	265	12.72	1.53	325	10.46	1.74
27	325	5.27	0.88	270	13.18	1.68	330	10.46	1.74
28	340	4.97	0.83	275	12.73	1.47	335	10.88	1.81
29	345	4.73	0.79	320	11.26	1.35	340	9.79	1.63
30	350	5.31	0.88	325	11.77	1.42	345	10.47	1.75
31	355	5.14	0.86	330	12.41	1.29	350	10.42	1.74
32	360	4.94	0.82	335	13.19	1.49	355	10.32	1.72
33	365	5.23	0.87	340	13.34	1.52	360	9.58	1.60
34	370	5.06	0.84	345	13.51	1.56	365	9.68	1.61
35	375	4.92	0.82	350	12.88	1.39	370	9.27	1.55
36	380	4.88	0.81	355	13.40	1.53	375	7.72	1.29
37	385	4.55	0.76	360	13.18	1.49	380	9.57	1.60
38	390	4.55	0.76	365	13.52	1.55	385	10.44	1.74
39	395	5.37	0.89	370	12.60	1.39	390	9.66	1.61
40	430	5.07	0.84	375	12.76	1.42	395	10.18	1.70
41	435	5.42	0.90	380	12.10	1.18	400	11.43	1.91
42	440	4.50	0.75	385	12.83	1.39	405	10.42	1.74
43	445	4.87	0.81	390	13.89	1.64	410	10.27	1.71
44	450	4.56	0.76	395	12.37	1.36	415	10.29	1.72
45	455	3.24	0.54	425	12.61	1.39	420	8.46	1.41
46	460	3.68	0.61	430	12.91	1.45	425	9.68	1.61
47	465	3.03	0.51	435	12.80	1.36	430	8.26	1.38
48	470	3.33	0.56	440	12.67	1.33	435	9.34	1.56
49	475	3.11	0.52	445	12.69	1.36	440	8.67	1.45
50	480	4.00	0.67	450	13.29	1.52	445	8.89	1.48

Giddings core A				Giddings core B			Giddings core C		
Sample	Depth (cm)	Dry weight (g)	Density (g cm^{-3})	Depth (cm)	Dry weight (g)	Density (g cm^{-3})	Depth (cm)	Dry weight (g)	Density (g cm^{-3})
51	485	4.20	0.70	455	12.97	1.50	450	6.65	1.11
52	490	3.66	0.61	460	12.53	1.34	455	7.22	1.20
53	495	3.40	0.57	465	11.13	1.17	460	6.71	1.12
54	515	3.60	0.60	470	13.42	1.57	465	9.26	1.54
55	520	3.29	0.55	475	12.74	1.44	470	8.86	1.48
56	525	3.76	0.63	480	11.94	1.09	475	8.27	1.38
57	530	4.03	0.67	485	12.04	1.18	480	7.11	1.19
58	535	5.43	0.90	490	12.39	1.30	485	7.99	1.33
59	540	4.07	0.68	495	12.18	1.36	490	7.01	1.17
60	545	5.23	0.87	515	12.48	1.44	495	7.78	1.30
61	550	5.05	0.84	520	11.97	1.35	500	6.36	1.06
62	555	5.69	0.95	525	11.17	1.24	505	8.06	1.34
63	560	5.85	0.97	530	9.84	0.91	510	6.12	1.02
64	565	5.76	0.96	535	12.53	1.40	515	7.86	1.31
65	570	5.52	0.92	540	12.63	1.44	520	8.15	1.36
66	575	5.42	0.90	545	9.89	0.89	525	7.25	1.21
67	580	5.32	0.89	550	11.40	1.04	530	7.72	1.29
68	585	5.08	0.85	555	11.68	1.24	535	6.95	1.16
69	590	5.99	1.00	560	11.64	1.05	540	6.66	1.11
70	595	3.80	0.63	565	11.24	1.04	545	7.56	1.26
71	600	4.84	0.81	570	12.50	1.34	550	6.34	1.06
72	605	5.08	0.85	575	11.50	1.05	555	7.14	1.19
73	610	6.05	1.01	580	13.02	1.51	560	7.52	1.25
74	615	6.46	1.08	585	12.02	1.23	565	6.15	1.03
75	620	6.09	1.02	590	12.00	1.13	570	6.54	1.09
76	625	6.11	1.02	595	11.57	1.04	575	6.98	1.16
77	630	6.39	1.06	630	11.73	1.11	580	6.40	1.07
78	635	6.58	1.10	635	9.97	0.86	585	6.40	1.07
79	640	9.15	1.52	640	11.13	1.00	590	7.43	1.24
80	645	5.66	0.94	645	11.96	1.15	595	6.69	1.12
81	650	12.76	2.13	650	11.18	0.98	600	7.23	1.21
82	655	12.31	2.05	655	11.93	1.13	605	6.81	1.14
83	660	11.28	1.88	660	13.70	1.61	610	6.94	1.16
84	665	12.22	2.04	665	11.02	0.94	615	5.51	0.92
85	670	10.90	1.82	670	11.50	1.08	620	5.61	0.94
86	675	11.69	1.95	675	12.40	1.28	625	5.92	0.99
87	680	11.56	1.93	680	11.76	1.16	630	5.97	1.00
88	685	10.96	1.83	685	11.77	1.20	635	5.26	0.88
89	750	8.84	1.47	690	11.36	1.03	640	7.62	1.27
90	755	7.62	1.27	695	12.54	1.47	645	6.76	1.13
91	760	11.54	1.92	725	10.27	0.93	650	6.54	1.09
92	765	11.57	1.93	730	10.41	0.93	655	6.31	1.05
93	770	8.67	1.45	735	11.08	0.94	660	7.15	1.19
94	775	9.45	1.57	740	10.92	0.93	665	6.36	1.06
95	780	9.56	1.59	745	11.08	0.94	670	7.15	1.19
96	785	10.48	1.75	750	11.59	1.09	675	5.82	0.97
97	790	8.40	1.40	755	11.91	1.14	680	7.29	1.22
98	795	9.47	1.58	760	11.39	1.08	685	6.07	1.01
99	800	10.26	1.71	765	11.28	1.02	690	6.45	1.08
100	805	11.14	1.86	770	11.02	1.00	695	5.69	0.95

Giddings core A				Giddings core B			Giddings core C		
Sample	Depth (cm)	Dry weight (g)	Density (g cm^{-3})	Depth (cm)	Dry weight (g)	Density (g cm^{-3})	Depth (cm)	Dry weight (g)	Density (g cm^{-3})
101	810	10.98	1.83	775	11.11	1.06	770	9.25	1.77
102	815	10.65	1.78	780	11.03	1.02	775	8.67	1.80
103	820	9.67	1.61	785	10.86	0.97	780	8.04	1.34
104	825	10.42	1.74	790	10.67	0.92	785	8.26	1.38
105	905	10.60	1.77	795	8.53	0.72	790	7.39	1.23
106	910	11.28	1.88	800	10.89	1.16	795	6.47	1.08
107	915	9.04	1.51	805	10.16	0.84	800	6.87	1.15
108	920	11.47	1.91	810	11.44	1.05	805	6.60	1.10
109	925	11.02	1.84	815	11.92	1.16	810	6.90	1.15
110	930	5.46	0.91	820	12.02	1.21	815	7.32	1.22
111	935	5.46	0.91	825	11.95	1.17	820	8.43	1.41
112	940	5.15	0.86	830	10.97	1.03	825	7.90	1.32
113	945	5.79	0.97	835	11.53	1.15	830	6.16	1.03
114	950	9.19	1.53	840	11.89	1.22	835	6.46	1.08
115	955	9.78	1.63	845	11.91	1.20	840	6.91	1.15
116	960	11.07	1.85	850	11.83	1.19	845	7.27	1.21
117	965	11.66	1.94	855	11.93	1.21	850	6.45	1.08
118	970	11.57	1.93	860	11.58	1.15	855	3.90	0.65
119	975	11.12	1.85	865	10.87	1.07	860	8.87	1.48
120	980	11.88	1.98	870	11.12	1.11	865	5.47	0.91
121	985	11.85	1.98	875	10.26	0.99	870	5.34	0.89
122	990	12.66	2.11	880	10.40	1.02	875	7.06	1.18
123	995	12.36	2.06	900	9.25	1.54	880	6.01	1.00
124	1000	11.93	1.99	905	9.62	1.60	885	4.77	0.80
125	1005	11.72	1.95	910	10.10	1.68	890	6.34	1.06
126	1010	11.39	1.90	915	9.53	1.59	895	7.50	1.25
127	1015	13.29	2.21	920	9.48	1.58	900	6.89	1.15
128				925	7.86	1.31	905	6.06	1.01
129				930	9.38	1.56	910	6.54	1.09
130				935	7.61	1.27	915	7.77	1.30
131				940	5.44	0.91	920	6.56	1.09
132				945	6.56	1.09	925	7.05	1.18
133				950	6.09	1.02	930	6.41	1.07
134				955	7.16	1.19	935	6.84	1.14
135				960	7.61	1.27	940	5.56	0.93
136				965	6.30	1.05	945	9.77	1.63
137				970	5.88	0.98	950	8.96	1.49
138				975	6.73	1.12	955	8.13	1.36
139				990	3.29	0.55	960	9.67	1.61
140				995	5.45	0.91	965	8.75	1.46
141				1000	11.01	1.84	970	9.78	1.63
142				1005	10.31	1.72	975	10.51	1.75
143				1010	9.71	1.62	980	8.25	1.38
144				1015	9.40	1.57	985	6.95	1.16
145				1020	9.85	1.64	990	9.46	1.58
146				1025	9.62	1.60	995	9.42	1.57
147				1030	9.95	1.66	1000	6.44	1.07
148				1035	8.70	1.45	1005	7.13	1.19
149				1040	7.51	1.25	1010	5.89	0.98
150				1045	7.60	1.27	1015	6.70	1.12

Giddings core A				Giddings core B			Giddings	7.93	1.32167
Sample	Depth (cm)	Dry weight (g)	Density (g cm^{-3})	Depth (cm)	Dry weight (g)	Density (g cm^{-3})	Depth (cm)	8.58	1.43
151				1050	7.29	1.22	1020	8.11	1.35
152				1055	6.22	1.04	1025	4.91	0.82
153				1060	7.08	1.18	1030	7.93	1.32
154				1065	7.24	1.21	1035	6.78	1.13
155				1070	6.19	1.03	1040	6.53	1.09
156				1075	5.78	0.96	1045	5.92	0.99
157				1080	6.21	1.04	1050	8.05	1.34
158				1085	7.37	1.23	1055	9.82	1.64
159				1090	6.14	1.02	1060	10.37	1.73
160				1095	7.97	1.33	1065	8.43	1.41
161				1100	9.52	1.59	1070	8.63	1.44
162				1105	9.47	1.58	1075	8.07	1.35
163				1110	8.78	1.46	1080	8.63	1.44
164				1115	8.11	1.35	1085	10.12	1.69
165				1120	9.99	1.67	1090	8.79	1.47
166				1125	9.98	1.66	1095	10.35	1.73
167				1130	8.93	1.49	1100	10.63	1.77
168				1135	8.77	1.46	1105	10.54	1.76
169				1140	9.47	1.58	1110	10.36	1.73
170				1145	7.91	1.32	1115	9.68	1.61
171				1150	7.28	1.21	1120	9.83	1.64
172				1155	6.48	1.08	1125	9.60	1.60
173				1160	6.24	1.04	1130	9.09	1.52
174				1165	5.50	0.92	1135	9.93	1.66
175				1170	6.59	1.10	1140	7.19	1.20
176				1175	6.51	1.09	1145	7.93	1.32
177				1180	7.26	1.21	1150	6.86	1.14
178				1185	6.59	1.10	1155	7.36	1.23
179				1190	7.22	1.20	1160	7.36	1.23
180				1260	8.82	1.47	1165	7.38	1.23
181				1265	9.46	1.58	1170	7.15	1.19
182				1270	9.87	1.65	1175	6.69	1.12
183				1275	10.36	1.73	1180	6.73	1.12
184				1280	10.45	1.74	1185	6.31	1.05
185				1285	9.96	1.66	1190	7.96	1.33
186				1290	7.29	1.22	1195	7.53	1.26
187				1295	6.19	1.03	1200	7.88	1.31
188				1300	9.36	1.56	1205	7.15	1.19
189				1305	8.75	1.46	1210	7.59	1.27
190				1310	8.32	1.39	1215	8.84	1.47
191				1315	9.54	1.59	1220	8.99	1.50
192				1320	10.46	1.74	1225	6.84	1.14
193				1325	7.84	1.31	1230	6.84	1.14
194				1330	10.21	1.70	1235	6.20	1.03
195				1335	9.91	1.65	1240	6.41	1.07
196				1340	9.08	1.51	1245	6.93	1.16
197				1345	10.15	1.69	1250	6.41	1.07
198				1350	10.07	1.68	1255	7.00	1.17
199				1355	9.82	1.64	1260	7.26	1.21
200				1360	10.25	1.71	1265	7.49	1.25

Giddings core A				Giddings core B			Giddings	6.78	1.13
Sample	Depth (cm)	Dry weight (g)	Density (g cm^{-3})	Depth (cm)	Dry weight (g)	Density (g cm^{-3})	Depth (cm)	7.36	1.2266667
201				1365	9.38	1.56	1270	6.50	1.08
202				1370	9.16	1.53	1275	9.69	1.62
203				1375	8.43	1.41	1280	10.63	1.77
204				1380	7.43	1.24	1285	10.16	1.69
205				1385	6.07	1.01	1290	8.53	1.42
206				1390	5.78	0.96	1295	8.63	1.44
207				1395	5.45	0.91	1300	10.97	1.83
208				1400	7.49	1.25	1305	5.95	0.99
209				1405	9.72	1.62	1310	6.34	1.06
210				1410	10.38	1.73	1315	7.14	1.19
211				1415	9.35	1.56	1320	7.36	1.23
212				1420	9.32	1.55	1325	6.78	1.13
213				1425	8.78	1.46	1330	7.20	1.20
214				1430	9.56	1.59	1335	6.78	1.13
215				1435	10.22	1.70	1340	5.97	1.00
216				1440	10.51	1.75	1345	10.79	1.80
217				1445	9.95	1.66	1350	5.88	0.98
218				1450	9.87	1.65	1355	6.18	1.03
219				1455	9.91	1.65	1360	6.93	1.16
220				1460	10.16	1.69	1365		0.00
221				1465	10.45	1.74	1370		0.00
222				1470	8.19	1.37	1375		0.00
223				1475	9.87	1.65	1380		0.00
224				1480	6.36	1.06			
225				1485	6.85	1.14			

Sample	Depth (cm)	Dry weight (g)	Density (g cm^{-3})	Depth (cm)	Dry weight (g)	Density (g cm^{-3})	Depth (cm)	Dry weight (g)	Density (g cm^{-3})	Depth (cm)	Dry weight (g)	Density (g cm^{-3})
	Gormire core 1			**Gormire core 2**			**Gormire core 3**			**Gormire core 4**		
1	2.65	1.09	0.18	2.54	2.57	0.45	2.57	1.30	0.22	2.60	1.91	0.32
2	5.3	1.64	0.27	5.08	5.14	0.47	5.14	1.25	0.21	5.20	1.91	0.32
3	7.95	1.65	0.28	7.62	7.71	0.49	7.71	1.38	0.23	7.80	1.87	0.31
4	10.6	1.94	0.32	10.16	10.28	0.54	10.28	1.31	0.22	10.40	1.79	0.30
5	13.25	1.85	0.31	12.70	12.85	0.61	12.85	1.65	0.28	13.00	1.88	0.31
6	15.9	1.98	0.33	15.24	15.42	0.54	15.42	1.57	0.26	15.60	1.80	0.30
7	18.55	2.53	0.42	17.78	17.99	0.61	17.99	1.55	0.26	18.20	2.11	0.35
8	21.2	2.7	0.45	20.32	20.56	0.53	20.56	1.64	0.27	20.80	2.22	0.37
9	23.85	1.8	0.30	22.86	23.13	0.51	23.13	1.97	0.33	23.40	2.10	0.35
10	26.5	1.82	0.30	25.40	25.70	0.51	25.70	1.97	0.33	26.00	2.07	0.35
11	29.15	1.68	0.28	27.94	28.27	0.51	28.27	2.13	0.36	28.60	2.22	0.37
12	31.8	1.8	0.30	30.48	30.84	0.43	30.84	2.14	0.36	31.20	2.52	0.42
13	34.45	2.07	0.35	33.02	33.41	0.43	33.41	2.44	0.41	33.80	2.34	0.39
14	37.1	2.14	0.36	35.56	35.98	0.39	35.98	2.17	0.36	36.40	2.18	0.36
15	39.75	2.44	0.41	38.10	38.55	0.31	38.55	2.20	0.37	39.00	2.14	0.36
16	42.4	2.27	0.38	40.64	41.12	0.27	41.12	2.07	0.35	41.60	2.09	0.35
17	45.05	2.41	0.40	43.18	43.69	0.28	43.69	1.99	0.33	44.20	1.84	0.31
18	47.7	2.18	0.36	45.72	46.26	0.26	46.26	2.05	0.34	46.80	1.89	0.32
19	50.35	1.99	0.33	48.26	48.83	0.25	48.83	1.80	0.30	49.40	1.81	0.30
20	53	1.86	0.31	50.80	51.40	0.26	51.40	1.51	0.25	52.00	1.48	0.25
21	55.65	1.55	0.26	53.34	53.97	0.22	53.97	1.55	0.26	54.60	1.31	0.22
22	58.3	1.74	0.29	55.88	56.54	0.23	56.54	1.79	0.30	57.20	1.45	0.24
23	60.95	1.83	0.31	58.42	59.11	0.22	59.11	1.61	0.27	59.80	1.22	0.20
24	63.6	1.98	0.33	60.96	61.68	0.23	61.68	1.70	0.28	62.40	1.37	0.23
25	66.25	1.75	0.29	63.50	64.25	0.40	64.25	1.64	0.27	65.00	1.25	0.21
26	68.9	1.61	0.27	66.04	66.82	0.00	66.82	1.62	0.27	67.60	1.21	0.20
27	71.55	1.56	0.26	68.58	69.39	0.00	69.39	1.44	0.24	70.20	1.27	0.21
28	74.2	1.47	0.25	71.12	71.96	0.00	71.96	1.45	0.24	72.80	1.24	0.21
29	76.85	1.88	0.31	73.66	74.53	0.00	74.53	1.61	0.27	75.40	1.41	0.24
30				76.20	77.10	0.00	77.10	1.62	0.27	78.00	1.47	0.25

Sample	Depth (cm)	Dry weight (g)	Density (g cm^{-3})	Depth (cm)	Dry weight (g)	Density (g cm^{-3})	Depth (cm)	Dry weight (g)	Density (g cm^{-3})
	Hornsea Mere 1			**Hornsea Mere 2**			**Hornsea Mere 3**		
1	2.56	11.86	1.186	2.65	2.65	0.245	2.62	2.89	0.289
2	5.12	12	1.2	5.3	5.3	0.316	5.24	3.1	0.31
3	7.68	8.78	0.878	7.95	7.95	0.369	7.86	3.47	0.347
4	10.24	9.05	0.905	10.6	10.6	0.331	10.48	3.51	0.351
5	12.8	7.07	0.707	13.25	13.25	0.342	13.1	3.69	0.369
6	15.36	7.87	0.787	15.9	15.9	0.338	15.72	4.23	0.423
7	17.92	7.78	0.778	18.55	18.55	0.339	18.34	3.74	0.374
8	20.48	7.57	0.757	21.2	21.2	0.317	20.96	3.72	0.372
9	23.04	7.2	0.72	23.85	23.85	0.353	23.58	3.74	0.374
10	25.6	7.34	0.734	26.5	26.5	0.342	26.2	4	0.4
11	28.16	6.12	0.612	29.15	29.15	0.344	28.82	3.92	0.392
12	30.72	6.56	0.656	31.8	31.8	0.336	31.44	4.5	0.45
13	33.28	5.79	0.579	34.45	34.45	0.315	34.06	5.19	0.519
14	35.84	5.91	0.591	37.1	37.1	0.326	36.68	5.8	0.58
15	38.4	5.5	0.55	39.75	39.75	0.348	39.3	4.96	0.496
16	40.96	5.26	0.526	42.4	42.4	0.367	41.92	4.69	0.469
17	43.52	5.68	0.568	45.05	45.05	0.369	44.54	5	0.5
18	46.08	6.07	0.607	47.7	47.7	0.368	47.16	5.55	0.555
19	48.64	5.67	0.567	50.35	50.35	0.37	49.78	5.14	0.514
20	51.2	6.07	0.607	53	53	0.37	52.4	4.95	0.495
21	53.76	7.11	0.711	55.65	55.65	0.396	55.02	5.23	0.523
22	56.32	7.42	0.742	58.3	58.3	0.427	57.64	5.02	0.502
23	58.88	6.2	0.62	60.95	60.95	0.426	60.26	4.65	0.465
24	61.44	5.32	0.532				62.88	4.88	0.488
25	64	5.16	0.516				65.5	4.7	0.47
26	66.56	4.77	0.477				68.12	4.31	0.431
27	69.12	5.88	0.588				70.74	4.49	0.449
28	71.68	5.48	0.548				73.36	4.2	0.42
29	74.24	5.57	0.557				75.98	4.69	0.469
30	76.8	6.13	0.613						

Sample	Depth (cm)	Dry weight (g)	Density (g cm^{-3})	Depth (cm)	Dry weight (g)	Density (g cm^{-3})	Depth (cm)	Dry weight (g)	Density (g cm^{-3})
	Hornsea Mere 4			**Hornsea Mere 5**			**Hornsea Mere 6**		
1	2.56	2.33	0.233	2.56	1.96	0.196	2.63	3.76	0.376
2	5.12	3.34	0.334	5.12	2.17	0.217	5.26	3.69	0.369
3	7.68	3.4	0.34	7.68	2.18	0.218	7.89	3.65	0.365
4	10.24	3.91	0.391	10.24	2.18	0.218	10.52	3.72	0.372
5	12.8	3.89	0.389	12.8	2.5	0.25	13.15	3.82	0.382
6	15.36	3.73	0.373	15.36	2.57	0.257	15.78	3.98	0.398
7	17.92	3.69	0.369	17.92	2.9	0.29	18.41	4.18	0.418
8	20.48	4.06	0.406	20.48	2.76	0.276	21.04	4.08	0.408
9	23.04	4.07	0.407	23.04	3	0.3	23.67	3.83	0.383
10	25.6	3.56	0.356	25.6	3.11	0.311	26.3	3.95	0.395
11	28.16	3.32	0.332	28.16	2.87	0.287	28.93	3.95	0.395
12	30.72	4.94	0.494	30.72	3.13	0.313	31.56	3.81	0.381
13	33.28	4.6	0.46	33.28	2.97	0.297	34.19	3.91	0.391
14	35.84	3.63	0.363	35.84	3.12	0.312	36.82	4.14	0.414
15	38.4	3.94	0.394	38.4	3.01	0.301	39.45	3.72	0.372
16	40.96	4.43	0.443	40.96	2.89	0.289	42.08	3.9	0.39
17	43.52	4.82	0.482	43.52	3.13	0.313	44.71	3.94	0.394
18	46.08	4.95	0.495	46.08	2.94	0.294	47.34	3.76	0.376
19	48.64	5.09	0.509	48.64	3.14	0.314	49.97	3.74	0.374
20	51.2	5.08	0.508	51.2	3.1	0.31	52.6	3.76	0.376
21	53.76	5.42	0.542	53.76	2.96	0.296	55.23	3.87	0.387
22	56.32	5.66	0.566	56.32	2.95	0.295	57.86	3.82	0.382
23	58.88	5.08	0.508	58.88	2.93	0.293	60.49	3.56	0.356
24	61.44	5.42	0.542	61.44	3.08	0.308	63.12	3.3	0.33
25	64	5.65	0.565	64	3.03	0.303	65.75	3.43	0.343
26	66.56	5.39	0.539	66.56	2.89	0.289	68.38	3.27	0.327
27	69.12	5.37	0.537	69.12	2.78	0.278	71.01	3.1	0.31
28	71.68	5.08	0.508	71.68	2.7	0.27	73.64	3.29	0.329
29	74.24	4.61	0.461	74.24	2.73	0.273	76.27	3.11	0.311
30	76.8	4.36	0.436	76.8	2.81	0.281	78.9	3.1	0.31
31	79.36	4.57	0.457	79.36	2.48	0.248			
32	81.92	4.3	0.43	81.92	2.79	0.279			

Sample	Depth (cm)	Dry weight (g)	Density (g cm^{-3})	Depth (cm)	Dry weight (g)	Density (g cm^{-3})	Depth (cm)	Dry weight (g)	Density (g cm^{-3})
	Hornsea Mere core 7			**Hornsea Mere core 8**			**Hornsea Mere core 9**		
1	2.62	1.77	0.177	2.69	1.95	0.195	2.58	1.84	0.184
2	5.24	2.19	0.219	5.38	2.07	0.207	5.16	2.18	0.218
3	7.86	2.52	0.252	8.07	2.21	0.221	7.74	2.42	0.242
4	10.48	3.15	0.315	10.76	2.53	0.253	10.32	2.62	0.262
5	13.1	2.39	0.239	13.45	2.66	0.266	12.9	2.64	0.264
6	15.72	3.01	0.301	16.14	2.79	0.279	15.48	3.03	0.303
7	18.34	2.81	0.281	18.83	2.98	0.298	18.06	3.08	0.308
8	20.96	2.95	0.295	21.52	3.52	0.352	20.64	3.19	0.319
9	23.58	2.86	0.286	24.21	2.58	0.258	23.22	3.44	0.344
10	26.2	3.02	0.302	26.9	3	0.3	25.8	3.5	0.35
11	28.82	3.01	0.301	29.59	3.01	0.301	28.38	3.64	0.364
12	31.44	3.29	0.329	32.28	3.15	0.315	30.96	4.07	0.407
13	34.06	3.06	0.306	34.97	3.5	0.35	33.54	3.82	0.382
14	36.68	3.51	0.351	37.66	3.35	0.335	36.12	3.69	0.369
15	39.3	3.26	0.326	40.35	3.89	0.389	38.7	3.93	0.393
16	41.92	3.02	0.302	43.04	3.62	0.362	41.28	3.92	0.392
17	44.54	3.36	0.336	45.73	4.14	0.414	43.86	4.11	0.411
18	47.16	3.34	0.334	48.42	3.65	0.365	46.44	4.43	0.443
19	49.78	3.44	0.344	51.11	3.7	0.37	49.02	5.03	0.503
20	52.4	3.39	0.339	53.8	3.48	0.348	51.6	5.13	0.513
21	55.02	3.33	0.333	56.49	3.3	0.33	54.18	4.89	0.489
22	57.64	3.58	0.358	59.18	3.51	0.351	56.76	4.66	0.466
23	60.26	3.41	0.341	61.87	3.64	0.364	59.34	4.56	0.456
24	62.88	3.22	0.322	64.56	3.43	0.343	61.92	4.43	0.443
25	65.5	3.23	0.323	67.25	3.48	0.348	64.5	4.64	0.464
26	68.12	3.39	0.339	69.94	3.31	0.331	67.08	4.13	0.413
27	70.74	3.28	0.328				69.66	4.18	0.418
28	73.36	3.48	0.348				72.24	3.91	0.391
29	75.98	3.23	0.323				74.82	3.67	0.367

Sample	Depth (cm)	Dry weight (g)	Density (g cm^{-3})
	Hornsea Mere core 10		
1	2.54	1.76	0.176
2	5.08	1.87	0.187
3	7.62	2.12	0.212
4	10.16	2.38	0.238
5	12.7	2.87	0.287
6	15.24	3.15	0.315
7	17.78	3.42	0.342
8	20.32	3.83	0.383
9	22.86	4.12	0.412
10	25.4	4.64	0.464
11	27.94	4.48	0.448
12	30.48	4.46	0.446
13	33.02	5.12	0.512
14	35.56	4.46	0.446
15	38.1	4.11	0.411
16	40.64	3.65	0.365
17	43.18	3.62	0.362
18	45.72	3.59	0.359
19	48.26	3.5	0.35
20	50.8	3.23	0.323
21	53.34	3.29	0.329
22	55.88	2.94	0.294
23	58.42	2.92	0.292
24	60.96	2.73	0.273
25	63.5	2.91	0.291
26	66.04	2.88	0.288
27	68.58	2.95	0.295
28	71.12	2.69	0.269
29	73.66	3.07	0.307
30	76.2	3.08	0.308
31	78.74	3.38	0.338
32	81.28	3.14	0.314
33	83.82	3.21	0.321
34	86.36	3.24	0.324
35	88.9	3.04	0.304

Appendix I

Giddings core sediment descriptions

Giddings core A

Altitude OD (m)	Thickness (m)	Stratigraphy	Boundary
249.00	0.50	Unrecovered	
248.50	0.50	Peat	
248.00	0.50	Unrecovered	
247.50	0.44	50% clay, 25% silt, 25% shells	Gradual
247.06	0.29	50% silt, 25% clay, 25% shells	Gradual
246.77	0.07	50% silt, 50% clay	
246.70	0.10	Unrecovered	
246.60	0.60	50% silt, 50% clay	
246.00	0.30	Unrecovered	
245.70	0.70	50% silt, 25% clay, 25% shells	
245.00	0.15	Unrecovered	
244.85	1.23	50% clay, 25% silt, 25% shells	Gradual
243.62	0.11	75% clay, 25% silt	Gradual
243.51	0.07	75% silt, 25% clay	Gradual
243.44	0.01	50% silt, 50% clay	Sharp
243.43	0.02	100% sand	Sharp, erosive base
243.41	0.07	75% silt, 25% clay	Sharp
243.34	0.01	75% sand, 25% gravel	Sharp
243.33	0.01	100% sand	Sharp, erosive base
243.32	0.01	100% silt	Sharp
234.31	0.07	75% sand, 25% gravel	Sharp
243.24	0.13	75% silt, 25% clay	
243.11	0.12	Unrecovered	
242.99	0.70	75% sand, 25% silt	Sharp
242.29	0.08	50% silt, 50% sand	
242.21	0.22	Unrecovered	
241.99	0.27	25% silt, 75% sand	
241.72	0.72	Unrecovered	
241.00	0.19	50% silt, 50% clay	Sharp
240.81	0.19	50% silt, 50% sand	Gradual
240.62	0.33	75% sand, 25% silt	Gradual
240.29	1.20	50% sand, 50% silt	Base of core

Giddings core B

Altitude (m)	Thickness (m)	Stratigraphy	Boundary
249.00	1.00	Unrecovered	
248.00	0.25	Peat/soil	Sharp
247.75	0.37	75% sand, 25% silt	
247.38	0.38	Unrecovered	
247.00	1.00	75% sand, 25% silt	Gradual
246.00	0.83	50% silt, 50% clay	
245.17	0.17	Unrecovered	
245.00	0.50	50% silt, 50% clay	Gradual
244.50	0.16	75% clay, 25% silt	
244.34	0.34	Unrecovered	
244.00	0.83	50% silt, 50% clay	
243.17	0.17	Unrecovered	
243.00	0.68	50% silt, 50% clay	
242.32	0.32	Unrecovered	
242.00	1.53	50% silt, 50% clay	Gradual
240.47	0.50	50% sand, 25% silt, 25% clay	Sharp
239.97	0.08	100% peat	Sharp
239.89	0.12	50% sand, 25% silt, 25% clay	Sharp
239.77	0.30	75% sand, 25% silt	Diffuse
239.47	0.70	50% silt, 50% clay	Diffuse
238.77	0.57	75% sand, 25% silt	
238.20	0.08	Unrecovered	
238.12	0.35	50% sand, 25% silt, 25% clay	
237.77	0.65	Unrecovered	
237.12	0.64	75% sand, 25% silt	Gradual
236.48	0.36	50% silt, 25% clay, 25% sand	Gradual
236.12	0.79	100% silt	Sharp
235.33	0.15	50% silt, 50% sand	Base of core

Giddings core C

Altitude (m)	Thickness (m)	Stratigraphy	Boundary
249.00	2.00	Unrecovered	
274.00	2.35	75% sand, 25% silt	Gradual
244.65	1.90	50% silt, 50% sand	Gradual
242.75	0.65	75% sand, 25% silt	
242.10	0.70	Unrecovered	
241.40	2.40	75% sand, 25% silt	Gradual
239.00	3.60	50% sand, 50% silt	Base of core

Appendix J

Lake Sediment Magnetic Data

Giddings core A

Sample	Depth	χ	ARM	IRM_{100}	SIRM
	cm	$\mu\ m^3\ kg^{-1}$	$mA\ m^2\ kg^{-1}$	$mA\ m^2\ kg^{-1}$	$mA\ m^2\ kg^{-1}$
1	150	0.0411	0.0153	0.1039	0.1392
2	155	0.0186	0.0091	0.0773	0.1000
3	160	0.0055	0.0250	0.1417	0.2042
4	165	0.0059	0.0167	0.0681	0.0861
5	170	0.0000	0.2800	0.9800	1.2600
6	175	0.0073	0.0341	0.1415	0.1854
7	180	0.0000	0.0271	0.1034	0.1356
8	185	0.0000	0.0586	0.2655	0.3517
9	190	0.0000	0.1045	0.6091	1.0091
10	195	0.0000	0.1050	0.4300	0.5500
11	200	0.0184	0.0811	0.5622	0.7486
12	250	0.0216	0.0397	0.3300	0.4960
13	255	0.0229	0.0254	0.1734	0.2433
14	260	0.0171	0.0266	0.1605	0.2319
15	265	0.0104	0.0297	0.1620	0.2227
16	270	0.0111	0.0253	0.1050	0.1355
17	275	0.0230	0.1620	0.7339	0.8542
18	280	0.0465	0.3153	1.7465	1.9355
19	285	0.0485	0.2489	1.9072	2.1964
20	290	0.0240	0.1470	0.8102	0.9473
21	295	0.0256	0.1097	0.6607	0.8813
22	300	0.0276	0.0601	0.3390	0.4506
23	305	0.0210	0.0539	0.3240	0.4376
24	310	0.0158	0.0193	0.1205	0.1736
25	315	0.0173	0.0358	0.2679	0.4653
26	320	0.0146	0.0454	0.1981	0.2558
27	325	0.0326	0.1385	0.6121	0.6743
28	340	0.0268	0.1179	0.5171	0.5637
29	345	0.0180	0.0834	0.3742	0.4260
30	350	0.0283	0.1232	0.6709	0.8066
31	355	0.0260	0.0768	0.4533	0.5891
32	360	0.0231	0.0656	0.4112	0.6079
33	365	0.0292	0.1110	0.7209	0.9752
34	370	0.0203	0.0677	0.3097	0.3983
35	375	0.0984	0.3320	2.3736	2.9103
36	380	0.1066	0.4096	2.7709	3.4301
37	385	0.0668	0.2053	1.4027	1.8615
38	390	0.0871	0.2429	1.6904	2.1277
39	395	0.0633	0.1463	0.8937	1.1873
40	430	0.0285	0.0779	0.4336	0.5590
41	435	0.0569	0.1358	0.8557	1.1801
42	440	0.0316	0.0784	0.3798	0.4420
43	445	0.0393	0.2068	1.1826	1.4114
44	450	0.0270	0.1308	0.7286	0.9662
45	455	0.0573	0.1855	1.3877	2.0742
46	460	0.0982	0.3450	2.3840	2.9971
47	465	0.0862	0.2481	1.6984	2.1519
48	470	0.0743	0.2367	1.4804	1.9653

49	475	0.0673	0.1657	0.9686	1.1884
50	480	0.0792	0.2250	1.5481	2.0497
51	485	0.0691	0.2045	1.3149	1.7748
52	490	0.0620	0.1975	1.1916	1.5394
53	495	0.0547	0.1510	0.8179	0.9871
54	515	0.0439	0.0933	0.5156	0.6210
55	520	0.0405	0.1199	0.7732	1.0759
56	525	0.0690	0.2030	1.4289	1.8588
57	530	0.0564	0.1974	1.1774	1.6440
58	535	0.0433	0.1785	1.0597	1.3319
59	540	0.0260	0.0981	0.4359	0.5017
60	545	0.0486	0.1771	1.2185	1.5251
61	550	0.0541	0.1792	1.1730	1.5131
62	555	0.0569	0.1331	0.6114	1.1804
63	560	0.0319	0.0881	0.4618	0.5609
64	565	0.0426	0.1054	0.6447	0.8288
65	570	0.0550	0.1388	0.8169	0.9914
66	575	0.0632	0.1583	0.8779	1.1160
67	580	0.0570	0.1361	0.7699	0.9294
68	585	0.0403	0.0851	0.4895	0.5871
69	590	0.1035	0.2405	1.7423	2.2128
70	595	0.0410	0.0812	0.5472	0.8595
71	600	0.0302	0.0826	0.4253	0.5109
72	605	0.0481	0.1577	1.0165	1.3209
73	610	0.0520	0.1322	0.9539	1.4352
74	615	0.0458	0.1193	0.8133	1.2744
75	620	0.0501	0.1236	0.7649	1.1091
76	625	0.0548	0.1560	0.9895	1.2829
77	630	0.0586	0.1548	0.9524	1.2119
78	635	0.0435	0.0821	0.5214	0.7868
79	640	0.0556	0.0413	0.2490	0.8608
80	645	0.0632	0.0352	0.3026	0.9683
81	650	0.0518	0.0060	0.0608	0.0952
82	655	0.0805	0.0058	0.0713	0.1127
83	660	0.0488	0.0042	0.0363	0.0638
84	665	0.0697	0.0067	0.0607	0.1018
85	670	0.0395	0.0041	0.0253	0.0468
86	675	0.0385	0.0116	0.0942	0.1486
87	680	0.0303	0.0074	0.0490	0.0790
88	685	0.0822	0.0076	0.0860	0.1333
89	750	0.0397	0.0103	0.0851	0.1842
90	755	0.0304	0.0055	0.0598	0.1362
91	760	0.0443	0.0095	0.1043	0.1703
92	765	0.0468	0.0076	0.0795	0.1253
93	770	0.0382	0.0068	0.1057	0.1801
94	775	0.0341	0.0054	0.0439	0.1027
95	780	0.0378	0.0066	0.0623	0.1199
96	785	0.0450	0.0063	0.0566	0.0961
97	790	0.0477	0.0066	0.0550	0.1026
98	795	0.0456	0.0057	0.0409	0.0808
99	800	0.0440	0.0055	0.0430	0.0851
100	805	0.0513	0.0062	0.0530	0.0917
101	810	0.0420	0.0063	0.0547	0.0991
102	815	0.0461	0.0085	0.1093	0.2746

103	820	0.0310	0.0116	0.1235	0.2561
104	825	0.0452	0.0056	0.0408	0.0714
105	905	0.0483	0.0163	0.1637	0.2424
106	910	0.0489	0.0125	0.1427	0.2150
107	915	0.0467	0.0115	0.1225	0.2075
108	920	0.0455	0.0093	0.0909	0.1656
109	925	0.0474	0.0098	0.1055	0.1724
110	930	0.0592	0.1709	1.2976	1.5465
111	935	0.0754	0.1836	1.2998	1.5740
112	940	0.0284	0.0646	0.3933	0.4711
113	945	0.0713	0.1710	1.1277	1.3399
114	950	0.0575	0.0525	0.4343	0.6550
115	955	0.0541	0.0472	0.3863	0.5804
116	960	0.0551	0.0332	0.2413	0.4649
117	965	0.0558	0.0315	0.2793	0.4583
118	970	0.0553	0.0277	0.2515	0.4155
119	975	0.0585	0.0232	0.2414	0.4343
120	980	0.0539	0.0244	0.2419	0.3957
121	985	0.0541	0.0223	0.2107	0.3495
122	990	0.0530	0.0220	0.2096	0.3672
123	995	0.0543	0.0227	0.2266	0.3664
124	1000	0.0512	0.0338	0.1933	0.2788
125	1005	0.0615	0.0189	0.1758	0.2719
126	1010	0.0571	0.0297	0.2064	0.3044
127	1015	0.0646	0.0190	0.1831	0.2805

Giddings core B					
Sample	Depth	χ	ARM	IRM_{100}	SIRM
	cm	$\mu m^3 kg\text{-}1$	$mA\ m^2\ kg^{-1}$	$mA\ m^2\ kg^{-1}$	$mA\ m^2\ kg^{-1}$
1	140	0.0864	0.1003	2.4042	2.9516
2	145	0.0769	0.0721	1.2542	1.5686
3	150	0.0364	0.0370	0.5620	0.6870
4	155	0.0367	0.0555	1.2709	1.5479
5	160	0.0082	0.0166	0.2865	0.3436
6	165	0.0011	0.0074	0.0756	0.1016
7	170	0.0034	0.0091	0.0770	0.1055
8	175	0.0039	0.0086	0.0785	0.1203
9	180	0.0010	0.0045	0.0437	0.0623
10	185	0.0087	0.0057	0.0603	0.1021
11	190	0.0053	0.0039	0.0419	0.0610
12	195	0.0039	0.0041	0.0497	0.0796
13	200	0.0010	0.0051	0.0727	0.0990
14	205	0.0085	0.0068	0.1040	0.1445
15	210	0.0030	0.0055	0.0721	0.1226
16	215	0.0164	0.0090	0.2094	0.2413
17	220	0.0136	0.0066	0.1035	0.1626
18	225	0.0037	0.0076	0.1297	0.2160
19	230	0.0042	0.0091	0.1538	0.2387
20	235	0.0075	0.0074	0.1386	0.2349
21	240	0.0051	0.0049	0.0515	0.0906
22	245	0.0000	0.0035	0.0360	0.0603
23	250	0.0255	0.0053	0.1144	0.1295
24	255	0.0116	0.0054	0.0481	0.0664
25	260	0.0259	0.0068	0.0549	0.0725
26	265	0.0207	0.0087	0.0822	0.1288
27	270	0.0030	0.0076	0.1213	0.1973
28	275	0.0329	0.0138	0.1430	0.2347
29	320	0.0285	0.0360	0.3214	0.4296
30	325	0.0341	0.0400	0.4398	0.6396
31	330	0.0452	0.1373	0.7977	0.9610
32	335	0.0471	0.0812	0.7290	1.0013
33	340	0.0275	0.0913	0.8143	1.1152
34	345	0.0300	0.0706	0.5907	0.8317
35	350	0.0347	0.0913	0.6799	0.9097
36	355	0.0337	0.0779	0.6758	0.9423
37	360	0.0291	0.0844	0.6051	0.8845
38	365	0.0313	0.0687	0.5625	0.8202
39	370	0.0372	0.0736	0.5520	0.7801
40	375	0.0423	0.0608	0.5223	0.7633
41	380	0.0594	0.1310	0.7751	0.9501
42	385	0.0431	0.0684	0.4929	0.6929
43	390	0.0336	0.0451	0.4280	0.7112
44	395	0.0355	0.0539	0.4302	0.7104
45	425	0.0396	0.0335	0.2885	0.4859
46	430	0.0403	0.0472	0.3687	0.5183
47	435	0.0380	0.0655	0.5360	0.8423
48	440	0.0528	0.0577	0.5090	0.7947
49	445	0.0380	0.0484	0.4382	0.6532
50	450	0.0274	0.0556	0.4924	0.7717
51	455	0.0278	0.0461	0.6278	0.9873

52	460	0.0410	0.0463	0.7448	1.1075
53	465	0.0486	0.0311	0.4973	0.8089
54	470	0.0341	0.0331	0.6438	1.0979
55	475	0.0347	0.0328	0.5247	0.9910
56	480	0.0930	0.0470	0.5305	0.8197
57	485	0.0592	0.0394	0.4616	0.7594
58	490	0.0463	0.0349	0.4093	0.7429
59	495	0.0393	0.0273	0.4031	0.7140
60	515	0.0406	0.0339	0.5291	0.8933
61	520	0.0409	0.0332	0.5942	1.0031
62	525	0.0459	0.0489	1.3034	2.0954
63	530	0.0807	0.0398	0.7017	1.1083
64	535	0.0428	0.0394	0.6302	1.0364
65	540	0.0440	0.0449	0.8840	1.4735
66	545	0.0752	0.0462	0.7472	1.0731
67	550	0.1204	0.0421	0.6205	0.9644
68	555	0.0538	0.0464	0.9175	1.4997
69	560	0.1053	0.0359	0.4523	0.7348
70	565	0.1127	0.0314	0.4301	0.7098
71	570	0.0461	0.0299	0.5461	0.9484
72	575	0.1067	0.0376	0.5099	0.7420
73	580	0.0310	0.0487	1.1069	1.8478
74	585	0.1248	0.0431	0.8973	1.4402
75	590	0.0971	0.0285	0.3700	0.6296
76	595	0.0353	0.0424	0.5777	0.9273
77	630	0.0630	0.0282	0.4955	0.8043
78	635	0.0716	0.0294	0.4174	0.7433
79	640	0.1156	0.0278	0.3310	0.5536
80	645	0.0984	0.0375	0.6809	1.1968
81	650	0.1145	0.0256	0.2528	0.3920
82	655	0.0798	0.0253	0.2871	0.4812
83	660	0.0393	0.0346	0.7372	1.4491
84	665	0.0728	0.0291	0.3426	0.5250
85	670	0.0616	0.0305	0.3712	0.6276
86	675	0.1240	0.0176	0.1892	0.3185
87	680	0.0519	0.0254	0.3313	0.6326
88	685	0.0514	0.0256	0.3581	0.7158
89	690	0.0761	0.0252	0.3437	0.6299
90	695	0.0398	0.0292	0.4308	0.7366
91	725	0.0716	0.0274	0.3275	0.5730
92	730	0.1331	0.0218	0.2351	0.4041
93	735	0.0730	0.0260	0.2495	0.4281
94	740	0.0964	0.0273	0.2709	0.4482
95	745	0.0851	0.0259	0.2333	0.3777
96	750	0.1087	0.0205	0.2069	0.3516
97	755	0.0613	0.0282	0.3715	0.6842
98	760	0.1125	0.0205	0.2428	0.4162
99	765	0.0768	0.0232	0.2505	0.3933
100	770	0.0718	0.0252	0.2596	0.4304
101	775	0.1020	0.0212	0.2444	0.4254
102	780	0.0718	0.0209	0.2140	0.4558
103	785	0.0687	0.0225	0.2270	0.3931
104	790	0.0758	0.0247	0.2650	0.3899
105	795	0.0930	0.0244	0.2365	0.5572

106	800	0.0562	0.0184	0.2370	0.2298
107	805	0.1198	0.0192	0.1641	0.4697
108	810	0.0669	0.0169	0.0196	0.2006
109	815	0.0706	0.0170	0.1764	0.2905
110	820	0.0871	0.0142	0.1683	0.3089
111	825	0.0669	0.0169	0.2000	0.3478
112	830	0.0711	0.0181	0.2037	0.4653
113	835	0.0551	0.0197	0.2643	0.3577
114	840	0.0521	0.0181	0.2996	0.4697
115	845	0.0485	0.0162	0.2371	0.6007
116	850	0.0912	0.0187	0.3592	0.9893
117	855	0.0523	0.0118	0.1501	0.3488
118	860	0.0539	0.0127	0.1501	0.3355
119	865	0.0594	0.0116	0.1631	0.4386
120	870	0.0630	0.0127	0.1498	0.3612
121	875	0.0643	0.0130	0.1469	0.3330
122	880	0.0392	0.0153	0.2269	0.6972
123	900	0.0195	0.0169	0.1219	0.1484
124	905	0.0114	0.0136	0.0963	0.1213
125	910	0.0099	0.0138	0.0939	0.1165
126	915	0.0168	0.0247	0.1468	0.1765
127	920	0.0316	0.0485	0.3257	0.4389
128	925	0.0471	0.0603	0.3379	0.4144
129	930	0.0299	0.0469	0.3131	0.4108
130	935	0.0394	0.0198	0.1603	0.2151
131	940	0.0754	0.0164	0.1557	0.2033
132	945	0.0640	0.0163	0.1694	0.2299
133	950	0.0673	0.0149	0.1384	0.1849
134	955	0.0573	0.0173	0.1703	0.2310
135	960	0.0841	0.0145	0.1495	0.2097
136	965	0.0825	0.0146	0.1389	0.1941
137	970	0.0901	0.0207	0.2029	0.3082
138	975	0.0594	0.0083	0.0813	0.1256
139	990	0.0152	0.0049	0.0450	0.0590
140	995	0.0459	0.0059	0.0661	0.1024
141	1000	0.0091	0.0157	0.1426	0.1918
142	1005	0.0097	0.0151	0.1797	0.2748
143	1010	0.0010	0.0070	0.0532	0.0673
144	1015	0.0160	0.0234	0.2422	0.3644
145	1020	0.0071	0.0138	0.1008	0.1285
146	1025	0.0042	0.0079	0.0533	0.0672
147	1030	0.0211	0.0325	0.1840	0.2195
148	1035	0.0322	0.0229	0.1784	0.2264
149	1040	0.0546	0.0186	0.1903	0.2486
150	1045	0.0592	0.0178	0.2117	0.2982
151	1050	0.0713	0.0165	0.2102	0.3055
152	1055	0.0579	0.0219	0.2458	0.3518
153	1060	0.0706	0.0198	0.1986	0.2850
154	1065	0.0552	0.0164	0.1678	0.2448
155	1070	0.0824	0.0116	0.1142	0.1704
156	1075	0.0779	0.0149	0.1465	0.2249
157	1080	0.0789	0.0158	0.1488	0.2245
158	1085	0.0570	0.0148	0.1687	0.2693
159	1090	0.0717	0.0181	0.2319	0.3106

160	1095	0.0778	0.0345	0.4605	0.5645
161	1100	0.0053	0.0111	0.1075	0.1517
162	1105	0.0032	0.0116	0.1036	0.1478
163	1110	0.0091	0.0146	0.1263	0.1866
164	1115	0.0012	0.0060	0.0485	0.0615
165	1120	0.0030	0.0066	0.0540	0.0757
166	1125	0.0080	0.0118	0.0719	0.0915
167	1130	0.0090	0.0155	0.0888	0.1129
168	1135	0.0137	0.0465	0.2120	0.2465
169	1140	0.0264	0.0446	0.2344	0.2862
170	1145	0.0405	0.0197	0.2071	0.3005
171	1150	0.0687	0.0174	0.1816	0.2596
172	1155	0.0633	0.0216	0.1988	0.2769
173	1160	0.0769	0.0191	0.2510	0.4011
174	1165	0.0909	0.0216	0.2202	0.3605
175	1170	0.0819	0.0203	0.2246	0.4024
176	1175	0.0922	0.0200	0.2098	0.4061
177	1180	0.0813	0.0229	0.2977	0.6065
178	1185	0.0895	0.0205	0.2173	0.4109
179	1190	0.0706	0.0188	0.2402	0.3874
180	1260	0.0057	0.0118	0.0896	0.1125
181	1265	0.0032	0.0093	0.0793	0.1061
182	1270	0.0061	0.0116	0.1139	0.1740
183	1275	0.0029	0.0085	0.0892	0.1310
184	1280	0.0010	0.0060	0.0502	0.0707
185	1285	0.0020	0.0064	0.0440	0.0613
186	1290	0.0713	0.0182	0.2472	0.3678
187	1295	0.0501	0.0208	0.2288	0.3735
188	1300	0.0021	0.0066	0.0488	0.0660
189	1305	0.0080	0.0118	0.0744	0.0984
190	1310	0.0060	0.0091	0.0700	0.0938
191	1315	0.0052	0.0077	0.0567	0.0777
192	1320	0.0000	0.0050	0.0379	0.0496
193	1325	0.0115	0.0128	0.0796	0.1071
194	1330	0.0069	0.0094	0.0937	0.1414
195	1335	0.0091	0.0117	0.1147	0.1792
196	1340	0.0088	0.0123	0.1229	0.1852
197	1345	0.0049	0.0084	0.0833	0.1233
198	1350	0.0060	0.0101	0.0911	0.1390
199	1355	0.0102	0.0137	0.1146	0.1618
200	1360	0.0088	0.0132	0.0888	0.1160
201	1365	0.0288	0.0630	0.3092	0.3699
202	1370	0.0328	0.0448	0.2486	0.3228
203	1375	0.0344	0.0527	0.3442	0.4516
204	1380	0.0485	0.0293	0.3245	0.4890
205	1385	0.0824	0.0142	0.1372	0.2033
206	1390	0.0900	0.0156	0.1521	0.1984
207	1395	0.0550	0.0160	0.1967	0.3299
208	1400	0.0080	0.0085	0.0680	0.0923
209	1405	0.0031	0.0063	0.0525	0.0713
210	1410	0.0010	0.0049	0.0394	0.0529
211	1415	0.0043	0.0061	0.0536	0.0740
212	1420	0.0075	0.0053	0.0428	0.0569
213	1425	0.0034	0.0065	0.0630	0.0814

214	1430	0.0021	0.0063	0.0454	0.0581
215	1435	0.0020	0.0060	0.0447	0.0598
216	1440	0.0010	0.0050	0.0403	0.0536
217	1445	0.0010	0.0049	0.0388	0.0527
218	1450	0.0041	0.0051	0.0462	0.0608
219	1455	0.0050	0.0145	0.0730	0.0911
220	1460	0.0020	0.0048	0.0383	0.0516
221	1465	0.0038	0.0075	0.0526	0.0704
222	1470	0.0293	0.0806	0.3643	0.4255
223	1475	0.0314	0.0467	0.2429	0.2954
224	1480	0.0692	0.0217	0.3248	0.5266
225	1485	0.0569	0.0133	0.1788	0.3127

Giddings core C					
Sample	Depth	χ	ARM	IRM_{100}	SIRM
	cm	$\mu m^3 kg^{-1}$	$mA m^2 kg^{-1}$	$mA m^2 kg^{-1}$	$mA m^2 kg^{-1}$
1	200	0.0071	0.0100	0.0943	0.1807
2	205	0.0179	0.0171	0.3610	0.7588
3	210	0.0138	0.0162	0.2846	0.5183
4	215	0.0091	0.0138	0.2223	0.3788
5	220	0.0137	0.0211	0.4201	0.6741
6	225	0.0134	0.0092	0.0705	0.1411
7	230	0.0359	0.0098	0.0791	0.2697
8	235	0.0300	0.0069	0.0444	0.0687
9	240	0.0242	0.0106	0.0742	0.1215
10	245	0.0320	0.0115	0.0834	0.2948
11	250	0.0252	0.0114	0.1226	0.4076
12	255	0.0206	0.0176	0.2408	0.4882
13	260	0.0137	0.0199	0.3175	0.5578
14	265	0.0098	0.0190	0.2933	0.5371
15	270	0.0000	0.0073	0.0332	0.0513
16	275	0.0000	0.0057	0.0306	0.0459
17	280	0.0152	0.0128	0.2302	0.2988
18	285	0.0208	0.0102	0.1620	0.2104
19	290	0.0079	0.0126	0.1808	0.2459
20	295	0.0163	0.0107	0.1829	0.2376
21	300	0.0182	0.0190	0.3787	0.5822
22	305	0.0150	0.0186	0.3696	0.5207
23	310	0.0167	0.0146	0.4291	0.5055
24	315	0.0038	0.0062	0.0276	0.0432
25	320	0.0053	0.0052	0.0207	0.0326
26	325	0.0163	0.0060	0.0299	0.0598
27	330	0.0210	0.0066	0.0337	0.0727
28	335	0.0055	0.0084	0.0541	0.1327
29	340	0.0031	0.0070	0.0430	0.0857
30	345	0.0430	0.0065	0.0389	0.1011
31	350	0.0067	0.0067	0.0401	0.0883
32	355	0.0068	0.0073	0.0443	0.0892
33	360	0.0292	0.0095	0.0722	0.2126
34	365	0.0217	0.0093	0.0750	0.1500
35	370	0.0205	0.0166	0.2876	0.7575
36	375	0.0363	0.0108	0.0820	0.3201
37	380	0.0303	0.0085	0.0559	0.2131
38	385	0.0383	0.0055	0.0218	0.0332
39	390	0.0455	0.0054	0.0212	0.0334
40	395	0.0236	0.0058	0.0231	0.0488
41	400	0.0297	0.0049	0.0194	0.0311
42	405	0.0393	0.0057	0.0241	0.0385
43	410	0.0380	0.0053	0.0198	0.0315
44	415	0.0447	0.0054	0.0226	0.0393
45	420	0.0189	0.0066	0.0307	0.0595
46	425	0.0269	0.0062	0.0275	0.0506
47	430	0.0266	0.0067	0.0297	0.0581
48	435	0.0161	0.0063	0.0301	0.0514
49	440	0.0277	0.0089	0.0527	0.1927
50	445	0.0405	0.0097	0.0699	0.2449
51	450	0.0511	0.0146	0.1211	0.4208

52	455	0.0208	0.0154	0.2201	0.6988
53	460	0.0387	0.0145	0.1340	0.3337
54	465	0.0367	0.0092	0.0661	0.1837
55	470	0.0361	0.0100	0.0623	0.1536
56	475	0.1064	0.0115	0.0805	0.2256
57	480	0.0464	0.0142	0.1217	0.4153
58	485	0.0213	0.0104	0.0691	0.1781
59	490	0.0228	0.0107	0.0738	0.2234
60	495	0.0437	0.0099	0.0599	0.1447
61	500	0.0440	0.0132	0.1061	0.4237
62	505	0.0310	0.0098	0.0691	0.2639
63	510	0.0392	0.0105	0.0727	0.2209
64	515	0.0305	0.0135	0.1101	0.3364
65	520	0.0344	0.0148	0.1566	0.3508
66	525	0.0455	0.0277	0.3934	0.8186
67	530	0.0376	0.0368	0.6820	1.3517
68	535	0.0734	0.0289	0.4491	0.8695
69	540	0.0315	0.0284	0.4318	0.8246
70	545	0.0556	0.0185	0.2671	0.5094
71	550	0.0457	0.0218	0.2721	0.5636
72	555	0.0476	0.0202	0.2570	0.5399
73	560	0.0426	0.0261	0.3719	0.8089
74	565	0.0748	0.0353	0.4650	0.9475
75	570	0.0566	0.0327	0.4228	0.8437
76	575	0.0501	0.0324	0.4281	0.8536
77	580	0.0781	0.0375	0.5594	1.1258
78	585	0.0484	0.0397	0.5872	1.1427
79	590	0.0404	0.0358	0.5748	1.1215
80	595	0.0493	0.0335	0.5746	1.1215
81	600	0.1120	0.0322	0.4635	0.9491
82	605	0.0426	0.0388	0.6260	1.3209
83	610	0.0548	0.0356	0.5137	1.0261
84	615	0.0907	0.0407	0.6000	1.1278
85	620	0.0660	0.0439	0.6510	1.2262
86	625	0.0541	0.0309	0.4059	0.7471
87	630	0.0452	0.0320	0.4615	0.8762
88	635	0.0760	0.0452	0.6456	1.1863
89	640	0.0446	0.0262	0.4672	0.9436
90	645	0.0414	0.0284	0.5075	1.0543
91	650	0.1162	0.0196	0.1864	0.4257
92	655	0.0729	0.0177	0.1464	0.3323
93	660	0.0531	0.0199	0.2204	0.5495
94	665	0.0597	0.0182	0.1517	0.3623
95	670	0.0378	0.0162	0.1558	0.3741
96	675	0.0567	0.0284	0.4438	1.0806
97	680	0.0480	0.0189	0.2251	0.4848
98	685	0.0544	0.0206	0.2498	0.5303
99	690	0.0636	0.0200	0.2611	0.5960
100	695	0.0492	0.0204	0.2302	0.5371
101	770	0.0160	0.0069	0.1494	0.1969
102	775	0.0110	0.0057	0.1248	0.1665
103	780	0.0560	0.0239	0.4011	0.6230
104	785	0.0472	0.0213	0.3990	0.6726
105	790	0.0487	0.0106	0.2313	0.5271

106	795	0.0510	0.0104	0.2128	0.4759
107	800	0.0306	0.0060	0.1108	0.2760
108	805	0.0742	0.0056	0.1121	0.2623
109	810	0.0406	0.0062	0.1528	0.3504
110	815	0.0833	0.0044	0.0881	0.2120
111	820	0.0320	0.0034	0.0709	0.1553
112	825	0.0316	0.0049	0.0878	0.1820
113	830	0.0373	0.0036	0.0841	0.2019
114	835	0.0433	0.0062	0.1167	0.3217
115	840	0.0420	0.0056	0.1132	0.2669
116	845	0.0454	0.0052	0.0966	0.2505
117	850	0.0248	0.0036	0.0969	0.2127
118	855	0.0487	0.0031	0.1108	0.2210
119	860	0.0361	0.0112	0.2336	0.3717
120	865	0.0347	0.0020	0.0786	0.1234
121	870	0.0337	0.0026	0.0700	0.1427
122	875	0.0567	0.0016	0.0579	0.1092
123	880	0.0732	0.0030	0.0874	0.1825
124	885	0.0273	0.0040	0.1145	0.2438
125	890	0.0536	0.0066	0.1722	0.3986
126	895	0.0413	0.0029	0.0692	0.1311
127	900	0.0319	0.0038	0.0977	0.1952
128	905	0.0297	0.0054	0.1149	0.2233
129	910	0.0413	0.0041	0.0953	0.2032
130	915	0.0270	0.0031	0.0694	0.1398
131	920	0.0335	0.0035	0.0806	0.1909
132	925	0.0312	0.0033	0.0711	0.1638
133	930	0.1420	0.0036	0.0874	0.2016
134	935	0.0263	0.0029	0.0756	0.1497
135	940	0.0306	0.0023	0.0833	0.1486
136	945	0.0113	0.0066	0.1841	0.2271
137	950	0.0458	0.0241	0.4432	0.7015
138	955	0.0492	0.0235	0.4652	0.7598
139	960	0.0341	0.0171	0.3362	0.5290
140	965	0.0457	0.0274	0.5309	0.8063
141	970	0.0419	0.0294	0.5951	0.8099
142	975	0.0295	0.0171	0.3420	0.5103
143	980	0.0642	0.0362	0.6796	0.9680
144	985	0.0777	0.0412	0.8986	1.2350
145	990	0.0275	0.0135	0.3119	0.3923
146	995	0.0340	0.0140	0.3392	0.4482
147	1000	0.0792	0.0067	0.1533	0.4523
148	1005	0.0323	0.0056	0.1080	0.3115
149	1010	0.0289	0.0066	0.1509	0.3669
150	1015	0.0388	0.0081	0.1733	0.4278
151	1020	0.0567	0.0034	0.0734	0.1919
152	1025	0.0536	0.0021	0.0503	0.1209
153	1030	0.0222	0.0026	0.0644	0.1619
154	1035	0.0326	0.0029	0.1053	0.1957
155	1040	0.0404	0.0126	0.2531	0.4603
156	1045	0.0590	0.0168	0.3060	0.5681
157	1050	0.0521	0.0165	0.3609	0.7083
158	1055	0.0625	0.0255	0.5012	0.8905
159	1060	0.0435	0.0194	0.4103	0.7032

160	1065	0.0316	0.0149	0.3337	0.5279
161	1070	0.0270	0.0147	0.3108	0.4762
162	1075	0.0356	0.0168	0.3827	0.6603
163	1080	0.0382	0.0159	0.3496	0.5723
164	1085	0.0384	0.0149	0.3192	0.5550
165	1090	0.0359	0.0133	0.3205	0.5542
166	1095	0.0267	0.0117	0.2567	0.3890
167	1100	0.0307	0.0150	0.3334	0.5564
168	1105	0.0280	0.0137	0.3269	0.5167
169	1110	0.0263	0.0131	0.2964	0.4277
170	1115	0.0323	0.0130	0.3081	0.4459
171	1120	0.0454	0.0126	0.3129	0.5124
172	1125	0.0289	0.0139	0.3097	0.4312
173	1130	0.0275	0.0121	0.2622	0.3575
174	1135	0.0260	0.0124	0.2661	0.3568
175	1140	0.0308	0.0109	0.2468	0.3363
176	1145	0.0393	0.0157	0.3411	0.4943
177	1150	0.0487	0.0050	0.1114	0.0042
178	1155	0.0416	0.0030	0.0665	0.1427
179	1160	0.0539	0.0031	0.0598	0.1233
180	1165	0.0476	0.0035	0.0732	0.1605
181	1170	0.0394	0.0046	0.0834	0.1920
182	1175	0.0474	0.0039	0.0757	0.1900
183	1180	0.0629	0.0042	0.0821	0.1839
184	1185	0.0419	0.0036	0.0692	0.1389
185	1190	0.0357	0.0045	0.0844	0.1877
186	1195	0.0428	0.0033	0.0742	0.1567
187	1200	0.0540	0.0023	0.0560	0.1073
188	1205	0.0345	0.0029	0.0629	0.1218
189	1210	0.0482	0.0020	0.0536	0.0947
190	1215	0.0336	0.0024	0.0618	0.1145
191	1220	0.1252	0.0025	0.0615	0.0918
192	1225	0.0328	0.0113	0.2402	0.3698
193	1230	0.1368	0.0020	0.0406	0.0600
194	1235	0.0322	0.0020	0.0580	0.1013
195	1240	0.0409	0.0047	0.0665	0.1193
196	1245	0.0419	0.0026	0.0594	0.0984
197	1250	0.0421	0.0034	0.0577	0.1069
198	1255	0.0462	0.0030	0.0662	0.1325
199	1260	0.0437	0.0030	0.0671	0.1273
200	1265	0.0414	0.0029	0.0586	0.1100
201	1270	0.0606	0.0019	0.0472	0.0782
202	1275	0.0534	0.0023	0.0471	0.0745
203	1280	0.0428	0.0019	0.0397	0.0609
204	1285	0.0557	0.0026	0.0481	0.0727
205	1290	0.0508	0.0022	0.0503	0.0758
206	1295	0.0506	0.0229	0.4615	0.6732
207	1300	0.0433	0.0188	0.4618	0.7174
208	1305	0.0453	0.0183	0.4640	0.6802
209	1310	0.0445	0.0158	0.3742	0.5448
210	1315	0.0545	0.0126	0.3071	0.4064
211	1320	0.0410	0.0213	0.5138	0.6176
212	1325	0.0387	0.0027	0.0578	0.0950
213	1330	0.0489	0.0039	0.0614	0.1476

214	1335	0.0434	0.0036	0.0583	0.1214
215	1340	0.0421	0.0034	0.0535	0.0970
216	1345	0.0487	0.0031	0.0547	0.1105
217	1350	0.1764	0.0021	0.0496	0.0808
218	1355	0.0605	0.0034	0.0543	0.1022
219	1360	0.0687	0.0042	0.0581	0.1204
220	1365	0.0445	0.0024	0.0310	0.0576
221	1370	0.0850	0.0043	0.0590	0.1105
222	1375	0.0744	0.0044	0.0623	0.1285
223	1380	0.0649	0.0038	0.0655	0.1349

Semer Water core SL2					
Sample	Depth	χ	ARM	IRM_{100}	SIRM
	cm	$\mu m^3 kg^{-1}$	$mA m^2 kg^{-1}$	$mA m^2 kg^{-1}$	$mA m^2 kg^{-1}$
1	2.36	0.114	0.282	1.361	1.612
2	4.72	0.103	0.202	1.183	1.438
3	7.08	0.110	0.198	1.387	1.733
4	9.44	0.111	0.201	1.333	1.604
5	11.8	0.125	0.238	1.635	1.966
6	14.16	0.119	0.238	1.450	1.736
7	16.52	0.133	0.309	1.548	1.876
8	18.88	0.130	0.244	1.908	2.437
9	21.24	0.143	0.263	1.618	1.964
10	23.6	0.165	0.324	2.319	2.961
11	25.96	0.205	0.392	3.154	4.009
12	28.32	0.196	0.420	2.876	3.650
13	30.68	0.195	0.433	2.889	3.599
14	33.04	0.201	0.441	3.513	4.676
15	35.4	0.187	0.379	3.174	4.226
16	37.76	0.179	0.349	3.008	3.987
17	40.12	0.182	0.342	3.142	4.292
18	42.48	0.152	0.269	2.439	3.306
19	44.84	0.197	0.405	3.585	4.869
20	47.2	0.163	0.312	2.443	3.147
21	49.56	0.163	0.274	2.309	3.047
22	51.92	0.159	0.247	2.050	2.679
23	54.28	0.170	0.301	2.273	2.935
24	56.64	0.181	0.359	2.371	2.922
25	59	0.186	0.369	2.596	3.288
26	61.36	0.186	0.288	2.451	3.243
27	63.72	0.195	0.366	2.696	3.409
28	66.08	0.180	0.359	2.552	3.241
29	68.44	0.204	0.391	3.029	3.924
30	70.8	0.210	0.414	3.079	3.984
31	73.16	0.205	0.415	3.099	4.018
32	75.52	0.198	0.396	2.765	3.555
33	77.88	0.202	0.398	2.821	3.591
34	80.24	0.202	0.391	2.902	3.698
35	82.6	0.193	0.381	2.742	3.423
36	84.96	0.189	0.386	2.587	3.155
37	87.32	0.188	0.377	2.608	3.255
38	89.68	0.185	0.357	2.500	3.152
39	92.04	0.178	0.348	2.299	2.854
40	94.4	0.175	0.347	2.474	3.171
41	96.76	0.183	0.334	2.703	3.548
42	99.12	0.183	0.365	2.816	3.651
43	101.48	0.189	0.370	3.057	4.002
44	103.84	0.178	0.351	2.573	3.271
45	106.2	0.200	0.385	3.051	3.982
46	108.56	0.199	0.393	3.155	4.155
47	110.92	0.199	0.395	3.362	4.406
48	113.28	0.215	0.428	3.789	5.024
49	115.64	0.198	0.415	3.224	4.116
50	118	0.190	0.394	2.857	3.708
51	120.36	0.197	0.411	3.226	4.187

52	122.72	0.198	0.400	2.873	3.744
53	125.08	0.218	0.414	3.537	4.703
54	127.44	0.196	0.405	3.336	4.409
55	129.8	0.205	0.423	3.277	4.249
56	132.16	0.199	0.398	3.186	4.258
57	134.52	0.221	0.460	4.026	5.317
58	136.88	0.221	0.479	4.059	5.321
59	139.24	0.230	0.499	4.411	5.664
60	141.6	0.242	0.531	4.641	6.086
61	143.96	0.234	0.530	4.246	5.607
62	146.32	0.233	0.495	4.097	5.441
63	148.68	0.202	0.460	3.548	4.609
64	151.04	0.212	0.466	3.274	4.234
65	153.4	0.211	0.437	3.323	4.397
66	155.76	0.225	0.441	3.687	4.956
67	158.12	0.216	0.453	3.594	4.859
68	160.48	0.236	0.467	4.231	5.787
69	162.84	0.234	0.457	4.409	6.141
70	165.2	0.246	0.460	5.030	6.823
71	167.56	0.238	0.432	4.311	5.964
72	169.92	0.240	0.454	4.749	6.575
73	172.28	0.221	0.435	3.765	5.237
74	174.64	0.215	0.418	3.761	5.220
75	177	0.226	0.422	4.065	5.465
76	179.36	0.203	0.372	3.331	4.598
77	181.72	0.208	0.365	3.450	4.690
78	184.08	0.221	0.394	4.038	5.516
79	186.44	0.210	0.386	3.665	5.074
80	188.8	0.199	0.362	3.376	4.549
81	191.16	0.186	0.352	2.978	3.978
82	193.52	0.201	0.376	4.196	5.754
83	195.88	0.194	0.340	2.978	3.952
84	198.24	0.192	0.337	2.972	4.048
85	200.6	0.179	0.329	2.712	3.637
86	202.96	0.175	0.328	2.711	3.681
87	205.32	0.167	0.286	2.306	3.178
88	207.68	0.171	0.288	2.519	3.485
89	210.04	0.152	0.239	2.023	2.740
90	212.4	0.146	0.220	1.842	2.525
91	214.76	0.146	0.214	1.561	2.077
92	217.12	0.141	0.188	1.397	1.874
93	219.48	0.152	0.208	1.595	2.187
94	221.84	0.144	0.215	1.533	2.016
95	224.2	0.160	0.230	1.867	2.568
96	226.56	0.158	0.248	2.193	3.002
97	228.92	0.152	0.246	1.871	2.615
98	231.28	0.143	0.215	1.683	2.405
99	233.64	0.139	0.227	1.835	2.626
100	236	0.143	0.221	1.915	2.753
101	238.36	0.150	0.249	2.411	3.516
102	240.72	0.153	0.286	2.555	3.629
103	243.08	0.153	0.290	2.826	3.937
104	245.44	0.139	0.251	2.221	3.127

Semer Water core SL1					
Sample	Depth	χ	ARM	IRM_{100}	SIRM
	cm	$\mu m^3 kg^{-1}$	$mA m^2 kg^{-1}$	$mA m^2 kg^{-1}$	$mA m^2 kg^{-1}$
1	2.19	0.125	0.361	1.731	1.971
2	4.38	0.128	0.355	1.736	1.962
3	6.56	0.126	0.304	1.621	1.779
4	8.75	0.124	0.282	1.466	1.692
5	10.94	0.117	0.257	1.400	1.633
6	13.13	0.137	0.340	1.787	1.993
7	15.32	0.134	0.315	1.849	1.952
8	17.50	0.145	0.328	1.793	2.034
9	19.69	0.141	0.335	1.901	2.113
10	21.88	0.145	0.331	1.964	2.182
11	24.07	0.164	0.377	2.388	2.687
12	26.26	0.177	0.388	2.744	2.932
13	28.44	0.165	0.436	2.447	2.766
14	30.63	0.184	0.448	2.680	3.000
15	32.82	0.187	0.461	2.391	2.609
16	35.01	0.179	0.432	2.529	2.763
17	37.20	0.182	0.377	3.014	3.425
18	39.38	0.187	0.408	2.786	3.130
19	41.57	0.187	0.403	3.004	4.170
20	43.76	0.206	0.435	3.676	4.269
21	45.95	0.190	0.409	2.974	3.420
22	48.14	0.189	0.427	3.938	4.402
23	50.32	0.185	0.413	2.622	2.937
24	52.51	0.179	0.425	2.674	2.967
25	54.70	0.169	0.416	2.980	3.490
26	56.89	0.171	0.417	3.167	3.667
27	59.08	0.165	0.378	2.770	3.165
28	61.26	0.153	0.371	2.460	2.782
29	63.45	0.166	0.348	2.682	3.079
30	65.64	0.170	0.364	2.377	2.716
31	67.83	0.158	0.386	2.169	2.279
32	70.02	0.177	0.424	3.160	3.681
33	72.20	0.178	0.387	3.064	3.535
34	74.39	0.177	0.397	2.744	3.155
35	76.58	0.150	0.401	2.372	2.490
36	78.77	0.170	0.435	2.935	3.333
37	80.96	0.180	0.463	3.608	4.196
38	83.14	0.186	0.425	2.893	4.000
39	85.33	0.194	0.452	2.995	3.502
40	87.52	0.224	0.482	3.306	3.755
41	89.71	0.218	0.496	5.121	6.008
42	91.90	0.249	0.507	3.982	4.570
43	94.08	0.227	0.489	3.972	4.539
44	96.27	0.221	0.445	5.448	6.483
45	98.46	0.119	0.255	1.804	2.149
46	100.65	0.116	0.244	1.457	1.704
47	102.84	0.116	0.244	1.465	1.671
48	105.02	0.114	0.226	1.411	1.655
49	107.21	0.122	0.241	1.624	1.980
50	109.40	0.124	0.247	2.163	2.500
51	111.59	0.109	0.224	1.585	1.913

52	113.78	0.117	0.234	1.811	2.228
53	115.96	0.128	0.251	2.207	2.709
54	118.15	0.137	0.324	2.386	2.843
55	120.34	0.140	0.311	2.355	2.791
56	122.53	0.129	0.262	2.017	2.269
57	124.72	0.120	0.251	2.063	2.507
58	126.90	0.114	0.240	1.456	1.723
59	129.09	0.111	0.224	1.442	1.707
60	131.28	0.105	0.194	1.207	1.390
61	133.47	0.101	0.180	1.127	1.319
62	135.66	0.098	0.170	1.095	1.326
63	137.84	0.099	0.233	1.519	1.802
64	140.03	0.102	0.249	1.415	1.631
65	142.22	0.100	0.182	1.028	1.215
66	144.41	0.103	0.194	1.075	1.238
67	146.60	0.101	0.159	0.901	1.048
68	148.78	0.108	0.218	1.367	1.631
69	150.97	0.116	0.247	1.439	1.667
70	153.16	0.112	0.233	1.496	1.781
71	155.35	0.137	0.317	1.914	2.229
72	157.54	0.132	0.325	2.562	3.140
73	159.72	0.114	0.295	2.197	2.778
74	161.91	0.108	0.264	1.918	2.374
75	164.10	0.108	0.252	2.207	2.748
76	166.29	0.105	0.268	1.875	2.350
77	168.48	0.106	0.269	2.206	2.806
78	170.66	0.080	0.232	1.269	1.455
79	172.85	0.077	0.143	1.056	1.197
80	175.04	0.072	0.122	0.718	0.844
81	177.23	0.076	0.128	0.832	0.995
82	179.42	0.076	0.125	0.738	0.904
83	181.60	0.078	0.115	0.656	0.783
84	183.79	0.091	0.084	0.568	0.758
85	185.98	0.097	0.095	0.677	0.930
86	188.17	0.106	0.211	1.891	2.151
87	190.36	0.108	0.293	1.883	2.176
88	192.54	0.109	0.275	1.763	2.101
89	194.73	0.097	0.194	1.210	1.431
90	196.92	0.091	0.159	1.157	1.322
91	199.11	0.093	0.199	1.277	1.602
92	201.30	0.092	0.193	1.170	1.417
93	203.48	0.088	0.143	0.742	0.898
94	205.67	0.080	0.107	0.572	0.693
95	207.86	0.103	0.085	0.590	0.646
96	210.05	0.094	0.090	0.512	0.635
97	212.24	0.084	0.094	0.645	0.695
98	214.42	0.089	0.109	0.620	0.744
99	216.61	0.101	0.187	1.129	1.313
100	218.80	0.082	0.182	0.911	1.063
101	220.99	0.078	0.140	0.698	0.825

Hornsea Mere core 1					
Sample	Depth	χ	ARM	IRM_{100}	SIRM
	cm	$\mu m^3 kg^{-1}$	$mA m^2 kg^{-1}$	$mA m^2 kg^{-1}$	$mA m^2 kg^{-1}$
1	2.56	0.104	0.054	1.247	1.587
2	5.12	0.123	0.099	2.451	4.599
3	7.68	0.237	0.283	6.843	13.929
4	10.24	0.221	0.245	5.382	10.544
5	12.80	0.164	0.159	2.291	3.706
6	15.36	0.161	0.185	2.044	3.126
7	17.92	0.161	0.214	1.951	3.018
8	20.48	0.173	0.213	1.950	2.831
9	23.04	0.153	0.244	1.594	2.347
10	25.60	0.168	0.292	1.857	2.614
11	28.16	0.172	0.374	1.778	2.234
12	30.72	0.169	0.442	2.117	2.816
13	33.28	0.185	0.528	2.442	3.093
14	35.84	0.178	0.511	2.415	3.058
15	38.40	0.178	0.597	2.431	3.036
16	40.96	0.186	0.656	2.548	3.163
17	43.52	0.180	0.580	2.391	2.979
18	46.08	0.181	0.580	2.557	3.224
19	48.64	0.185	0.637	2.785	3.462
20	51.20	0.191	0.615	2.888	3.554
21	53.76	0.208	0.545	2.297	4.748
22	56.32	0.193	0.434	3.012	3.827
23	58.88	0.190	0.541	2.832	3.439
24	61.44	0.212	0.666	3.218	3.882
25	64.00	0.219	0.709	3.304	4.012
26	66.56	0.233	0.743	3.646	4.392
27	69.12	0.214	0.677	3.315	4.009
28	71.68	0.215	0.681	3.318	3.965
29	74.24	0.214	0.696	3.199	3.815
30	76.80	0.214	0.590	3.281	3.987

Hornsea Mere core 2					
Sample	Depth	χ	ARM	IRM_{100}	SIRM
	cm	$\mu\ m^3\ kg^{-1}$	$mA\ m^2\ kg^{-1}$	$mA\ m^2\ kg^{-1}$	$mA\ m^2\ kg^{-1}$
1	2.65	0.135	0.208	1.759	2.211
2	5.30	0.117	0.171	1.589	2.005
3	7.95	0.114	0.149	1.493	1.889
4	10.60	0.115	0.118	1.450	1.812
5	13.25	0.114	0.135	1.488	1.879
6	15.90	0.109	0.096	1.379	1.743
7	18.55	0.109	0.093	1.360	1.726
8	21.20	0.117	0.096	1.426	1.824
9	23.85	0.119	0.094	1.450	1.820
10	26.50	0.111	0.083	1.377	1.771
11	29.15	0.119	0.098	1.544	1.937
12	31.80	0.104	0.089	1.292	1.645
13	34.45	0.124	0.118	1.581	2.003
14	37.10	0.126	0.118	1.586	2.023
15	39.75	0.132	0.117	1.716	2.218
16	42.40	0.136	0.135	1.779	2.289
17	45.05	0.138	0.144	1.802	2.351
18	47.70	0.136	0.165	1.908	2.434
19	50.35	0.146	0.171	1.965	2.541
20	53.00	0.151	0.182	2.057	2.657
21	55.65	0.149	0.180	2.045	2.648
22	58.30	0.150	0.203	2.028	2.627
23	60.95	0.148	0.192	2.040	2.624

Hornsea Mere core 3					
	Depth	χ	ARM	IRM_{100}	SIRM
	cm	$\mu m^3 kg^{-1}$	$mA m^2 kg^{-1}$	$mA m^2 kg^{-1}$	$mA m^2 kg^{-1}$
1	2.62	0.125	0.304	1.986	2.402
2	5.24	0.152	0.310	2.217	2.703
3	7.86	0.144	0.277	2.071	2.538
4	10.48	0.151	0.236	2.067	2.563
5	13.1	0.125	0.161	1.640	2.034
6	15.72	0.121	0.103	1.513	1.925
7	18.34	0.123	0.098	1.512	1.906
8	20.96	0.142	0.140	1.878	2.351
9	23.58	0.150	0.178	2.102	2.640
10	26.2	0.155	0.226	2.217	2.790
11	28.82	0.173	0.335	2.773	3.576
12	31.44	0.160	0.356	2.524	3.128
13	34.06	0.162	0.392	2.473	3.137
14	36.68	0.174	0.481	2.697	3.327
15	39.3	0.167	0.437	2.567	3.235
16	41.92	0.181	0.543	2.875	3.644
17	44.54	0.188	0.604	2.901	3.683
18	47.16	0.184	0.577	2.872	3.654
19	49.78	0.187	0.645	2.947	3.740
20	52.4	0.194	0.693	3.014	3.808
21	55.02	0.191	0.670	2.962	3.738
22	57.64	0.193	0.676	3.000	3.766
23	60.26	0.202	0.673	3.058	3.855
24	62.88	0.193	0.619	2.944	3.783
25	65.5	0.206	0.696	3.062	3.875
26	68.12	0.209	0.712	3.158	3.999
27	70.74	0.212	0.722	3.222	4.065
28	73.36	0.202	0.755	3.160	3.994
29	75.98	0.205	0.693	3.073	3.913

Hornsea Mere core 4					
Sample	Depth	χ	ARM	IRM_{100}	SIRM
	cm	$\mu m^3 kg^{-1}$	$mA m^2 kg^{-1}$	$mA m^2 kg^{-1}$	$mA m^2 kg^{-1}$
1	2.56	0.133	0.323	2.024	2.546
2	5.12	0.144	0.260	2.115	2.591
3	7.68	0.144	0.299	2.128	2.593
4	10.24	0.146	0.220	1.956	2.440
5	12.8	0.136	0.152	1.838	2.242
6	15.36	0.121	0.117	1.535	1.870
7	17.92	0.108	0.091	1.314	1.628
8	20.48	0.118	0.111	1.606	1.983
9	23.04	0.135	0.137	1.810	2.216
10	25.6	0.129	0.140	1.936	2.406
11	28.16	0.163	0.186	2.308	2.901
12	30.72	0.121	0.143	1.766	2.207
13	33.28	0.143	0.168	2.122	2.741
14	35.84	0.152	0.227	2.300	2.907
15	38.4	0.137	0.187	1.913	2.481
16	40.96	0.156	0.272	2.145	2.763
17	43.52	0.174	0.406	2.442	3.068
18	46.08	0.158	0.537	2.725	3.425
19	48.64	0.189	0.595	2.909	3.644
20	51.2	0.187	0.570	2.856	3.639
21	53.76	0.188	0.575	2.831	3.589
22	56.32	0.189	0.562	2.772	3.541
23	58.88	0.199	0.638	2.916	3.696
24	61.44	0.192	0.587	2.895	3.724
25	64	0.198	0.593	2.942	3.821
26	66.56	0.206	0.693	3.074	3.918
27	69.12	0.201	0.700	3.008	3.828
28	71.68	0.211	0.744	3.113	3.936
29	74.24	0.223	0.795	3.211	4.029
30	76.8	0.245	0.874	3.325	4.209
31	79.36	0.239	0.819	3.201	3.983

Hornsea Mere core 5					
Sample	Depth	χ	ARM	IRM_{100}	SIRM
	cm	$\mu\ m^3\ kg^{-1}$	$mA\ m^2\ kg^{-1}$	$mA\ m^2\ kg^{-1}$	$mA\ m^2\ kg^{-1}$
1	2.56	0.148	0.475	2.239	2.626
2	5.12	0.143	0.447	2.157	2.565
3	7.68	0.147	0.455	2.270	2.672
4	10.24	0.151	0.445	2.000	2.463
5	12.8	0.140	0.363	2.132	2.714
6	15.36	0.148	0.378	0.378	2.628
7	17.92	0.162	0.369	2.348	2.749
8	20.48	0.163	0.356	2.333	2.523
9	23.04	0.160	0.290	2.120	2.179
10	25.6	0.151	0.207	1.834	2.115
11	28.16	0.150	0.180	1.777	2.018
12	30.72	0.150	0.136	1.702	1.916
13	33.28	0.145	0.106	1.620	1.754
14	35.84	0.131	0.103	1.457	1.948
15	38.4	0.143	0.108	1.607	2.062
16	40.96	0.149	0.119	1.691	2.088
17	43.52	0.150	0.123	1.716	2.190
18	46.08	0.160	0.127	1.786	1.836
19	48.64	0.134	0.107	1.506	1.665
20	51.2	0.123	0.096	1.381	1.668
21	53.76	0.122	0.099	1.363	1.920
22	56.32	0.136	0.128	1.578	2.099
23	58.88	0.143	0.147	1.719	2.238
24	61.44	0.149	0.171	1.815	2.393
25	64	0.155	0.216	1.983	2.519
26	66.56	0.156	0.243	2.096	2.606
27	69.12	0.155	0.267	2.167	2.681
28	71.68	0.159	0.299	2.259	2.667
29	74.24	0.158	0.290	2.225	2.673
30	76.8	0.157	0.309	2.236	2.921
31	79.36	0.157	0.296	2.425	2.729

Hornsea Mere core 6					
Sample	Depth	χ	ARM	IRM_{100}	SIRM
	cm	$\mu\ m^3\ kg^{-1}$	$mA\ m^2\ kg^{-1}$	$mA\ m^2\ kg^{-1}$	$mA\ m^2\ kg^{-1}$
1	2.63	0.170	0.441	2.064	2.210
2	5.26	0.146	0.348	1.886	1.922
3	7.89	0.137	0.248	1.635	1.767
4	10.52	0.137	0.169	1.495	1.852
5	13.15	0.141	0.168	1.559	1.881
6	15.78	0.143	0.150	1.573	1.615
7	18.41	0.134	0.102	1.357	1.385
8	21.04	0.125	0.076	1.166	1.158
9	23.67	0.104	0.069	1.007	1.036
10	26.3	0.089	0.062	0.880	1.137
11	28.93	0.101	0.068	0.971	1.187
12	31.56	0.097	0.078	1.004	1.383
13	34.19	0.110	0.090	1.156	1.627
14	36.82	0.118	0.112	1.346	1.988
15	39.45	0.137	0.133	1.637	2.142
16	42.08	0.141	0.150	1.750	2.226
17	44.71	0.142	0.180	1.806	2.307
18	47.34	0.146	0.203	1.864	3.202
19	49.97	0.158	0.301	2.583	2.804
20	52.6	0.162	0.335	2.325	2.685
21	55.23	0.155	0.343	2.220	2.916
22	57.86	0.157	0.522	2.454	3.542
23	60.49	0.177	0.721	3.002	4.220
24	63.12	0.203	0.981	3.630	4.533
25	65.75	0.216	1.168	3.894	4.801
26	68.38	0.235	1.215	4.095	5.165
27	71.01	0.255	1.402	4.514	4.770
28	73.64	0.237	1.326	4.139	4.793
29	76.27	0.238	1.315	4.093	4.954
30	78.9	0.248	1.376	2.090	2.511

Hornsea Mere core 7					
Sample	Depth	χ	ARM	IRM_{100}	SIRM
	cm	$\mu\ m^3\ kg^{-1}$	$mA\ m^2\ kg^{-1}$	$mA\ m^2\ kg^{-1}$	$mA\ m^2\ kg^{-1}$
1	2.62	0.124	0.440	2.100	2.496
2	5.24	0.132	0.405	1.984	2.362
3	7.86	0.127	0.315	1.302	1.598
4	10.48	0.102	0.156	1.590	1.905
5	13.1	0.134	0.131	1.096	1.318
6	15.72	0.100	0.077	0.996	1.188
7	18.34	0.085	0.065	0.780	0.918
8	20.96	0.068	0.056	0.699	0.809
9	23.58	0.056	0.058	0.695	0.836
10	26.2	0.056	0.061	0.764	0.899
11	28.82	0.056	0.070	0.942	1.116
12	31.44	0.070	0.080	1.275	1.504
13	34.06	0.092	0.109	1.567	1.869
14	36.68	0.117	0.133	1.718	2.068
15	39.3	0.123	0.143	1.954	2.420
16	41.92	0.136	0.195	2.143	2.680
17	44.54	0.146	0.258	2.246	2.742
18	47.16	0.144	0.282	2.209	2.640
19	49.78	0.148	0.372	2.714	3.213
20	52.4	0.168	0.601	3.483	4.073
21	55.02	0.192	0.909	3.743	4.328
22	57.64	0.204	1.092	4.047	4.702
23	60.26	0.220	1.135	4.130	4.791
24	62.88	0.224	1.174	3.932	4.548
25	65.5	0.211	1.153	3.805	4.417
26	68.12	0.212	1.155	3.933	4.617
27	70.74	0.226	1.155	3.908	4.592
28	73.36	0.230	1.123	3.932	4.644
29	75.98	0.235	1.070	2.208	2.637

Hornsea Mere core 8					
Sample	Depth	χ	ARM	IRM_{100}	SIRM
	cm	$\mu\ m^3\ kg^{-1}$	$mA\ m^2\ kg^{-1}$	$mA\ m^2\ kg^{-1}$	$mA\ m^2\ kg^{-1}$
1	2.69	0.138	0.449	2.308	2.735
2	5.38	0.150	0.462	2.214	2.628
3	8.07	0.145	0.403	1.925	2.291
4	10.76	0.134	0.300	1.772	2.100
5	13.45	0.132	0.229	1.493	1.800
6	16.14	0.122	0.132	1.216	1.466
7	18.83	0.104	0.084	1.045	1.256
8	21.52	0.085	0.068	1.213	1.443
9	24.21	0.097	0.093	0.929	1.096
10	26.9	0.073	0.068	0.917	1.095
11	29.59	0.073	0.071	1.072	1.279
12	32.28	0.079	0.084	1.273	1.517
13	34.97	0.094	0.098	1.395	1.675
14	37.66	0.104	0.120	1.543	1.869
15	40.35	0.111	0.119	1.824	2.251
16	43.04	0.130	0.151	1.850	2.292
17	45.73	0.130	0.173	2.160	2.703
18	48.42	0.151	0.256	2.087	2.684
19	51.11	0.146	0.244	1.891	2.400
20	53.8	0.149	0.289	2.030	2.896
21	56.49	0.158	0.390	2.217	3.254
22	59.18	0.177	0.584	2.630	3.860
23	61.87	0.192	0.807	3.437	4.252
24	64.56	0.207	1.008	3.549	4.183
25	67.25	0.201	1.046	3.756	4.424
26	69.94	0.218	1.087	2.063	2.543

Hornsea Mere core 9					
Sample	Depth	χ	ARM	IRM_{100}	SIRM
	cm	$\mu\ m^3\ kg^{-1}$	$mA\ m^2\ kg^{-1}$	$mA\ m^2\ kg^{-1}$	$mA\ m^2\ kg^{-1}$
1	2.58	0.130	0.449	1.973	2.391
2	5.16	0.124	0.390	2.318	2.774
3	7.74	0.145	0.428	2.172	2.569
4	10.32	0.141	0.383	1.729	2.072
5	12.9	0.129	0.209	1.347	1.623
6	15.48	0.112	0.117	1.130	1.363
7	18.06	0.094	0.079	0.962	1.155
8	20.64	0.078	0.071	1.105	1.317
9	23.22	0.084	0.085	1.557	1.887
10	25.8	0.111	0.119	1.896	2.301
11	28.38	0.132	0.164	1.962	2.479
12	30.96	0.140	0.186	1.982	2.571
13	33.54	0.147	0.205	1.918	2.488
14	36.12	0.154	0.273	2.193	2.725
15	38.7	0.163	0.440	2.595	3.195
16	41.28	0.179	0.581	2.744	3.400
17	43.86	0.185	0.642	3.004	3.739
18	46.44	0.199	0.700	3.026	3.851
19	49.02	0.205	0.680	3.128	3.962
20	51.6	0.211	0.700	2.993	3.864
21	54.18	0.207	0.656	3.020	3.864
22	56.76	0.212	0.715	2.914	3.646
23	59.34	0.208	0.796	2.995	3.759
24	61.92	0.214	0.811	3.026	3.849
25	64.5	0.224	0.819	3.191	4.008
26	67.08	0.235	0.862	3.098	3.880
27	69.66	0.239	0.833	3.224	4.055
28	72.24	0.248	0.864	3.189	3.999
29	74.82	0.243	0.899	2.174	2.626

Hornsea Mere core 10					
Sample	Depth	χ	ARM	IRM_{100}	SIRM
	cm	$\mu\ m^3\ kg^{-1}$	$mA\ m^2\ kg^{-1}$	$mA\ m^2\ kg^{-1}$	$mA\ m^2\ kg^{-1}$
1	2.54	0.136	0.439	3.311	3.759
2	5.08	0.198	0.425	2.066	2.460
3	7.62	0.127	0.365	1.797	2.151
4	10.16	0.122	0.217	1.414	1.726
5	12.7	0.111	0.125	1.333	1.636
6	15.24	0.108	0.121	1.151	1.399
7	17.78	0.096	0.084	1.283	1.543
8	20.32	0.097	0.091	1.414	1.719
9	22.86	0.104	0.113	1.912	2.404
10	25.4	0.129	0.142	1.968	2.480
11	27.94	0.141	0.161	1.714	2.279
12	30.48	0.139	0.144	1.649	2.243
13	33.02	0.158	0.125	1.755	2.446
14	35.56	0.146	0.158	1.234	1.766
15	38.1	0.144	0.132	1.380	2.010
16	40.64	0.148	0.144	1.859	2.630
17	43.18	0.157	0.163	2.162	3.151
18	45.72	0.162	0.175	1.735	2.351
19	48.26	0.163	0.163	1.959	2.714
20	50.8	0.164	0.163	1.865	2.536
21	53.34	0.164	0.164	1.945	2.680
22	55.88	0.170	0.187	1.965	2.645
23	58.42	0.171	0.194	2.085	2.762
24	60.96	0.179	0.204	2.015	2.574
25	63.5	0.179	0.197	1.917	2.503
26	66.04	0.174	0.177	1.917	2.479
27	68.58	0.173	0.205	1.933	2.601
28	71.12	0.178	0.214	1.918	2.624
29	73.66	0.176	0.206	1.851	2.553
30	76.2	0.172	0.205	1.870	2.562
31	78.74	0.178	0.207	1.915	2.567
32	81.28	0.172	0.228	1.792	2.286
33	83.82	0.168	0.217	1.859	2.464
34	86.36	0.170	0.228	1.948	2.568

Gormire core 1					
Sample	Depth	χ	ARM	IRM_{100}	SIRM
	cm	$\mu\ m^3\ kg^{-1}$	$mA\ m^2\ kg^{-1}$	$mA\ m^2\ kg^{-1}$	$mA\ m^2\ kg^{-1}$
1	2.65	0.5	1.213	8.595	10.640
2	5.3	0.4	0.665	5.671	7.248
3	7.95	0.2	0.521	3.836	4.892
4	10.6	0.1	0.351	2.196	2.836
5	13.25	0	0.318	2.230	2.867
6	15.9	0	0.263	2.008	2.664
7	18.55	0	0.192	1.187	1.546
8	21.2	0	0.191	1.133	1.420
9	23.85	0	0.228	2.362	3.707
10	26.5	0	0.179	1.586	2.460
11	29.15	0	0.183	1.490	2.064
12	31.8	0	0.150	1.433	2.068
13	34.45	0	0.122	1.286	1.913
14	37.1	0	0.100	1.033	1.500
15	39.75	0	0.084	0.574	0.793
16	42.4	0	0.074	0.411	0.515
17	45.05	0	0.068	0.373	0.489
18	47.7	0	0.060	0.300	0.363
19	50.35	0	0.059	0.276	0.324
20	53	0	0.060	0.287	0.356
21	55.65	0	0.077	0.399	0.446
22	58.3	0	0.075	0.426	0.675
23	60.95	0	0.051	0.252	0.352
24	63.6	0	0.035	0.155	0.186
25	66.25	0	0.040	0.171	0.215
26	68.9	0	0.043	0.183	0.242
27	71.55	0	0.049	0.231	0.290
28	74.2	0	0.050	0.216	0.273
29	76.85	0	0.054	0.254	0.380

Gormire core 2					
Sample	Depth	χ	ARM	IRM_{100}	SIRM
	cm	$\mu\ m^3\ kg^{-1}$	$mA\ m^2\ kg^{-1}$	$mA\ m^2\ kg^{-1}$	$mA\ m^2\ kg^{-1}$
1	2.54	1.1	0.478	7.375	10.361
2	5.08	1.4	0.852	13.412	17.725
3	7.62	1	0.917	12.688	17.437
4	10.16	0.4	0.892	3.565	4.258
5	12.7	0.4	1.158	3.909	4.562
6	15.24	0.3	1.045	3.786	4.364
7	17.78	0.2	0.850	3.026	3.508
8	20.32	0.1	0.697	2.874	3.433
9	22.86	0	0.571	2.263	2.691
10	25.4	0	0.143	0.600	0.735
11	27.94	0	0.099	0.409	0.500
12	30.48	0	0.090	0.415	0.585
13	33.02	0	0.068	0.297	0.389
14	35.56	0	0.055	0.227	0.284
15	38.1	0	0.060	0.247	0.312
16	40.64	0	0.078	0.464	0.900
17	43.18	0	0.073	0.442	0.747
18	45.72	0	0.066	0.354	0.571
19	48.26	0	0.051	0.253	0.354
20	50.8	0	0.045	0.210	0.272
21	53.34	0	0.045	0.230	0.295
22	55.88	0	0.045	0.230	0.301
23	58.42	0	0.054	0.260	0.311
24	60.96	0	0.056	0.262	0.331

Gormire core 3					
Sample	Depth	χ	ARM	IRM_{100}	SIRM
	cm	$\mu\ m^3\ kg^{-1}$	$mA\ m^2\ kg^{-1}$	$mA\ m^2\ kg^{-1}$	$mA\ m^2\ kg^{-1}$
1	3	0.5	1.245	9.578	12.228
2	2.57	0.6	1.530	12.518	15.465
3	5.14	0.6	1.637	12.219	15.063
4	7.71	0.5	1.414	10.608	13.285
5	10.28	0.5	1.688	9.158	10.995
6	12.85	0.4	2.222	8.555	10.250
7	15.42	0.1	2.174	7.530	8.681
8	17.99	0.2	1.901	6.516	7.766
9	20.56	0	1.376	4.742	5.534
10	23.13	0.3	1.117	3.999	4.717
11	25.7	0.2	0.765	2.952	3.398
12	28.27	0.2	0.739	2.843	3.178
13	30.84	0	0.703	2.773	3.292
14	33.41	0.1	0.898	3.457	4.146
15	35.98	0.3	0.594	2.436	2.881
16	38.55	0.2	0.254	1.446	1.871
17	41.12	0.1	0.156	1.158	1.618
18	43.69	0	0.111	0.602	0.789
19	46.26	0	0.112	0.581	0.772
20	48.83	0	0.091	0.613	0.919
21	51.4	0	0.095	0.725	1.121
22	53.97	0	0.069	0.408	0.587
23	56.54	0	0.073	0.383	0.535
24	59.11	0	0.059	0.321	0.484
25	61.68	0	0.052	0.283	0.385
26	64.25	0	0.041	0.227	0.317
27	66.82	0	0.044	0.228	0.319
28	69.39	0	0.049	0.216	0.290
29	71.96	0	0.055	0.263	0.380
30	74.53	0	0.043	0.204	0.271

Gormire core 4					
Sample	Depth	χ	ARM	IRM_{100}	SIRM
	cm	$\mu m^3 kg^{-1}$	$mA m^2 kg^{-1}$	$mA m^2 kg^{-1}$	$mA m^2 kg^{-1}$
1	2.6	0.8	0.653	7.373	8.864
2	5.2	0.9	0.727	10.138	11.661
3	7.8	1.9	1.903	37.481	46.620
4	10.4	1.9	2.783	45.246	56.374
5	13	2.1	3.041	49.766	63.824
6	15.6	0.3	1.886	7.317	7.417
7	18.2	0.2	1.477	4.987	5.408
8	20.8	0.5	1.124	3.989	4.359
9	23.4	0.4	1.250	4.300	4.992
10	26	0.3	0.714	2.728	2.825
11	28.6	0.3	0.665	2.949	3.252
12	31.2	0.2	0.683	2.768	3.342
13	33.8	0	0.488	2.095	2.314
14	36.4	0.2	0.349	1.502	1.745
15	39	0	0.179	0.800	0.621
16	41.6	0	0.122	0.571	0.733
17	44.2	0	0.108	0.517	0.679
18	46.8	0	0.085	0.423	0.575
19	49.4	0	0.070	0.333	0.454
20	52	0	0.068	0.282	0.311
21	54.6	0	0.066	0.260	0.261
22	57.2	0	0.059	0.228	0.261
23	59.8	0	0.066	0.260	0.261
24	62.4	0	0.058	0.228	0.266
25	65	0	0.062	0.251	0.291
26	67.6	0	0.074	0.294	0.350
27	70.2	0	0.074	0.273	0.326
28	72.8	0	0.074	0.294	0.357
29	75.4	0	0.084	0.394	0.502
30	78	0	0.067	0.285	0.356

Appendix K

Davis-Merrick (Constrained) Resistivity Inversion Data

	Depth (m)	ohm-m
SEM 1	0	137.523
	0.21516	137.523
	0.21516	15.0000
	0.21616	15.0000
	0.21616	100.000
	22.2045	100.000
	22.2045	2500.00
SEM 2	0	188.852
	1.17080	188.852
	1.17080	1574.43
	9.63814	1574.43
	9.63814	2500.00
SEM 3	0	25.5774
	0.78269	25.5774
	0.78269	586.308
	2.17007	586.308
	2.17007	15.0000
	20.6318	15.0000
	20.6318	100.000
	34.5624	100.000
	34.5624	2500.00
SEM4	0	109.275
	0.737714	109.275
	0.737714	78.5816
	10.07012	78.5816
	10.07012	15.0000
	33.4598	15.0000
	33.4598	100.000
	33.4598	100.000
	33.4598	2500.00
SEM 5	0	118.594
	0.606760	118.594
	0.606760	60.1729
	8.69615	60.1729
	8.69615	15.000
	28.4558	15.000
	28.4558	100.000
	28.4568	100.000
	28.4568	2500.00
SEM 6	0	22.1827
	0.135262	22.1827
	0.135262	59.1154
	2.00102	59.1154
	2.00102	15.0000
	18.6710	15.0000
	18.6710	100.000
	18.6720	100.000
	18.6720	2500.00
SEM 7	0	39.5047
	2.82289	39.5047
	2.82289	15.0000
	22.0222	15.0000
	22.0222	100.000
	22.0232	100.000
	22.0232	2500.00
SEM 8	0	29.4003
	0.26594	29.4003
	0.26594	35.5309
	4.13665	35.5309
	4.13665	15.0000
	25.4970	15.0000
	25.4970	100.000
	28.8626	100.000
	28.8626	2500.00
SEM 9	0	123.919
	0.49097	123.919
	0.49097	91.8357
	8.52227	91.8357
	8.52227	15.0000
	21.8893	15.0000
	21.8893	100.000
	21.8893	100.000
	21.8893	2500.00
SEM 10	0	72.9438
	0.96883	72.9438
	0.96883	312.419
	1.98269	312.419
	1.98269	100.000
	93.8075	100.000
	93.8075	2500.00
SEM 11	0	164.506
	1.92836	164.506
	1.92836	100.000
SEM 12	0	64.8348
	0.647015	64.8348
	0.647015	41.0327
	5.26483	41.0327
	5.26483	15.0000
	7.75552	15.0000
	7.75552	100.000
	49.5609	100.000
	49.5609	2500.0
SEM 13	0	96.7926
	55.6890	96.7926
	55.6890	100.000
	55.7175	100.000
	55.7175	2500.00

Appendix L

Gully Size Classification in Raydale

A	Semer Water	B	Cragdale Water
1	S	1	S
2	S	2	L
3	M	3	S
4	S	4	S
5	S	5	L
6	S	6	L
7	S	7	L
8	S		
9	S		
10	S		

C	Raydale Beck	D	Bardale Beck
1	S	1	M
2	S	2	M
3	S	3	M
4	S	4	S
5	S	5	S
6	S	6	S
7	S	7	M
8	S	8	S
9	S	9	S
10	L	10	L
11	M	11	S
12	L	12	S
13	M	13	L
14	S	14	S
15	L	15	M
16	S	16	S
17	L	17	S
18	S	18	S
19	S	19	M